

200-DV-1 Operable Unit S-Complex Field Summary Report

Prepared for the U.S. Department of Energy
Assistant Secretary for Environmental Management

Contractor for the U.S. Department of Energy
under Contract DE-AC06-08RL14788

CH2MHILL
Plateau Remediation Company

**P.O. Box 1600
Richland, Washington 99352**

200-DV-1 Operable Unit S-Complex Field Summary Report

Date Published
March 2020

Prepared for the U.S. Department of Energy
Assistant Secretary for Environmental Management

Contractor for the U.S. Department of Energy
under Contract DE-AC06-08RL14788

CH2MHILL
Plateau Remediation Company
P.O. Box 1600
Richland, Washington 99352

APPROVED
By Sarah Harrison at 3:55 pm, Mar 03, 2020

Release Approval

Date

TRADEMARK DISCLAIMER

Reference herein to any specific commercial product, process, or service by tradename, trademark, manufacturer, or otherwise, does not necessarily constitute or imply its endorsement, recommendation, or favoring by the United States Government or any agency thereof or its contractors or subcontractors.

This report has been reproduced from the best available copy.

Printed in the United States of America

Contents

1	Introduction	1-1
1.1	Background on 200-DV-1 OU and the S Complex Waste Sites	1-1
1.1.1	216-S-9 Crib.....	1-1
1.1.2	216-S-13 Crib.....	1-3
1.1.3	216-S-21 Crib.....	1-5
1.2	Hydrogeology of the 200-DV-1 Operable Unit S Complex Area.....	1-8
2	Field Methods	2-1
2.1	Drilling	2-1
2.2	Sampling and Analysis.....	2-3
2.3	Geologic Logging.....	2-9
2.4	Geophysical Logging	2-9
2.5	Core Logging.....	2-10
2.6	Borehole Decommissioning	2-10
2.7	Waste Management	2-10
3	Borehole Results	3-1
3.1	Borehole C9512 at the 216-S-9 Crib.....	3-1
3.2	Borehole C9513 at the 216-S-13 Crib.....	3-10
3.3	Borehole C9514 at the 216-S-21 Crib.....	3-23
4	Conclusions	4-1
5	References	5-1

Appendices

A	Borehole Drilling Summaries.....	A-i
B	Borehole Geophysical Log Reports	B-i
C	Borehole Core Log Reports and Photographs.....	C-i
D	Contaminant Attenuation and Transport Characterization of 200-DV-1 Operable Unit Sediment Samples (PNNL-26208).....	D-i

Figures

Figure 1-1.	Map of S Complex Area Showing 200-DV-1 OU Characterization Borehole Locations and the Borehole Location at the 216-S-9 Crib	1-2
Figure 1-2.	Configuration of the 216-S-9 Crib.....	1-3
Figure 1-3.	Map of S Complex Area Showing 200-DV-1 OU Characterization Borehole Locations and the Borehole Location at the 216-S-13 Crib	1-4
Figure 1-4.	Configuration of the 216-S-13 Crib.....	1-5

Figure 1-5.	Map of S Complex Area Showing 200-DV-1 OU Characterization Borehole Locations and the Borehole Location at the 216-S-21 Crib	1-6
Figure 1-6.	Configuration of the 216-S-21 Crib.....	1-7
Figure 2-1.	200-DV-1 OU Drilling Schematics for Boreholes C9512 and C9514.....	2-1
Figure 2-2.	200-DV-1 OU Drilling Schematics for Borehole C9513	2-2
Figure 2-3.	200-DV-1 OU Becker Hammer Drill Rigs: Foremost AP-1000.....	2-3
Figure 2-4.	200-DV-1 OU Sonic Drill Rigs: 600C Full-Size Track-Mounted Rig (Left), Terra Sonic 150CC Track-Mounted Rig (Right).....	2-3
Figure 2-5.	200-DV-1 OU Shallow Soil Samplers: Becker Hammer Split Spoon, Sonic Sleeves (Left to Right).....	2-4
Figure 2-6.	200-DV-1 OU Deep Soil Samplers: Sonic Core.....	2-4
Figure 2-7.	Geophysical Logging: Sonde Above Borehole, Sonde Getting Sleeved, Sleeved Sonde Lowered in a Borehole (Left to Right)	2-9
Figure 2-8.	Example Core from 90 to 95 ft bgs in Borehole C9513 Showing a Very Distinct Color Change in the Silt from Reddish-Brown to Bluish-Grey at 90.8 ft bgs.....	2-10
Figure 3-1.	As-Built Diagram for Borehole C9512.....	3-3
Figure 3-2.	Geophysical Log and Sample Depths for Borehole C9512	3-4
Figure 3-3.	Composite Log Profile for Borehole C9512.....	3-9
Figure 3-4.	As-Built Design Diagram for Borehole C9513	3-11
Figure 3-5.	Geophysical Log and Sample Depths for Borehole C9513	3-12
Figure 3-6.	Composite Log Profile for Borehole C9513.....	3-22
Figure 3-7.	Microtomography Images of a Longitudinal Cross Section from Borehole C9513, 222.5 to 223.5 ft bgs	3-23
Figure 3-8.	As-Built Diagram for Borehole C9514.....	3-24
Figure 3-9.	Geophysical Log and Sample Depths for Borehole C9514	3-25
Figure 3-10.	Composite Log Profile for Borehole C9514.....	3-31

Tables

Table 1-1.	216-S-9 Crib Inventory of Mobile Contaminants.....	1-3
Table 1-2.	216-S-13 Crib Inventory of Mobile Contaminants.....	1-5
Table 1-3.	216-S-21 Crib Inventory of Mobile Contaminants	1-7
Table 2-1.	200-DV-1 OU Analytical Methods.....	2-5
Table 3-1.	Deviations from the 200-DV-1 OU SAP for S Complex Boreholes	3-2
Table 3-2.	Radiological Contaminant Concentrations in Samples Collected from Borehole C9512	3-5
Table 3-3.	Nonradiological Contaminant Concentrations in Samples Collected from Borehole C9512	3-6
Table 3-4.	Radiological Contaminant Concentrations in Samples Collected from Borehole C9513	3-13

Table 3-5. Nonradiological Contaminant Concentrations in Samples Collected from Borehole C95133-15

Table 3-6. Organic Contaminant Concentrations in Samples Collected from Borehole C95133-19

Table 3-7. Radiological Contaminant Concentrations in Samples Collected from Borehole C95143-27

Table 3-8. Nonradiological Contaminant Concentrations Collected from C95143-28

This page intentionally left blank.

Terms

BDS	Borehole Deviation System
bgs	below ground surface
CCU	Cold Creek unit
CCUc	Cold Creek unit caliche
CCUz	Cold Creek unit silt
COPC	contaminant of potential concern
CSM	conceptual site model
FY	fiscal year
Hf	Hanford formation
Hf1	Hanford formation unit 1
Hf2	Hanford formation unit 2
KUT	potassium, uranium, thorium
MIBK	methyl isobutyl ketone
OU	operable unit
PNNL	Pacific Northwest National Laboratory
REDOX	reduction-oxidation
Rtf	Ringold Formation member of Taylor Flat
Rwie	Ringold Formation member of Wooded Island – unit E
SAP	sampling and analysis plan
TD	total depth

This page intentionally left blank.

1 Introduction

This field summary report documents the drilling, sampling, and decommissioning of three vadose zone characterization boreholes installed in the 200-DV-1 Operable Unit (OU) within the Central Plateau of the Hanford Site in fiscal years (FYs) 2016 and 2017. These boreholes were drilled as part of the 200-DV-1 OU remedial investigation to characterize the deep vadose zone beneath 200-DV-1 OU waste sites located in the S Complex Area. The boreholes were drilled and sampled as defined in DOE/RL-2011-104, *Characterization Sampling and Analysis Plan for the 200-DV-1 Operable Unit* (hereinafter called the sampling and analysis plan [SAP]). The purpose of this document is to describe field methods and results from drilling and sampling three characterization boreholes in the S Complex Area.

1.1 Background on 200-DV-1 OU and the S Complex Waste Sites

The 200-DV-1 OU comprises 43 waste sites in three distinct geographical areas of Central Plateau: the B Complex Area, the T Complex Area, and the S Complex Area. This OU includes the vadose zone from the ground surface to the water table at these 43 waste sites. The 200-DV-1 OU was created in 2010 to support remedy selection for waste sites with deep vadose contamination. The deep vadose zone begins approximately 15.2 m (50 ft) below ground surface (bgs) and extends to the water table at depths ranging from 55 to 82 m (180 to 270 ft) bgs. The deep vadose zone was contaminated during disposal of hazardous waste associated with plutonium separation processes. In the S Complex Area, the reduction-oxidation (REDOX) process operating at the 202S Plant (S Plant) used methyl isobutyl ketone (MIBK) to separate plutonium and uranium from the dissolved fuel rod solutions. From 1952 through 1967, S Plant processed approximately 24,000 tons of uranium fuel rods. The lingering contamination in the deep vadose zone is a potential source for continued release of mobile contaminants to the groundwater. The deep vadose zone is being characterized by drilling boreholes and collecting soil samples at selected depths.

The primary contaminants in the deep vadose zone at the S Complex Area that are driving long-term risk are uranium and technetium-99 because of their adverse health effects, mobility, and long half-lives. Additional mobile contaminants of long-term concern are iodine-129, chromium (assumed to be hexavalent chromium), tritium, nitrate, and MIBK (DOE/RL-2010-89, *Long-Range Deep Vadose Zone Program Plan*). The S Complex Area includes three waste sites in the 200-DV-1 OU associated with S Plant.

Three boreholes were drilled at three waste sites:

1. Borehole C9512 at the 216-S-9 Crib
2. Borehole C9513 at the 216-S-13 Crib
3. Borehole C9514 at the 216-S-21 Crib

1.1.1 216-S-9 Crib

The 216-S-9 Crib is located east of the S-SX and SY Tank Farms as displayed in Figure 1-1. The waste site was a 91 m (300 ft) long by 9.1 m (30 ft) deep crib fed by a perforated vitrified clay pipe, as shown in Figure 1-2. From 1965 to 1969 the crib received 49.5 million L (13.1 million gal) of condensate from S Plant. The crib was taken out of service when it reached its radionuclide limit. Table 1-1 shows the total estimated inventory of mobile contaminants discharged to the 216-S-9 Crib, which included large quantities of uranium, tritium, and nitrate. In 2016, borehole C9512 was drilled near the influent end of the crib, near the leak discovered in 1969 at the junction of the pipelines that re-routed the waste to the replacement crib.

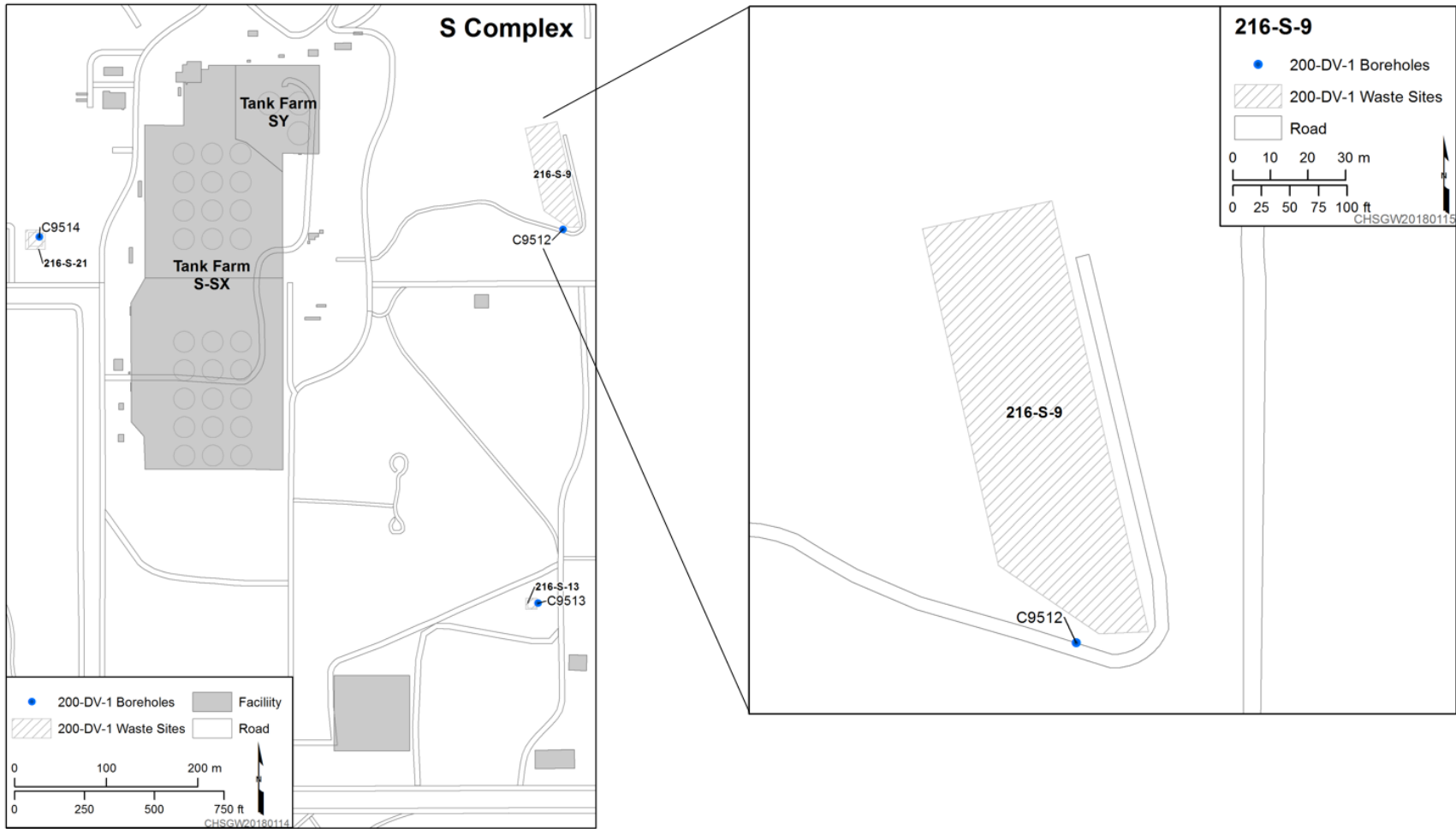
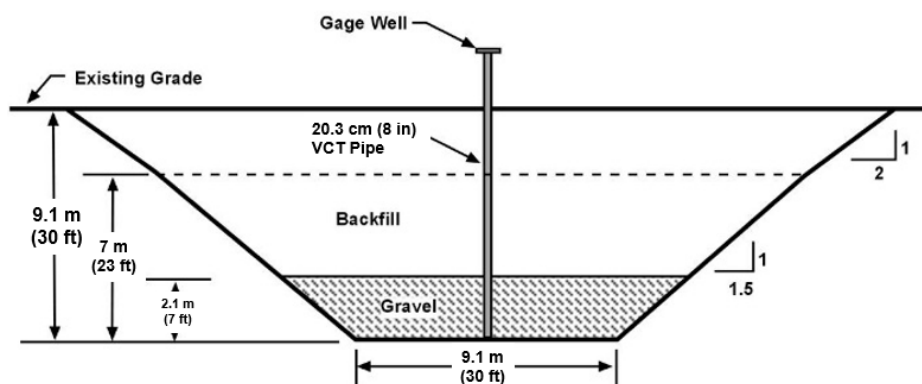


Figure 1-1. Map of S Complex Area Showing 200-DV-1 OU Characterization Borehole Locations and the Borehole Location at the 216-S-9 Crib



Source: Appendix A of CP-49279, *Central Plateau Waste Site Dimensions*.

Figure 1-2. Configuration of the 216-S-9 Crib

Table 1-1. 216-S-9 Crib Inventory of Mobile Contaminants

Contaminant	Inventory
Uranium (total)	2.76×10^2 kg
Technetium-99	1.04×10^{-1} Ci
Iodine-129	2.95×10^{-2} Ci
Cobalt-60	1.12×10^{-2} Ci
Tritium	1.17×10^3 Ci
Nitrate	4.18×10^4 kg
Fluoride	None
Ferrocyanide	None
Chromium*	None

Source: RPP-26744, *Hanford Soil Inventory Model, Rev. 1*.

Note: In RPP-26744, radionuclides are decayed to January 1, 2001.

*The Soil Inventory Model in RPP-26744 does not provide speciation information for chromium. All chromium inventories are assumed to be hexavalent unless other information is available.

1.1.2 216-S-13 Crib

The 216-S-13 Crib is located west of the solvent storage and makeup building as displayed in Figure 1-3. The waste site was a 3.7 by 3.7 m (12 by 12 ft) square wooden box with an open bottom, fed by one inlet pipe near the top of the box as shown in Figure 1-4. From 1952 to 1972 the crib received 4.9 million L (1.3 million gal) of liquid waste from decontaminated metal and MIBK solvent storage facilities and sump waste from the uranyl nitrate hexahydrate storage facility. The crib was removed from service when the storage facilities were deactivated. Table 1-2 shows the total estimated inventory of mobile contaminants discharged to the 216-S-13 Crib, which included large quantities of uranium, tritium, nitrate, and chromium. Additionally, 10,000 kg of MIBK and 10,000 kg of sodium dichromate were disposed in the crib (DOE/RL-2007-02-VOLII-ADD3, *Site-Specific Field Sampling Plans for the 216-B-42 Trench, 216-S-13 Crib, 216-S-21 Crib, 216-T-18 Crib, and 216-T-19 Crib and Tile Field in the 200-TW-1/PW-5 Operable Units*). In 2017, deep borehole C9513 was drilled near the influent (eastern) side of the crib to address the zone that is expected to have the highest contamination. The location selected in DOE/RL-2011-104 was within the footprint of the crib but during characterization planning, the borehole was relocated outside the crib footprint because of subsidence concerns.

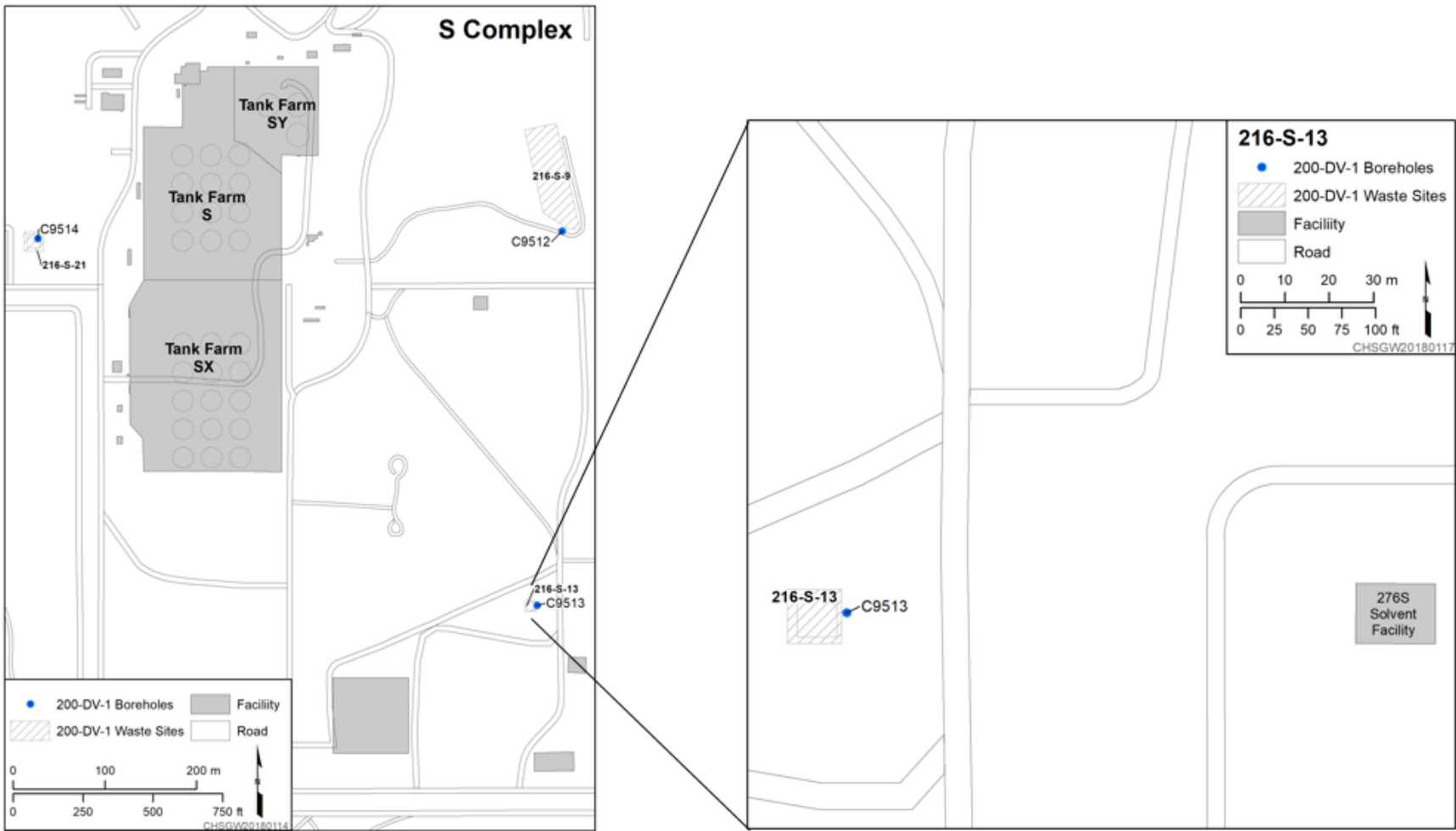
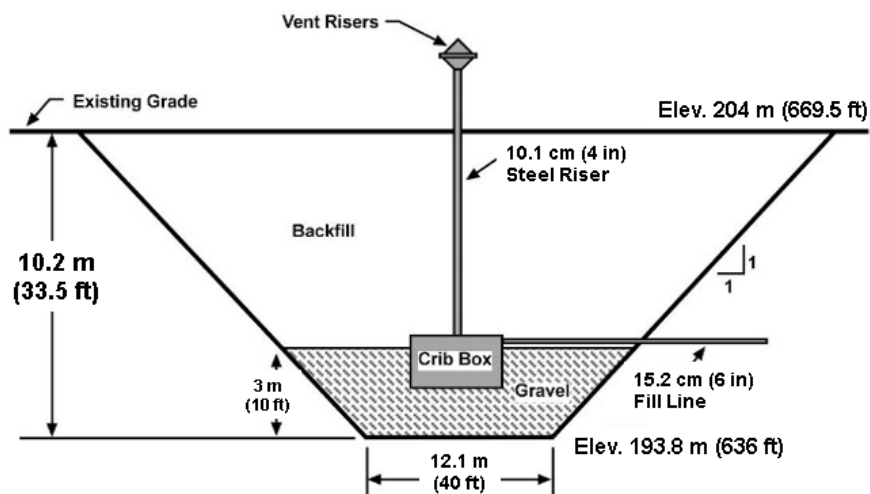


Figure 1-3. Map of S Complex Area Showing 200-DV-1 OU Characterization Borehole Locations and the Borehole Location at the 216-S-13 Crib



Source: DOE/RL-2007-02-VOLII-ADD3, *Site-Specific Field Sampling Plans for the 216-B-42 Trench, 216-S-13 Crib, 216-S-21 Crib, 216-T-18 Crib, and 216-T-19 Crib and Tile Field in the 200-TW-1/PW-5 Operable Units.*

Figure 1-4. Configuration of the 216-S-13 Crib

Table 1-2. 216-S-13 Crib Inventory of Mobile Contaminants

Contaminant	Inventory
Uranium (total)	3.05 kg
Technetium-99	4.40×10^{-1} Ci
Iodine-129	None
Cobalt-60	1.85×10^{-3} Ci
Tritium	4.31×10^1 Ci
Nitrate	3.48×10^4 kg
Fluoride	4.79×10^1 kg
Ferrocyanide	None
Chromium*	1.21×10^1 kg

Source: RPP-26744, *Hanford Soil Inventory Model, Rev. 1.*

Note: In RPP-26744, radionuclides are decayed to January 1, 2001.

*The Soil Inventory Model in RPP-26744 does not provide speciation information for chromium. All chromium inventories are assumed to be hexavalent unless other information is available.

1.1.3 216-S-21 Crib

The 216-S-21 Crib is located west of the S-SX Tank Farm as displayed in Figure 1-5. The crib was a 4.8 by 4.8 m (16 by 16 ft) wooden box with two vent risers and one test well going through the center of the box, as shown in Figure 1-6. From 1954 to 1970 the crib received 87 million L (23 million gal) of condensate from the 241-SX-401 Building condensers. Table 1-3 shows the total estimated inventory of mobile contaminants discharged to the 216-S-21 Crib, which included large quantities of technetium-99, tritium, nitrate, and chromium. Borehole C9514 was drilled in 2016 near the influent (eastern) side of the crib to address the zone that was expected to have the highest contamination. The location selected in DOE/RL-2011-104 was closer to the center of the crib, but during characterization planning, the borehole was relocated further away from the crib center because of subsidence concerns.

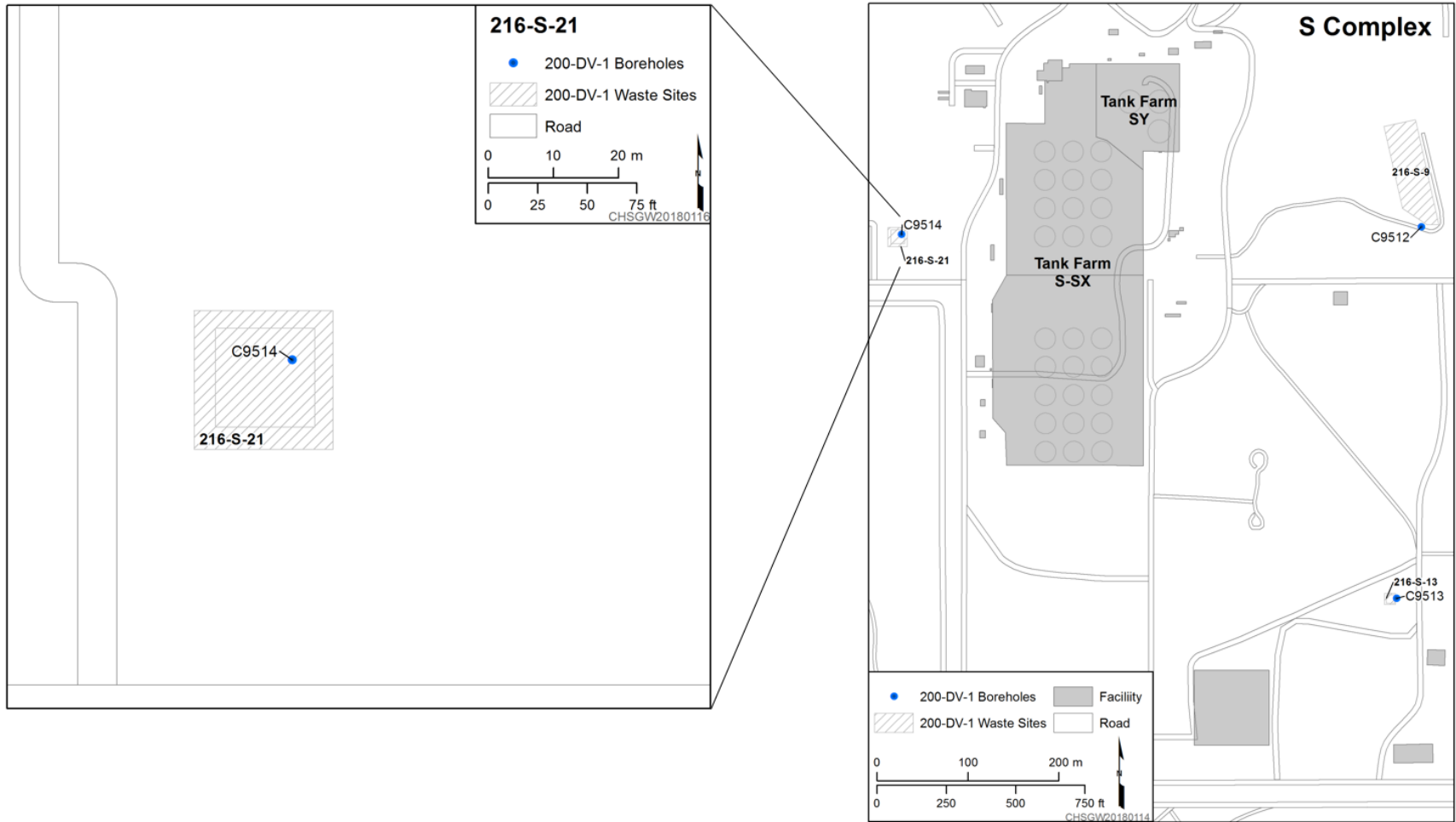
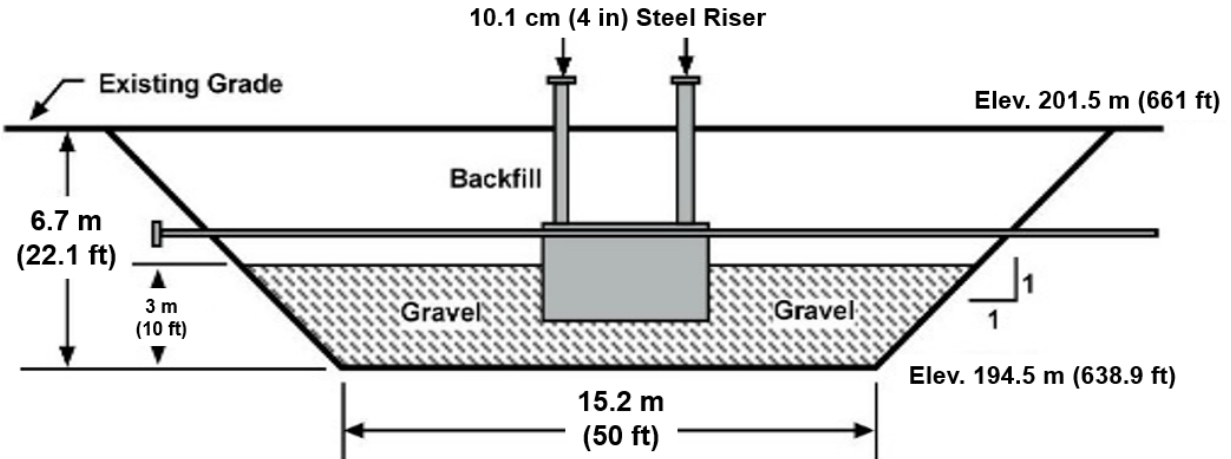


Figure 1-5. Map of S Complex Area Showing 200-DV-1 OU Characterization Borehole Locations and the Borehole Location at the 216-S-21 Crib



Source: DOE/RL-2007-02-VOLII-ADD3, *Site-Specific Field Sampling Plans for the 216-B-42 Trench, 216-S-13 Crib, 216-S-21 Crib, 216-T-18 Crib, and 216-T-19 Crib and Tile Field in the 200-TW-1/PW-5 Operable Units.*

Figure 1-6. Configuration of the 216-S-21 Crib

Table 1-3. 216-S-21 Crib Inventory of Mobile Contaminants

Contaminant	Inventory
Uranium (total)	1.06×10^{-1} kg
Technetium-99	2.11×10^{-1} Ci
Iodine-129	3.23×10^{-4} Ci
Cobalt-60	3.36×10^{-2} Ci
Tritium	2.54×10^3 Ci
Nitrate	4.91×10^2 kg
Fluoride	2.19×10^1 kg
Ferrocyanide	None
Chromium*	5.08×10^1 kg

Source: RPP-26744, *Hanford Soil Inventory Model, Rev. 1.*

Note: In RPP-26744, radionuclides are decayed to January 1, 2001.

*The Soil Inventory Model in RPP-26744 does not provide speciation information for chromium. All chromium inventories are assumed to be hexavalent unless other information is available.

1.2 Hydrogeology of the 200-DV-1 Operable Unit S Complex Area

The 200-DV-1 OU is located in the Central Plateau of the Hanford Site, which is the topographically elevated region formed during the Pleistocene cataclysmic floods (DOE/RL-2002-39, *Standardized Stratigraphic Nomenclature for Post-Ringold-Formation Sediments Within the Central Pasco Basin*). These paleo-floods deposited thick sequences of unconsolidated silt, sand, and gravel known as the Hanford formation (Hf) onto older sediments of the Cold Creek unit (CCU) and Ringold Formation, creating a mega flood bar. The unique depositional setting of the Hf sediments created a series of erosional unconformities that result in heterogeneities within the stratigraphic unit. All 200-DV-1 OU waste sites are located within the Central Plateau on this ancestral flood bar.

In the S Complex Area, the vadose zone is 67.4 to 72.5 m (221 to 238 ft) thick and is composed of two of the three units of the Hf (Hanford formation unit 1 [Hf1] and Hanford formation unit 2 [Hf2]), the Cold Creek unit silt (CCUz) and Cold Creek unit caliche (CCUc), the Ringold Formation upper fines (Ringold Formation member of Taylor Flat [Rtf]), and part of the Ringold Formation member of Wooded Island – unit E (Rwie). The Hf comprises about one half of the vadose thickness and consists of an upper open framework gravel unit (Hf1) and a sand-dominated unit (Hf2). The Hanford sediments typically have higher permeability and hydraulic conductivity compared to the older, more consolidated CCU and Ringold Formation. The CCUz is a fine-grained silt to sand facies that overlies the CCUc, which is a variably cemented calcium carbonate fine- to coarse-grained deposit. Underlying the CCU is the Ringold Formation, which is locally composed of predominantly fine-grained silt and sand (Rtf) atop a fluvial deposit of silty, sandy gravel (Rwie). The S Complex vadose zone overlies an unconfined aquifer, contained within the Rwie. The saturated thickness of the aquifer in the S Complex ranges from 102 to 108 m (335 to 355 ft).

2 Field Methods

Drilling was carried out in accordance with SGW-58552, *Description of Work for the Characterization of 200-DV-1 Operable Unit, FY2015*. Sampling, sample quality assurance, and quality control were carried out under the direction of the following documents:

- DOE/RL-2011-104, *Characterization Sampling and Analysis Plan for the 200-DV-1 Operable Unit*
- DOE/RL-2011-104-ADD1, *Characterization Sampling and Analysis Plan for the 200-DV-1 Operable Unit Addendum 1: Attenuation Process Characterization*
- DOE/RL-2011-104-ADD2, *Characterization Sampling and Analysis Plan for the 200-DV-1 Operable Unit Addendum 2: Supplemental Shallow Soil Risk Characterization Sampling*

Stillwater LLC, Layne Christensen Company, Cascade Drilling L.P., Great West Drilling, and Holt Services drilled the three boreholes between April 2016 and September 2017 under the direction of CH2M HILL Plateau Remediation Company. Freestone Environmental Services provided well site geology services and Stoller Newport News Nuclear provided geophysical logging services.

2.1 Drilling

Boreholes C9512, C9513, and C9514 were drilled in the S Complex Area to characterize the mobile contaminants in the vadose zone at or near the waste sites. Geophysical logs from nearby wells had previously identified a zone of high radiological contamination between 4.6 and 15 m (15 and 50 ft) bgs. In order to protect the work site personnel, samples and drill cuttings from this zone could not be brought to the surface. Therefore, one type of drill rig pushed through the high radiological zone and another type of rig cored through the vadose zone as shown in Figure 2-1. Borehole C9513 was deeper than the other two boreholes and the casing was downsized to meet the same objective, as shown in Figure 2-2.

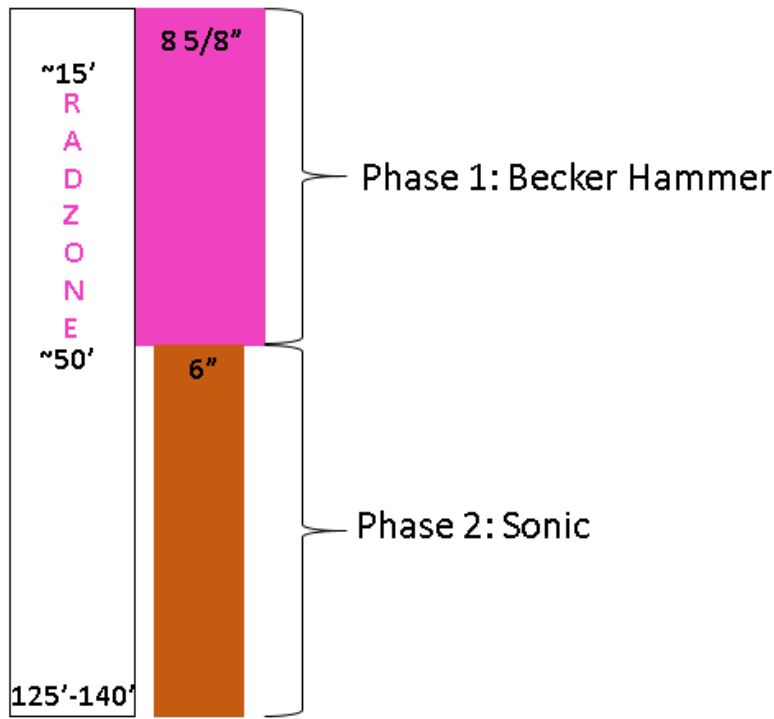


Figure 2-1. 200-DV-1 OU Drilling Schematics for Boreholes C9512 and C9514

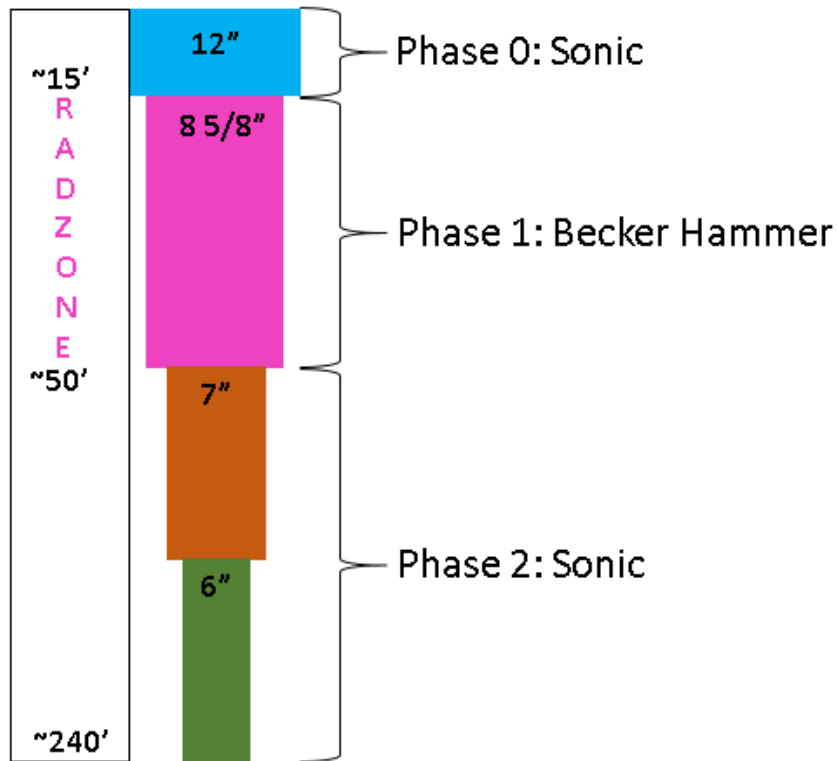


Figure 2-2. 200-DV-1 OU Drilling Schematics for Borehole C9513

Figure 2-3 shows the first phase of drilling using a Foremost AP-1000® Becker Hammer drill rig to push through the high radiological zone to approximately 15 m (50 ft) bgs. The Becker Hammer rig drove 8.625 in. diameter temporary casing with a removable 6.625 in. diameter inner drive rod using a 600 horsepower diesel hammer. Following installation of casing, the borehole was geophysically logged to determine if the Becker Hammer had drilled through the radiological contamination. If the high radiological zone had successfully been drilled through, then drilling proceeded to the second phase.

The second phase of drilling used either a 600C full-size, track-mounted sonic drill rig or a Terra Sonic 150CC track-mounted sonic rig (Figure 2-4), to core from the bottom of the high radiological zone to total depth (TD). The sonic drill rig used vibrational, rotational, and downward force to drive 6 in. diameter temporary casing to depths around 38 to 73 m (125 to 240 ft) bgs. Appendix A contains the drilling summaries for boreholes C9512, C9513, and C9514.

® Foremost AP-1000 Becker Hammer drills are a tradename of Foremost, Surrey, British Columbia, Canada.



Figure 2-3. 200-DV-1 OU Becker Hammer Drill Rigs: Foremost AP-1000



Figure 2-4. 200-DV-1 OU Sonic Drill Rigs: 600C Full-Size Track-Mounted Rig (Left), Terra Sonic 150CC Track-Mounted Rig (Right)

2.2 Sampling and Analysis

Soil samples were collected in the shallow vadose zone above 4.6 m (15 ft) bgs and in the deep vadose zone from approximately 15 m (50 ft) bgs to TD. The Becker Hammer used a split-spoon sampler and the sonic rig used plastic sleeves to collect shallow soil samples (0 to 4.6 m [15 ft] bgs) at preselected intervals during phase 1 of drilling as shown in Figure 2-5. Both split-spoon soil and sleeve samples were bottled at the drill site and subsequently shipped to offsite analytical laboratories. During phase 2 of drilling, the sonic rig collected intact continuous core samples using 5 ft long by 4 in. diameter plastic LEXAN[®] liners, as shown in Figure 2-6. The cores were surveyed for temperature and radiological contamination, labeled, and sent to the 6267 Sample Packaging, Shipping, and Receiving Building, just east of the 200 West Area, to be stored in a refrigerator while awaiting transport to the RJ Lee soil laboratory for lithological logging and subsampling. Preselected cores were also sent to Pacific Northwest National Laboratory (PNNL) for analysis of contaminant attenuation and transport per DOE/RL-2011-104-ADD1.

[®] LEXAN is a registered trademark of SABIC, Riyadh, Saudi Arabia.



Figure 2-5. 200-DV-1 OU Shallow Soil Samplers: Becker Hammer Split Spoon, Sonic Sleeves (Left to Right)



Figure 2-6. 200-DV-1 OU Deep Soil Samplers: Sonic Core

After the sonic rig reached TD, the borehole was geophysically logged. Adjustments to the planned sample interval depths per DOE/RL-2011-104 were made based on identification of man-made radiological contaminants, high moisture peaks, and lithologic transitions identified in the geophysical logs. Additionally, the core samples were assessed based on the core temperature readings to ensure that cores with the lowest (or acceptable) temperature readings were selected for subsampling. Heat generated during sonic drilling can result in increased core temperatures; therefore, the temperature of the core was measured using both an infrared gun and temperature tape. All soil samples were analyzed for contaminants of potential concern (COPCs) per DOE/RL-2011-104 at either Test America Laboratories or GEL Laboratory. The analytical methods used by the laboratories are detailed in Table 2-1.

Table 2-1. 200-DV-1 OU Analytical Methods

Constituent	Method [HEIS Method Name]	Description	Sample Preparation
Radiological			
Am-241	AEA [AMCMISO_EIE_PREC_AEA] [AMCMISO_EIE_PLT_AEA]	Isotopic americium/curium analysis by alpha spectrometry	Acid extraction, separation by sequential Eichrom ion-exchange resin, and precipitated on a filter
C-14	LSC [C14_LSC] [C14_CHEM_LSC]	C-14 analysis by liquid scintillation counter	Burn sample in a furnace and collect gas
Cs-137 Co-60 Eu-152 Eu-124 Eu-155	GS [GAMMA_GS]	Gamma-emitting radionuclide analysis by GS using germanium high energy detectors	No sample preparation
I-129	LEPS [I129_SEP_LEPS_GS]	Iodine-129 analysis by LEPS	Solvent extraction and precipitation
Np-237	AEA [NP237_IE_PRECIP_AEA] [NP237_LLE_PLATE_AEA]	Neptunium-237 analysis by alpha spectrometry	Acid leach, separation by ion exchange, and precipitated on a filter
Ni-63	LSC [NI63_LSC]	Nickel-63 analysis by liquid scintillation counter	Acid leach and separation by ion exchange
Pu-238 Pu-239/240	AEA [PUIISO_PLATE_AEA] [PUIISO_IE_PRECIP_AEA]	Isotopic plutonium analysis by alpha spectrometry	Acid leach and separation by ion exchange
Sr-90	GPC [SRISO_SEP_PRECIP_GPC] [SRTOT_SEP_PRECIP_GPC]	Total beta strontium analysis by GPC	Acid leach, chemical separation, and precipitated on a filter
Tc-99	LSC [TC99_EIE_LSC] [TC99_ETVDSK_LSC]	Technetium-99 analysis by liquid scintillation counter	Acid leach and separation by Eichrom ion-exchange resin
H-3	LSC [TRITIUM_DIST_LSC]	Tritium analysis by LSC	Burn sample in a furnace and collect gas

Table 2-1. 200-DV-1 OU Analytical Methods

Constituent	Method [HEIS Method Name]	Description	Sample Preparation
U-233/234 U-235 U-238	AEA [UIISO_IE_PRECIP_AEA] [UIISO_IE_PLATE_AEA] [UIISO_IE_PLATE_AEA]	Isotopic uranium analysis by alpha spectrometry	Acid leach, separation by ion-exchange resin, and precipitated on a filter
Nonradiological			
Al As Ba Cd Cr Cu Pb Mn Ni Se U	6020 Metals (EPA 846) [6020_METALS_ICPMS]	Metal analysis by ICP-MS	Acid leach
NH ₃	350.1 Ammonia (EPA 846) [350.1_AMMONIA]	Ammonium analysis by automated colorimetry	Sulfuric acid extraction
Sb Ag	6010 Metals (EPA 846) [6010_METALS_ICP]	Metal analysis by ICP-AES	Acid leach
Cl ⁻ F ⁻ NO ₃ ⁻ NO ₂ ⁻ PO ₄ ³⁻ SO ₄ ²⁻	300 Anions (EPA 600) or 9056 Anions (EPA 846) [300.0_ANIONS_IC] [9056_ANIONS_IC]	Anion analysis by ion chromatography	10:1 water extraction
CN ⁻	9012 Cyanide (EPA 846) or equivalent [9012_CYANIDE]	Cyanide analysis by automated colorimetry	Water leach with a base
Cr(VI)	7196 Hexavalent Chromium (EPA 846) [7196_CR6]	Hexavalent chromium analysis by colorimetry	Alkaline leach
Hg	7471 Mercury (EPA 846) [7471_HG_CVAA]	Mercury analysis by cold vapor atomic absorption	Chemical vapor generation

Table 2-1. 200-DV-1 OU Analytical Methods

Constituent	Method [HEIS Method Name]	Description	Sample Preparation
Geochemical			
Al Ba Ca Fe Mg Mn K Na	6010 Metals (EPA 846) [6010M_ICP_WE]	Metal analysis by ICP-AES or ICP-MS	1:1 water extraction
Ca Fe Mg K Na	6010 Metals (EPA 846) [6010_METALS_ICP]	Metal analysis by ICP-AES	Acid leach
Al Ba Mn	6020 Metals (EPA 846) [6020_METALS_ICPMS]	Metals by ICP-MS	Acid leach
TIC	9060 TOC (EPA 846) [9060_TOC] [9060_TOC_WE]	TIC analysis by measuring CO ₂ after acid purging	Water leach
TOC		TOC analysis by measuring CO ₂ after chemical oxidation	
Physical			
pH	9045 PH (EPA 846) [9045_PH]	pH of soils using an electrode	--
Specific Conductance	9050 Specific Conductivity (EPA 846) [9050_CONDUCT]	Specific conductance is measured using a self-contained conductivity meter (Wheatstone bridge-type or equivalent)	--
Bulk Density	D2937 Bulk Density (ASTM) [D2937_DENSITY]	Standard test method for density of soil in place by the drive-cylinder method (vol. 4.08)	--
% Moisture	D2216 Percent Moisture (ASTM) [D2216_%MOIS]	Percent moisture in soils measured by drying soil in an oven	--
Particle Size	D422 Particle Size (ASTM) [D422_PARTCLSIZE]	Particle size distribution using a sieve	--

Table 2-1. 200-DV-1 OU Analytical Methods

Constituent	Method [HEIS Method Name]	Description	Sample Preparation
Organics			
Kerosene	Total Petroleum Hydrocarbons (WDOE) [WTPH_DIESEL]	Total petroleum hydrocarbon analysis by gas chromatography-flame ionization detector	Solvent extraction
TBP	8270 Semi-Volatile Organic Analysis (EPA 846) [8270_SVOA_GCMS]	Semi-volatile organic compound analysis by GC-MS	Solvent extraction
MIBK	8260 Volatile Organic Analysis (EPA 846) [8260_VOA_GCMS]	Volatile organic compound analysis by GC-MS	Gas purge
PCB	8082 PCB (EPA 846) [8082_PCB_GC]	PCB analysis by gas chromatography-electron capture detector	Solvent extraction

- | | | | | | |
|---------|---|--|------|---|--|
| AEA | = | alpha energy analysis | LSC | = | liquid scintillation counter |
| ASTM | = | ASTM International (formerly American Society for Testing and Materials) | PCB | = | polychlorinated biphenyl |
| GC-MS | = | gas chromatography-mass spectrometry | TBP | = | tributyl phosphate |
| GPC | = | gas proportional counting | TIC | = | total inorganic carbon |
| GS | = | gamma spectroscopy | TOC | = | total organic carbon |
| HEIS | = | Hanford Environmental Information System | MIBK | = | methyl isobutyl ketone |
| ICP-AES | = | inductively coupled plasma-atomic emission spectroscopy | OU | = | operable unit |
| ICP-MS | = | inductively coupled plasma-mass spectrometry | WDOE | = | Washington State Department of Ecology |
| LEPS | = | low energy photon spectroscopy | | | |

2.3 Geologic Logging

Geologic logging was conducted concurrently with borehole drilling in accordance with standard methods for geologic logging. Geologic logging activities included preparing daily reports, borehole logs, and well summary sheets. In most cases during phase 2 drilling, due to sediment collection via the continuous core, detailed geologic descriptions were not possible in the field but were completed in the RJ Lee soil laboratory when the cores were opened for core logging and subsampling. Appendix A contains the well site geologist's drilling summary reports for boreholes C9512, C9513, and C9514.

2.4 Geophysical Logging

Geophysical logging was conducted to characterize the nature and vertical extent of gamma contamination, identify sediment layers suitable for sampling, define geologic units with potential for lateral correlation, and evaluate the straightness of the borehole.

The Spectral Gamma Logging System, High Rate Logging System, Neutron Moisture Logging System, Borehole Deviation System (BDS), and Passive Neutron Logging System were all used during this project. As shown in Figures 2-1 and 2-2, each borehole consisted of either two or four casing strings, with each casing string logged separately with the exception of the BDS, which was deployed once when total depth was reached within the respective casing strings.

After drilling of each casing string was completed, a radiological control technician swabbed and checked the borehole to assess the downhole environment and determine if there was any internal contamination that could contaminate the logging tools. As a matter of practice, it was decided to sleeve the logging tools in 4 mil (0.004 in.) thick plastic during logging to prevent the Sonde from coming in contact with the casing, as shown in Figure 2-7.



Figure 2-7. Geophysical Logging: Sonde Above Borehole, Sonde Getting Sleeved, Sleeved Sonde Lowered in a Borehole (Left to Right)

Prior to using each logging system, verification checks were conducted to ensure proper tool operation. Logging was conducted to within approximately 0.3 m (1 ft) of the bottom of the borehole. The bottom 0.3 m (1 ft) was not logged to limit the potential for contaminated material to be brought up to the surface following a log run. The High Rate Logging System and Passive Neutron Logging System log runs focused on intervals of high radioactivity, as determined during initial Spectral Gamma Logging System logging. A centralizer was used during logging of each first casing string to keep the logging tool near the center of the borehole axis. Due to the smaller diameter of the second casing string, no centralizer was used except when logging with the BDS. Verification checks were conducted following each logging day. Repeat log runs were conducted over 10% of the logged intervals as another quality check to confirm both proper tool operation and depth repeatability. Appendix B contains the geophysical log data reports.

2.5 Core Logging

The intact 1.5 m (5 ft) long continuous cores collected during sonic drilling were sent to the RJ Lee soil laboratory for lithologic logging and subsampling. Prior to cutting the core, the outside of the LEXAN liner was surveyed with hand-held instruments for alpha, beta, and gamma radiation. Each LEXAN liner was then cut lengthwise on each side, as shown in Figure 2-8. After opened, the soil was surveyed again. Pictures of each core were taken using a digital camera. The lithology of each core was logged in detail per the standard methods for geologic logging. Preselected soil intervals were subsampled, bottled, labeled, and shipped to offsite analytical laboratories for analysis. Appendix C contains the detailed core descriptions and digital photographs.



Figure 2-8. Example Core from 27.4 to 29.0 m (90 to 95 ft) bgs in Borehole C9513 Showing a Very Distinct Color Change in the Silt from Reddish-Brown to Bluish-Grey at 27.7 m (90.8 ft) bgs

2.6 Borehole Decommissioning

Boreholes C9512, C9513, and C9514 were decommissioned from total depth to approximately 0.6 m (2 ft) bgs with bentonite chips. Concrete was poured from 0 to 0.6 m (2 ft) bgs and a brass marker was placed at ground surface for identification.

2.7 Waste Management

The waste generated from 200-DV-1 OU drilling, sampling, geophysical logging, and borehole decommissioning activities was managed according to DOE/RL-2012-20, *Waste Control Plan for the 200-DV-1 Operable Unit*.

3 Borehole Results

This chapter details the borehole as-built diagrams and analytical results (sediment and geophysical log plots). It presents a composite borehole log showing the overall borehole lithology, contaminant depth profile, and geophysical logging profile for each of the three characterization boreholes. Additionally, some preliminary observations based on the soil and geophysical data from the three characterization boreholes are noted in this chapter. These observations focus on the mobile contaminants with the largest quantities discharged to the waste sites (uranium, technetium-99, iodine-129, tritium, nitrate, and chromium), as shown in Tables 1-1 through 1-3.

All required data analyses were completed. Data from the 200-DV-1 OU boreholes in the S Complex Area have been reviewed and verified as part of the quality assurance process in accordance with the SAP (Section 2.4 of DOE/RL-2011-104). Data validation will be documented in separate data validation reports and discussed in the data usability assessment report. Detailed interpretations of the borehole and analytical data and an updated 200-DV-1 OU conceptual site model (CSM) will be presented in future reports.

Table 3-1 details the number of samples collected, total depth achieved for each borehole, and deviations from the SAP (DOE/RL-2011-104, DOE/RL-2011-104-ADD1, and DOE/RL-2011-104-ADD2). In general, the number of SAP samples stayed the same but the sample depths were moved to avoid the high radiological zone (Section 2.1) and to sample at optimal depths after reviewing the geophysical logs (Section 2.2). Additionally, supplemental samples were collected to satisfy the SAP addenda (DOE/RL-2011-104-ADD1 and DOE/RL-2011-104-ADD2).

3.1 Borehole C9512 at the 216-S-9 Crib

Borehole C9512 is located at the 216-S-9 Crib. The Becker Hammer drill rig pushed 8.625 in. diameter casing from ground surface to 11.1 m (36.4 ft) bgs and the sonic rig drilled 6 in. diameter casing to TD of 43.4 m (142.5 ft) bgs (Figure 3-1). C9512 was geophysically logged and final sample depths were selected, as shown in Figure 3-2. The sediment samples were analyzed for COPCs, as displayed in Tables 3-2 and 3-3, and the lithology was logged and plotted with mobile COPCs and borehole geophysics, as shown in Figure 3-3.

The sediment samples collected at approximately 19 m (61 ft) bgs and approximately 32 m (104 ft) bgs contained elevated concentrations of nitrate (212,000 and 288,000 $\mu\text{g}/\text{kg}$, respectively). Tritium was present in the lower portion of the borehole with concentrations increasing with depth; concentrations were 54, 100, and 417 pCi/g at 32, 40, and 43 m (104, 130, and 140 ft) bgs, respectively. The sample with the highest tritium concentration was collected from a zone of high moisture at the CCUz. Low concentrations of iodine-129 were detected in the two deepest samples from the borehole (40 and 43 m [130 and 140 ft] bgs). Borehole geophysical logs show cesium-137 contamination from ground surface to approximately 20 m (64 ft) bgs.

Borehole C9512 encountered the Hf1 and Hf2 and a portion of the uppermost fine-grained CCU. No soil was evaluated from 4.6 to 10 m (15 to 32 ft) bgs due to the Becker Hammer drilling method. Therefore, the base of the crib fill at borehole C9512 is inferred from geophysical logs showing an abrupt increase in cesium-137 at 7.9 m (26 ft) bgs, although the contact could potentially be shallower. The sandy and silty gravel intervals encountered at the start of sonic drilling at 9.8 m (32 ft) bgs indicates the borehole is well into the gravel-dominated Hf1. A transition at 17 m (56 ft) bgs to massive sand followed by well-bedded sand and silty sand indicates the top of the Hf2. This transition can also be seen in the geophysical logs where an increase in natural potassium, uranium, and thorium indicate an increase in clay minerals and fine-grained sediments. At 39 m (128 ft) bgs the silt content increases to 90% but then drops back down to 15% from 39.8 to 40.3 m (130.7 to 132.2 ft) bgs. At 40 m (132 ft) bgs the unit is 100% laminated, light

yellowish-brown silt. This is the top of the CCU, specifically the CCUz, which persists to TD of the borehole at 43.4 m (142.5 ft) bgs.

Table 3-1. Deviations from the 200-DV-1 OU SAP for S Complex Boreholes

Waste Site	Borehole	Planned (SAP)	Actual	Reason for Deviation
216-S-9 Crib	C9512	Samples: 7 Depth: 42.6 m (140 ft)	Samples: 11 Depth: 43.4 m (142.5 ft)	Samples: Two supplemental shallow samples collected for risk assessment per DOE/RL-2011-104-ADD2, and two supplemental vadose zone samples collected for PNNL per DOE/RL-2011-104-ADD1. Depth: Not applicable
216-S-13 Crib	C9513	Samples: 11 Depth: 74.7 m (245 ft)	Samples: 21 Depth: 73.3 m (240.5 ft)	Samples: Seven supplemental shallow samples collected for risk assessment, and three supplemental vadose zone samples collected for PNNL per DOE/RL-2011-104-ADD1. Depth: Stopped drilling 4.5 ft above planned depth to avoid drilling into the groundwater per the Washington State Department of Ecology.
216-S-21 Crib	C9514	Samples: 7 Depth: 38.1 m (125 ft)	Samples: 9 Depth: 38.9 m (127.6 ft)	Samples: Two supplemental shallow samples collected for risk assessment per DOE/RL-2011-104-ADD2. Depth: Not applicable

References: DOE/RL-2011-104-ADD1, *Characterization Sampling and Analysis Plan for the 200-DV-1 Operable Unit Addendum 1: Attenuation Process Characterization.*

DOE/RL-2011-104-ADD2, *Characterization Sampling and Analysis Plan for the 200-DV-1 Operable Unit Addendum 2: Supplemental Shallow Risk Characterization Sampling.*

OU = operable unit

PNNL = Pacific Northwest National Laboratory

SAP = sampling and analysis plan

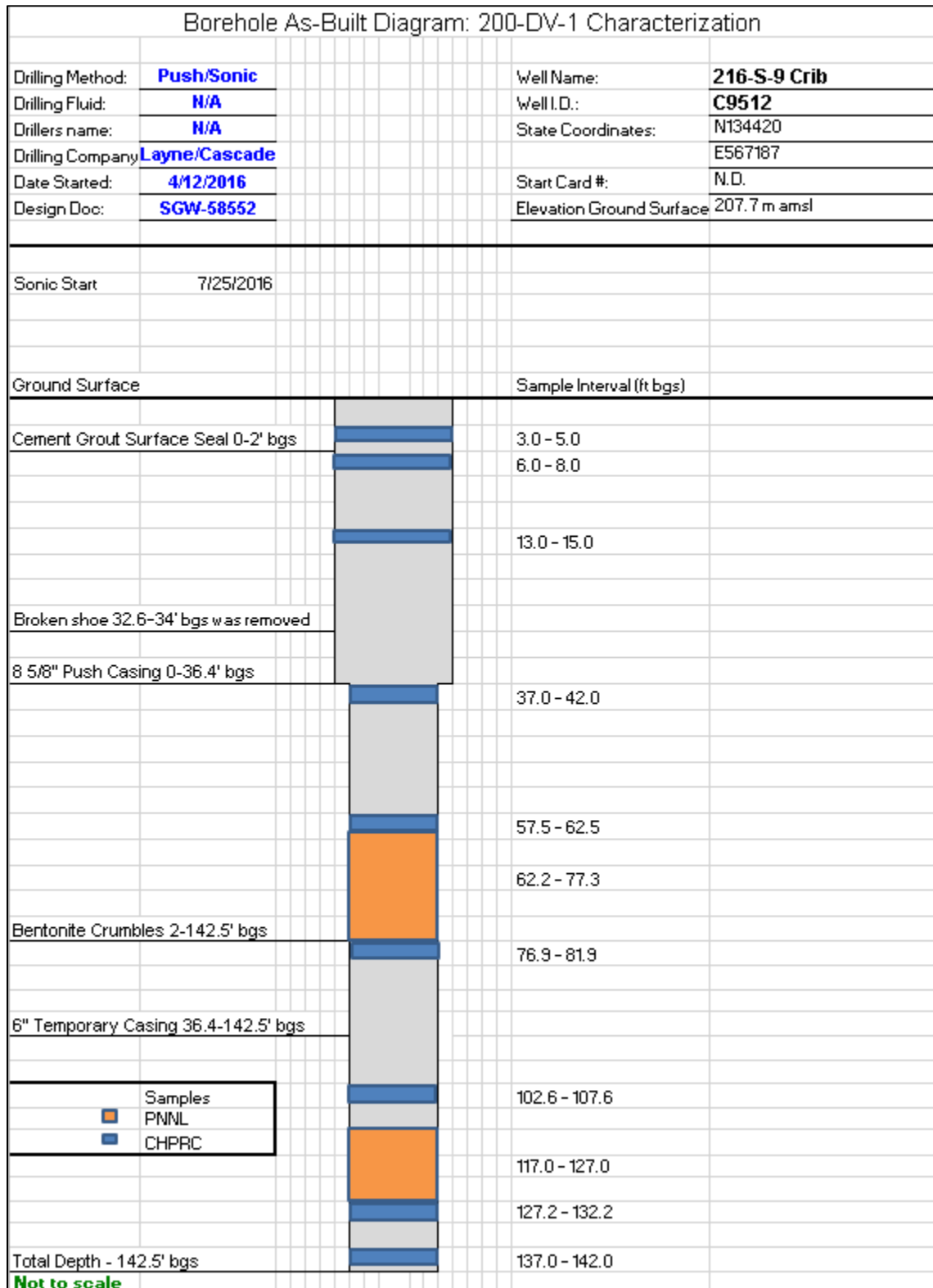
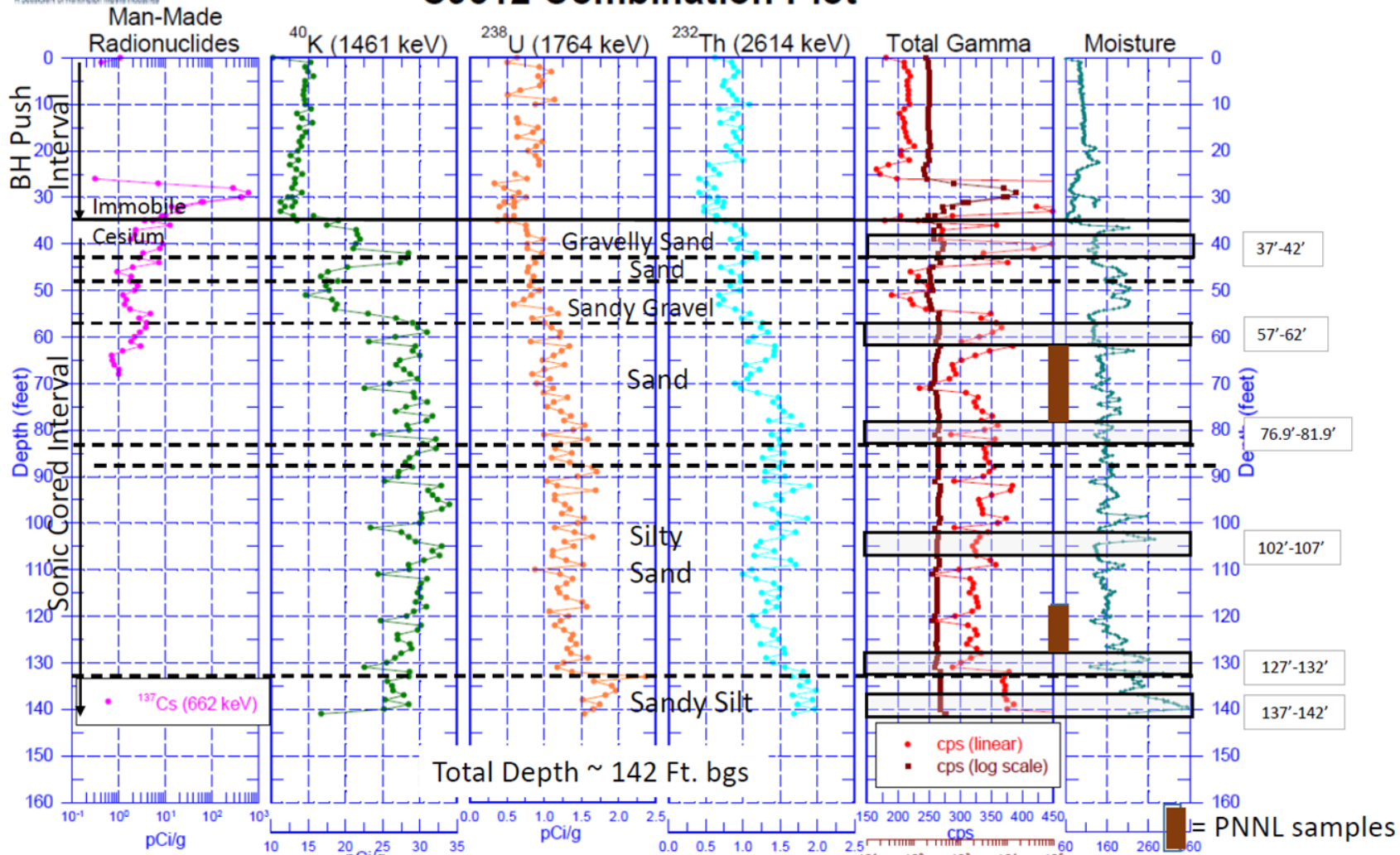


Figure 3-1. As-Built Diagram for Borehole C9512



Stoller Newport News Nuclear
A Subsidiary of Hamamatsu Inertial Industries

C9512 Combination Plot



3-4

SGW-61596, REV. 1

Note: Appendix B contains the complete geophysical log report.

Figure 3-2. Geophysical Log and Sample Depths for Borehole C9512

Table 3-2. Radiological Contaminant Concentrations in Samples Collected from Borehole C9512

Sample Interval (ft bgs)	Sample Number (HEIS #)	Am-241 (pCi/g)	C-14 (pCi/g)	Cs-137 (pCi/g)	Co-60 (pCi/g)	Eu-152 (pCi/g)	Eu-154 (pCi/g)	Eu-155 (pCi/g)	I-129 (pCi/g)	Np-237 (pCi/g)	Ni-63 (pCi/g)	Pu-238 (pCi/g)	Pu-239/240 (pCi/g)	Sr-90 (pCi/g)	Tc-99 (pCi/g)	H-3 (pCi/g)	U-233/234 (pCi/g)	U-235 (pCi/g)	U-238 (pCi/g)
3.2 - 5.5	B33XV3	0.0266 U	0.18 U	0.721	0.0163 U	0.0365 U	0.0524 U	0.0458 U		0.0286 U	276	0.038 U	0.0367 U	0.258 U	0.577 U	0.189 U		0.0241 U	0.254
6 - 8.2	B33XV4	0.0308 U	0.187 U	0.463	0.0157 U	0.0314 U	0.0492 U	0.0297 U		0.0285 U	5.86 U	0.0391 U	0.17	0.347 U	0.575 U	0.183 U		0.0289	0.26
13 - 15.3	B33XV5	0.0469 U	0.185 U	0.0365	0.0155 U	0.0319 U	0.0483 U	0.031	0.121 U	0.044 U	4.37 U	0.0348 U	0.0291 U	0.231 U	0.56 U	4.88		0.0268 U	0.371
40.7 - 41.5	B37FF9	0.701	8.29	5.36	0.0111 U	0.0312 U	0.0364 U	0.026 U	0.127 U	0.0818 U	5.67 U	0.0905	0.671	0.32	0.808 U	30.3	0.562	0.038 U	0.605
60.8 - 62	B37FH1	0.243	0.795	1.24	0.0134 U	0.027 U	0.0452 U	0.023 U	0.141 U	0.0437 U	6.6 U	0.123	0.267	0.359	1.06 U	14.6	0.165	0.0545 U	0.178
	B37FH3	0.349	0.564 U	1.2	0.0116 U	0.0248 U	0.0364 U	0.0234 U	0.158 U	0.0591 U	7.38 U	0.0801 U	0.244	0.288	1.09 U	15.8	0.217	0.0586 U	0.308
78.5 - 79.8	B37FH5	0.0661 U	0.272 U	0.0103 U	0.0128 U	0.0223 U	0.0411 U	0.021 U	0.167 U	0.0752 U	7.62 U	0.0698 U	0.0511 U	0.268 U	1.1 U	10.1	0.258	0.0471 U	0.271
103.1 - 104.6	B37FH7	0.0831 U	1.05	0.0102 U	0.0124 U	0.0278 U	0.0392 U	0.0348 U	0.0577 U	0.0547 U	7.45 U	0.0635 U	0.0527 U	0.272 U	1.04 U	53.7	0.124	0.0442 U	0.218
129.2 - 130.2	B37FH9	0.0918 U	0.269 U	0.0124 U	0.0143 U	0.0281 U	0.046 U	0.027 U	0.729	0.0556 U	6.49 U	0.0873 U	0.069 U	0.346 U	0.932 U	100	0.279	0.054 U	0.172
139 - 140.5	B37FJ1	0.084 U	0.393	0.0191 U	0.0217 U	0.0528 U	0.0673 U	0.0638 U	0.691	0.0603 U	6.59 U	0.0876 U	0.105 U	0.366 U	1.09 U	417	0.178	0.0522 U	0.168

Notes: Blank cells indicate no result for sample number.
 Undetected radionuclide value reported is the minimum detectable concentration.
 bgs = below ground surface
 HEIS = Hanford Environmental Information System
Data qualifier
 U =analyzed for but not detected

Table 3-3. Nonradiological Contaminant Concentrations in Samples Collected from Borehole C9512

Sample Interval (ft bgs)	Sample Number (HEIS #)	Al (µg/kg)	NH ₃ (µg/kg)	Sb (µg/kg)	As (µg/kg)	Ba (µg/kg)	Cd (µg/kg)	Cl ⁻ (µg/kg)	Cr (µg/kg)	Cu (µg/kg)	CN ⁻ (µg/kg)	F ⁻ (µg/kg)	Cr(VI) (µg/kg)	Pb (µg/kg)	Mn (µg/kg)	Hg (µg/kg)	Ni (µg/kg)	NO ₃ ⁻ (µg/kg)	NO ₂ ⁻ (µg/kg)	PO ₄ ³⁻ (µg/kg)	Se (µg/kg)	Ag (µg/kg)	SO ₄ ²⁻ (µg/kg)	Kerosene (µg/kg)	TBP (µg/kg)	U (µg/kg)	
3.2 - 5.5	B33XT3							1,900 B				1,100						31,400 N	102 U	3,800 BN			6,900				
	B33XT8	6,060,000 D		480 BD	7,100 D	86,900 DN	140 BD		7,000 D	14,800 D	120 U			5,600 D		14 B	11,300 D				1,600 BD	190 BD		350 U	48 U	550 D	
6 - 8.2	B33XT4							1,800 B				1,500						27,400 N	112 B	2,300 BN			7,900				
	B33XT9	6,080,000 D		510 BD	8,700 D	132,000 DN	140 BD		11,500 D	21,400 D	120 U			7,200 D		10 U	15,500 D				1,800 BD	210 BD		350 U	48 U	710 D	
13 - 15.3	B33XT5							31,000				1,200						35,000 N	102 U	1,300 BN			120,000				
	B33VX0	6,440,000 D	158 BN	490 BD	8,000 D	109,000 DN	110 BD		11,000 D	21,100 D	120 U			6,900 D		11 U	15,000 D				2,000 BD	120 U		350 U	48 U	640 D	
	B33XV5												200 B														
40.7 - 41.5	B37FF9							10,000				500	150 U					66,400	624 U	1,260 U			19,000				
	B37FH0	5,570,000 D	6,570 N	460 UD	2,900 D	52,400 D	140 D		9,200 D	11,000 D	110 U			3,800 D	285,000 D	15 B	10,400 D				810 UD	190 UD		340 U	47 U	880 D	
60.8 - 62	B37FH1							1,000 B				510	150 U					212,000	1,020 B	1,230 U			2,100 B				
	B37FH2	7,700,000 D	9,360 N	470 UD	6,700 D	135,000 D	120 BD		13,400 D	15,000 D	120 U			6,300 D	617,000 D	11 U	13,100 D				910 BD	190 UD		340 U	47 U	580 D	
	B37FH3							1,100 B				520	150 U					212,000	1,050 B	1,260 U			2,100 B				
	B37FH4	7,490,000 D	11,100 N	500 UD	5,600 D	83,800 D	74 BD		12,700 D	15,000 D	110 U			6,200 D	379,000 D	10 U	18,200 D				930 BD	190 UD		340 U	47 UZH	550 D	
78.5 - 79.8	B37FH5							1,900 B				810	150 U					93,000 Z	624 UZ	1,260 UZ			1,500 B				
	B37FH6	8,450,000 D	888 CN	480 UD	6,700 D	142,000 D	92 BD		14,200 D	18,100 D	110 U			6,300 D	580,000 DN	11 U	13,400 D				710 UD	170 UD		340 U	47 U	1,100 D	
103.1 - 104.6	B37FH7							8,400				1,500	150 U					288,000 DZY	2,100 Z	1,260 UZ			4,200				
	B37FH8	9,850,000 D	863 CN	480 BD	6,700 D	84,400 D	110 BD		18,200 D	15,600 D	120 U			6,400 D	429,000 DN	12 B	19,000 D				1,000 BD	190 UD		350 U	48 U	780 D	
129.2 - 130.2	B37FH9							990 U				840	150 U					33,200 Z	624 UZ	1,720 BZ			3,400				
	B37FJ0	11,800,000 D	705 CN	530 BD	9,600 D	116,000 D	170 D		21,800 D	22,500 D	120 U			8,500 D	409,000 DN	14 B	24,800 D				1,200 BD	190 UD		350 U	49 U	930 D	

Table 3-3. Nonradiological Contaminant Concentrations in Samples Collected from Borehole C9512

Sample Interval (ft bgs)	Sample Number (HEIS #)	Al (µg/kg)	NH ₃ (µg/kg)	Sb (µg/kg)	As (µg/kg)	Ba (µg/kg)	Cd (µg/kg)	Cl ⁻ (µg/kg)	Cr (µg/kg)	Cu (µg/kg)	CN ⁻ (µg/kg)	F ⁻ (µg/kg)	Cr(VI) (µg/kg)	Pb (µg/kg)	Mn (µg/kg)	Hg (µg/kg)	Ni (µg/kg)	NO ₃ ⁻ (µg/kg)	NO ₂ ⁻ (µg/kg)	PO ₄ ³⁻ (µg/kg)	Se (µg/kg)	Ag (µg/kg)	SO ₄ ²⁻ (µg/kg)	Kerosene (µg/kg)	TBP (µg/kg)	U (µg/kg)	
139 - 140.5	B37FJ1							2,600				1,000	210 B					27,400	624 U	2,330 B			11,000				
	B37FJ2	9,050,000 D	1,060 CN	550 UD	5,200 D	92,900 D	100 BD		12,500 D	18,200 D	130 U			9,300 D	382,000 DN	12 U	14,400 D				1,200 BD	200 UD		390 U	53 U	690 D	

Note: Blank cells indicate no result for sample number.

bgs = below ground surface

HEIS = Hanford Environmental Information System

TBP = tributyl phosphate

Data qualifiers

B = analyte was detected at less than the quantitation limit but greater than the method detection limit

C = analyte was detected in both the sample and the quality control blank

D = analyte was reported at a secondary dilution factor

H = laboratory holding time exceeded before the sample was analyzed

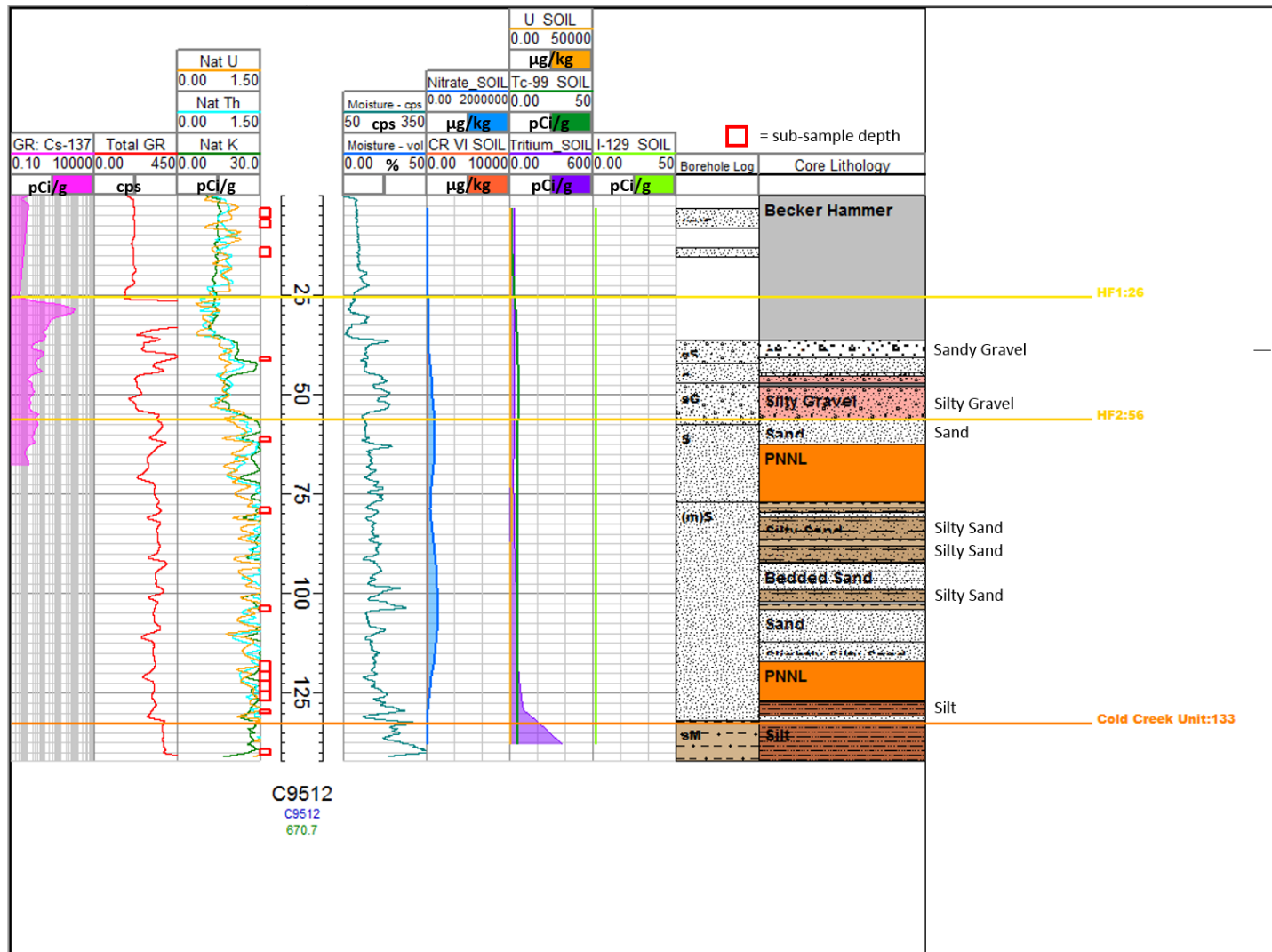
N = spike and/or spike duplicate recovery is outside control limits

U = analyzed for but not detected

Y = result is suspect

Z = miscellaneous circumstances exist; additional information available in database comment field

This page intentionally left blank.



Notes: The contaminant scale changes with each borehole. The ground surface elevation at borehole C9512 is 204.4 m (670.7 ft). Appendix C contains the complete borehole core log report and photographs.

Figure 3-3. Composite Log Profile for Borehole C9512

3.2 Borehole C9513 at the 216-S-13 Crib

Borehole C9513 is located at the 216-S-13 Crib. The sonic rig drove 12 in. diameter casing from ground surface to 3.6 m (11.9 ft) bgs and the Becker Hammer rig pushed 8.625 in. diameter casing to 13.1 m (43 ft) bgs. The sonic rig returned to drill 7 in. diameter casing to 48.9 m (160.3 ft) bgs and 6 in. diameter casing to TD at 73.3 m (240.5 ft) bgs as shown in Figure 3-4. Borehole C9513 was geophysically logged and final sample depths were selected, as shown in Figure 3-5. The sediment samples were analyzed for COPCs, as displayed in Tables 3-4, 3-5, and 3-6, and the lithology was logged and plotted with mobile COPCs and borehole geophysics, as shown in Figure 3-6.

Sediment samples collected from approximately 28 m (91 ft) bgs to approximately 59 m (192 ft) bgs had significantly high concentrations of hexavalent chromium with concentrations increasing to a peak (9,790 $\mu\text{g}/\text{kg}$) in the moist CCUz (approximately 45 m [147 ft] bgs) and then decreasing below the CCUc in the Rtf (approximately 59 m [192 ft] bgs). Similarly, concentrations of MIBK were elevated from 29 to 53 m (95 to 173 ft) bgs with a maximum concentration (1,900,000 $\mu\text{g}/\text{kg}$) at the CCUz (approximately 44 m [143 ft] bgs) and lower concentrations in sediments collected from the Rtf (approximately 52 m [170 ft] bgs). High uranium concentrations (32,700 and 36,800 $\mu\text{g}/\text{kg}$) were found at 27.7 m (91 ft) bgs in the Hf2 and at 40.2 m (132 ft) bgs at the CCU contact. Technetium-99 was detected (11.4 pCi/g) at approximately 35.4 m (116 ft) bgs. Borehole geophysical logs show cesium-137, cobalt-60, uranium-235, and protactinium-234 contamination at approximately 9 to 17 m (30 to 55 ft) bgs, with sporadic hits of uranium-235 and protactinium-234 throughout the borehole to approximately 46 m (150 ft) bgs.

Borehole C9513 is a deep borehole drilled through the Hf1 and Hf2, the CCU and CCUc, the Rtf and a portion of the Rwie to TD just above the water table. The crib fill material extends from the ground surface to at least 4.6 m (15 ft) bgs where the Becker Hammer drilling method commenced and continued to 14 m (45 ft) bgs. There is a marked change in the geophysical log response at 12 m (39 ft) bgs where all the spectral components increase, indicating a change in lithology to finer-grained sediments and the Hf2 contact. Once the sonic drilling began at 14 m (45 ft) bgs, the Hf2 was revealed to be alternating sand and silty sand with distinct bedding structures. There are several silt beds within the Hf2 where core observations correlate well with neutron moisture log response. The volume percent moisture in those beds is as high as 25%. One high moisture bed at 27 m (90 ft) bgs corresponds to high concentrations of uranium and MIBK as well as a very distinct color change from reddish brown silt to bluish gray silt, as shown in Figure 2-8. The upper CCU was encountered at 40 m (132 ft) bgs where the thorium and neutron moisture logs increase and the lithology transitions into a more silt-dominated system. The CCU displays multiple soft sediment deformation structures, including a coarser-grained injectite structure from 43.6 to 44.2 m (143 to 145 ft) bgs. Injectites are soft sediment deformation structures resulting from rapid sedimentation loading overpressured saturated sediments below. The CCUc contact is interpreted at 46 m (150 ft) bgs from the characteristic spectral gamma signature (increased natural uranium and a substantial decrease in potassium and thorium). The CCUc contact is contained within the cores sent to PNNL and preserved intact for hydraulic analyses; therefore, a textural description of the CCUc is not available for this well.

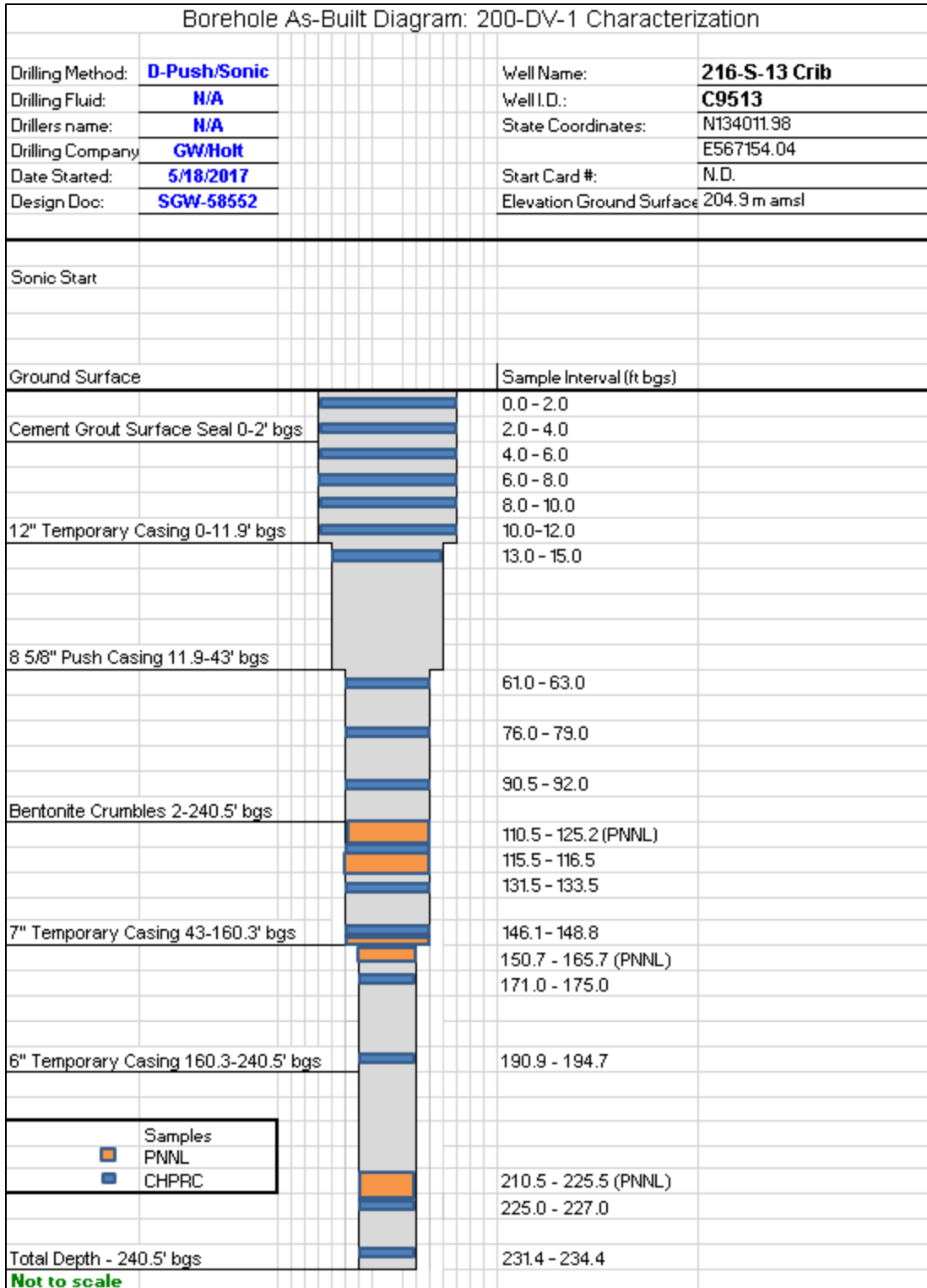
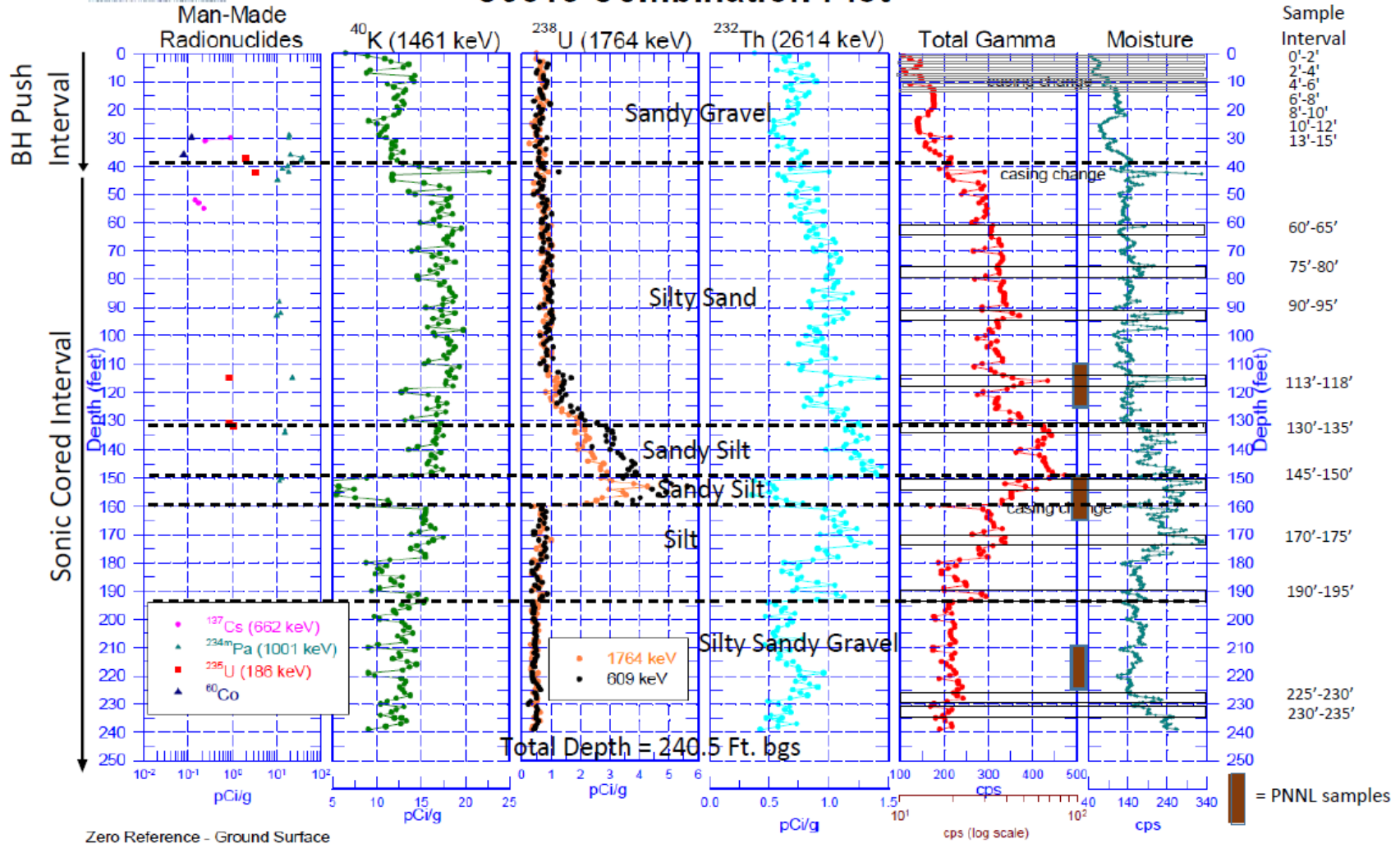


Figure 3-4. As-Built Design Diagram for Borehole C9513



Stellar Newport News Nuclear
A Subsidiary of Huntington Energy Solutions

C9513 Combination Plot



Zero Reference - Ground Surface

Note: Appendix B contains the complete geophysical log report.

Figure 3-5. Geophysical Log and Sample Depths for Borehole C9513

Table 3-4. Radiological Contaminant Concentrations in Samples Collected from Borehole C9513

Sample Depth Interval (ft bgs)	Sample Number (HEIS #)	Am-241 (pCi/g)	C-14 (pCi/g)	Cs-137 (pCi/g)	Co-60 (pCi/g)	Eu-152 (pCi/g)	Eu-154 (pCi/g)	Eu-155 (pCi/g)	I-129 (pCi/g)	Np-237 (pCi/g)	Ni-63 (pCi/g)	Pu-238 (pCi/g)	Pu-239/240 (pCi/g)	Sr-90 (pCi/g)	Tc-99 (pCi/g)	H-3 (pCi/g)	U-233/234 (pCi/g)	U-235 (pCi/g)	U-238 (pCi/g)
0 - 2	B39WN2	0.0599 U	0.138 U	0.0207 U	0.0263 U	0.0449 U	0.0757 U	0.0432 U	0.113 U	0.0457 U	6.98 U	0.0639 U	0.0552 U	0.147 U	0.378 U	0.712 U	0.0829	0.0536 U	0.113
2 - 4	B39WN7	0.0625 U	0.136 U	0.0254 U	0.0288 U	0.0585 U	0.097 U	0.0547 U	0.112 U	0.0504 U	7.01 U	0.0719 U	0.0785 U	0.157 U	0.415 U	0.737 U	0.205	0.0581 U	0.187
4 - 6	B39WP2	0.155 U	0.139 U	0.0214 U	0.0234 U	0.0512 U	0.0673 U	0.0617 U	0.133 U	0.055 U	6.87 U	0.0694 U	0.0754 U	0.143 U	0.42 U	0.723 U	0.108	0.0473 U	0.165
6 - 8	B39WP7	0.0742 U	0.137 U	0.0236 U	0.026 U	0.0522 U	0.0853 U	0.0487 U	0.123 U	0.0606 U	7.7 U	0.0686 U	0.0549 U	0.154 U	0.403 U	0.729 U	0.338	0.0497 U	0.148
8 - 10	B39WR2	0.0809 U	0.136 U	0.0218 U	0.0258 U	0.0498 U	0.0867 U	0.0462 U	0.135 U	0.0592 U	5.77 U	0.0653 U	0.0771 U	0.121 U	0.477 U	0.744 U	0.137	0.0394 U	0.126
10 - 12	B39WR7	0.097 U	0.135 U	0.0202 U	0.0268 U	0.0471 U	0.0812 U	0.0447 U	0.0927 U	0.0447 U	6.41 U	0.0816 U	0.0815 U	0.119 U	0.38 U	0.746 U	0.27	0.0453 U	0.271
13 - 15	B39WT2	0.0792 U	0.139 U	0.0255 U	0.0246 U	0.0724 U	0.0853 U	0.0944 U	0.148	0.0609 U	6.77 U	0.0829 U	0.103 U	0.136 U	0.441 U	0.729 U	0.198	0.0487 U	0.146
61 - 63	B3DCF8	0.348 U	3.96 U	0.0364 U	0.0407 U	0.0812 U	0.119 U	0.0736 U	1.58 U	0.681 U	6.5 U	0.521 U	0.602 U	2.34	3.24 U	27 U	2.01	0.444 U	1.56
	B3DCH3	0.424 U	3.92 U	0.0362 U	0.0529 U	0.109 U	0.139 U	0.131 UXR	0.882 U	0.691 U	5.16 U	0.558 U	0.302 U	3.22	3.76 U	26.7 U	1.77	0.605 U	1.64
76 - 79	B3DCH8	0.462 U	4.02 U	0.0322 U	0.0332 U	0.073 U	0.1 U	0.0616 UXR	1.58 U	0.517 U	6.43 U	0.56 U	0.666 U	1.63	3.19 U	26.9 U	3.25	0.425	1.96
90.5 - 92	B3DCJ3	0.221 U	4.02 U	0.0221 U	0.0234 U	0.0519 U	0.0748 UXR	0.0491 UXR	0.671 U	0.722 U	6.2 U	0.305 U	0.669 U	2.18	3.76 U	27.3 U	12.1	1	12
115.5 - 116.5	B3F941	0.973 UA	3.89 UA	0.0374 UA	0.0434 UA	0.0956 UA	0.11 UA	0.0874 UXA	1.13 UA	0.37 UA	5.95 UA	0.537 UA	0.515 UA	1.51 UA	11.4 BA	23.8 UA	2.86 A	0.42 UA	2.82 A
131.5 - 133.5	B3DCJ8	0.445 U	3.96 U	0.0343 U	0.0368 U	0.0939 U	0.131 U	0.109 UXR	1.18 U	0.449 U	5.19 U	0.607 U	0.686 U	1.44 U	2.9 B	28.4 U	8.72	0.827	10.7
146.1 - 148.8	B3DCK3	0.46 U	4.06 U	0.0313 U	0.0307 U	0.0762 U	0.0879 U	0.0885 UXR	1.04	0.561 U	6.43 U	0.477 U	0.477 U	1.77 U	2.45 U	27.5 U	0.736 U	0.523 U	0.696
171 - 175	B3DCK8	0.591 U	4.15 U	0.0345 U	0.0333 U	0.0991 U	0.124 U	0.115 U	0.93 U	0.448 U	6.77 U	0.423 U	0.423 U	1.83 U	2.7 U	26.9 U	1.13	0.465 U	0.858
190.9 - 194.7	B3DCL3	0.765 U	4.13 U	0.041 U	0.0416 U	0.0862 U	0.142 U	0.104 U	1.41 U	0.432 U	6.51 U	0.458 U	0.554 U	1.15 U	3.44 U	27.3 U	0.912	0.568 U	0.63
225 - 227	B3DCL8	0.572 U	4.08 U	0.0362 U	0.0427 U	0.0831 U	0.138 U	0.0939 U	0.541 U	0.526 U	6.14 U	0.496 U	0.629 U	1.01 U	2.47 U	28.2 U	0.951	0.515 U	0.397

Table 3-4. Radiological Contaminant Concentrations in Samples Collected from Borehole C9513

Sample Depth Interval (ft bgs)	Sample Number (HEIS #)	Am-241 (pCi/g)	C-14 (pCi/g)	Cs-137 (pCi/g)	Co-60 (pCi/g)	Eu-152 (pCi/g)	Eu-154 (pCi/g)	Eu-155 (pCi/g)	I-129 (pCi/g)	Np-237 (pCi/g)	Ni-63 (pCi/g)	Pu-238 (pCi/g)	Pu-239/240 (pCi/g)	Sr-90 (pCi/g)	Tc-99 (pCi/g)	H-3 (pCi/g)	U-233/234 (pCi/g)	U-235 (pCi/g)	U-238 (pCi/g)
231.4 - 234.4	B3DCM3	0.458 UA	4.02 UA	0.0365 AU	0.0366 UA	0.0785 UA	0.125 UA	0.0887 UA	0.656 UA	0.562 UA	5.33 UA	0.466 UA	0.445 UA	0.998 UA	2.49 UA	27.6 UA	1.25 A	0.562 A	0.541 A

Note: Undetected radionuclide value reported is the minimum detectable concentration.

bgs = below ground surface

HEIS = Hanford Environmental Information System

Data qualifiers

A = Discrepancy in chain-of-custody paperwork

R = Do not use. Further review indicates the result is not valid

U = Analyzed for but not detected

X = Indicates a result-specific comment is provided in the data report or case narrative

Table 3-5. Nonradiological Contaminant Concentrations in Samples Collected from Borehole C9513

Sample Depth Interval (ft bgs)	Sample Number (HEIS #)	Al (µg/kg)	NH ₃ (µg/kg)	Sb (µg/kg)	As (µg/kg)	Ba (µg/kg)	Cd (µg/kg)	Cl (µg/kg)	Cr (µg/kg)	Cu (µg/kg)	CN ⁻ (µg/kg)	F ⁻ (µg/kg)	Cr(VI) (µg/kg)	Pb (µg/kg)	Mn (µg/kg)	Hg (µg/kg)	Ni (µg/kg)	NO ₃ ⁻ (µg/kg)	NO ₂ ⁻ (µg/kg)	PO ₄ ³⁻ (µg/kg)	Se (µg/kg)	Ag (µg/kg)	SO ₄ ²⁻ (µg/kg)	Kerosene (µg/kg)	TBP (µg/kg)	U (µg/kg)	
0 - 2	B39WN2												180 B														
	B39WN3	8,320,000 D	365 BN	470 UD	7,100 D	111,000 D	100 BD	1,300 BC	12,000 D	18,600 D	120 U	1,100		6,800 D	498,000 DN	11 U	14,000 D	1,370	194 U	2,500 B	1,500 D	180 UD	2,000 B	2,600 U	49 U	650 D	
2 - 4	B39WN7												150 U														
	B39WN8	8,020,000 D	292 UN	470 UD	7,200 D	110,000 D	110 BD	1,400 BC	10,700 D	21,000 D	120 U	1,200		7,100 D	519,000 DN	11 U	15,500 D	5,310	194 U	2,400 B	1,500 D	190 UD	4,600 B	2,600 U	49 U	850 D	
4 - 6	B39WP2												150 U														
	B39WP3	6,970,000 D	292 UN	480 UD	7,300 D	120,000 D	110 BD	1,600 BC	8,600 D	19,800 D	120 U	910 B		5,100 D	658,000 DN	11 U	12,300 D	6,200	191 U	2,000 B	1,400 D	190 UD	5,300	2,600 U	48 U	650 D	
6 - 8	B39WP7												230 B														
	B39WP8	6,180,000 D	292 UN	470 UD	5,500 D	80,500 D	88 BD	7,500	8,000 D	15,300 D	120 U	1,400		5,100 D	383,000 DN	11 U	9,800 D	17,300	194 U	3,600 B	1,500 D	180 UD	8,200	2,600 U	49 UR	750 D	
8 - 10	B39WR2												150 U														
	B39WR3	8,080,000 D	328 BN	450 UD	7,700 D	129,000 D	130 D	7,300	10,900 D	21,600 D	120 U	1,500		6,100 D	656,000 DN	11 U	14,100 D	19,000	194 U	4,300 B	1,600 D	180 UD	4,900 B	2,600 U	49 U	2,100 D	
10 - 12	B39WR7												180 B														
	B39WR8	8,510,000 D	292 UN	500 UD	6,200 D	169,000 D	100 BD	3,400	10,300 D	19,500 D	120 U	1,300		6,900 D	762,000 DN	12 U	15,300 D	14,200	194 U	2,700 B	1,500 D	190 UD	4,100 B	2,600 U	49 U	660 D	
13 - 15	B39WT2												150 U														
	B39WT3	8,550,000 D	292 UN	470 UD	5,900 D	113,000 D	110 BD	1,500 BC	11,100 D	18,600 D	120 U	990 B		6,500 D	530,000 DN	10 U	16,200 D	12,000	194 U	3,200 B	1,400 D	190 UD	4,500 B	2,600 U	49 U	650 D	
61 - 63	B3DCF8																								307 UXH		
	B3DCF9												127 U														
	B3DCH0							2,320				534 B						9,120	1,070 U	2,030 UN			5,160				
	B3DCH1	5,340,000 DA	1,460 CA	470 UDA	3,900 DA	62,000 DA	56 DA			13,800 DA	11,200 DA	110 UNA		4,100 DA	255,000 DA	34 A	10,600 DA				440 BDA	74 UDA				3,400 DA	
	B38CH3																								307 UXH		
	B3DCH4													151 U													
	B3DCH5								2,600				518 B						10,500	1,090 U	2,060 UN			5,960			
B3DCH6	5,050,000 DA	1,460 CA	470 UDA	3,400 DA	55,200 DA	56 DA			11,500 DA	10,200 DA	110 UNA		3,700 DA	269,000 DA	34 A	82,00 DA				530 DA	75 UDA					3,100 DA	

Table 3-5. Nonradiological Contaminant Concentrations in Samples Collected from Borehole C9513

Sample Depth Interval (ft bgs)	Sample Number (HEIS #)	Al (µg/kg)	NH ₃ (µg/kg)	Sb (µg/kg)	As (µg/kg)	Ba (µg/kg)	Cd (µg/kg)	Cl ⁻ (µg/kg)	Cr (µg/kg)	Cu (µg/kg)	CN ⁻ (µg/kg)	F ⁻ (µg/kg)	Cr(VI) (µg/kg)	Pb (µg/kg)	Mn (µg/kg)	Hg (µg/kg)	Ni (µg/kg)	NO ₃ ⁻ (µg/kg)	NO ₂ ⁻ (µg/kg)	PO ₄ ³⁻ (µg/kg)	Se (µg/kg)	Ag (µg/kg)	SO ₄ ²⁻ (µg/kg)	Kerosene (µg/kg)	TBP (µg/kg)	U (µg/kg)
76 - 79	B3D3H8																								316 UXH	
	B3DCH9												129 U													
	B3DCJ0							4,210				1,250						23,800	1,140 B	2,080 UN			14,800			
	B3DCJ1	7,800,000 DA	1,580 CA	480 BDA	6,300 DA	91,700 DA	82 DA		17,100 DA	12,500 DA	120 UNA			5,500 DA	356,000 DA	10 UA	15,400 DA				610 DA	77 UDA				7,100 DA
90.5 - 92	B3DCJ3																								351 UXH	
	B3DCJ4												1,590													
	B3DCJ5							2,770				729 B						1,920 B	1,260 U	2,390 UN			3,870 B			
	B3DCJ6	10,800,000 D	2,550 C	870 BD	11,000 D	129,000 D	130 D		73,100 D	20,400 D	130 UN			13,200 D	510,000 D	13 U	16,600 D				1,300 D	76 BD				32,700 D
115.5 - 116.5	B3F941																								310 UXAH	
	B3F942												5,890													
	B3F943							1,650 BA				402 BA						1,510 UA	1,120 UA	2,130 UA			4,220 A			
	B3F944	7,130,000 DA	1,220 CA	500 UDA	4,900 DA	80,600 DA	89 BDA		39,900 DA	13,400 DA	120 UA			6,000 DA	349,000 DNA	11 UA	12,600 DA				800 UDA	190 UDA				7,000 DA
131.5 - 133.5	B3DCJ8																								318 UXH	
	B3DCJ9												6,090 D													
	B3DCK0							6,050				940 B						2,130 B	1,150 U	2,170 U			6,660			
	B3DCK1	13,100,000 D	1,700 C	500 UD	9,300 D	130,000 D	180 D		61,800 D	25,400 D	120 U			11,600 D	427,000 DN	11 U	25,300 D				1,300 DA	180 UD				36,800 D
146.1 - 148.8	B3DCK3																								344 UXH	
	B3DCK4												9,790 D													
	B3DCK5							3,760				375 U						1,790 B	1,200 U	2,260 U			10,200			
	B3DCK6	13,900,000 D	1,950 C	550 UD	7,100 D	153,000 D	160 D		84,700 D	28,500 D	130 U			14,300 D	555,000 DN	12 B	26,800 D				1,800 D	210 UD				1,100 D

Table 3-5. Nonradiological Contaminant Concentrations in Samples Collected from Borehole C9513

Sample Depth Interval (ft bgs)	Sample Number (HEIS #)	Al (µg/kg)	NH ₃ (µg/kg)	Sb (µg/kg)	As (µg/kg)	Ba (µg/kg)	Cd (µg/kg)	Cl ⁻ (µg/kg)	Cr (µg/kg)	Cu (µg/kg)	CN ⁻ (µg/kg)	F ⁻ (µg/kg)	Cr(VI) (µg/kg)	Pb (µg/kg)	Mn (µg/kg)	Hg (µg/kg)	Ni (µg/kg)	NO ₃ ⁻ (µg/kg)	NO ₂ ⁻ (µg/kg)	PO ₄ ³⁻ (µg/kg)	Se (µg/kg)	Ag (µg/kg)	SO ₄ ²⁻ (µg/kg)	Kerosene (µg/kg)	TBP (µg/kg)	U (µg/kg)	
171 - 175	B3DCK8																								332 UXH		
	B3DCK9												5,770														
	B3DCL0							6,660				872 B						1,630 U	1,210 U	2,290 U			5,320				
	B3DCL1	12,200,000 D	511 BC	500 UD	7,200 D	118,000 D	130 D		53,400 D	24,400 D	130 U			9,800 D	710,000 DN	12 U	24,400 D					1,400 D	190 UD				830 D
190.9 - 194.7	B3DCL3																									306 UXH	
	B3DCL4												1,150														
	B3DCL5							3,080				352 U						15,000	1,120 U	2,130 U				2,880 B			
	B3DCL6	6,460,000 D	1,110 C	490 UD	2,500 D	50,300 D	79 BD		17,600 D	12,700 D	110 U			4,400 D	425,000 DN	10 U	17,500 D					810 UD	190 UD				380 D
225 - 227	B3DCL8																									302 UXH	
	B3DCL9												160 U														
	B3DCM0							1,280 B				327 U						1,710 B	1,040 U	1,970 U				1,280 U			
	B3DCM1	4,690,000 D	535 BC	440 UD	1,600 BD	28,300 D	54 UD		10,400 D	11,500 D	110 U			3,000 D	222,000 DN	10 U	12,700 D					730 UD	170 UD				260 D
231.4 - 234.4	B3DCM3																									303 UXAH	
	B3DCM4												164 U														
	B3DCM5							2,570				344 U						1,750 B	1,100 U	2,080 U				1,580 B			
	B3DCM6	7,990,000 D	1,090 C	190 UD	980 UD	107,000 D	59 UD		17,500 D	17,700 D	110 U			3,400 D	496,000 DN	10 U	23,900 D					780 UD	180 UD				330 D

Note: Blank cells indicate no result for sample number.

bgs = below ground surface

Cr(VI) = hexavalent chromium

TBP = tributyl phosphate

HEIS = Hanford Environment Information System

Data qualifiers

A = discrepancy in chain-of-custody paperwork

B = analyte was detected at less than the quantitation limit but greater than the method detection limit

C = analyte was detected in both the sample and the quality control blank

D = analyte was reported at a secondary dilution factor

H = laboratory holding time exceeded before the sample was analyzed

N = spike and/or spike duplicate recovery is outside control limits

R = do not use; further review indicates the result is not valid

U = analyzed for but not detected

X = indicates a result-specific comment is provided in the data report or case narrative

This page intentionally left blank.

Table 3-6. Organic Contaminant Concentrations in Samples Collected from Borehole C9513

Sample Depth Interval (ft bgs)	Sample Number (HEIS #)	MIBK (µg/kg)	Polychlorinated Biphenyls								
			Aroclor-1016 (µg/kg)	Aroclor-1221 (µg/kg)	Aroclor-1232 (µg/kg)	Aroclor-1242 (µg/kg)	Aroclor-1248 (µg/kg)	Aroclor-1254 (µg/kg)	Aroclor-1260 (µg/kg)	Aroclor-1262 (µg/kg)	Aroclor-1268 (µg/kg)
0 - 2	B39WN3		10 U	10 U	10 U	10 U	10 U	8.6 U	8.6 U	8.6 U	8.6 U
	B39WN4	0.53 UT									
2 - 4	B39WN8		10 U	10 U	10 U	10 U	10 U	8.6 U	8.6 U	8.6 U	8.6 U
	B39WN9	0.53 UT									
4 - 6	B39WP3		10 U	10 U	10 U	10 U	10 U	8.4 U	8.4 U	8.4 U	8.4 U
	B39WP4	0.55 UT									
6 - 8	B39WP8		10 U	10 U	10 U	10 U	10 U	8.7 U	8.7 U	8.7 U	8.7 U
	B39WP9	0.53 UT									
8 - 10	B39WR3		10 U	10 U	10 U	10 U	10 U	8.5 U	8.5 U	8.5 U	8.5 U
	B39WR4	0.51 UT									
10 - 12	B39WR8		10 U	10 U	10 U	10 U	10 U	8.6 U	8.6 U	8.6 U	8.6 U
	B39WR9	0.5 UT									
12 - 15	B39WT3		10 U	10 U	10 U	10 U	10 U	8.6 U	8.6 U	8.6 U	8.6 U
	B39WT4	0.49 UT									

Table 3-6. Organic Contaminant Concentrations in Samples Collected from Borehole C9513

Sample Depth Interval (ft bgs)	Sample Number (HEIS #)	MIBK (µg/kg)	Polychlorinated Biphenyls								
			Aroclor-1016 (µg/kg)	Aroclor-1221 (µg/kg)	Aroclor-1232 (µg/kg)	Aroclor-1242 (µg/kg)	Aroclor-1248 (µg/kg)	Aroclor-1254 (µg/kg)	Aroclor-1260 (µg/kg)	Aroclor-1262 (µg/kg)	Aroclor-1268 (µg/kg)
45 - 47.5	B39WV1	62 T									
61 - 63	B3DCF8		3.41 U	3.41 U	3.41 U	3.41 U	3.41 U	3.41 U	3.41 U	3.41 U	3.41 U
	B3DCH3		3.43 U	3.43 U	3.43 U	3.43 U	3.43 U	3.43 U	3.43 U	3.43 U	3.43 U
75 - 80	B39WX1	23 T									
76 - 79	B3DCH8		3.54 U	3.54 U	3.54 U	3.54 U	3.54 U	3.54 U	3.54 U	3.54 U	3.54 U
90.5 - 92	B3DCJ3		3.93 U	3.93 U	3.93 U	3.93 U	3.93 U	3.93 U	3.93 U	3.93 U	3.93 U
95 - 100	B39WY2	220,000 D									
115.5 - 116.5	B3F941		3.5 UA	3.5 UA	3.5 UA	3.5 UA	3.5 UA	3.5 UA	3.5 UA	3.5 UA	3.5 UA
124.8 - 129.8	B39X19	96,000 DH									
131.5 - 133.5	B3DCJ8		3.56 U	3.56 U	3.56 U	3.56 U	3.56 U	3.56 U	3.56 U	3.56 U	3.56 U
140.5 - 145.5	B39X46	1,900,000 DH									
146.1 - 148.8	B3DCK3		3.85 U	3.85 U	3.85 U	3.85 U	3.85 U	3.85 U	3.85 U	3.85 U	3.85 U
154.9 - 159.9	B39X60	650,000 DTH									
170.5 - 175.5	B39X75	7,900 DT									

Table 3-6. Organic Contaminant Concentrations in Samples Collected from Borehole C9513

Sample Depth Interval (ft bgs)	Sample Number (HEIS #)	MIBK (µg/kg)	Polychlorinated Biphenyls								
			Aroclor-1016 (µg/kg)	Aroclor-1221 (µg/kg)	Aroclor-1232 (µg/kg)	Aroclor-1242 (µg/kg)	Aroclor-1248 (µg/kg)	Aroclor-1254 (µg/kg)	Aroclor-1260 (µg/kg)	Aroclor-1262 (µg/kg)	Aroclor-1268 (µg/kg)
171 - 175	B3DCK8		3.73 U	3.73 U	3.73 U	3.73 U	3.73 U	3.73 U	3.73 U	3.73 U	3.73 U
190.4 - 195.4	B39X86	16 T									
190.9 - 194.7	B3DCL3		3.44 U	3.44 U	3.44 U	3.44 U	3.44 U	3.44 U	3.44 U	3.44 U	3.44 U
214.9 - 219.9	B39XB4	0.65 U									
225 - 227	B3DCL8		3.42 U	3.42 U	3.42 U	3.42 U	3.42 U	3.42 U	3.42 U	3.42 U	3.42 U
231.4 - 234.4	B3DCM3		3.42 UA	3.42 UA	3.42 UA	3.42 UA	3.42 UA	3.42 UA	3.42 UA	3.42 UA	3.42 UA

Note: Blank cells indicate no result for sample number.

bgs = below ground surface

MIBK = methyl isobutyl ketone

HEIS = Hanford Environmental Information System

Data qualifiers

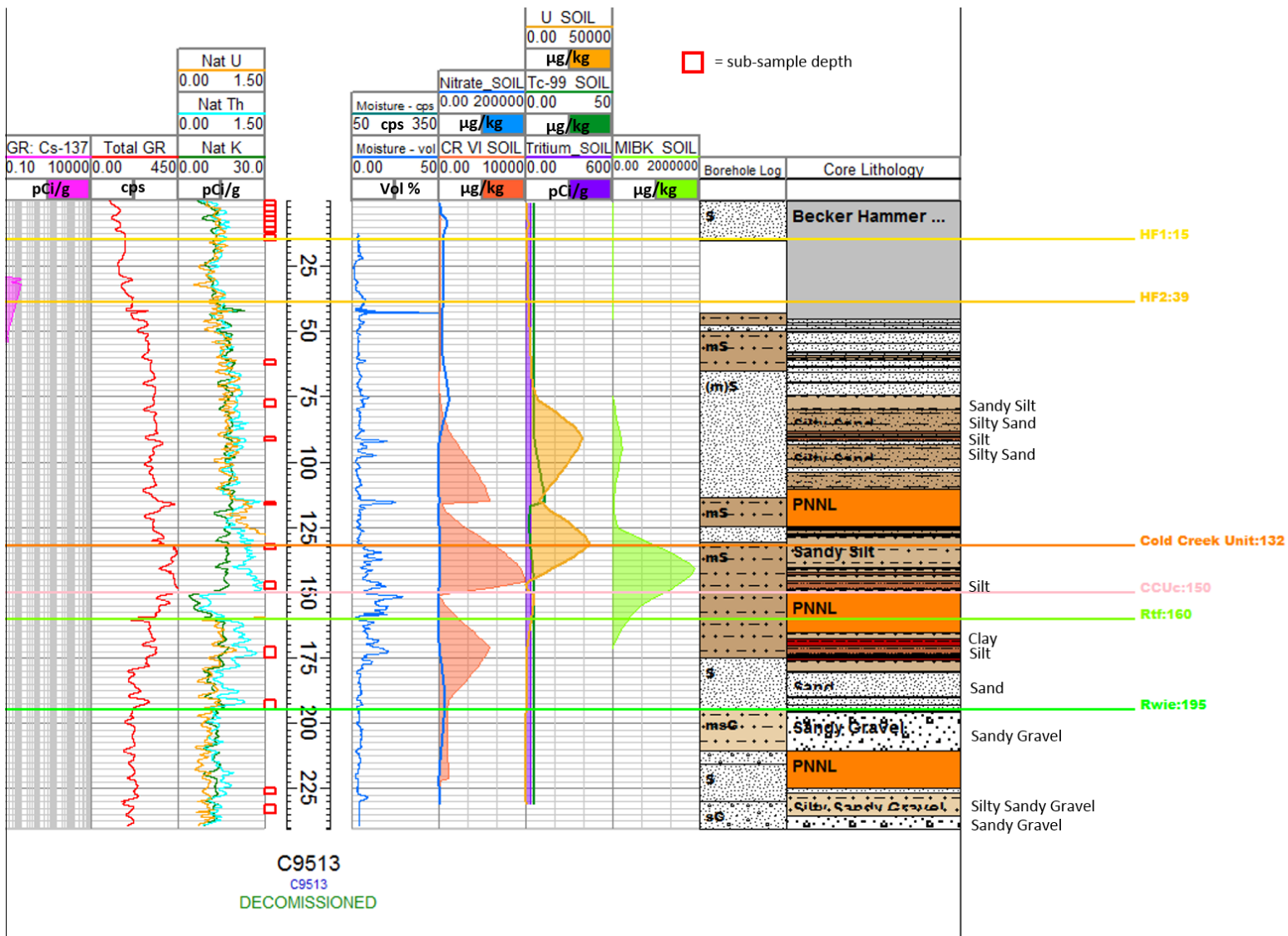
A = discrepancy in chain-of-custody paperwork

D = analyte was reported at a secondary dilution factor

H = laboratory holding time exceeded before the sample was analyzed

T = spike and/or spike duplicate recovery is outside control limits

U = analyzed for but not detected



Notes: The contaminant scale changes with each borehole. The ground surface elevation at borehole C9513 is 205.0 m (672.6 ft). Appendix C contains the complete borehole core log report and photographs.

Figure 3-6. Composite Log Profile for Borehole C9513

The contact with the Rtf is interpreted at 49 m (160 ft) bgs from the spectral gamma log response where the potassium, uranium, and thorium return to a standard siliciclastic signature (all three components roughly equal in proportion). The clay and silt content of the Rtf is high while the grain-size coarsens downward to the Rwie contact at 59 m (195 ft) bgs. The Rwie is dominated by sandy gravel to gravel with abundant silica cement. A 4.6 m (15 ft) thick interval (64 to 68.6 m [210 to 225 ft] bgs) of intact cores from the Rwie was sent to PNNL for analyses. The X-Ray microtomography images show that those cores are almost entirely sand, as displayed in Figure 3-7. The core from 69 to 70 m (225 to 230 ft) bgs has 0.6 m (2 ft) of the same sand at the top, indicating that the sand sequence is approximately 5 m (17 ft) thick. From 69 m (227 ft) bgs to TD of the borehole at 74 m (241 ft) bgs, the Rwie is felsic-dominated silty sandy gravel to sandy gravel.

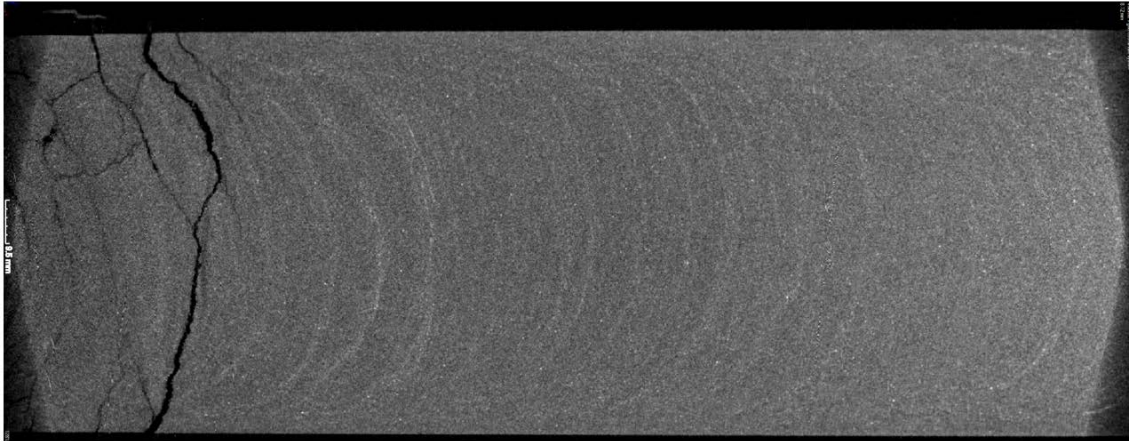


Figure 3-7. Microtomography Images of a Longitudinal Cross Section from Borehole C9513, 67.8 to 68.1 m (222.5 to 223.5 ft) bgs

3.3 Borehole C9514 at the 216-S-21 Crib

Borehole C9514 is located at the 216-S-21 Crib. The Becker Hammer rig pushed 8.625 in. diameter casing from ground surface to 13.4 m (44 ft) bgs and the sonic rig drilled 6 in. diameter casing to TD at 38.9 m (127.6 ft) bgs, as shown in Figure 3-8. Borehole C9514 was geophysically logged and final sample depths were selected, as shown in Figure 3-9. The sediment samples were analyzed for COPCs, as displayed in Tables 3-7 and 3-8, and the lithology was logged and plotted with mobile COPCs and borehole geophysics, as shown in Figure 3-10.

Sediment samples collected from approximately 14 m (45 ft) bgs to approximately 29 m (94 ft) bgs had elevated concentrations of nitrate that decreased with depth from 753,000 to 79,700 $\mu\text{g}/\text{kg}$. The hexavalent chromium concentration was also significantly high (14,200 $\mu\text{g}/\text{kg}$) at 14 m (45 ft) bgs, which was a high moisture silt layer in the Hf2. The highest concentration of technetium-99 (194 pCi/g) was found in the silt layer at approximately 14 m (45 ft) bgs; concentrations decreased with depth to 67.9 pCi/g at 24 m (79 ft) bgs. Tritium was present in sediment samples throughout the vadose zone deeper than 2.9 m (9.5 ft) bgs. The highest tritium concentration (208 pCi/g) was also found in the silt layer at 14 m (45 ft) bgs; concentrations decreased to 15.5 pCi/g at 21 m (68 ft) bgs, increased to an average of 155 pCi/g at 29 m (94 ft) bgs, and decreased again to 17.2 pCi/g at the bottom of the borehole (approximately 38 m [124 ft] bgs). Borehole geophysical logs show cesium-137 contamination from approximately 4.6 m (15 ft) bgs to approximately 18 m (60 ft) bgs.

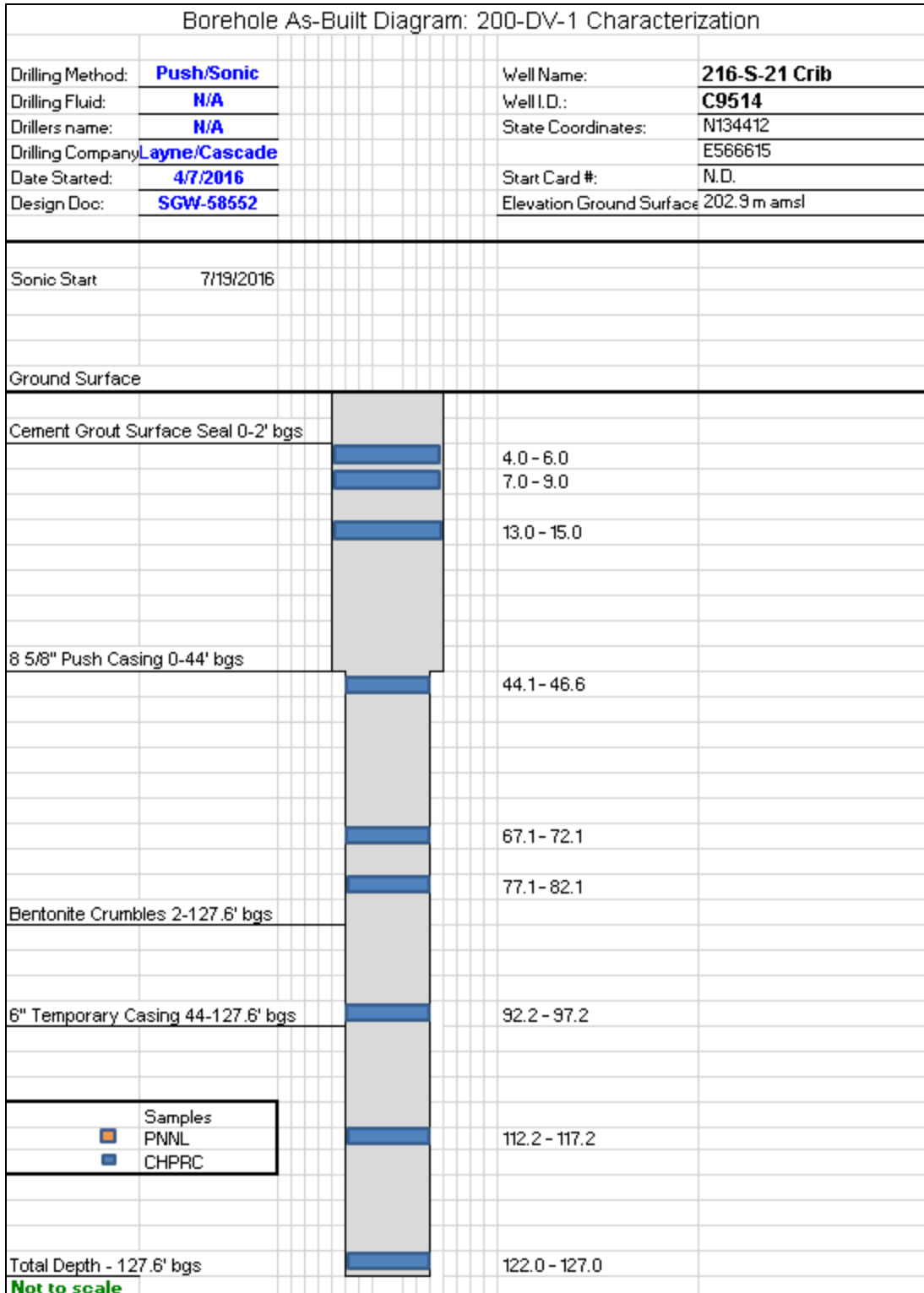
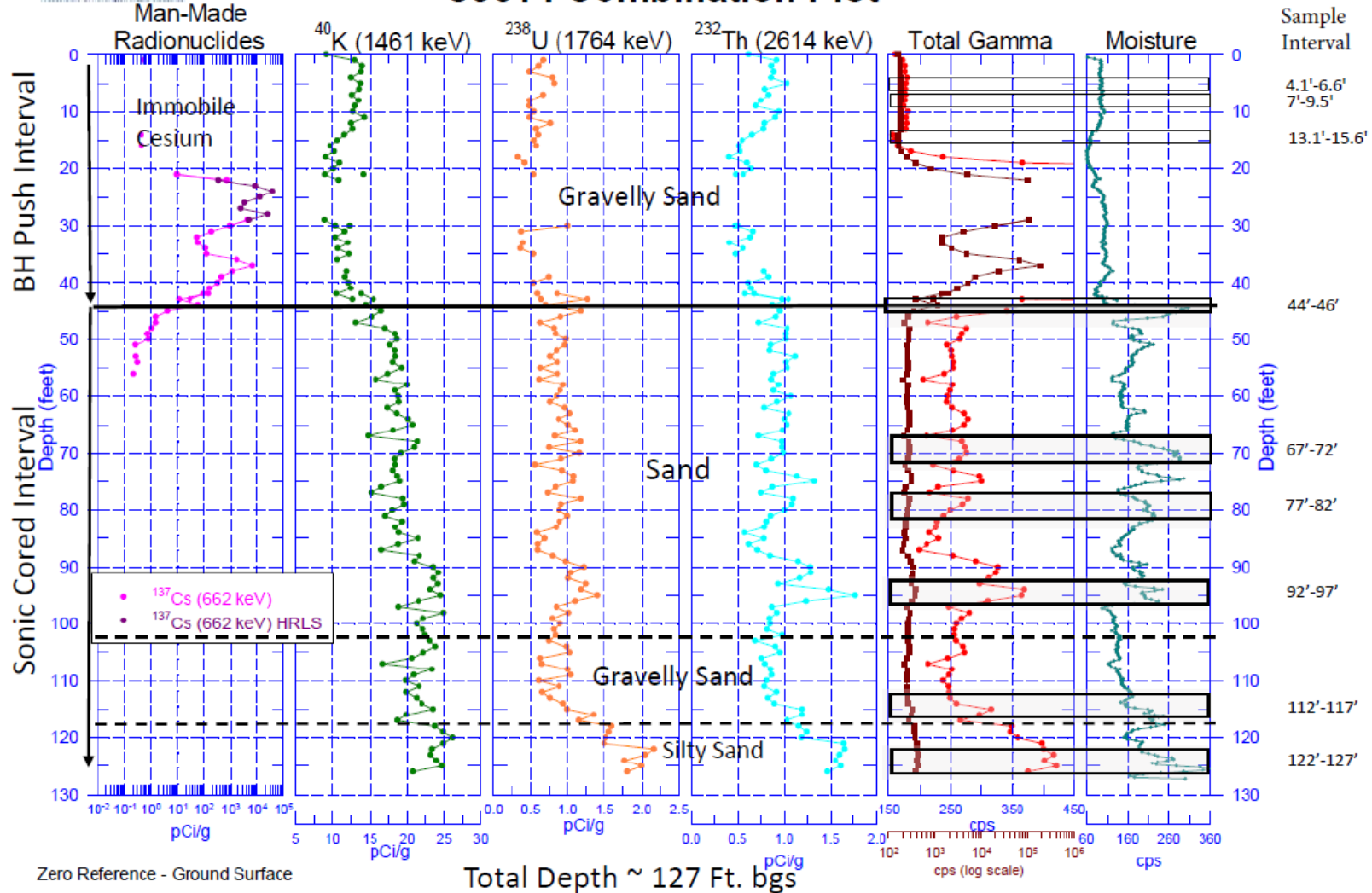


Figure 3-8. As-Built Diagram for Borehole C9514



Stoller Newport News Nuclear
A Subsidiary of Hamilton Infratec Industries

C9514 Combination Plot



Note: Appendix B contains the complete geophysical log report.

Figure 3-9. Geophysical Log and Sample Depths for Borehole C9514

This page intentionally left blank.

Table 3-7. Radiological Contaminant Concentrations in Samples Collected from Borehole C9514

Sample Interval (ft bgs)	Sample Number (HEIS #)	Am-241 (pCi/g)	C-14 (pCi/g)	Cs-137 (pCi/g)	Co-60 (pCi/g)	Eu-152 (pCi/g)	Eu-154 (pCi/g)	Eu-155 (pCi/g)	I-129 (pCi/g)	Np-237 (pCi/g)	Ni-63 (pCi/g)	Pu-238 (pCi/g)	Pu-239/240 (pCi/g)	Sr-90 (pCi/g)	Tc-99 (pCi/g)	H-3 (pCi/g)	U-233/234 (pCi/g)	U-235 (pCi/g)	U-238 (pCi/g)
4.1 - 6.6	B33XP6	0.0833 U	0.343 U	0.0392	0.0194 U	0.0399 U	0.0694 U	0.0384 U		0.0476 U	6.57 U	0.05771 U	0.0624 U	0.21 U	0.577 U	0.423 U		0.0495 U	0.484
7.0 - 9.5	B33XP7	0.0646 U	0.34 U	0.0229 U	0.0208 U	0.0624 U	0.0654 U	0.0762 U		0.0359 U	6.27 U	0.0576 U	0.0481 U	0.187 U	0.586 U	0.564 U		0.053 U	0.187
13.1 - 15.6	B33XR0	0.0487 U	0.348 U	0.11	0.0214 U	0.0638 U	0.0686 U	0.0799 U	0.0881 U	0.0284 U	6.53 U	0.074 U	0.0758 U	0.203 U	0.5815 U	12.7		0.0515 U	0.548
44.6 - 45.6	B36M84	0.102 U	0.629	0.428	0.0441	0.031 U	0.0398 U	0.041 U	0.117	0.0659 U	7.78	0.0613 U	0.0557 U	16.6	194	208	0.179	0.0416 U	0.181
67.8 - 69.5	B36M86	0.123 U	0.477 U	0.013 U	0.0124 U	0.0357 U	0.0407 U	0.0468 U	0.112 U	0.0671 U	7.07 U	0.0613 U	0.052 U	7.62	147	15.5	0.152	0.0351 U	0.218
78.3 - 79.8	B36M88	0.103 U	0.465 U	0.0108 U	0.0126 U	0.0238 U	0.0381 U	0.0231 U	0.0855 U	0.0396 U	6.28 U	0.0534 U	0.0443 U	0.28 U	67.9	103	0.224	0.0425 U	0.255
93.7 - 95.7	B36M90	0.136 U	0.471 U	0.0121 U	0.0137 U	0.0271 U	0.0467 U	0.0258 U	0.0966 U	0.0746 U	7.43 U	0.0744 U	0.0533 U	0.339 U	1.07 U	170	0.312	0.0442 U	0.349
	B36M92	0.135 U	0.473 U	0.0103 U	0.012 U	0.0225 U	0.0388 U	0.0203 U	0.0813 U	0.0593 U	7.5 U	0.073 U	0.0663 U	0.216 U	-974 U	142	0.177	0.0409 U	0.211
114.8 - 115-8	B36M94	0.194 U	0.263 U	0.0122 U	0.0143 U	0.0275 U	0.0442 U	0.0268 U	0.0902 U	0.0448 U	6.82 U	0.0834 U	0.0709 U	0.224 U	0.867 U	12.8	0.375	0.0536 U	0.318
123.5 - 125	B36M96	0.0907 U	0.26 U	0.0133 U	0.0143 U	0.0294 U	0.0468 U	0.0282 U	0.112 U	0.0356 U	7.23 U	0.0578 U	0.0777 U	0.232 U	2.67	17.2	0.182	0.0553 U	0.21

Notes: Blank cells indicate no result for sample number.
 Undetected radionuclide value reported is the minimum detectable concentration.
 bgs = below ground surface
 HEIS = Hanford Environmental Information System
Data qualifier:
 U = analyzed for but not detected above limiting criteria

Table 3-8. Nonradiological Contaminant Concentrations Collected from C9514

Sample Intervals (ft bgs)	Sample Number (HEIS #)	Al (µg/kg)	NH ₃ (µg/kg)	Sb (µg/kg)	As (µg/kg)	Ba (µg/kg)	Cd (µg/kg)	Cl ⁻ (µg/kg)	Cr (µg/kg)	Cu (µg/kg)	CN ⁻	F ⁻ (µg/kg)	Cr(VI) (µg/kg)	Pb (µg/kg)	Mn (µg/kg)	Hg (µg/kg)	Ni (µg/kg)	NO ₃ ⁻ (µg/kg)	NO ₂ ⁻ (µg/kg)	PO ₄ ³⁻ (µg/kg)	Se (µg/kg)	Ag (µg/kg)	SO ₄ ²⁻ (µg/kg)	Kerosene (µg/kg)	TBP (µg/kg)	U (µg/kg)	
4.1 - 6.6	B33XP0							1,800 B				880 B						34,100	256 BN	1,500 B			4,600 B				
	B33XP4	7,130,000 D		340 UN	4,500 BD	90,100 D	110 BD		8,400 D	14,500 D	130 U			5,600 D		12 U	11,000 D				1,400 BD	200 BD		380 U	52 U	450 BD	
7.0 - 9.5	B33XP1							3,400				780 B						33,200	223 UN	1,600 B			5,500 B				
	B33XP5	10,200,000 D		340 UN	6,000 D	119,000 D	120 BD		14,200 D	20,600 D	120 U			7,200 D		11 U	16,400 D				1,900 BD	200 BD		360 U	50 U	600 D	
13.1 - 15.6	B33XP2							4,000				760 B						48,700	194 UN	2,200 B			19,000				
	B33XP8	8,950,000 D	827 N	320 UN	5,500 D	101,000 D	100 BD		10,900 D	16,600 D	120 U			6,800 D		2,200 D	13,100 D				1,700 BD	120 U		360 U	49 U	1,100 D	
	B33XR0												240 B														
44.6 - 45.6	B36M84							29,000				550	14,200					753,000 D	755 B	1,230 U			9,600				
	B36M85	12,200,000 D	1,220 N	400 BD	6,600 D	216,000 DN	140 D		35,900 D	21,600 D	130 U			7,000 D	853,000 D	12 U	17,300 D				2,600 D	110 BD		380 U	53 U	790 D	
67.8 - 69.5	B36M86							2,800				390 B	230 B					292,000 D	5,910	1,260 U			3,000				
	B36M87	9,080,000 D	693 N	190 BD	4,200 D	96,200 D	65 BD		14,300 D	14,700 D	120 U			4,700 D	502,000 D	11 B	13,400 D				1,300 D	57 UD		350 U	48 U	480 D	
78.3 - 79.8	B36M88							2,400				920	150 U					226,000 D	1,450	24,800 UD			1,900 B				
	B36M89	12,400,000 D	3,650 N	370 BD	5,700 D	140,000 D	100 BD		19,400 D	18,000 D	120 U			6,000 D	551,000 D	13 B	18,600 D				900 BD	85 BD		360 U	49 U	660 D	
93.7 - 95.7	B36M90							1,400 B				970	150 U					111,000	624 U	1,720 B			2,500				
	B36M91	8,370,000 D	839 N	340 BD	6,700 D	83,600 D	89 BD		11,600 D	14,000 D	120 U			8,000 D	394,000 D	12 B	10,800 D				780 BD	63 BD		350 U	49 U	580 D	
	B36M92							2,000				600	150 U					79,700	624 U	1,630 B			2,000 B				
	B36M93	11,100,000 D	1,190 N	430 BD	10,200 D	122,000 D	110 BD		16,900 D	19,600 D	120 U			10,400 D	558,000 D	12 B	15,900 D				1,200 D	67 BD		360 U	49 U	730 D	
114.8 - 115.8	B36M94							11,000				570	150 U					1,550	624 U	1,590 B			2,700				
	B36M95	10,500,000 D	1,130 N	490 BD	7,700 D	97,300 DN	120 BD		17,000 D	17,700 D	120 U			7,400 D	376,000 D	12 U	17,800 D				1,600 D	65 BD		360 U	49 U	760 D	

Table 3-8. Nonradiological Contaminant Concentrations Collected from C9514

Sample Intervals (ft bgs)	Sample Number (HEIS #)	Al (µg/kg)	NH ₃ (µg/kg)	Sb (µg/kg)	As (µg/kg)	Ba (µg/kg)	Cd (µg/kg)	Cl ⁻ (µg/kg)	Cr (µg/kg)	Cu (µg/kg)	CN ⁻	F ⁻ (µg/kg)	Cr(VI) (µg/kg)	Pb (µg/kg)	Mn (µg/kg)	Hg (µg/kg)	Ni (µg/kg)	NO ₃ ⁻ (µg/kg)	NO ₂ ⁻ (µg/kg)	PO ₄ ³⁻ (µg/kg)	Se (µg/kg)	Ag (µg/kg)	SO ₄ ²⁻ (µg/kg)	Kerosene (µg/kg)	TBP (µg/kg)	U (µg/kg)	
123.5 - 125	B36M96							1,700 B				670	150 U					18,100	624 U	1,960 B			2,500				
	B36M97	10,000,000 D	1,340 N	420 BD	5,500 D	96,000 D	180 D		16,800 D	16,900 D	120 U			7,900 D	317,000 D	12 U	19,000 D				1,500 D	95 BD		360 U	50 U	790 D	

Note: Blank cells indicate no result for sample number.

bgs = below ground surface

Cr(VI) = hexavalent chromium

HEIS = Hanford Environmental Information System

TBP = tributyl phosphate

Data qualifiers

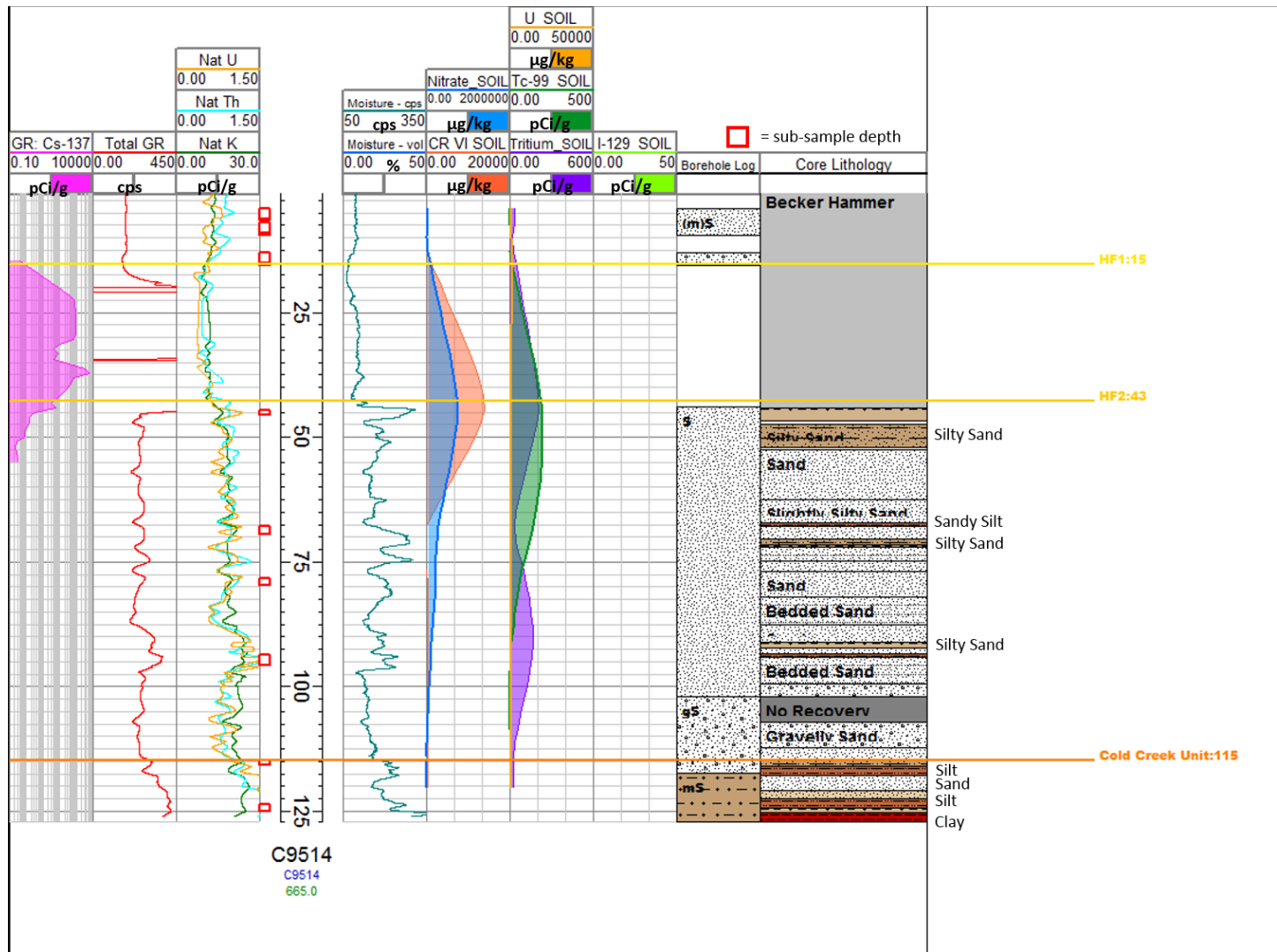
B = the analyte was detected at a value less than the contract required detection limit but greater than or equal to the instrument detection limit/method detection limit (as appropriate)

D = analyte was identified in an analysis at a secondary dilution factor

N = spike sample recovery is outside control limits

U = analyzed for but not detected above limiting criteria

This page intentionally left blank.



Notes: The contaminant scale changes with each borehole. The ground surface elevation at borehole C9514 is 202.7 m (665.0 ft). Appendix C contains the complete borehole core log report and photographs.

Figure 3-10. Composite Log Profile for Borehole C9514

The change from crib fill material to the gravel dominated Hf1 is estimated at 4.6 m (15 ft) bgs where geophysical logs indicate cesium-137 contamination begins. The top of the Hf2 is estimated at 13 m (43 ft) bgs where the character of the neutron moisture log changes. The Hf2 consists mostly of sand, slightly silty sand, and silty sand with distinct 3 to 5 cm thick fining upwards bedding sequences. There are three thin silt beds at 13.4 to 14.2, 20.5 to 20.7, and 28.5 to 28.7 m (44.1 to 46.6, 67.1 to 67.8, and 93.5 to 94.1 ft) bgs within the Hf2. The gravel content increases slightly with depth, up to 15% to 25% subrounded to rounded pebble-sized gravels. At 35 m (115 ft) bgs there is a well-defined contact between the Hf2 above and the CCU below. The contact is several centimeters thick, very fine-grained with dark wood fragments and abundant iron-staining. Below the contact the CCU persists to TD of the borehole at 38.9 m (127.6 ft) bgs and is 100% silt, moist, nonplastic with sharp cross-bedded lamination structures, occasionally interbedded with very-fine, iron-stained sand.

4 Conclusions

Characterization boreholes C9512, C9513, and C9514 were drilled in the S Complex Area during FYs 2016 and 2017 as part of the 200-DV-1 OU remedial investigation. The purpose of this characterization was to identify the nature and extent of the contamination in the vadose zone at three 200-DV-1 OU waste sites in the S Complex Area. A phased approach was used to drill these boreholes to prevent worker exposure to contaminated soil cuttings from a zone of high radiological contamination that exists beneath most of the waste sites (approximately 4.6 to 15 m [15 to 50 ft] bgs). A Becker Hammer rig was used for the first phase of drilling to push casing through the zone of high radiological contamination. During the second phase of drilling, a sonic rig was used to drill from the bottom of the high radiological contamination zone to TD. Sediment samples were collected in the shallow vadose zone above 4.6 m (15 ft) bgs using split-spoon samplers and sleeves, and from the vadose zone below 15 m (50 ft) bgs using continuous core. The sediment samples were analyzed for contaminants of potential concern in accordance with the SAP (DOE/RL-2011-104) and SAP addenda (DOE/RL-2011-104-ADD1 and DOE/RL-2011-104-ADD2). Additionally, the cores were logged for geophysics and lithology. These data will be integrated with other supporting information (e.g., hydraulic properties) as part of the evaluation and update of the CSM supporting DOE/RL-2011-102, *Remedial Investigation/Feasibility Study and RCRA Facility Investigation/Corrective Measures Study Work Plan for the 200-DV-1 Operable Unit*.

PNNL-26208, *Contaminant Attenuation and Transport Characterization of 200-DV-1 Operable Unit Sediment Samples*, identifies and evaluates attenuation processes and other factors that affect transport of contaminants present in vadose samples from the Hanford Site. PNNL characterized two depth intervals in borehole C9512 (216-S-9 Crib). Appendix D contains the report. Core samples from three depth intervals in borehole C9513 (216-S-13 Crib), which was drilled in FY 2017, were provided to PNNL for geochemical and physical characterization. The results are available in two PNNL reports issued in FY 2018: PNNL-27524, *Contaminant Attenuation and Transport Characterization of 200-DV-1 Operable Unit Sediment Samples from Boreholes C9497, C9498, C9603, C9488, and C9513*, and PNNL-27846, *Physical and Hydraulic Properties of Sediments from the 200-DV-1 Operable Unit*.

The following lessons were learned during the implementation of the 200-DV-1 OU characterization project:

- Intact soil cores are critical to capturing vadose zone heterogeneities, ground-truthing geophysical logs, and reducing uncertainties in the nature and extent of contamination. Continuous intact cores provide the sample material and flexibility needed to perform multiple phases of complex analyses and address characterization data gaps.
- The focus of characterization should be establishing the nature, extent, fate, and transport of contaminants. Therefore, a tiered/staged approach should be employed when determining whether advanced analyses, such as contaminant leachability, should be pursued. In general, as the tier level increases so does the level of sophistication in data collection.
 - Tier 1 analyses define nature and extent of contamination by characterizing sediment and pore water chemistry. The sample depths are selected based on specifications described in Section 2.2 of this report. Aliquots from each sample depth are saved. Determinations of whether the stored aliquots should proceed to tier 2 or 3 analyses should be made by an integrated multi-disciplinary project team.
 - Tier 2 analyses investigate contaminant mobility (leaching) and are performed with consideration of the geochemical and contaminant analysis of sediment and pore water.

- Tier 3 analyses fill any data gaps (i.e., hydraulic properties, isotopic analyses, and microbial studies).

The preliminary observations detailed in Chapter 3 were evaluated against data needs identified in Table 4-1 from DOE/RL-2011-102.

- **216-S-9 Crib.** The new characterization data from borehole C9512 aligned with the CSM that the 216-S-9 Crib has likely impacted groundwater in the past; iodine-129 was detected at low concentrations in the two deepest samples, just above and within the CCUz. It appears that tritium may have migrated from the crib as concentrations increased with depth to the CCUz. Nearly 49.5 million L (13.1 million gal) of waste containing 1,170 Ci of tritium was disposed to the crib during operations. An updated CSM report will evaluate whether these contaminants (iodine-129 and tritium) will infiltrate to groundwater beneath the CCU.
- **216-S-13 Crib.** The new characterization data from borehole C9513 at the 216-S-13 Crib, which received only 4.9 million L (1.3 million gal) of waste, identified significant concentrations of residual hexavalent chromium, MIBK, uranium, and technetium-99 in the vadose zone. Uranium and technetium-99 were only detected in sediments above the CCUc, indicating these mobile contaminants have not yet reached the groundwater. Hexavalent chromium and MIBK have both migrated through the CCUc and into the Rtf. An updated CSM report will evaluate whether these contaminants will infiltrate to groundwater beneath the Rwie.
- **216-S-21 Crib.** The new characterization data from borehole C9514 at the 216-S-21 identified significant concentrations of nitrate, hexavalent chromium, technetium-99, and tritium in a silt bed at approximately 13.7 m (45 ft) bgs. Concentration of all contaminants except tritium decrease with depth indicating these mobile contaminants have not yet reached the groundwater. Tritium concentrations vary throughout the borehole but decrease at and below the CCU. Approximately 87 million L (23 million gal) of waste containing 2,540 Ci of tritium was disposed to the crib. Further evaluation of the impacts of disposal at the 216-S-21 Crib will be evaluated in the updated CSM report.

The S Complex Area characterization data from this field summary report will be interpreted to accomplish the following tasks:

- Refine the CSM for each waste site.
- Create a detailed three-dimensional geologic model and map of the S Complex Area with a focus on the vertical heterogeneity observed in the continuous coring.
- Estimate key parameters (hydraulic properties, recharge rates, contaminant mass distribution, desorption distribution coefficient values, etc.) for the fate and transport model.
- Evaluate published literature related to S Complex Area fate and transport studies to build a comprehensive CSM.

The CSM resulting from these tasks will be updated and provided in a separate report.

5 References

- DOE/RL-2002-39, 2002, *Standardized Stratigraphic Nomenclature for Post-Ringold-Formation Sediments Within the Central Pasco Basin*, Rev. 0, U.S. Department of Energy, Richland Operations Office, Richland, Washington. Available at: <https://pdw.hanford.gov/document/0081471H>.
- CP-49279, 2011, *Central Plateau Waste Site Dimensions*, Rev. 0, CH2M HILL Plateau Remediation Company, Richland, Washington. <https://pdw.hanford.gov/document/AR-03298>.
- DOE/RL-2007-02-VOLII-ADD3, 2008, *Site-Specific Field-Sampling Plans for the 216-B-42 Trench, 216-S-13 Crib, 216-S-21 Crib, 216-T-18 Crib and 216-T-19 Crib and Tile Field in the 200-TW-1/200-PW-5 Operable Units*, Rev. 0, U.S. Department of Energy, Richland Operations Office, Richland, Washington. Available at: <http://pdw.hanford.gov/arpir/index.cfm/viewDoc?accession=0807090163>.
- DOE/RL-2010-89, 2010, *Long-Range Deep Vadose Zone Program Plan*, Rev. 0, U.S. Department of Energy, Richland Operations Office, Richland, Washington. Available at: <http://pdw.hanford.gov/arpir/index.cfm/viewDoc?accession=0084131>.
- DOE/RL-2011-102, 2016, *Remedial Investigation/Feasibility Study and RCRA Facility Investigation/Corrective Measures Study Work Plan for the 200-DV-1 Operable Unit*, Rev. 0, U.S. Department of Energy, Richland Operations Office, Richland, Washington. Available at: <http://pdw.hanford.gov/arpir/index.cfm/viewDoc?accession=0075538H>.
- DOE/RL-2011-104, 2012, *Characterization Sampling and Analysis Plan for the 200-DV-1 Operable Unit*, Rev. 0, U.S. Department of Energy, Richland Operations Office, Richland, Washington. Available at: <http://pdw.hanford.gov/arpir/index.cfm/viewDoc?accession=1202020261>.
- DOE/RL-2011-104-ADD1, 2017, *Characterization Sampling and Analysis Plan for the 200-DV-1 Operable Unit Addendum 1: Attenuation Process Characterization*, Rev. 0, U.S. Department of Energy, Richland Operations Office, Richland, Washington. Available at: <http://pdw.hanford.gov/arpir/index.cfm/viewDoc?accession=0071507H>.
- DOE/RL-2011-104-ADD2, 2017, *Characterization Sampling and Analysis Plan for the 200-DV-1 Operable Unit Addendum 2: Supplemental Shallow Soil Risk Characterization Sampling*, Rev. 0, U.S. Department of Energy, Richland Operations Office, Richland, Washington. Available at: <http://pdw.hanford.gov/arpir/index.cfm/viewDoc?accession=0071506H>.
- DOE/RL-2012-20, 2015, *Waste Control Plan for the 200-DV-1 Operable Unit*, Rev. 0, U.S. Department of Energy, Richland Operations Office, Richland, Washington. Available at: <http://pdw.hanford.gov/arpir/index.cfm/viewDoc?accession=1506301062>.
- PNNL-26208, 2017, *Contaminant Attenuation and Transport Characterization of 200-DV-1 Operable Unit Sediment Samples*, RPT-DVZ-AFRI-037, Pacific Northwest National Laboratory, Richland, Washington. Available at: <https://pdw.hanford.gov/arpir/index.cfm/viewDoc?accession=0069250H>.
- PNNL-27524, 2018, *Contaminant Attenuation and Transport Characterization of 200-DV-1 Operable Unit Sediment Samples from Boreholes C9497, C9498, C9603, C9488, and C9513*, RPT-DVZ-CHPRC-0004, Rev 0.0, Pacific Northwest National Laboratory, Richland, Washington. Available at: <https://www.osti.gov/biblio/1468977>.

PNNL-27846, 2018, *Physical and Hydraulic Properties of Sediments from the 200-DV-1 Operable Unit*, RPT-DVZ-CHPRC 0005, Rev 0, Pacific Northwest National Laboratory, Richland, Washington. Available at: <https://www.osti.gov/biblio/1468972>.

RPP-26744, 2005, *Hanford Soil Inventory Model, Rev. 1*, Rev. 0, Washington. CH2M HILL Hanford Group, Inc., Richland, Washington. Available at: <http://pdw.hanford.gov/arpir/index.cfm/viewDoc?accession=0081114H>.

SGW-58552, 2015, *Description of Work for the Characterization 200-DV-1 Operable Unit, FY2015*, Rev. 2, CH2M HILL Plateau Remediation Company, Richland, Washington. Available at: <https://pdw.hanford.gov/arpir/index.cfm/viewDoc?accession=0073390H>.

Appendix A
Borehole Drilling Summaries

This page intentionally left blank.

Tables

Table A-1. Borehole C9512 (216-S-9 Crib)	A-1
Table A-2. Borehole C9513 (216-S-13 Crib).....	A-4
Table A-3. Borehole C9514 (216-S-21 Crib).....	A-8

This page intentionally left blank.

Table A-1. Borehole C9512 (216-S-9 Crib)

Date	Depth Interval (ft bgs)	Recovery %	IR LEXAN Temperature	IR Drill Shoe Temperature (°Fahrenheit)	Irreversible Temperature Label	HEIS #
Becker Hammer						
11/24/2015	3.2 - 5.5	60	-	-	-	B33XT8, B33XV3, B33XT3
11/24/2015	6.0 - 8.2	30	-	-	-	B33XT4, B33XT9, B33XV4
11/24/2015	13.0 - 15.3	100	-	-	-	B33XR7, B33XT5, B33XV0, B33XV5, B33XT0
Sonic						
7/25/2016	35.5 - 37.0	100	35.5 ft bgs = 75 37.0 ft bgs = 94	127	-	B36159
7/25/2016	37.0 - 42.0	100	37.0 ft bgs = 98 39.5 ft bgs = 88 42.0 ft bgs = 114	110	-	B36161
7/25/2016	42.2 - 47.2	100	42.2 ft bgs = 93 44.7 ft bgs = 86 47.2 ft bgs = 131	110	-	B36163
7/25/2016	47.2 - 52.2	88	47.2 ft bgs = 125 49.7 ft bgs = 145 52.2 ft bgs = 124	283	-	B36165
7/25/2016	52.4 - 57.4	100	52.4 ft bgs = 115 54.9 ft bgs = 107 57.4 ft bgs = 141	128	-	B36167
7/25/2016	57.5 - 62.5	100	57.5 ft bgs = 88 60.0 ft bgs = 87 62.5 ft bgs = 95	118	-	B36169
7/26/2016	62.2 - 63.2	100	80	-	84	B36173
7/26/2016	63.2 - 64.2	100	81	-	84	B36175
7/26/2016	64.2 - 65.2	100	82	-	99	B36177
7/26/2016	65.2 - 66.2	100	83	-	84	B36179
7/26/2016	66.2 - 67.2	100	89	95	104	B36181
7/26/2016	67.2 - 68.2	100	86	-	93	B36183
7/26/2016	68.2 - 69.2	100	87	-	99	B36185
7/26/2016	69.2 - 70.2	100	93	-	115	B36187
7/26/2016	70.2 - 71.2	100	92	-	104	B36189

Table A-1. Borehole C9512 (216-S-9 Crib)

Date	Depth Interval (ft bgs)	Recovery %	IR LEXAN Temperature	IR Drill Shoe Temperature (°Fahrenheit)	Irreversible Temperature Label		HEIS #
7/26/2016	71.2 – 72.2	100	102	95	108		B36191
7/26/2016	72.3 – 73.3	100	76	-	93		B36193
7/26/2016	73.3 – 74.3	100	80	-	84		B36195
7/26/2016	74.3 – 75.3	100	81	-	84		B36197
7/26/2016	75.3 – 76.3	100	82	-	84		B36199
7/26/2016	76.3 – 77.3	100	91	109	115		B361B1
7/26/2016	76.9 – 81.9	100	76.9 ft bgs = 126 79.4 ft bgs = 100 81.9 ft bgs = 124	115	-		B361B3
7/26/2016	82.9 – 87.9	100	82.9 ft bgs = 98 85.4 ft bgs = 89 87.9 ft bgs = 113	100	-		B361B5
7/26/2016	87.0 – 92.0	100	87.0 ft bgs = 98 89.5 ft bgs = 98 92.0 ft bgs = 139	100	-		B361B7
7/26/2016	92.5 – 97.5	100	92.5 ft bgs = 96 95.0 ft bgs = 90 97.5 ft bgs = 104	101	-		B361B9
7/27/2016	97.0 – 102.0	100	97.0 ft bgs = 77 99.5 ft bgs = 78 102.0 ft bgs = 94	136	-		B361C1
7/27/2016	102.6 – 107.6	100	102.6 ft bgs = 89 105.1 ft bgs = 85 107.6 ft bgs = 113	103	-		B361C3
7/27/2016	107.0 – 112.0	100	107.0 ft bgs = 85 109.5 ft bgs = 77 112.0 ft bgs = 89	99	-		B361C5
7/27/2016	112.0 – 117.0	100	112.0 ft bgs = 104 114.5 ft bgs = 86 117.0 ft bgs = 89	105	-		B361C7
7/27/2016	117.0 – 118.0	100	127	-	144		B361C9
7/27/2016	118.0 – 119.0	100	130	-	160		B361D1

Table A-1. Borehole C9512 (216-S-9 Crib)

Date	Depth Interval (ft bgs)	Recovery %	IR LEXAN Temperature	IR Drill Shoe Temperature (°Fahrenheit)	Irreversible Temperature Label		HEIS #
7/27/2016	119.0 – 120.0	100	135	-	Unreadable		B361D3
7/27/2016	120.0 – 121.0	100	124	-	160		B361D5
7/27/2016	121.0 – 122.0	100	122	109	199		B361D7
7/27/2016	122.0 – 123.0	100	96	-	129		B361D9
7/27/2016	123.0 – 124.0	100	83	-	115		B361F1
7/27/2016	124.0 – 125.0	100	90	-	120		B361F3
7/27/2016	125.0 – 126.0	100	90	-	129		B361F5
7/27/2016	126.0 – 127.0	100	119	105	129		B361F7
7/27/2016	127.2 – 132.2	100	127.2 ft bgs = 105 129.7 ft bgs = 108 132.2 ft bgs = 119	122	-		B361F9
7/27/2016	132.0 – 137.0	100	132.0 ft bgs = 95 134.5 ft bgs = 95 137.0 ft bgs = 111	106	-		B361H1
7/27/2016	137.0 – 142.0	100	137.0 ft bgs = 99 139.5 ft bgs = 107 142.0 ft bgs = 110	108	-		B361H3

Notes:

bgs = below ground surface

HEIS = Hanford Environmental Information System

IR = Infrared

Table A-2. Borehole C9513 (216-S-13 Crib)

Date	Sample Depth (ft bgs)	Sample Method	IR LEXAN Temperature (°F)	Recovery %	HEIS number
7/10/2017	0.0 – 2.0	Grab	N/A	100	B39WN3, B39WN4, B39WN2
7/10/2017	2.0 – 4.0		N/A	100	B39WN8, B39WN9, B39WN7
7/10/2017	4.0 – 6.0		N/A	100	B39WP3, B39WP4, B39WP2
7/10/2017	6.0 – 8.0		N/A	100	B39WP8, B39WP9, B39WP7
7/10/2017	8.0 – 10.0		N/A	100	B39WR3, B39WR4, B39WR2
5/18/2017	10.0 – 12.0		N/A	100	B39WR8, B39WR9, B39WR7
5/18/2017	12.0 – 15.0		N/A	100	B39WT3, B39WT4, B39WT2
7/10/2017	45.0 – 47.5	LEXAN™ liner Core	45.0 ft bgs = 87 46.3 ft bgs = 89 47.5 ft bgs = 149	100	B39WV0, B39WV1, B39WV2
7/10/2017	47.5 – 50.0		47.5 ft bgs = 84 48.8 ft bgs = N/A 50.0 ft bgs = 92	50	B39WV4
7/10/2017	50.0 – 55.0		50.0 ft bgs = 104 52.5 ft bgs = 109 55.0 ft bgs = 159	100	B39WV6
7/10/2017	55.0 – 60.0		55.0 ft bgs = 102 57.5 ft bgs = 121 60.0 ft bgs = 151	100	B39WV8
7/10/2017	60.0 – 65.0		60.0 ft bgs = 96 62.5 ft bgs = 103 65.0 ft bgs = 94	100	B39WW0
7/11/2017	65.0 – 70.0		65.0 ft bgs = 79 67.5 ft bgs = 77 70.0 ft bgs = 92	100	B39WW2
7/11/2017	70.0 – 75.0		70.0 ft bgs = 76 72.5 ft bgs = 78 75.0 ft bgs = 113	100	B39WW4

Table A-2. Borehole C9513 (216-S-13 Crib)

Date	Sample Depth (ft bgs)	Sample Method	IR LEXAN Temperature (°F)	Recovery %	HEIS number
7/11/2017	75.0 – 80.0		75.0 ft bgs = 94 77.5 ft bgs = 96 80.0 ft bgs = 145	100	B39WX0, B39WX1, B39WX3
7/11/2017	80.0 – 85.0		80.0 ft bgs = 84 82.5 ft bgs = 89 85.0 ft bgs = 96	100	B39WX5
7/11/2017	85.0 – 90.0		85.0 ft bgs = 105 87.5 ft bgs = 108 90.0 ft bgs = 150	100	B39WX7
7/11/2017	90.0 – 95.0		90.0 ft bgs = 83 92.5 ft bgs = 87 95.0 ft bgs = 96	100	B39WX9
7/17/2017	95.0 – 100.0		95.0 ft bgs = 74 97.5 ft bgs = 76 100.0 ft bgs = 75	100	B39WY1, B39WY2, B39WY3, B39WY4
7/17/2017	100.0 – 105.0		100.0 ft bgs = 87 102.5 ft bgs = 94 105.0 ft bgs = 85	100	B39WY6
8/22/2017	105.5 – 110.5		105.5 ft bgs = 78 108.0 ft bgs = 83 110.5 ft bgs = 95	100	B39WY8
8/22/2017	110.5 – 115.5		110.5 ft bgs = 89 113.0 ft bgs = 87 115.5 ft bgs = 100	100	B39X04, B39X03, B39X02, B39X01, B39X00
8/22/2017	115.6 – 120.6		115.6 ft bgs = 92 118.1 ft bgs = 92 120.6 ft bgs = 105	100	B39X10, B39X09, B39X08, B39X07, B39X06
8/22/2017	120.2 – 125.2		120.2 ft bgs = 94 122.7 ft bgs = 98 125.2 ft bgs = 111	100	B39X16, B39X15, B39X14, B39X13, B39X12,
8/23/2017	124.8 – 129.8		124.8 ft bgs = 81 127.3 ft bgs = 81 129.8 ft bgs = 100	100	B39X20, B39X19, B39X18, B39X39
8/23/2017	130.5 – 135.5		130.5 ft bgs = 82 133.0 ft bgs = 82 135.5 ft bgs = 90	100	B39X41
8/23/2017	135.2 – 140.2		135.2 ft bgs = 99 137.7 ft bgs = 86 140.2 ft bgs = 116	100	B39X43

Table A-2. Borehole C9513 (216-S-13 Crib)

Date	Sample Depth (ft bgs)	Sample Method	IR LEXAN Temperature (°F)	Recovery %	HEIS number
8/23/2017	140.5 – 145.5		140.5 ft bgs = 89 143.0 ft bgs = 90 145.5 ft bgs = 108	100	B39X47, B39X46, B39X45
8/23/2017	145.1 – 150.1		145.1 ft bgs = 104 147.6 ft bgs = 102 150.1 ft bgs = 121	100	B39X50
8/23/2017	150.7 – 155.7		150.7 ft bgs = 106 153.2 ft bgs = 129 155.7 ft bgs = 136	100	B39X56, B39X55, B39X54, B39X53, B39X52
8/24/2017	154.9 – 159.9		154.9 ft bgs = N/A 157.4 ft bgs = N/A 159.9 ft bgs = N/A	100	B39X64, B39X63, B39X62, B39X61, B39X60, B39X59, B39X58
8/28/2017	160.7 – 165.7		160.7 ft bgs = 75 163.2 ft bgs = 76 165.7 ft bgs = 87	100	B39X70, B39X69, B39X68, B39X67, B39X66
8/28/2017	165.3 – 170.3		165.3 ft bgs = 84 167.8 ft bgs = 88 170.3 ft bgs = 100	100	B39X72
8/28/2017	170.5 – 175.5		170.5 ft bgs = 86 173.0 ft bgs = 94 175.5 ft bgs = 100	100	B39X77, B39X76, B39X75, B39X74
8/28/2017	175.1 – 180.1		175.1 ft bgs = 92 177.6 ft bgs = 92 180.1 ft bgs = 104	100	B39X78
8/28/2017	180.6 – 185.6		180.6 ft bgs = 86 183.1 ft bgs = 92 185.6 ft bgs = 103	100	B39X81
8/28/2017	184.9 – 189.9		184.9 ft bgs = 143 187.4 ft bgs = 115 190.9 ft bgs = 138	100	B39X83
8/29/2017	190.4 – 195.4		190.4 ft bgs = 75 192.9 ft bgs = 75 195.4 ft bgs = 97	98	B39X88, B39X87, B39X86, B39X85
8/29/2017	194.7 – 199.7		194.7 ft bgs = 94 197.2 ft bgs = 111 199.7 ft bgs = 102	100	B39X90
8/29/2017	200.5 – 205.5		200.5 ft bgs = 101 203.0 ft bgs = 107 205.5 ft bgs = 122	100	B39X92

Table A-2. Borehole C9513 (216-S-13 Crib)

Date	Sample Depth (ft bgs)	Sample Method	IR LEXAN Temperature (°F)	Recovery %	HEIS number
8/29/2017	205.5 – 210.5		205.5 ft bgs = 110 208.0 ft bgs = 113 210.5 ft bgs = 145	100	B39X94
8/30/2017	210.5 – 215.5		210.5 ft bgs = 86 213.0 ft bgs = 88 215.5 ft bgs = 102	100	B39XB0, B39X99, B39X98, B39X97, B39X96
8/30/2017	214.9 – 219.9		214.9 ft bgs = 111 217.1 ft bgs = 89 219.9 ft bgs = 137	100	B39XB8, B39XB7, B39XB6, B39XB5, B39XB4, B39XB3, B39XB2
8/30/2017	220.5 – 225.5		220.5 ft bgs = 86 223.0 ft bgs = 84 225.5 ft bgs = 89	100	B39XB2, B39XC4, B39XC3, B39XC2, B39XC1, B39XC0
8/30/2017	224.7 – 229.7		220.5 ft bgs = 91 223.0 ft bgs = 97 225.5 ft bgs = 152	92	B39XC6
8/31/2017	230.4 – 235.4		230.4 ft bgs = N/A 232.9 ft bgs = N/A 235.4 ft bgs = N/A	100	B39XC8
8/31/2017	235.5 – 240.5		235.5 ft bgs = 75 238.0 ft bgs = 78 240.5 ft bgs = 82	100	B39XD0

bgs = below ground surface

HEIS = Hanford Environmental Information System

Table A-3. Borehole C9514 (216-S-21 Crib)

Date	Depth Interval (ft bgs)	Recovery %	IR LEXAN		IR Drill Shoe Temperature	HEIS #
			Temperature (°Fahrenheit)	Temperature		
Becker Hammer						
4/7/2016	4.1 - 6.6	50	-	-	-	B33XN2, B33XP0, B33XP4, B33XP6
4/7/2016	7.0 - 9.5	40	-	-	-	B33XN3, B33XP1, B33XP5, B33XP7
4/7/2016	13.1 - 15.6	40	-	-	-	B33XN4, B33XN6, B33XP2, B33XP8, B33XR0
Sonic						
7/19/2016	44.1 - 46.6	100	44.1 ft bgs = 79 46.6 ft bgs = 115		107	B36107, B36106
7/20/2016	47.4 - 49.9	100	47.4 ft bgs = 68 49.9 ft bgs = 72		91.8	B36109
7/20/2016	49.6 - 52.1	100	49.6 ft bgs = 67 52.1 ft bgs = 71		83.4	B36111
7/20/2016	52.5 - 55.0	100	52.1 ft bgs = 75 55.0 ft bgs = 79		99.2	B36113
7/20/2016	54.7 - 57.2	100	54.7 ft bgs = 70 57.2 ft bgs = 75		91.4	B36115
7/20/2016	57.1 - 62.1	100	57.1 ft bgs = 78 59.6 ft bgs = 76 62.1 ft bgs = 95		115	B36117
7/20/2016	62.1 - 67.1	100	62.1 ft bgs = 85 64.6 ft bgs = 76 67.1 ft bgs = 110		117.8	B36119
7/20/2016	67.1 - 72.1	100	67.1 ft bgs = 108 69.6 ft bgs = 80 72.1 ft bgs = 111		118.6	B36121
7/20/2016	72.0 - 77.0	100	72.0 ft bgs = 92 74.5 ft bgs = 76 77.0 ft bgs = 98		101.8	B36123
7/20/2016	77.1 - 82.1	100	77.1 ft bgs = 87 79.6 ft bgs = 84 82.1 ft bgs = 125		114	B36125

Table A-3. Borehole C9514 (216-S-21 Crib)

Date	Depth Interval (ft bgs)	Recovery %	IR LEXAN Temperature (°Fahrenheit)		HEIS #
			IR LEXAN Temperature	IR Drill Shoe Temperature	
7/20/2016	82.5 – 87.5	100	82.5 ft bgs = 95 85.0 ft bgs = 81 87.5 ft bgs = 125	135	B36127
7/20/2016	87.2 – 92.2	100	87.2 ft bgs = 100 89.7 ft bgs = 81 92.2 ft bgs = 93	96.4	B36129
7/20/2016	92.2 – 97.2	100	92.2 ft bgs = 104 94.7 ft bgs = 81 97.2 ft bgs = 104	104	B36131
7/21/2016	97.1 - 102.1	100	97.1 ft bgs = 72 99.6 ft bgs = 76 102.1 ft bgs = 106	106.8	B36133
7/21/2016	102.0 - 107.0	16	~1' sample=92	96.4	B36135
7/21/2016	107.2 - 112.2	100	107.2 ft bgs = 87 109.7 ft bgs = 74 112.2 ft bgs = 102	113.6	B36137
7/21/2016	112.2 - 117.2	100	112.2 ft bgs = 78 114.7 ft bgs = 74 117.2 ft bgs = 83	108.6	B36139
7/21/2016	117.4 - 122.4	100	117.4 ft bgs = 77 119.9 ft bgs = 77 122.4 ft bgs = 106	114.8	B36141
7/21/2016	122.0 - 127.0	90	122.0 ft bgs = 87 124.5 ft bgs = 80 127.0 ft bgs = 94	116.2	B36143

Notes:
 bgs = below ground surface
 HEIS = Hanford Environmental Information System
 IR = Infrared

This page intentionally left blank.

Appendix B
Borehole Geophysical Log Reports

This page intentionally left blank.

Contents

C9512 (216-S-9 Crib) Log Data Report B-1
C9513 (216-S-13 Crib) Log Data ReportB-18
C9514 (216-S-21 Crib) Log Data ReportB-39

This page intentionally left blank.



Stoller Newport News Nuclear

C9512 Log Data Report

Borehole Information

Log Date	2016-07-28	Filename	C9512_HG-NM_2016-07-28	Site	216-S-9 (200- DV-1)
Coordinates (WA StPlane)		DTW¹ (ft)	None	DTW Date	07/28/16
North (m)	East (m)	Drill Date	TOC² Elevation	Total Depth (ft)	
N/A	N/A	07/27/16	N/A	142.5	

Casing Information

Casing Type	Drill Type	Stickup (ft)	Diameter (in.)		Thickness (in.)	Top (ft)	Bottom (ft)
			Outer	Inside			
Threaded Steel	Becker Hammer	0.3	8 5/8	7 3/8	5/8	0.3	36.4
Threaded Steel	Sonic	0.0	6	5	1/2	0.0	140.5

Borehole Notes

The onsite geologist provided the total depth and casing depth. A Becker Hammer push method was used to 36.4 ft. Subsequent drilling was conducted using a Sonic method. The logging engineer measured casing stick-up and casing diameters. No water existed inside the casing. The maximum logging depth achieved was 141 ft, approximately 0.5 ft below casing. Zero reference is ground surface.

Logging Equipment Information

Logging System	Gamma 5Tb	Type	60% HPGe SGLS ³
Effective Calibration Date	03/19/15	Serial No.	54-TP13441B
Calibration Reference	HGLP-CC-115, Rev. 0	Logging Procedure	SGRP-PRO-OP-53023, Rev. 0

Logging System	Gamma 1L	Type	60% HPGe SGLS
Effective Calibration Date	10/22/15	Serial No.	47-TP-32211A
Calibration Reference	HGLP-CC-130, Rev. 0	Logging Procedure	SGRP-PRO-OP-53010, Rev. 0

Logging System	Gamma 1H	Type	NMLS ⁴
Effective Calibration Date	10/21/15	Serial No.	H310700352
Calibration Reference	HGLP-CC-131, Rev. 1	Logging Procedure	SGRP-PRO-OP-53016, Rev. 0

Logging System	Gamma 5Tb	Type	60% HPGe SGLS
Effective Calibration Date	02/23/16	Serial No.	54-TP13441B
Calibration Reference	HGLP-CC-136, Rev. 2	Logging Procedure	SGRP-PRO-OP-53023, Rev. 0

Logging System	Gamma 5Pb	Type	NMLS
Effective Calibration Date	04/15/15	Serial No.	H34055445
Calibration Reference	HGLP-CC-116, Rev. 0	Logging Procedure	SGRP-PRO-OP-53024, Rev. 0

¹ depth to water inside casing

² top of casing

³ Spectral Gamma Logging System

⁴ Neutron Moisture Logging System



Stoller Newport News Nuclear

Logging System	Gamma 5Pb	Type	NMLS
Effective Calibration Date	05/02/16	Serial No.	H34055445
Calibration Reference	HGLP-CC-140, Rev. 0a	Logging Procedure	SGRP-PRO-OP-53024, Rev. 0

SGLS Log Run Information

Log Run	1	2 Repeat	5	6 Repeat	9
HEIS Number	1019686	1019687	1019688	1019689	1019690
Date	12/02/15	12/02/15	04/20/16	04/20/16	07/28/16
Logging Engineer	Spatz/Felt	Spatz/Felt	Spatz/Felt	Spatz/Felt	Spatz
Start Depth (ft)	0.0	27.0	30.0	34.0	34.0
Finish Depth (ft)	31.98	30.0	35.0	35.0	141.0
Count Time (sec)	100	100	100	100	200
Live/Real	R	R	R	R	R
Shield (Y/N)	N	N	N	N	N
MSA Interval (ft)	1.0	1.0	1.0	1.0	1.0
Log Speed (ft/min)	N/A	N/A	N/A	N/A	N/A
Pre-Verification	C9512FTB2015 1202AV00CAB 1	C9512FTB2015 1202AV00CAB 1	AL299CAB	AL299CAB	C9512FTB2016 0728AV00CAB 1
Start File	AD000000	BD002700	AL299000	AL299006	AD003400
Finish File	AD003198	BD003000	AL299005	AL299007	AD014100
Post-Verification	C9512FTB2015 1202BV00CAA 1	C9512FTB2015 1202BV00CAA 1	AL299CAA	AL299CAA	C9512FTB2016 0728BV00CAA 1
Depth Return Error (in.)	N/A	2.0 high	N/A	0.0	N/A
Comments	No fine gain adjustments made				

Log Run	10 Repeat				
HEIS Number	1019691				
Date	07/28/16				
Logging Engineer	Spatz				
Start Depth (ft)	129.0				
Finish Depth (ft)	141.0				
Count Time (sec)	200				
Live/Real	R				
Shield (Y/N)	N				
MSA Interval (ft)	1.0				
Log Speed (ft/min)	N/A				
Pre-Verification	C9512FTB2016 0728AV00CAB 1				
Start File	BD012900				
Finish File	BD014100				
Post-Verification	C9512FTB2016 0728BV00CAA 1				


Stoller Newport News Nuclear

Log Run	10 Repeat				
Depth Return Error (in.)	2.0 high				
Comments	No fine gain adjustments made				

NMLS Log Run Information

Log Run	3	4 Repeat	7	8 Repeat	11
HEIS Number	1019692	1019693	1019694	1019695	1019696
Date	12/02/15	12/02/15	04/20/16	04/20/16	07/28/16
Logging Engineer	Spatz/Felt	Spatz/Felt	Spatz/Felt	Spatz/Felt	Spatz
Start Depth (ft)	0.0	28.5	30.0	34.0	34.0
Finish Depth (ft)	32.01	31.51	35.5	35.0	141.0
Count Time (sec)	15	15	15	15	15
Live/Real	R	R	R	R	R
Shield (Y/N)	N	N	N	N	N
MSA Interval (ft)	0.25	0.25	0.25	0.25	0.25
Log Speed (ft/min)	N/A	N/A	N/A	N/A	N/A
Pre-Verification	C9512FPB20151 202AV00CAB1	C9512FPB20151 202AV00CAB1	AH241CAB	AH241CAB	C9512FPB20160 728AV00CAB1
Start File	AD000000	BD002850	AH241000	AH241023	AD003400
Finish File	AD003201	BD003151	AH241022	AH241027	AD014100
Post-Verification	C9512FPB20151 102BV00CAA1	C9512FPB20151 102BV00CAA1	AH241CAA	AH241CAA	C9512FPB20160 728BV00CAA1
Depth Return Error (in.)	N/A	0.5 high	N/A	0.5 high	N/A
Comments	None	None	None	None	None

Log Run	12 Repeat				
HEIS Number	1019697				
Date	07/28/16				
Logging Engineer	Spatz				
Start Depth (ft)	129.0				
Finish Depth (ft)	141.0				
Count Time (sec)	15				
Live/Real	R				
Shield (Y/N)	N				
MSA Interval (ft)	0.25				
Log Speed (ft/min)	N/A				
Pre-Verification	C9512FPB20160 728AV00CAB1				
Start File	BD012900				
Finish File	BD014100				
Post-Verification	C9512FPB20160 728BV00CAA1				
Depth Return Error (in.)	1.0 high				
Comments	None				



Stoller Newport News Nuclear

Logging Operation Notes

A centralizer was installed on the sondes for the first casing to 36.4 ft; no centralizer was used for the second casing due to the small internal diameter. As a precaution, the sondes were covered in plastic sleeving to prevent potential contamination of equipment for the second casing to 141 ft.

Pre- and post-survey verification measurements met the acceptance criteria for the established systems.

Analysis Notes

Analyst	P.D. Henwood	Date	09/22/16
Reference(s)	SGRP-PRO-OP-53040, Rev. 0; SGRP-PRO-OP-53051, Rev. 0; SGRP-PRO-OP-53052, Rev. 0		

A casing correction for a 5/8-in. thick casing was applied for the first Becker Hammer push to 36.4 ft and for a 1/2-in. thick casing for the remainder of the borehole drilled by the Sonic drill.

No water correction was necessary as water was not encountered.

SGLS spectra were processed in batch mode in APTEC SUPERVISOR to identify individual energy peaks and determine count rates. Concentrations from the SGLS were calculated in EXCEL templates identified as 5TB20150319, 5T20160223, and 1L20151022 using an efficiency function and corrections for casing and dead time as determined by annual calibrations.

An interpreted data set was created for this borehole. Depth overlaps were removed where two casings existed at 30, 34, and 35 ft. This results in a data set where only one data point is presented for each depth.

NMLS data are reported in counts per second.

HGU⁵ is an empirical unit of gamma activity proposed as a means to standardize gamma log response across multiple logging systems with different response characteristics. The HGU is defined in terms of measurements in the Hanford Borehole Calibration Facility, and the magnitude is selected such that 1 HGU is approximately equivalent to typical Hanford background activity, based on data from background samples as reported in *Hanford Site Background: Part 2, Soil Background for Radionuclides* (DOE/RL-96-12).

Results and Interpretations

Cs-137 was detected in this borehole near the ground surface and from 26 to 68 ft. A maximum concentration of approximately 608 pCi/g was measured at 29 ft.

No other manmade radionuclides were detected. MDLs for processed uranium (Pa-234m [U-238] and U-235) that are possible contaminants are plotted.

Casing joints are evident by reduced count rates for the moisture and gamma measurements at 5 and 10 ft intervals beginning at 41 ft.

The neutron moisture log primarily responds to moisture present in the surrounding formation. In general, an increase in count rate reflects an increase in moisture content. Moisture content may increase in sediments of relatively high silt or clay content.

The manmade, KUT, and moisture repeat plots indicate that the respective systems were working properly.

⁵ Hanford Gamma Unit



Stoller Newport News Nuclear

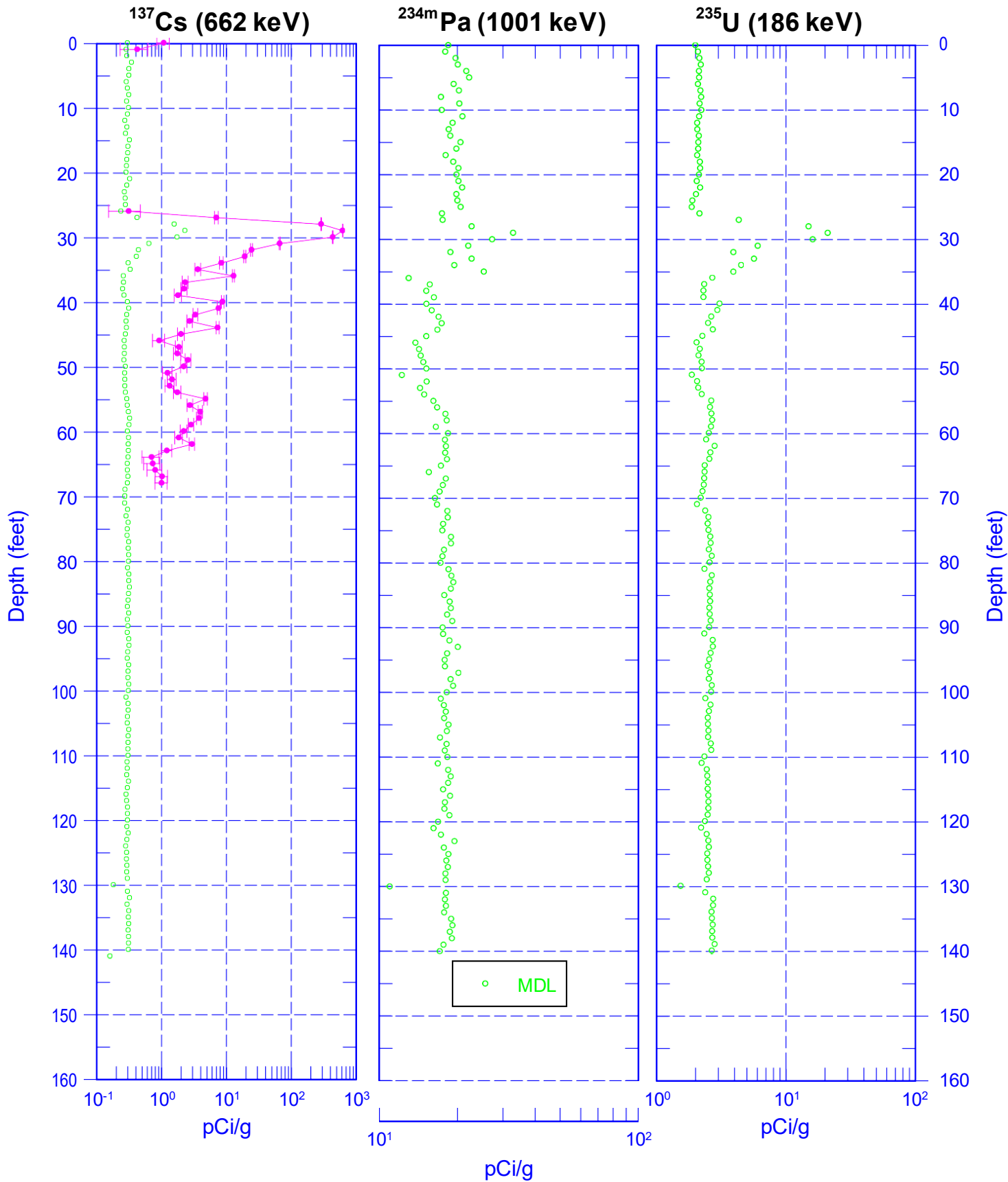
List of Log Plots

Depth Reference is ground surface.

- Manmade Radionuclides (0-160 ft)
- Natural Gamma Logs (0-160 ft)
- Combination Plot (0-120 ft)
- Combination Plot (110-230 ft)
- Combination Plot (0-160 ft)
- Total Gamma & Moisture (0-160 ft)
- Total Gamma & Hanford Gamma Unit (0-160 ft)
- Repeat of Manmade Radionuclides (27-35 ft)
- Repeat Section of Natural Gamma Logs (27-35 ft)
- Repeat Section of Natural Gamma Logs (129-141 ft)
- Moisture Repeat Section (28-35 ft)
- Moisture Repeat Section (129-141 ft)



C9512 Manmade Radionuclides

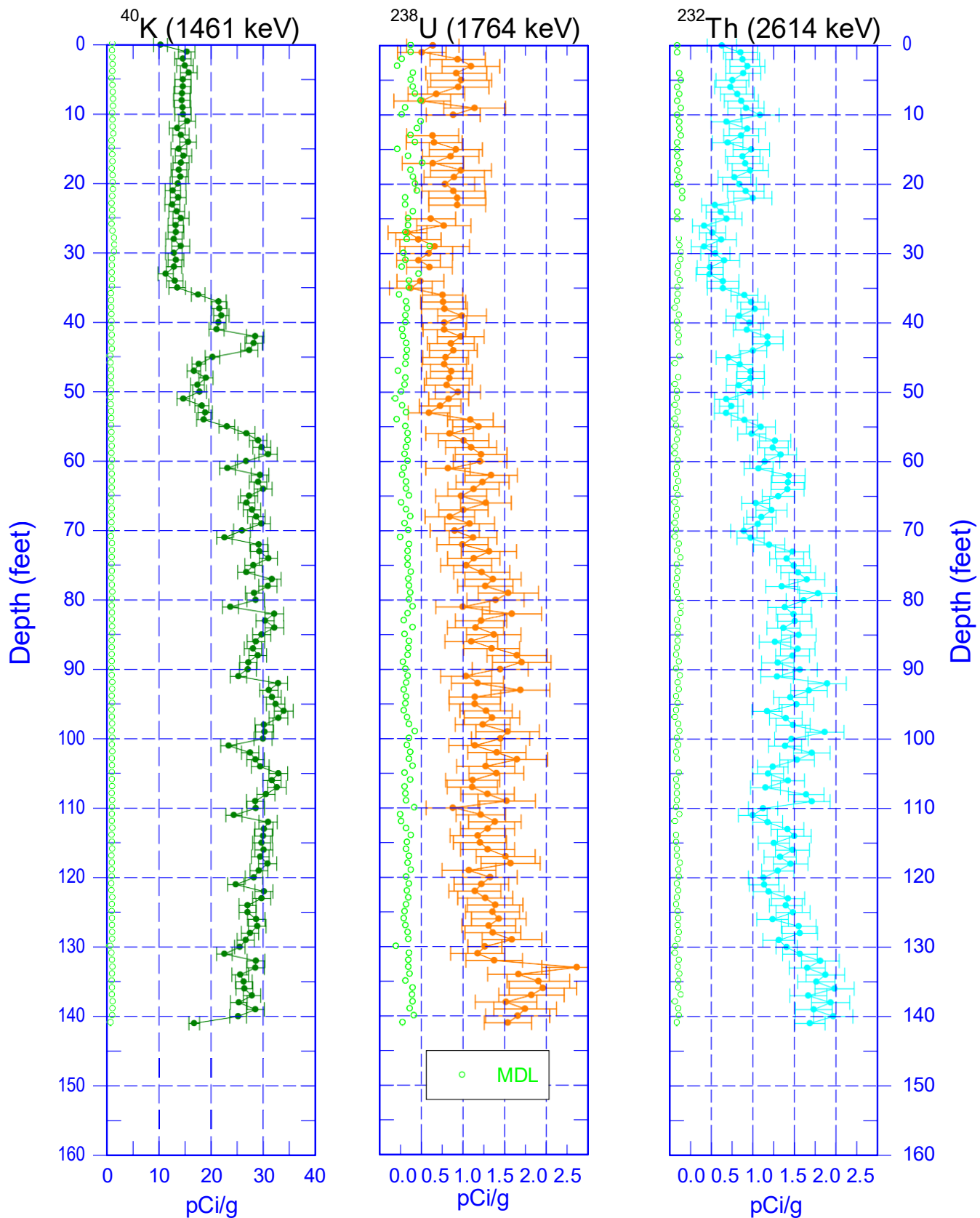


Zero Reference - Ground Surface



Stoller Newport News Nuclear
A Subsidiary of Huntington Ingalls Industries

C9512 Natural Gamma Logs

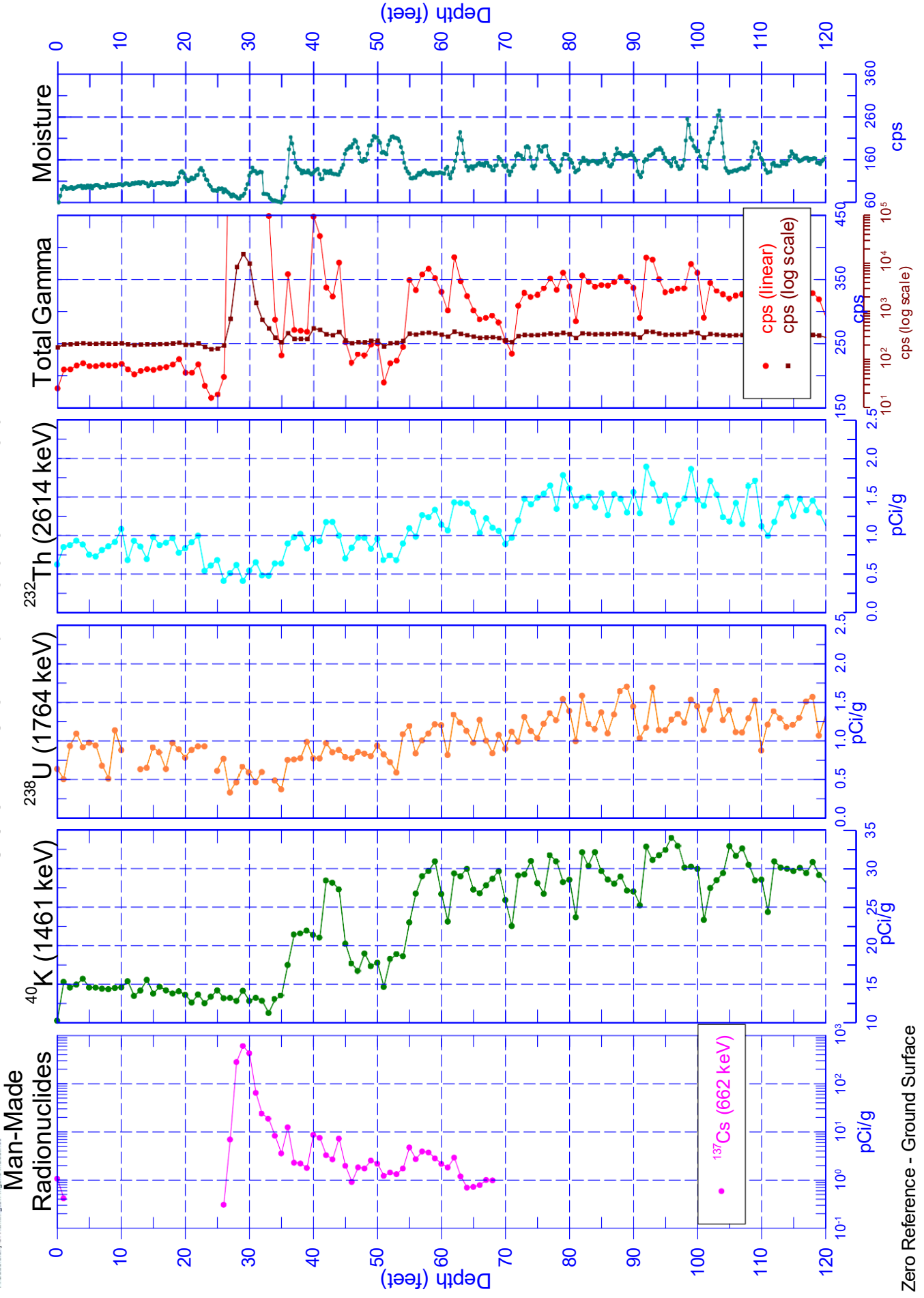


Zero Reference - Ground Surface



Stoller Newport News Nuclear
A Subsidiary of Huntington Ingalls Industries

C9512 Combination Plot

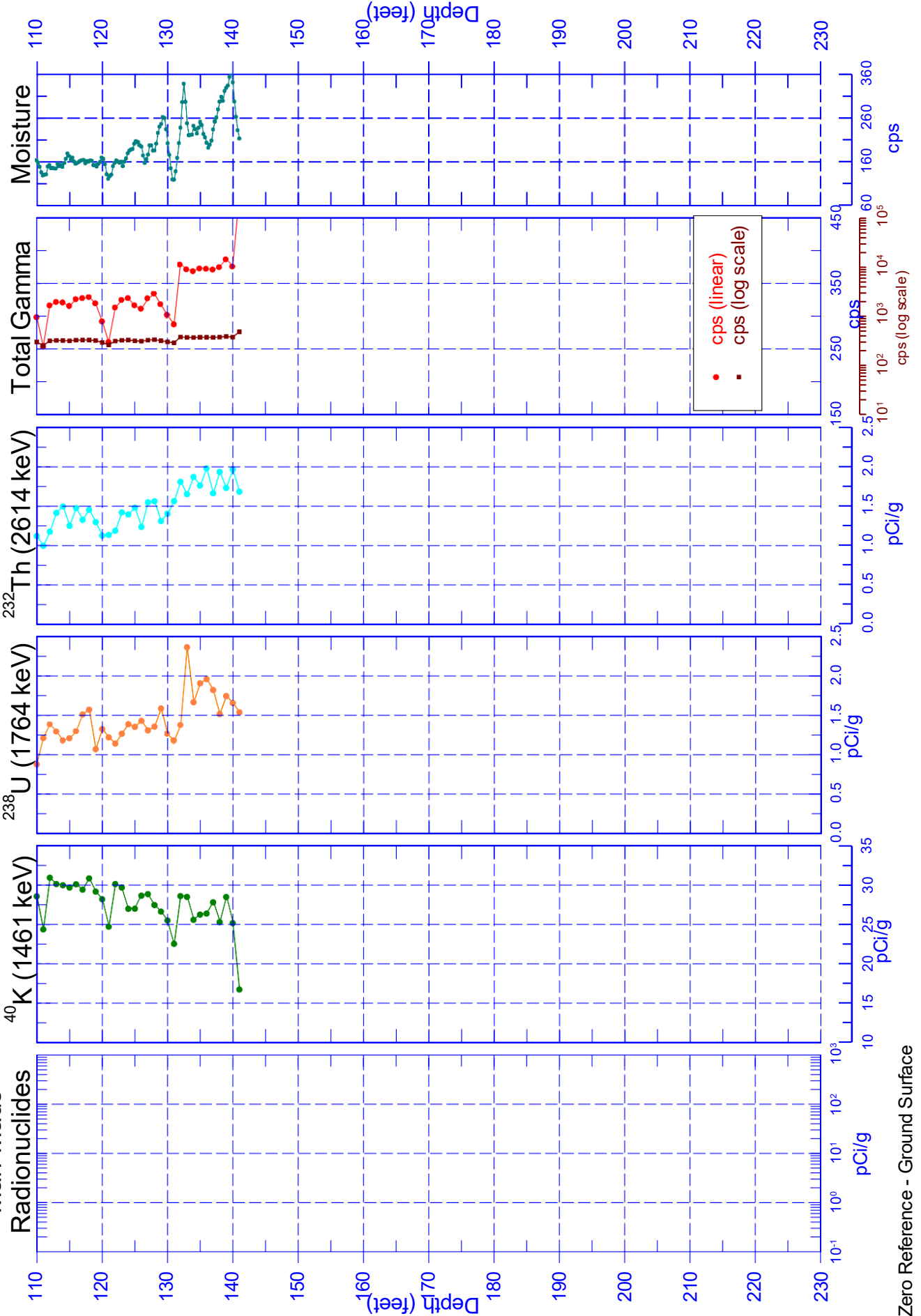




Stoller Newport News Nuclear
A Subsidiary of Huntington Ingalls Industries

C9512 Combination Plot

Man-Made
Radionuclides

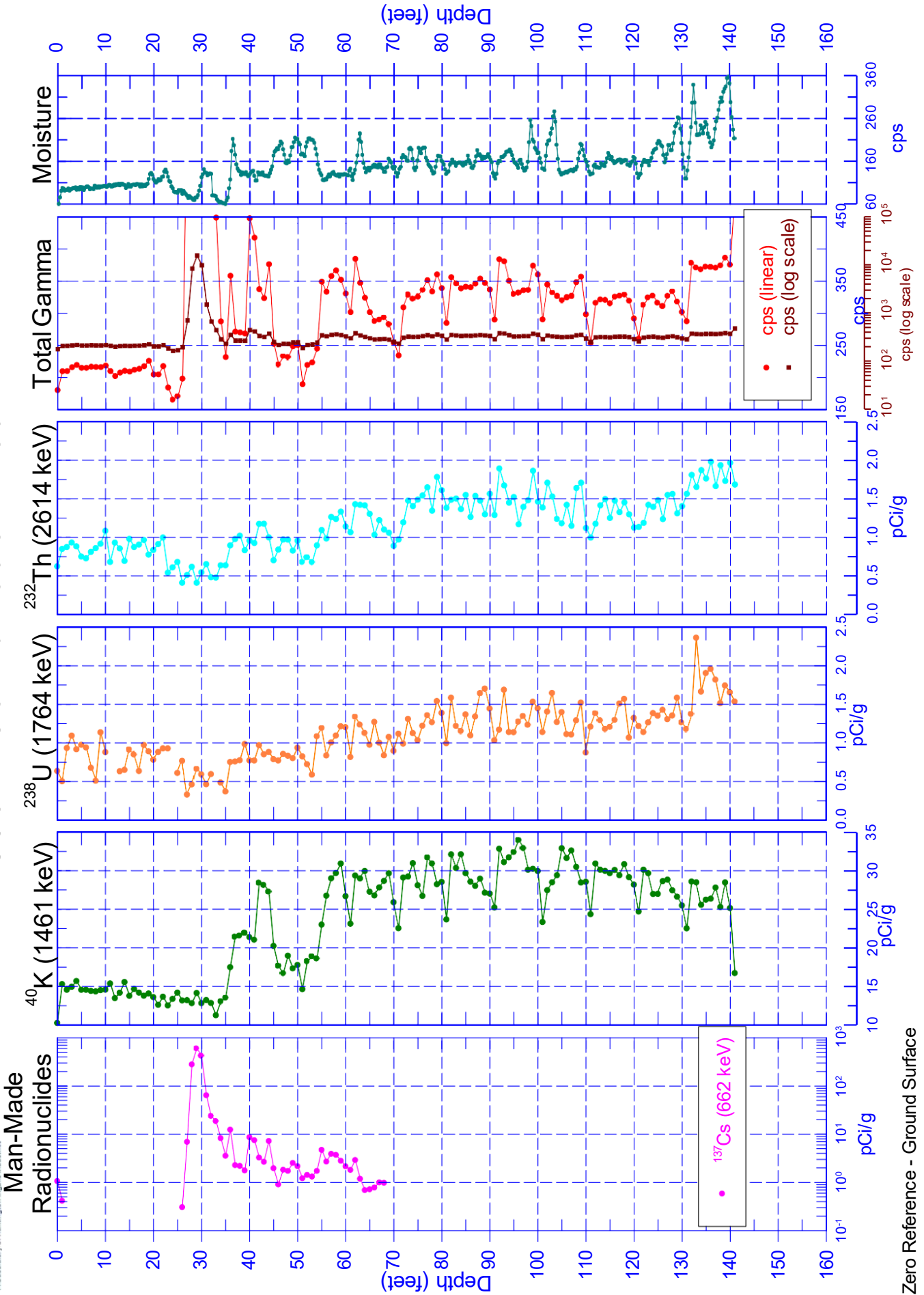


Zero Reference - Ground Surface



Stoller Newport News Nuclear
A Subsidiary of Huntington Ingalls Industries

C9512 Combination Plot



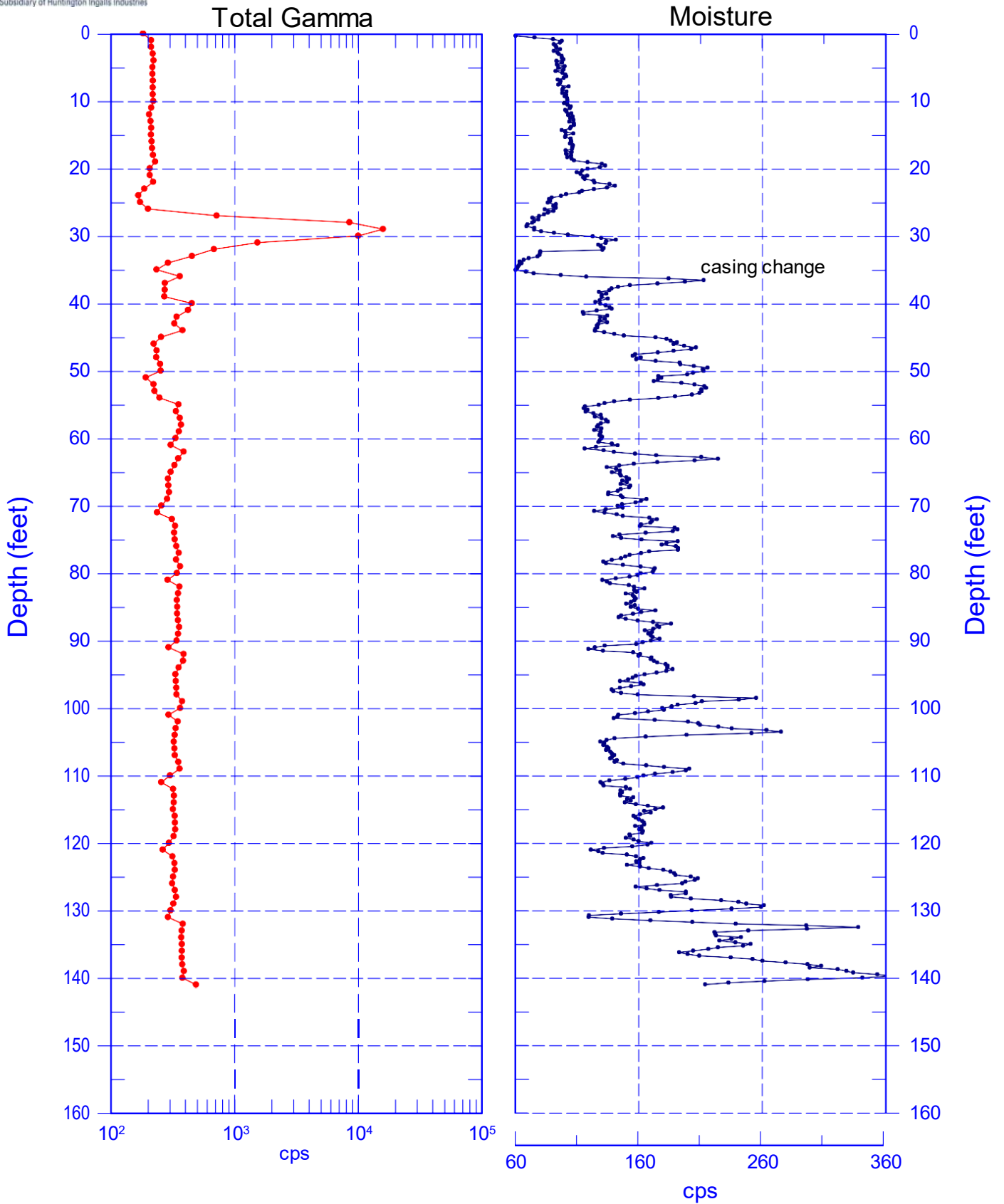
Zero Reference - Ground Surface



Stoller Newport News Nuclear
A Subsidiary of Huntington Ingalls Industries

C9512

Total Gamma & Moisture



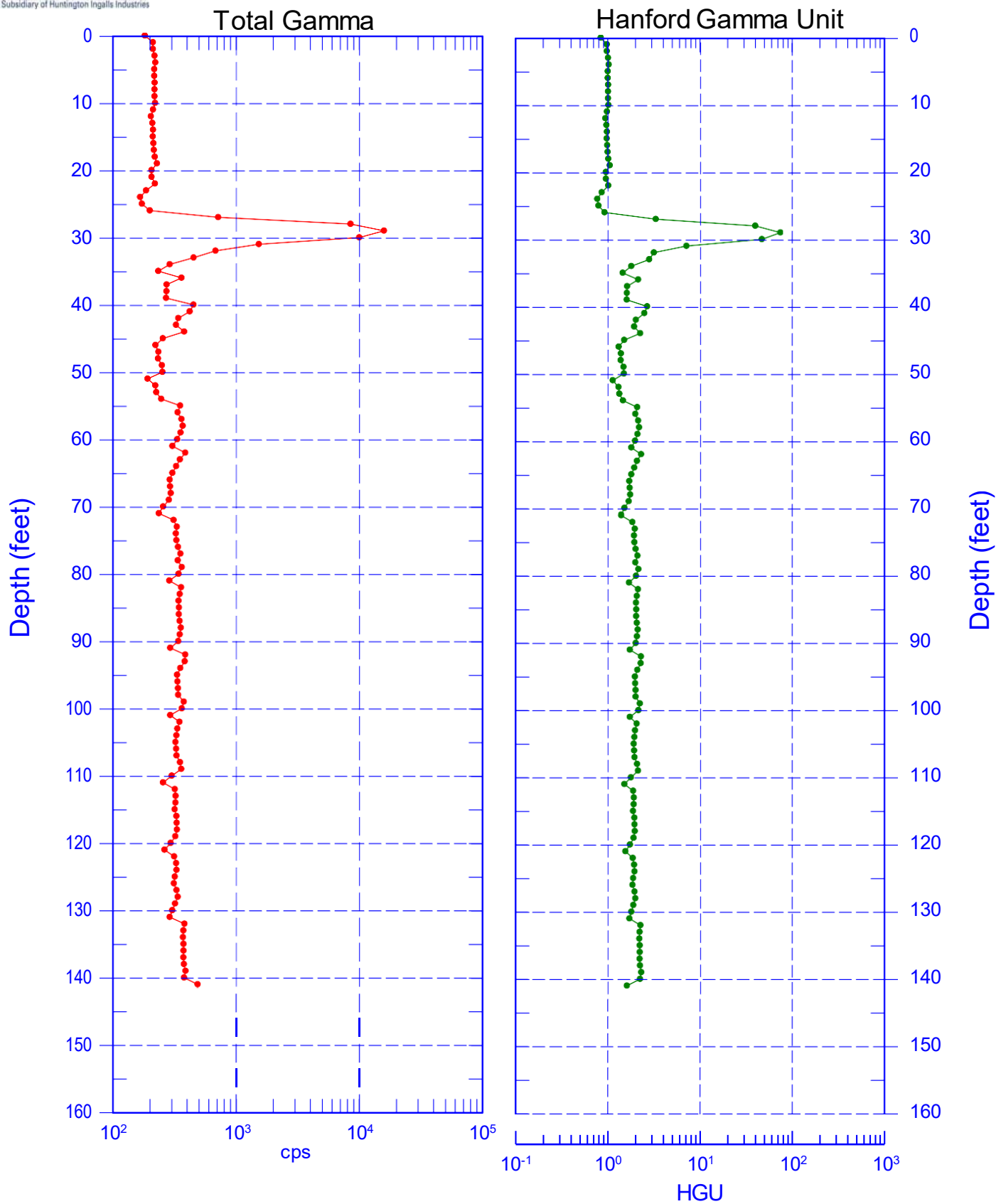
Zero Reference - Ground Surface



Stoller Newport News Nuclear
A Subsidiary of Huntington Ingalls Industries

C9512

Total Gamma & Hanford Gamma Unit



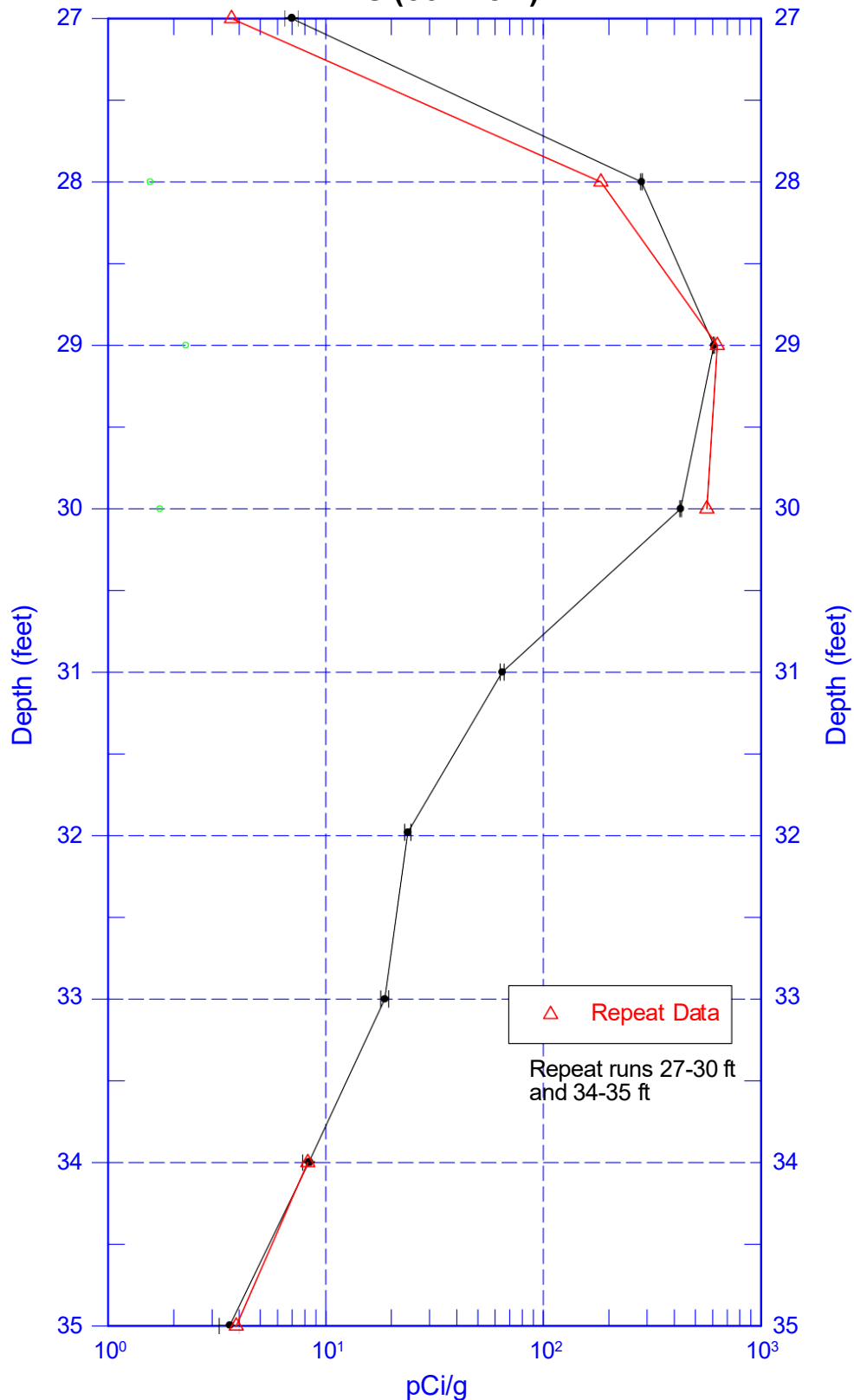
Zero Reference - Ground Surface



C9512

Repeat of Manmade Radionuclides

¹³⁷Cs (662 keV)



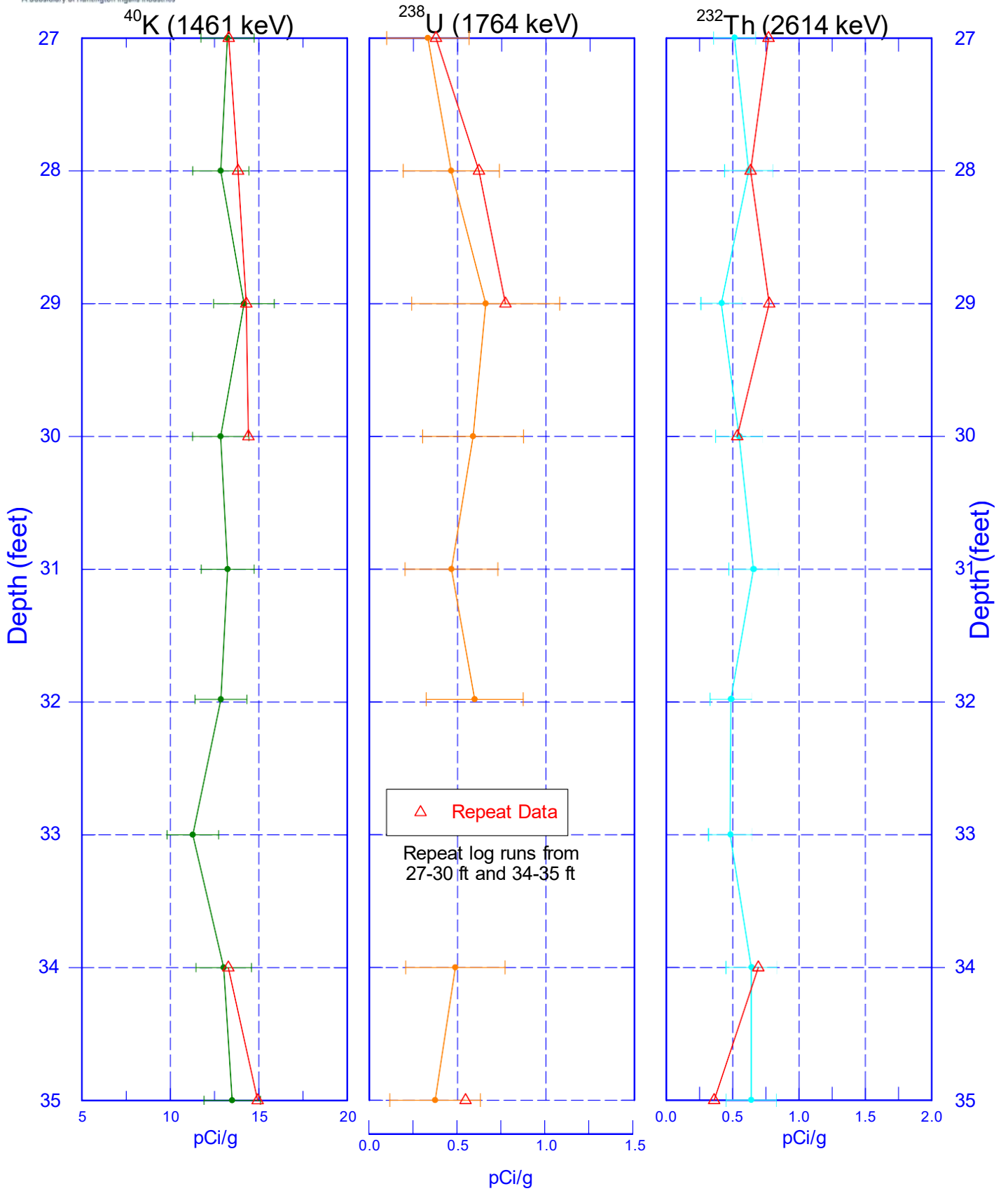
Zero Reference - Ground Surface



Stoller Newport News Nuclear
A Subsidiary of Huntington Ingalls Industries

C9512

Repeat Section of Natural Gamma Logs



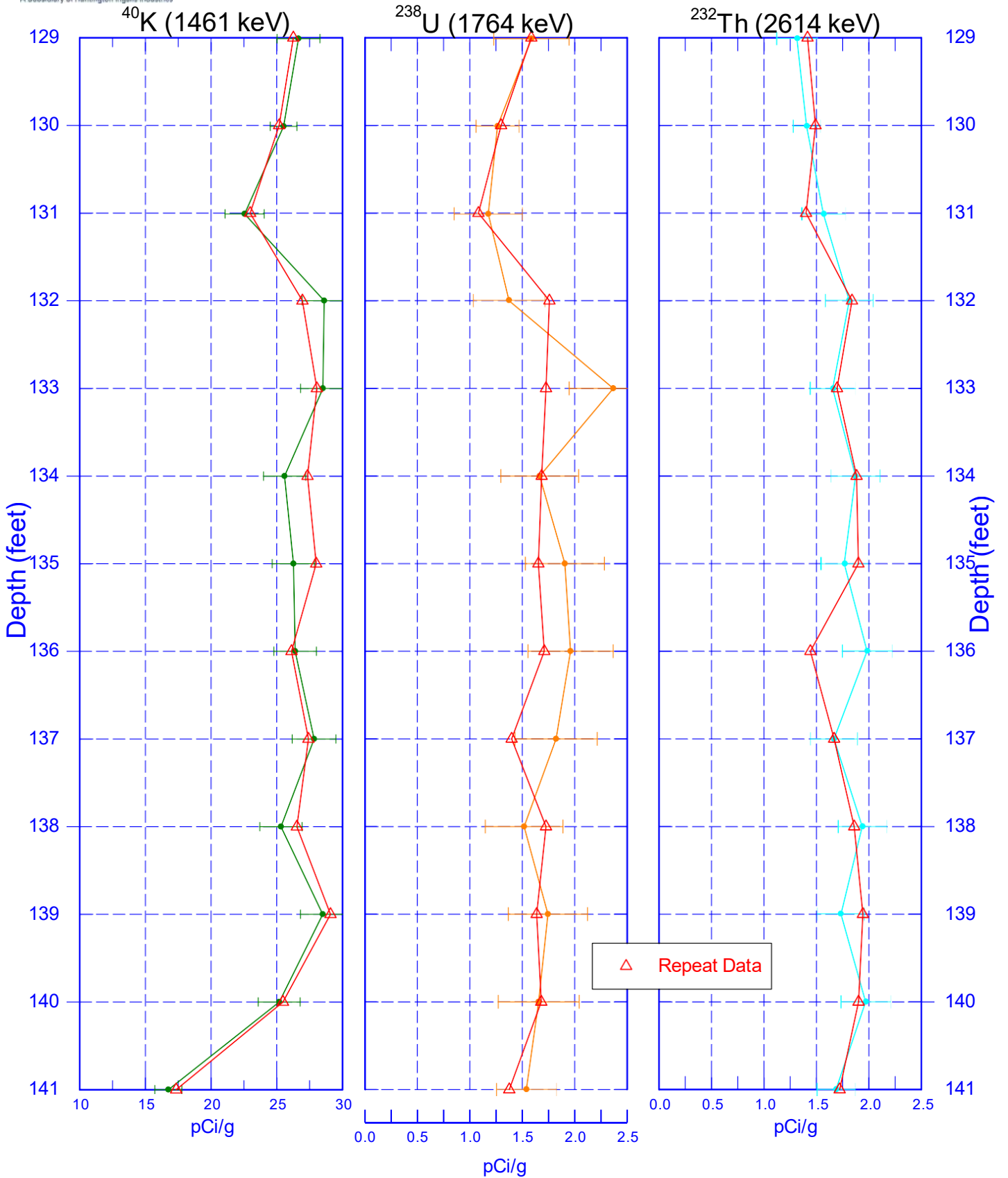
Zero Reference - Ground Surface



Stoller Newport News Nuclear
A Subsidiary of Huntington Ingalls Industries

C9512

Repeat Section of Natural Gamma Logs



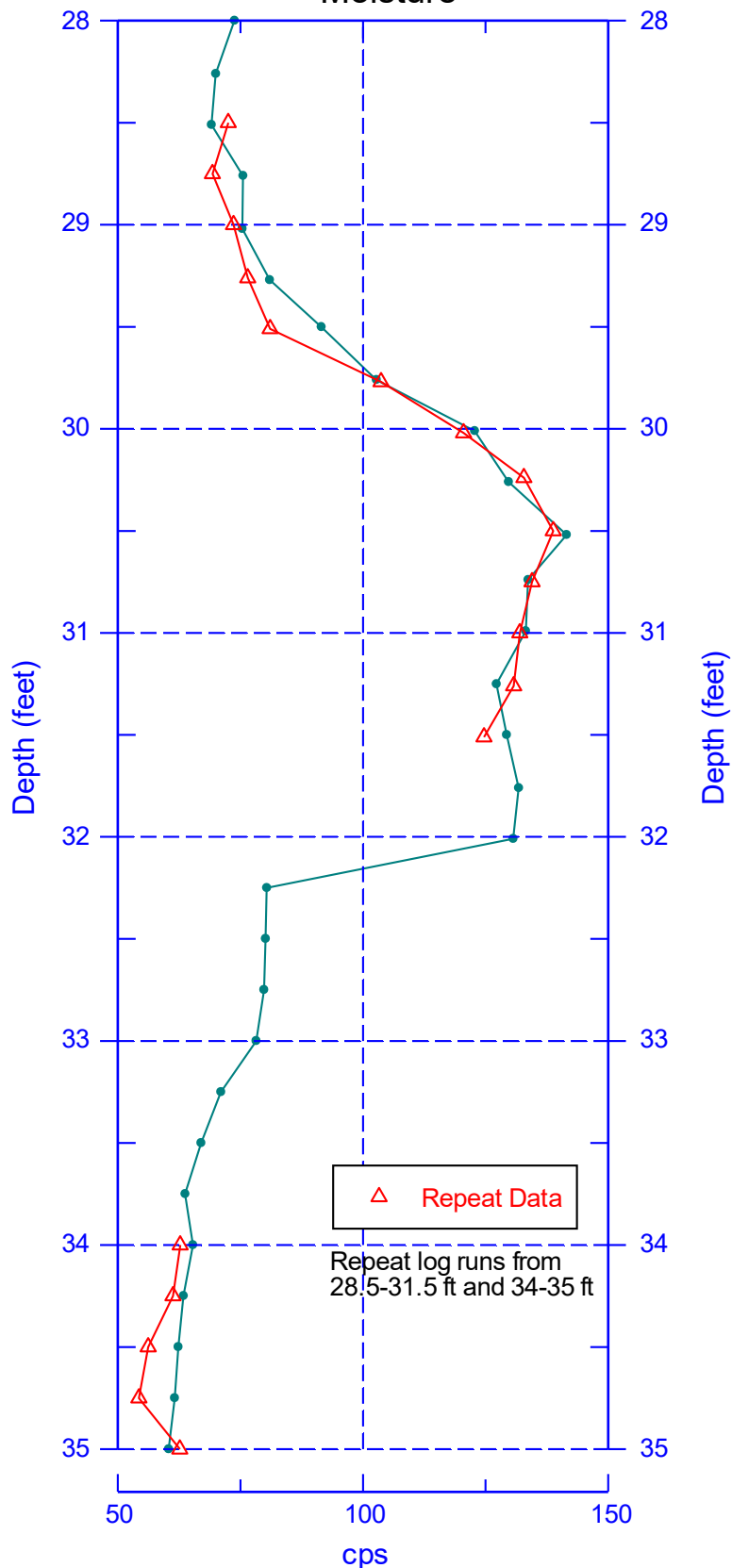
Zero Reference - Ground Surface



C9512

Moisture Repeat Section

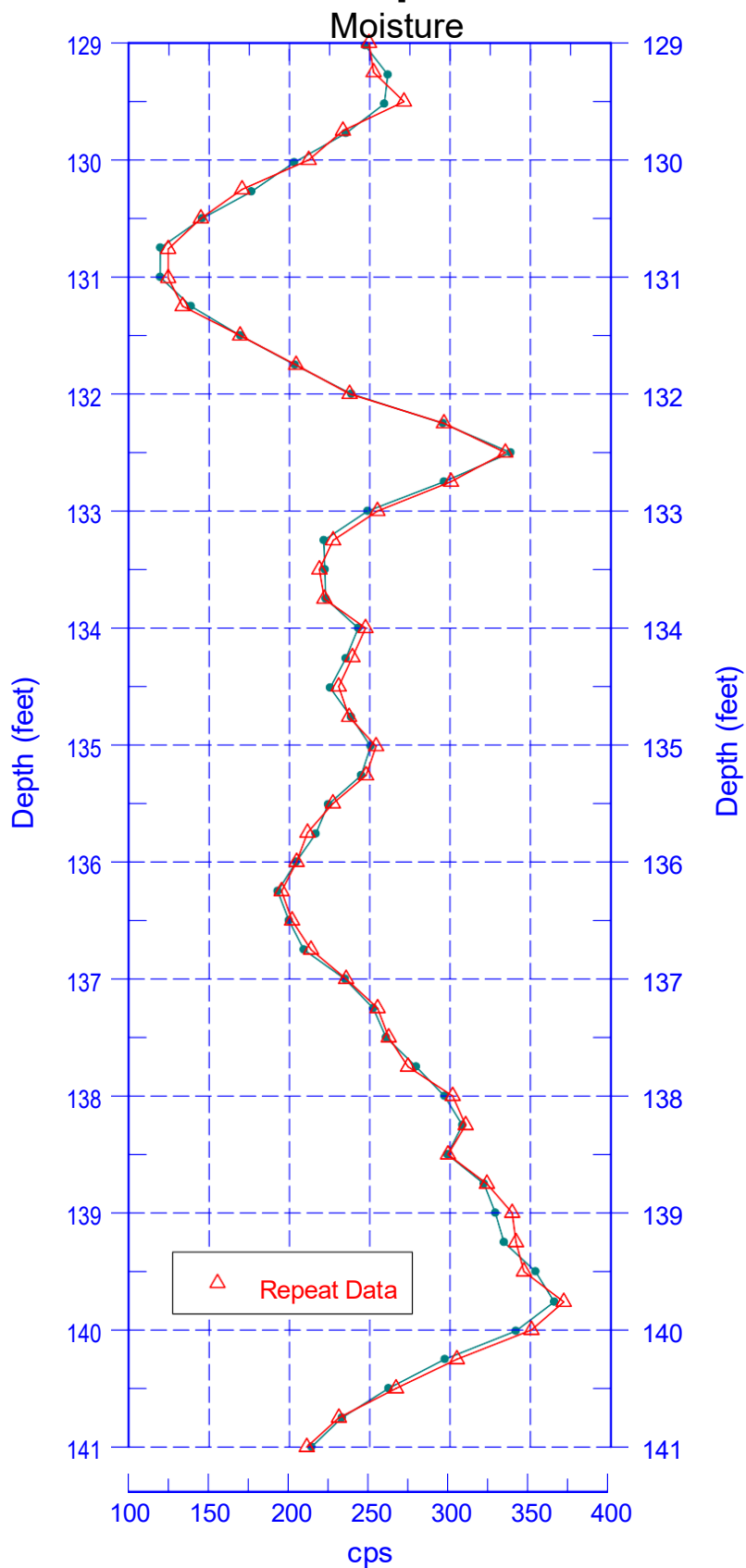
Moisture



Zero Reference - Ground Surface



C9512 Moisture Repeat Section



Zero Reference - Ground Surface

C9513 Log Data Report

Borehole Information

Log Date	2017-09-05	Filename	C9513_HG-NM_2017-09-05	Site	200-DV-1	
DTW¹ (ft)		DTW Date		Drill Date	Total Depth (ft)	Depth Datum
Dry		09/05/17	SN3	08/31/17	240.2	Ground Surface

Casing Information

Casing Type	Drill Type	Stickup (ft)	Diameter (in.)		Thickness (in.)	Top (ft)	Bottom (ft)
			Outer	Inside			
TerraSonic steel	Sonic	0.5	12	10.88-11.5	0.25-0.56	-0.5	11.9
Steel	Becker	0.2	8.625	7.511	0.557	-0.2	42.1
TerraSonic steel	Sonic	0.2	7.05	6.22-6.50	0.25-0.42	-0.2	160.3
TerraSonic steel	Sonic	0.2	6.0	5-5.5	0.25-0.5	-0.2	240.3

Borehole Notes

The on site geologist provided the total depth and casing depth. The logging engineer measured casing stick-up. Casing diameters are provided by the driller. The maximum logging depth achieved was 239 ft. Zero reference is ground surface.

Logging was started after the second casing had been drilled. The logged interval to 11.9 ft was conducted inside two casings.

Logging Equipment Information

Logging System	Gamma 5Tb	Type	60% HPGe SGLS ²
Effective Calibration Date	02/16/17	Serial No.	54-TP13441B
Calibration Reference	HGLP-CC-152, Rev. 0	Logging Procedure	SGRP-PRO-OP-53023, Rev. 0

Logging System	Gamma 5Pb	Type	NMLS ³
Effective Calibration Date	02/27/17	Serial No.	H34055445
Calibration Reference	HGLP-CC-153, Rev. 0	Logging Procedure	SGRP-PRO-OP-53024, Rev. 0

SGLS Log Run Information

Log Run	1	2 Repeat	5	6 Repeat	9
HEIS Number	1020010	1020011	1020012	1020013	1020014
Date	06/01/17	06/01/17	08/24/17	08/24/17	08/31/17
Logging Engineer	Felt/McClellan	Felt/McClellan	Felt/Meisner	Felt	Felt/Meisner
Start Depth (ft)	0.0	37.01	41.0	130.0	158.0
Finish Depth (ft)	42.01	42.01	159.02	142.01	235.01
Count Time (sec)	200	500	200	200	200
Live/Real	R	R	R	R	R

¹ depth to water inside casing

² Spectral Gamma Logging System

³ Neutron Moisture Logging System

Log Run	1	2 Repeat	5	6 Repeat	9
Shield (Y/N)	N	N	N	N	N
MSA Interval (ft)	1.0	1.0	1.0	1.0	1.0
Log Speed (ft/min)	N/A	N/A	N/A	N/A	N/A
Pre-Verification	C9513FTB2017 0601AV00CAB 1	C9513FTB2017 0601AV00CAB 1	C9513FTB2017 0824AV00CAB 1	C9513FTB2017 0824AV00CAB 1	C9513FTB2017 0831AV00CAB 1
Start File	AD000000	BD003701	AD004100	BD013000	AD015800
Finish File	AD004201	BD004201	AD015902	BD014201	AD023501
Post-Verification	C9513FTB2017 0601BV00CAA 1	C9513FTB2017 0601BV00CAA 1	C9513FTB2017 0824BV00CAA 1	C9513FTB2017 0824BV00CAA 1	C9513FTB2017 0831BV00CAA 1
Depth Return Error (in.)	N/A	0.0	N/A	3.0 high	N/A
Comments	Fine gain adjustment made after 29 ft	No fine gain adjustments made	Gain adjustment after file 56	No fine gain adjustments made	No fine gain adjustments made

Log Run	10	11 Repeat			
HEIS Number	1020015	1020016			
Date	08/31/17	08/31/17			
Logging Engineer	Felt/Meisner	Felt/Meisner			
Start Depth (ft)	235.0	230.0			
Finish Depth (ft)	239.01	238.0			
Count Time (sec)	200	200			
Live/Real	R	R			
Shield (Y/N)	N	N			
MSA Interval (ft)	1.0	1.0			
Log Speed (ft/min)	N/A	N/A			
Pre-Verification	C9513FTB2017 0831AV00CAB 1	C9513FTB2017 0831AV00CAB 1			
Start File	BD023500	CD023000			
Finish File	BD023901	CD023800			
Post-Verification	C9513FTB2017 0831BV00CAA 1	C9513FTB2017 0831BV00CAA 1			
Depth Return Error (in.)	N/A	5.0 high			
Comments	No fine gain adjustments made	No fine gain adjustments made			

NMLS Log Run Information

Log Run	3	4 Repeat	7	8 Repeat	12
HEIS Number	1020017	1020018	1020019	1020020	1020021
Date	06/05/17	06/05/17	08/24/17	08/24/17	09/05/17
Logging Engineer	Spatz/McClellan	Spatz/McClellan	Spatz/McClellan	Spatz/McClellan	Felt
Start Depth (ft)	0.0	36.0	41.0	130.0	158.0
Finish Depth (ft)	42.76	42.0	159.02	142.01	239.02
Count Time (sec)	15	15	15	15	15

Log Run	3	4 Repeat	7	8 Repeat	12
Live/Real	R	R	R	R	R
Shield (Y/N)	N	N	N	N	N
MSA Interval (ft)	0.25	0.25	0.25	0.25	0.25
Log Speed (ft/min)	N/A	N/A	N/A	N/A	N/A
Pre-Verification	C9513FPB20170 605AV00CAB1	C9513FPB20170 605AV00CAB1	C9513FPB20170 824AV00CAB1	C9513FPB20170 824AV00CAB1	C9513FPB20170 905AV00CAB1
Start File	AD000000	BD003600	AD004100	BD013000	AD015800
Finish File	AD004276	BD004200	AD015902	BD014201	AD023902
Post-Verification	C9513FPB20170 605BV00CAA1	C9513FPB20170 605BV00CAA1	C9513FPB20170 824BV00CAA1	C9513FPB20170 824BV00CAA1	C9513FPB20170 905BV00CAA1
Depth Return Error (in.)	N/A	High 0.5	N/A	2.0 high	N/A
Comments	None	None	None	None	None

Log Run	13 Repeat				
HEIS Number	1020022				
Date	09/05/17				
Logging Engineer	Felt				
Start Depth (ft)	225.0				
Finish Depth (ft)	233.0				
Count Time (sec)	15				
Live/Real	R				
Shield (Y/N)	N				
MSA Interval (ft)	0.25				
Log Speed (ft/min)	N/A				
Pre-Verification	C9513FPB20170 905AV00CAB1				
Start File	BD022500				
Finish File	BD023300				
Post-Verification	C9513FPB20170 905BV00CAA1				
Depth Return Error (in.)	1.0 high				
Comments	None				

Logging Operation Notes

A centralizer was not installed on the SGLS and NMLS sondes. The sondes were enveloped in plastic sleeving to prevent potential contamination.

Analysis Notes

Analyst	P.D. Henwood	Date	09/21/17
Reference(s)	SGRP-PRO-OP-53040, Rev. 0; SGRP-PRO-OP-53051, Rev. 0		

A combined casing correction of 0.807-in. was applied to the SGLS data to 11.9 ft and 0.557-in. to 43 ft. Casing corrections for a 1/4-in. thick casing were applied for the remainder of the borehole. No corrections were applied for the thicker casing joints associated with the sonic casing where the maximum thickness varies from 0.42-in. to 0.5-in and results in lower concentrations at 10-ft intervals.

No water correction was applied in this borehole as groundwater was not reached.

SGLS spectra were processed in batch mode in APTEC SUPERVISOR to identify individual energy peaks and determine count rates. Concentrations for the SGLS were calculated in an EXCEL template identified as ftB20170216, using an efficiency function and corrections for casing and dead time as determined by annual calibrations.

An interpreted data set was created for this borehole. Depth overlaps from consecutive log runs or where two casings existed were removed from 41 and 42 ft and from 158 and 159 ft. This results in a data set where only one data point is presented for each depth.

NMLS data are reported in counts per second.

HGU⁴ is an empirical unit of gamma activity proposed as a means to standardize gamma log response across multiple logging systems with different response characteristics. The HGU is defined in terms of measurements in the Hanford Borehole Calibration Facility, and the magnitude is selected such that 1 HGU is approximately equivalent to typical Hanford background activity, based on data from background samples as reported in *Hanford Site Background: Part 2, Soil Background for Radionuclides* (DOE/RL-96-12).

Results and Interpretations

Cs-137 and manmade uranium (Pa-234 [U-238] and U-235) were detected in this borehole. Cs-137 was detected at 30, 31, 52, 53 and 55 ft. The maximum concentration was approximately 1 pCi/g at 30 ft.

Pa-234m was detected at 29 and 30 ft, from 36 to 42 ft, and a few other intermittent depth locations deeper in the borehole. The maximum concentration was measured at 34 pCi/g at 38 ft. U-235 was measured at intermittent depths throughout the borehole with a maximum concentration measured at 3 pCi/g at 42 ft in depth.

Radon inside the casing is evident from 115 to 160 ft in depth where the Bi-214 energy peaks (609 and 1764 keV) used to assay naturally occurring uranium diverge in concentration.

The neutron moisture log primarily responds to moisture present in the surrounding formation. In general, an increase in count rate reflects an increase in moisture content. Moisture content may increase in sediments of relatively high silt or clay content. The depth interval from ground surface to 12 ft was logged within two casings.

The manmade, KUT, and moisture repeat plots indicate that the respective systems were working properly. The manmade repeat suggests some variation. The repeat data acquired at 500 seconds rather than 200 seconds probably reflect the most accurate concentrations.

List of Log Plots

Depth Reference is ground surface.

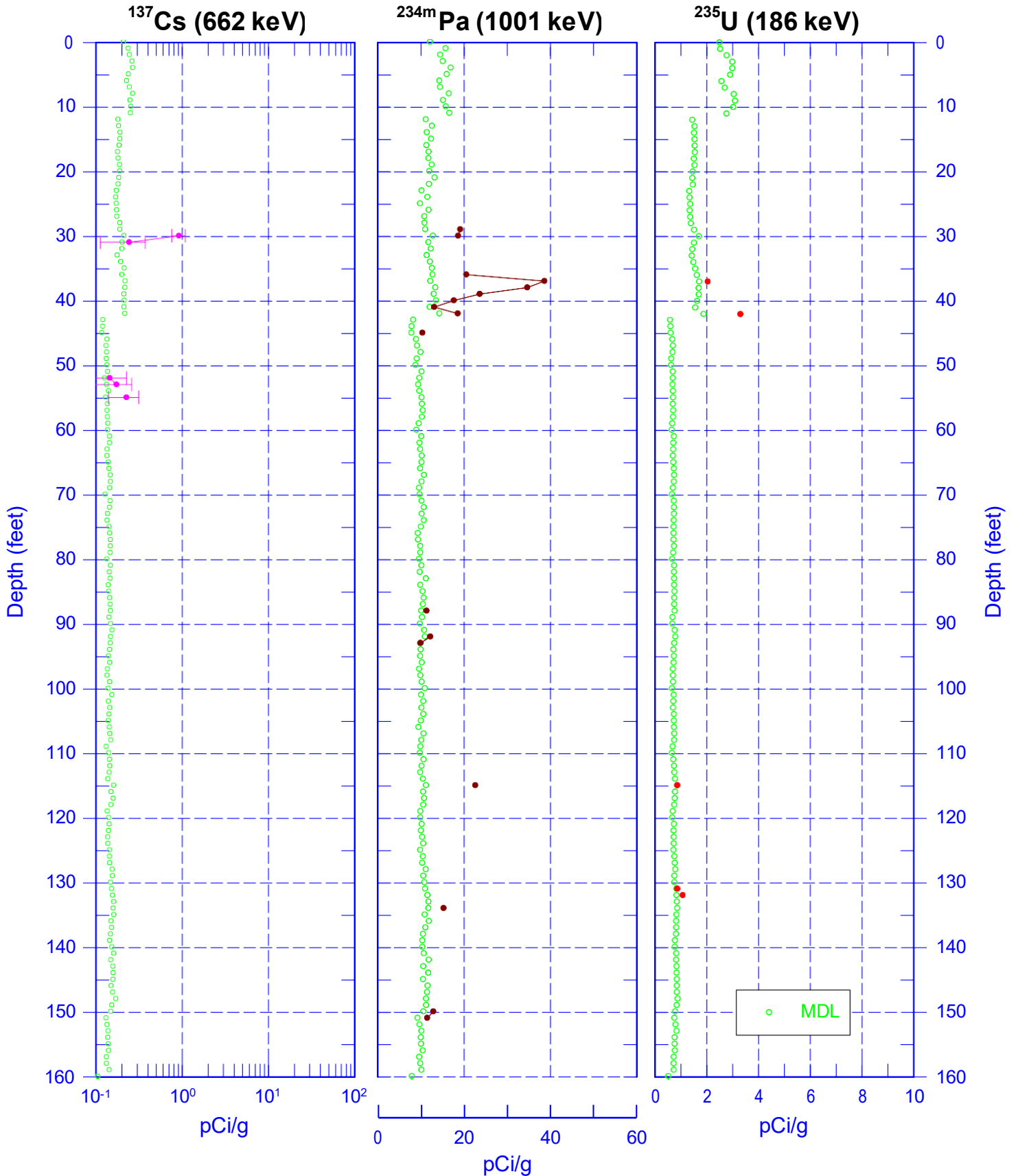
Manmade Radionuclides (0-160 ft)
 Manmade Radionuclides (150-310 ft)
 Natural Gamma Logs (0-160 ft)
 Natural Gamma Logs (150-310 ft)
 Combination Plot (0-120 ft)
 Combination Plot (120-240 ft)
 Combination Plot (0-250 ft)
 Total Gamma & Moisture (0-160 ft)
 Total Gamma & Moisture (150-310 ft)
 Total Gamma & Hanford Gamma Unit (0-250 ft)
 Manmade Radionuclides Repeat (36-43 ft)
 Repeat Section of Natural Gamma Logs (37-43 ft)
 Repeat Section of Natural Gamma Logs (130-143 ft)
 Repeat Section of Natural Gamma Logs (230-238 ft)
 Moisture Repeat Section (36-42 ft)
 Moisture Repeat Section (130-142 ft)
 Moisture Repeat Section (225-233 ft)

⁴ Hanford Gamma Unit



C9513

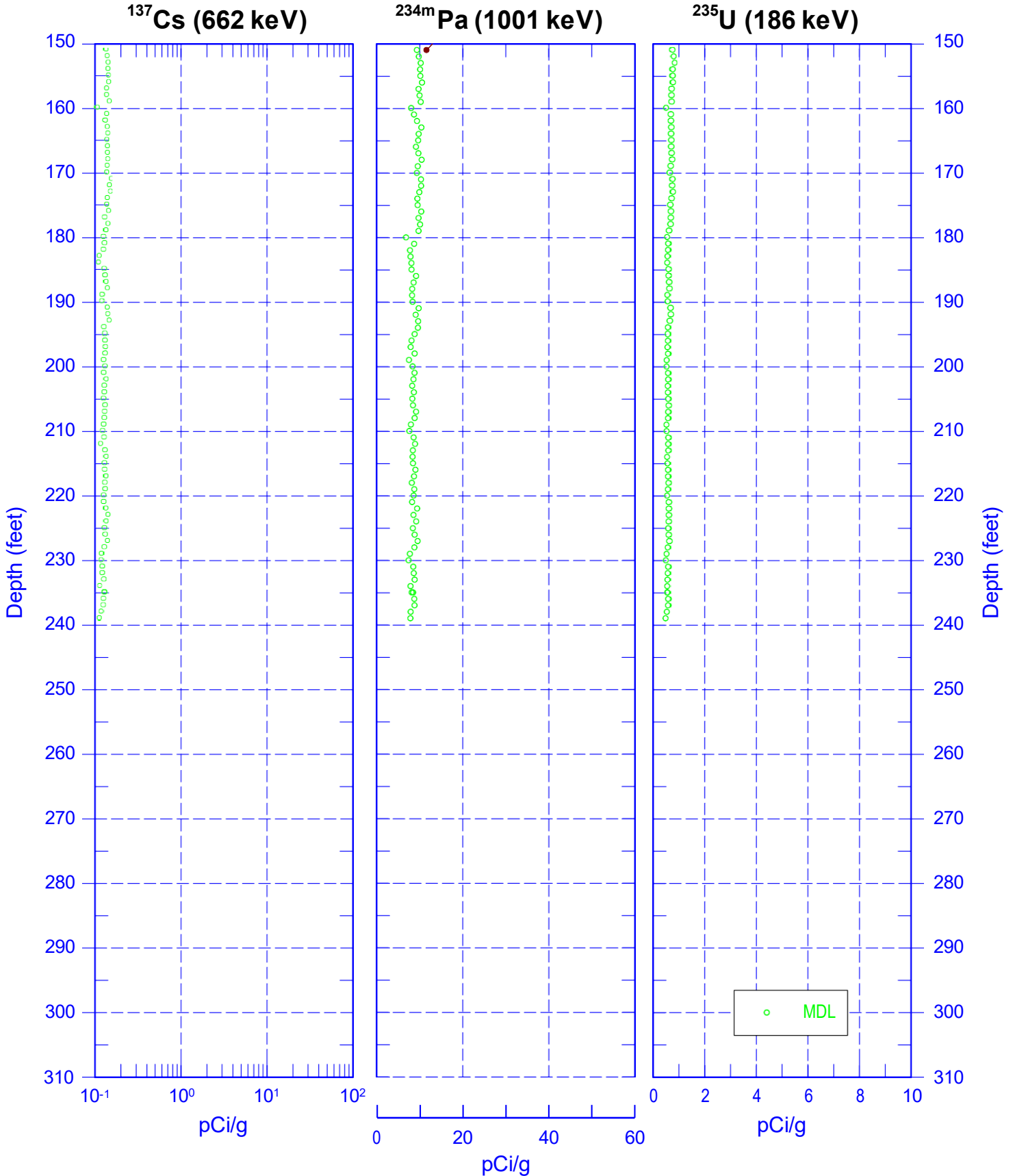
Manmade Radionuclides



Zero Reference - Ground Surface



C9513 Manmade Radionuclides

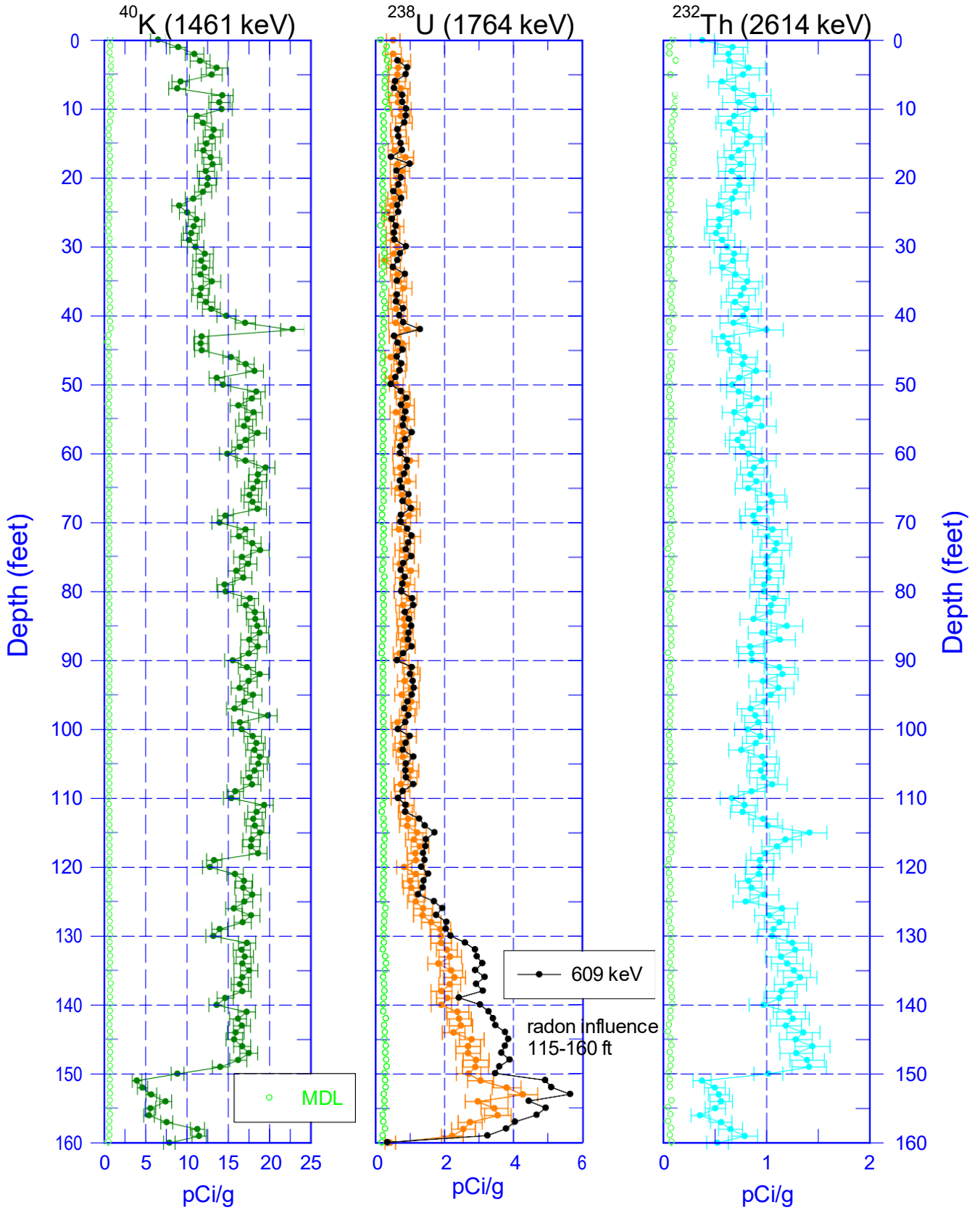


Zero Reference - Ground Surface



Stoller Newport News Nuclear
A Subsidiary of Huntington Ingalls Industries

C9513 Natural Gamma Logs

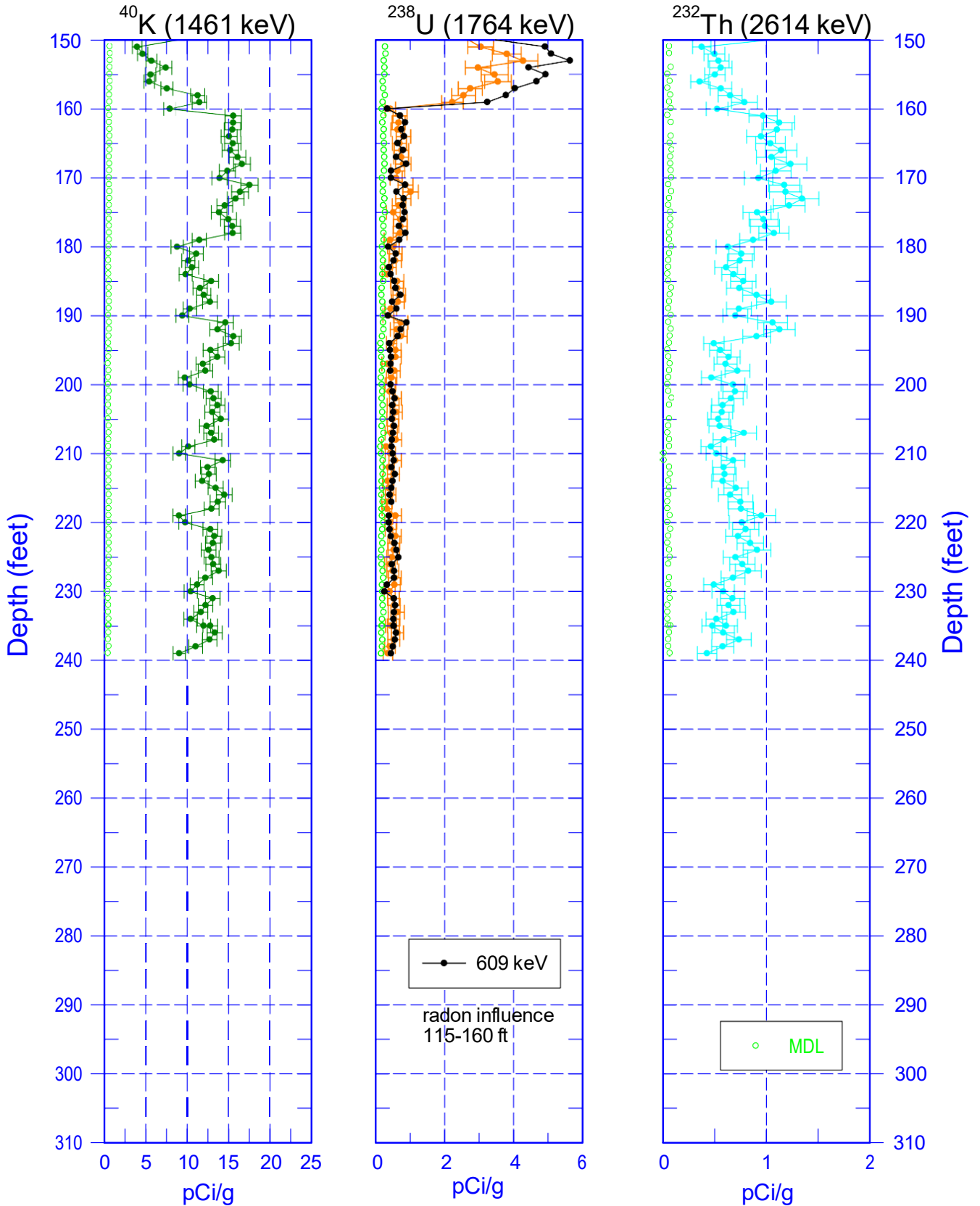


Zero Reference - Ground Surface



Stoller Newport News Nuclear
A Subsidiary of Huntington Ingalls Industries

C9513 Natural Gamma Logs



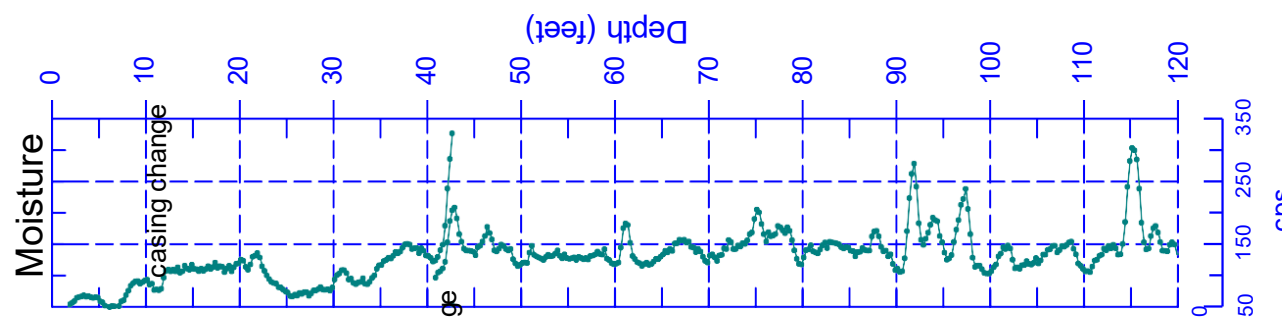
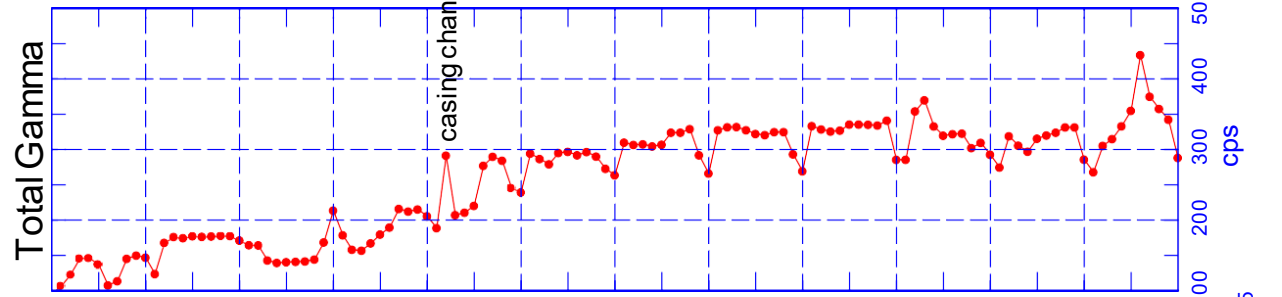
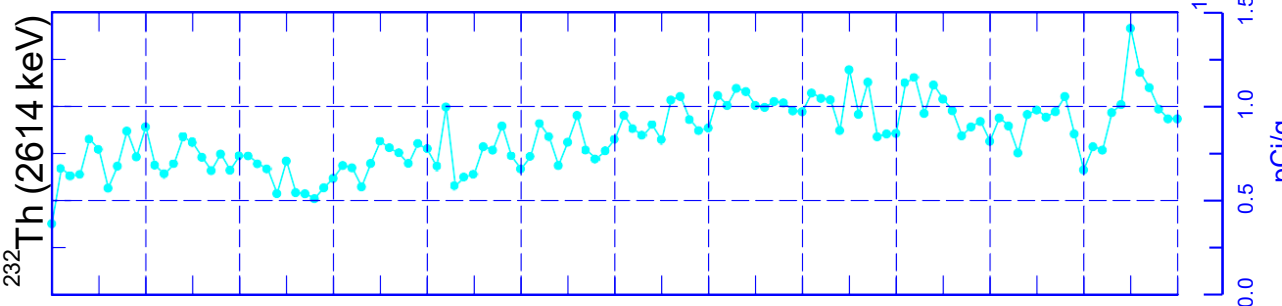
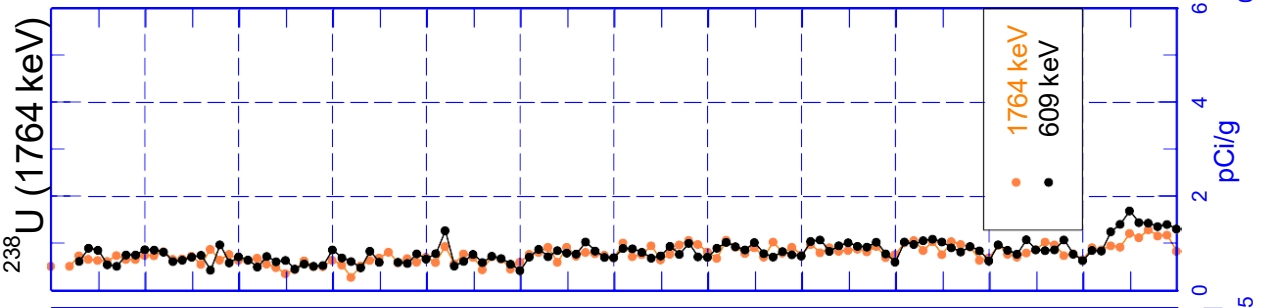
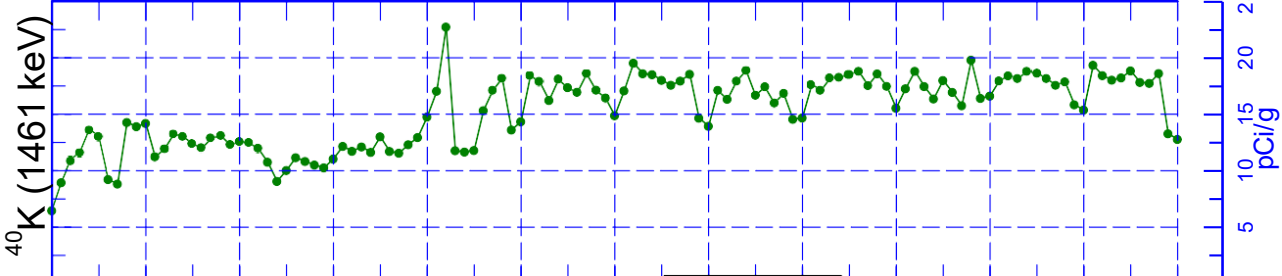
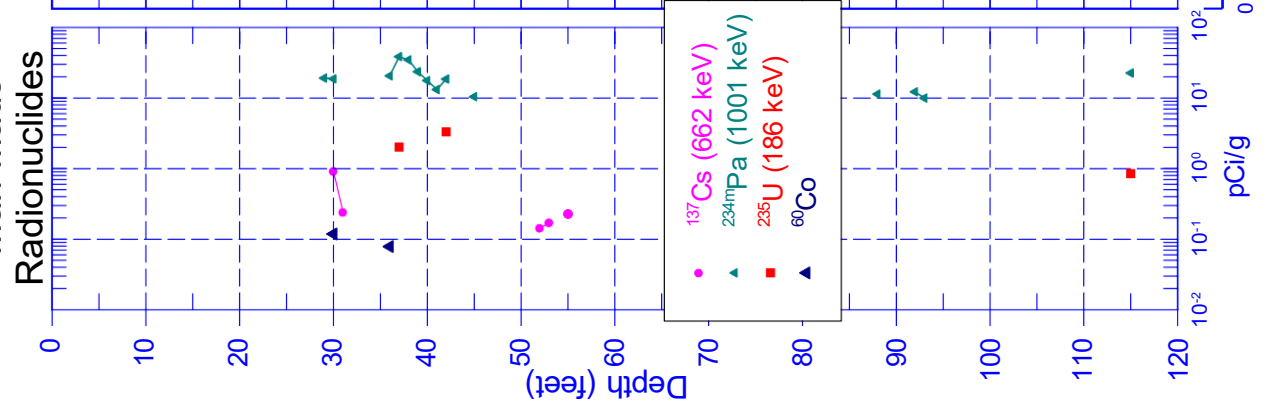
Zero Reference - Ground Surface

C9513 Combination Plot



Stoller Newport News Nuclear
A Subsidiary of Huntington Ingalls Industries

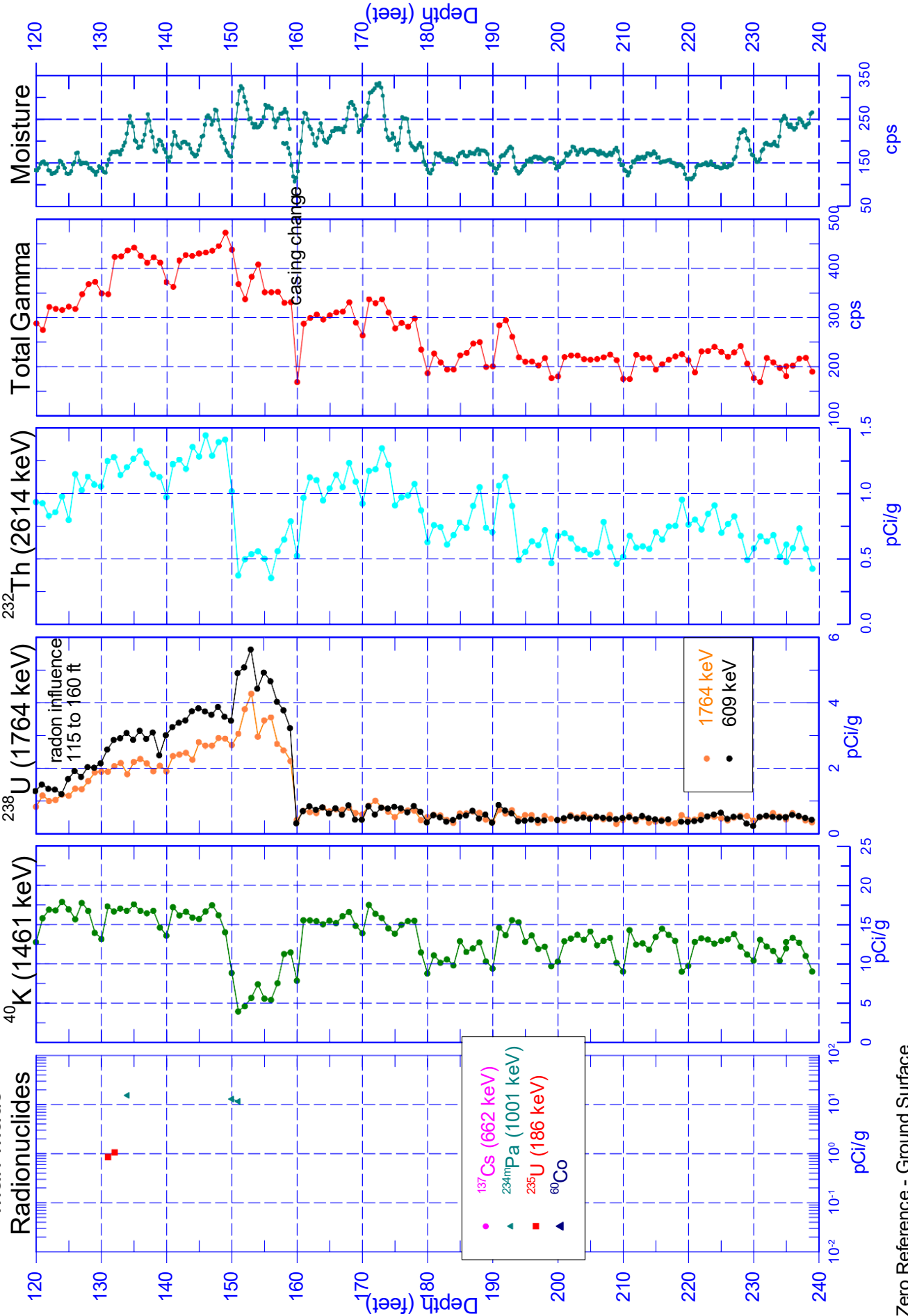
Man-Made Radionuclides





C9513 Combination Plot

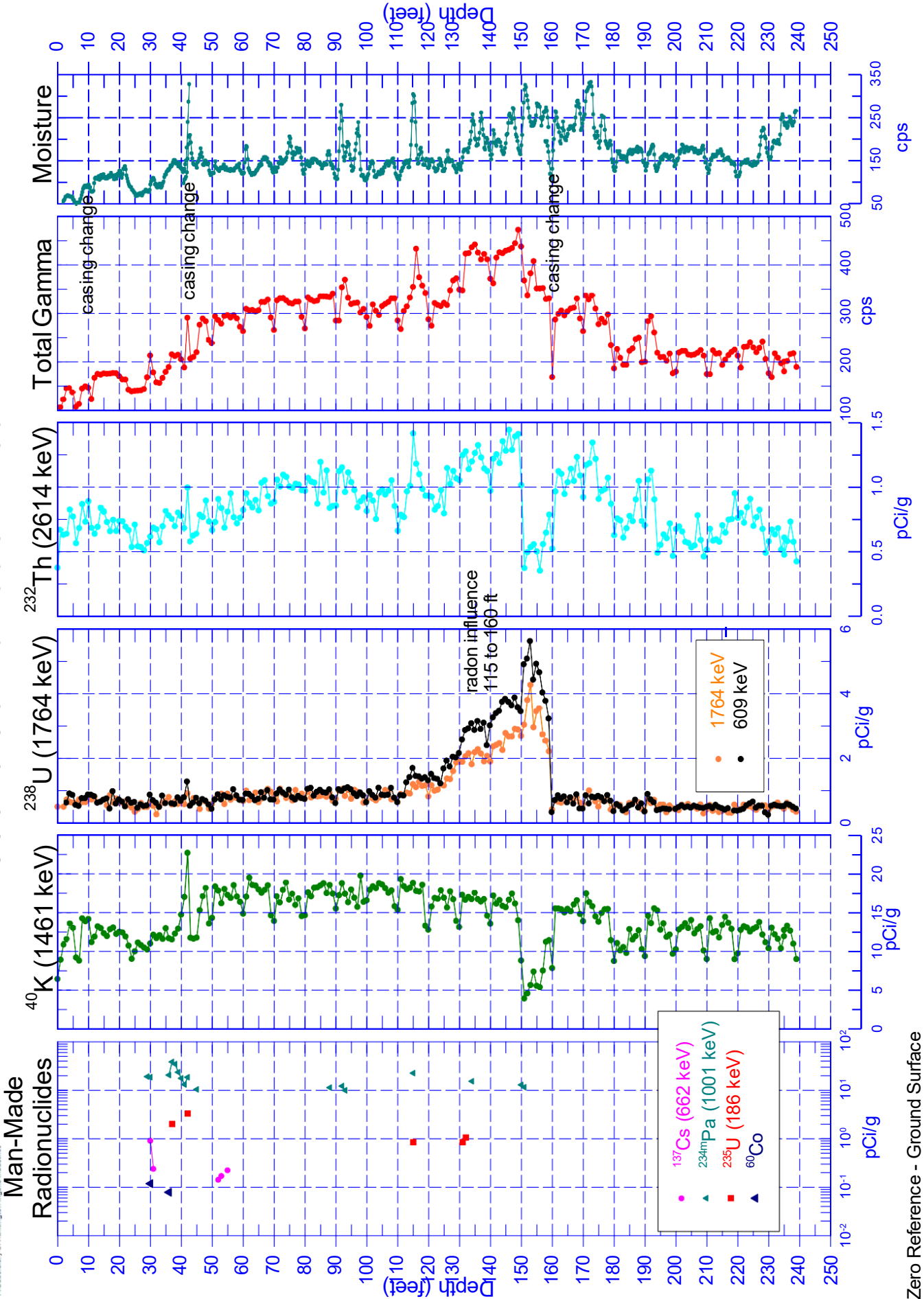
Man-Made Radionuclides



Zero Reference - Ground Surface



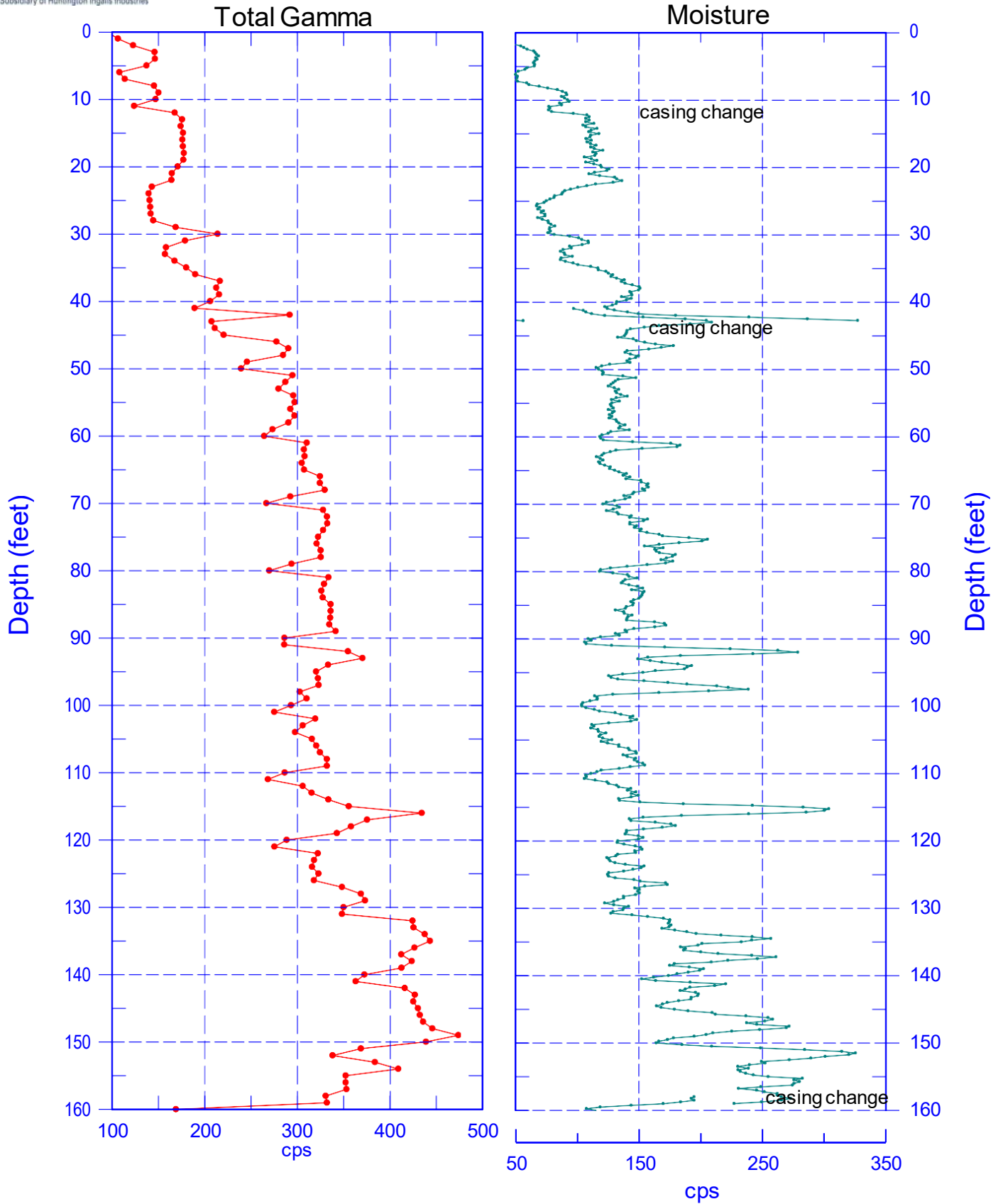
C9513 Combination Plot





C9513

Total Gamma & Moisture

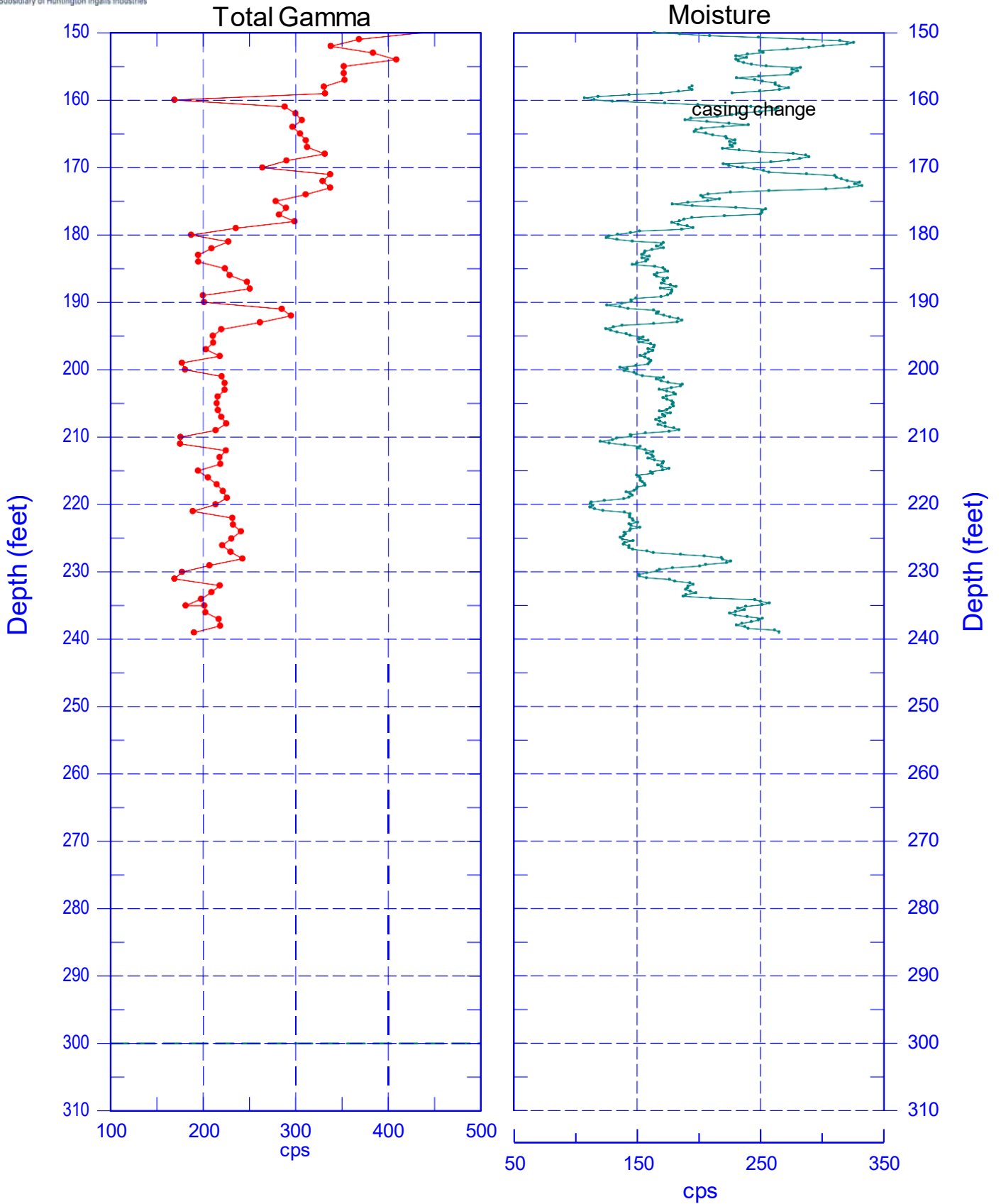


Zero Reference - Ground Surface



C9513

Total Gamma & Moisture

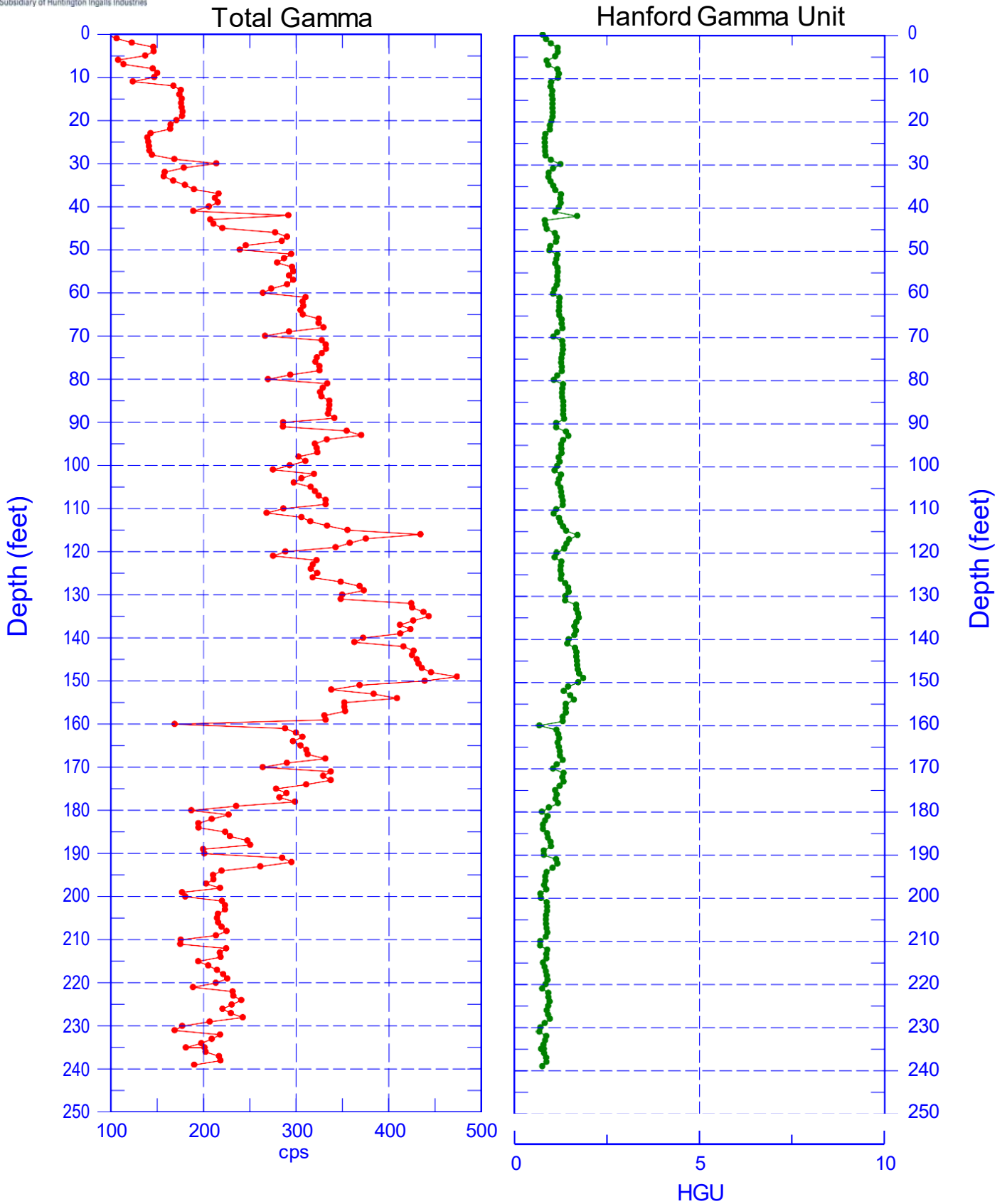


Zero Reference - Ground Surface



C9513

Total Gamma & Hanford Gamma Unit

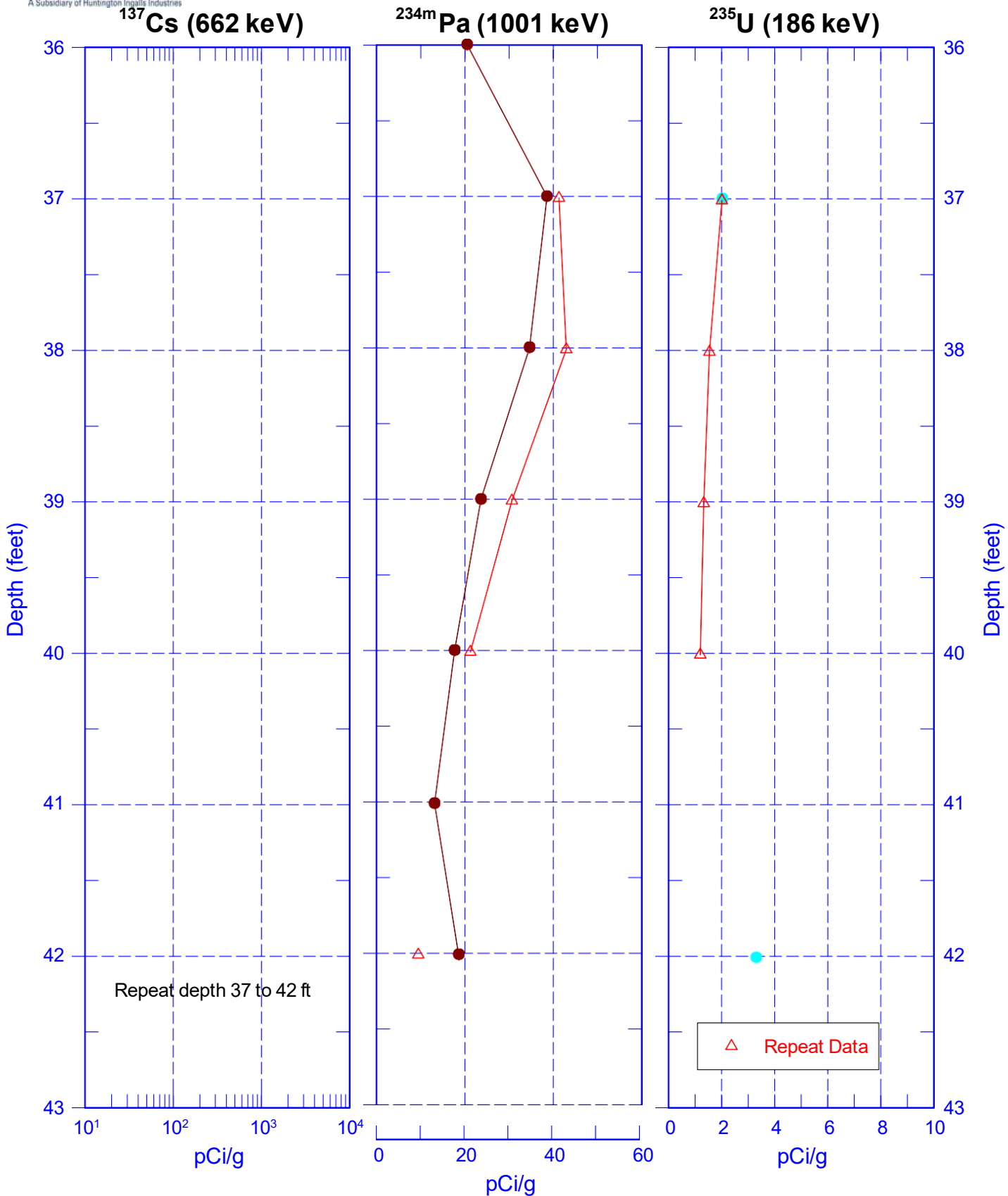


Zero Reference - Ground Surface



Stoller Newport News Nuclear
A Subsidiary of Huntington Ingalls Industries

C9513 Manmade Radionuclides Repeat



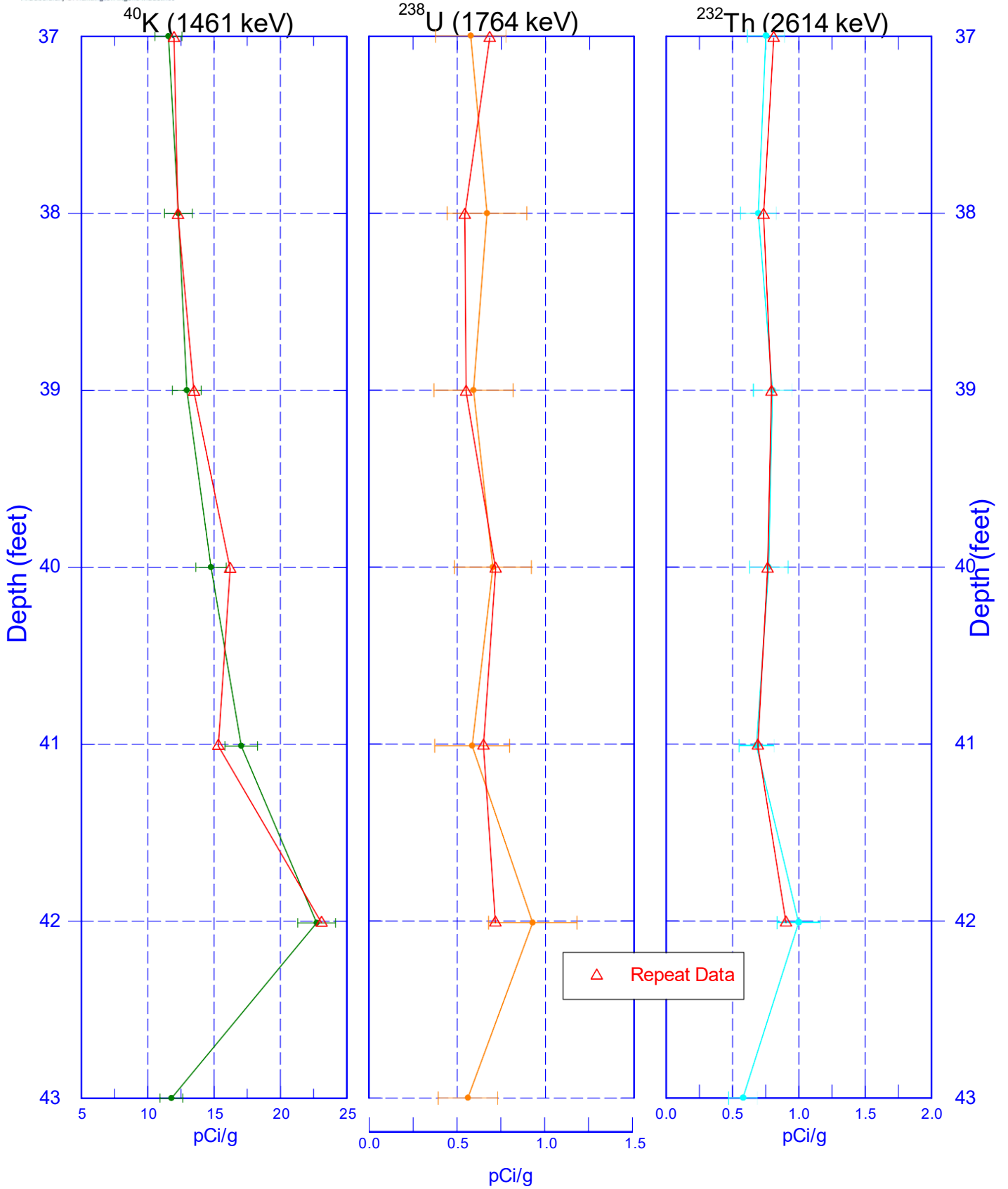
Zero Reference - Ground Surface



Stoller Newport News Nuclear
A Subsidiary of Huntington Ingalls Industries

C9513

Repeat Section of Natural Gamma Logs



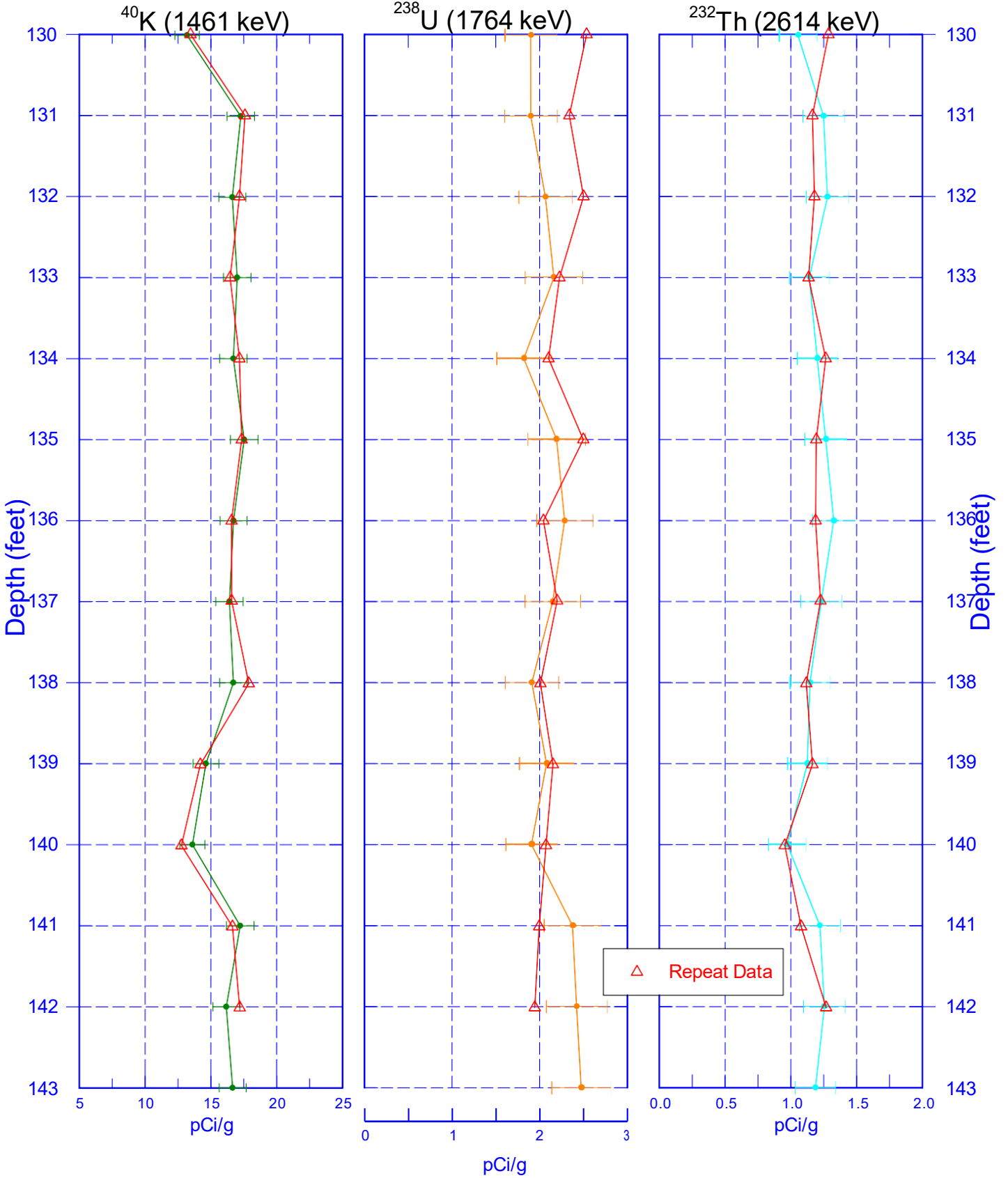
Zero Reference - Ground Surface



Stoller Newport News Nuclear
A Subsidiary of Huntington Ingalls Industries

C9513

Repeat Section of Natural Gamma Logs



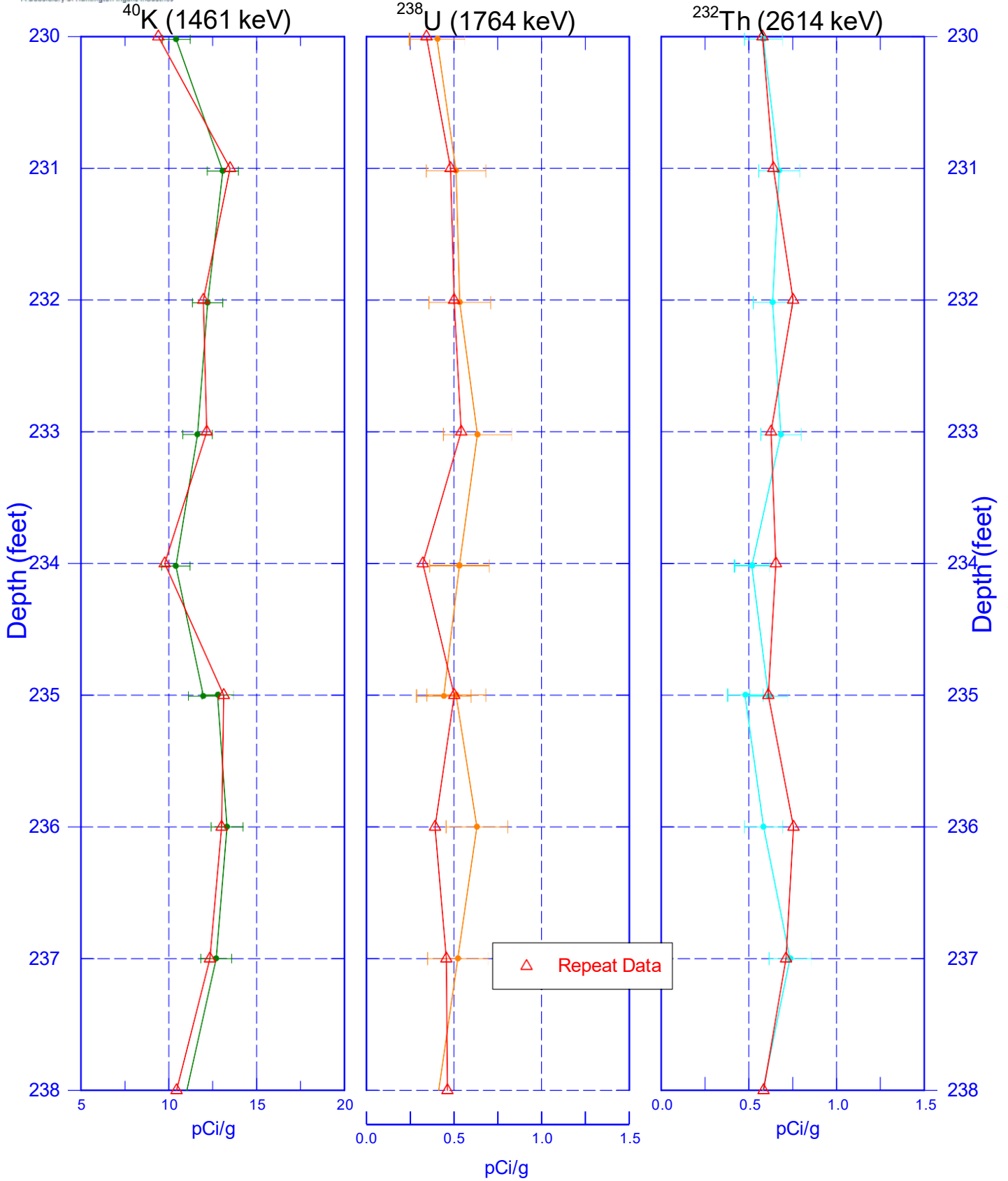
Zero Reference - Ground Surface



Stoller Newport News Nuclear
A Subsidiary of Huntington Ingalls Industries

C9513

Repeat Section of Natural Gamma Logs

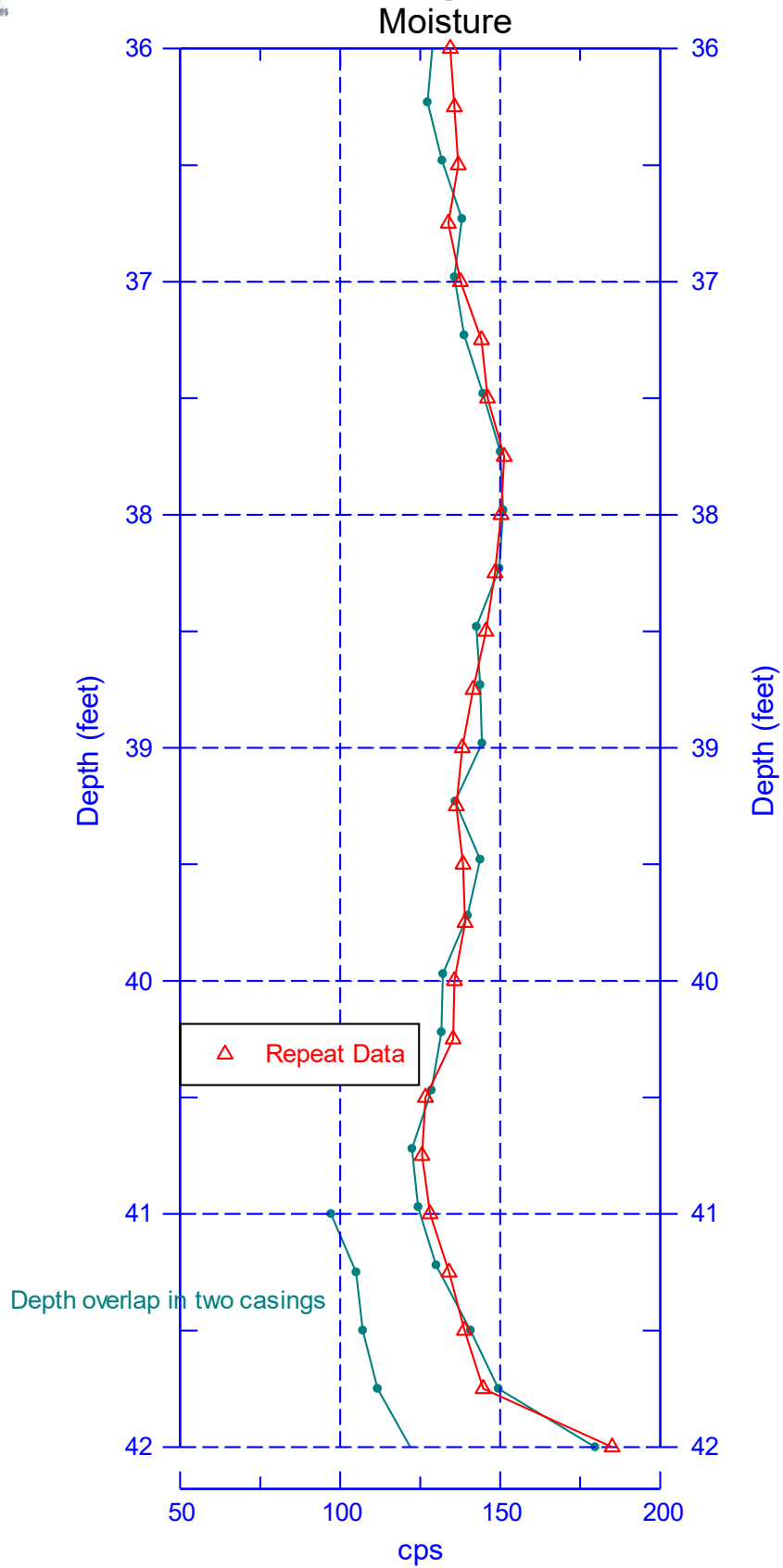


Zero Reference - Ground Surface



C9513

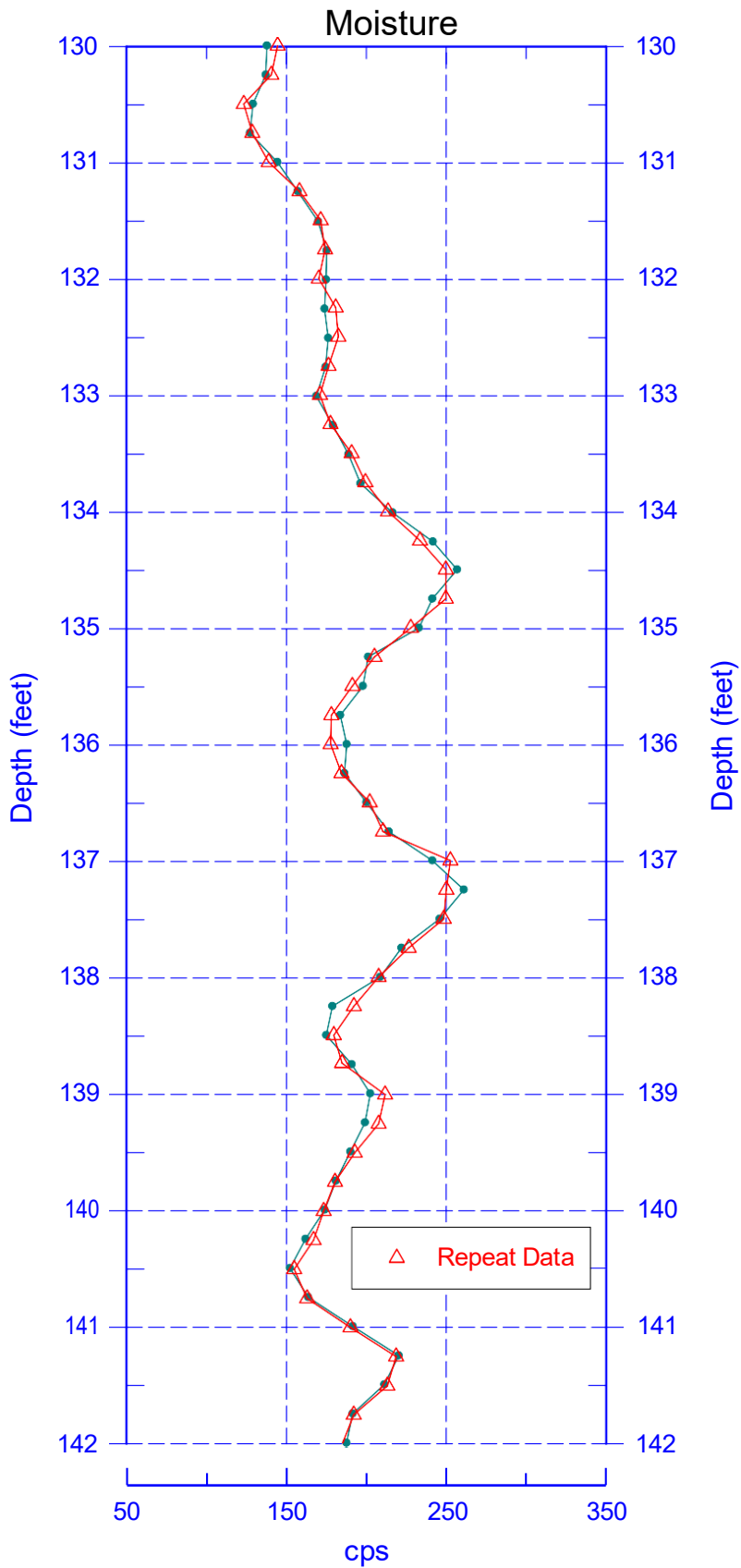
Moisture Repeat Section



Zero Reference - Ground Surface



C9513 Moisture Repeat Section

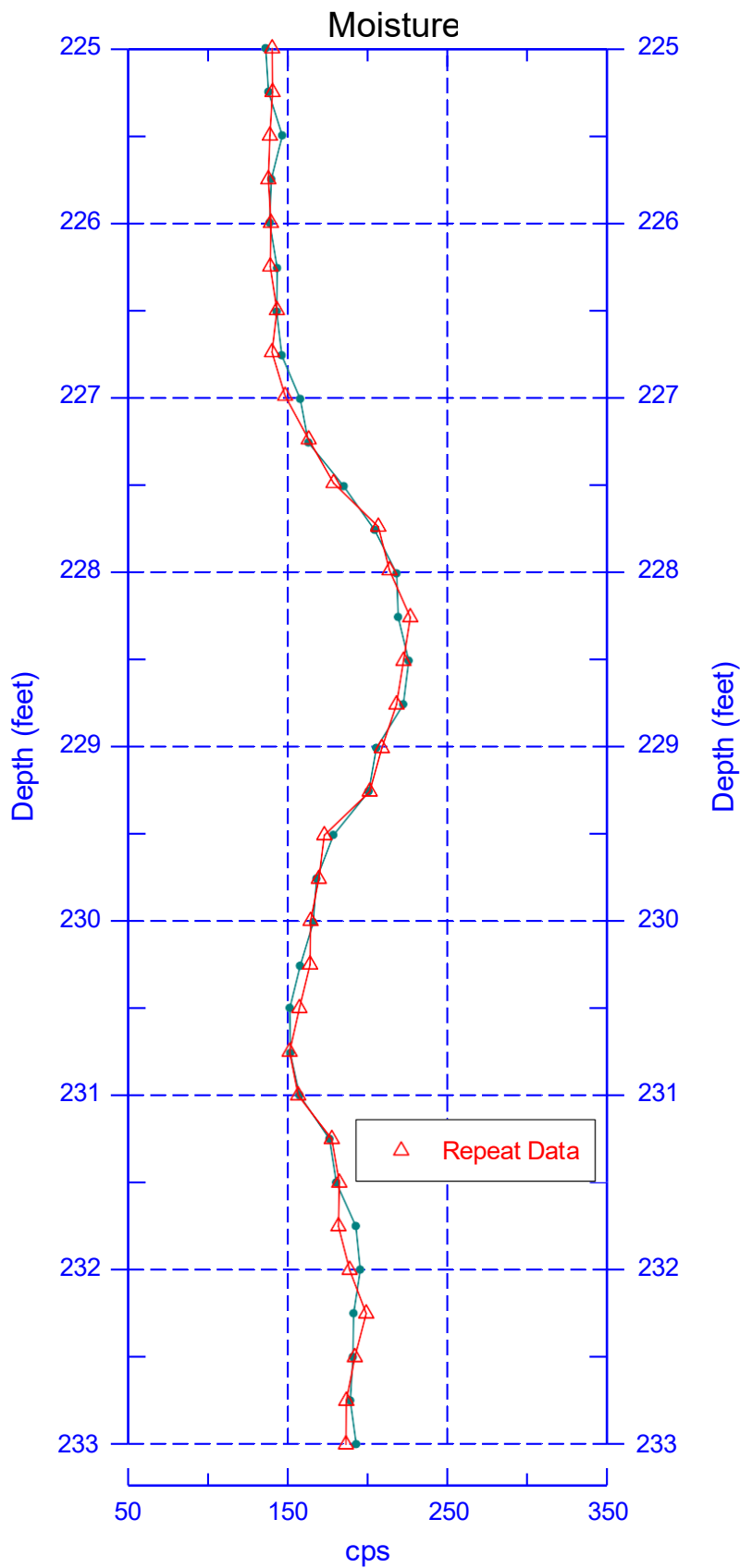


Zero Reference - Ground Surface



C9513

Moisture Repeat Section



Zero Reference - Ground Surface



Stoller Newport News Nuclear

C9514 Log Data Report

Borehole Information

Log Date	2016-07-25	Filename	C9514_HG-NM_2016-07-25	Site	216-S-21 (200-DV-1)
Coordinates (WA StPlane)		DTW¹ (ft)	N/A	DTW Date	07/21/16
North (m)	East (m)	Drill Date	TO C² Elevation		Total Depth (ft)
N/A	N/A	07/21/16	N/A		127.6

Casing Information

Casing Type	Drill Type	Stickup (ft)	Diameter (in.)		Thickness (in.)	Top (ft)	Bottom (ft)
			Outer	Inside			
Threaded Steel	Becker Hammer	0.2	8 5/8	7 3/8	5/8	-0.3	44
Threaded Steel	Sonic	-1.5	6.0	5.0	1/2	+1.5	127.5

Borehole Notes

Drill depth and casing depth were provided by the wellsite geologist. A Becker Hammer push method was used to 44 ft. Subsequent drilling was completed using a Sonic drilling method to total depth. Casing stick up and diameter were measured by the logging engineer. The maximum logging depth achieved was 127.26 ft. Zero reference is ground surface.

Logging Equipment Information

Logging System	Gamma 5Tb	Type	60% HPGe SGLS ³
Effective Calibration Date	02/23/16	Serial No.	54-TP13441B
Calibration Reference	HGLP-CC-136, Rev. 0	Logging Procedure	SGRP-RRO-OP-53023, Rev. 0

Logging System	Gamma 5Pb	Type	NMLS ⁴
Effective Calibration Date	04/15/15	Serial No.	H34055445
Calibration Reference	HGLP-CC-116, Rev. 0	Logging Procedure	SGRP-PRO-OP-53024, Rev. 0

Logging System	Gamma 5Tb	Type	60% HPGe SGLS
Effective Calibration Date	02/23/16	Serial No.	54-TP13441B
Calibration Reference	HGLP-CC-136, Rev. 1	Logging Procedure	SGRP-RRO-OP-53023, Rev. 0

Logging System	Gamma 5Pb	Type	NMLS
Effective Calibration Date	05/02/16	Serial No.	H34055445
Calibration Reference	HGLP-CC-140, Rev. 0a	Logging Procedure	SGRP-PRO-OP-53024, Rev. 0

Logging System	Gamma 5Cb	Type	HRLS ⁵
Effective Calibration Date	07/30/15	Serial No.	39A314
Calibration Reference	HGLP-CC-123, Rev. 0	Logging Procedure	SGRP-PRO-OP-53050, Rev. 0

¹ depth to water inside casing

² top of casing

³ Spectral Gamma Logging System

⁴ Neutron Moisture Logging System

⁵ High Rate Logging System

A SUBSIDIARY OF HUNTINGTON INGALLS INDUSTRIES

2439 Robertson Drive • Richland, WA 99354 • Telephone (509) 946-6455 •

www.stoller.com


Stoller Newport News Nuclear
SGLS Log Run Information

Log Run	1	2	3	4 Repeat	11
HEIS Number	1019653	N/A	1019654	1019655	1019662
Date	04/11/16	04/11/16	04/11/16	04/11/16	07/25/16
Logging Engineer	Spatz	Spatz	Spatz	Spatz	Felt
Start Depth (ft)	0.0	21.0	29.0	39.0	42.0
Finish Depth (ft)	24.01	30.02	43.0	42.0	126.01
Count Time (sec)	100	20	100	100	200
Live/Real	R	R	R	R	R
Shield (Y/N)	NA	NA	NA	NA	N
MSA Interval (ft)	1.0	1.0	1.0	1.0	1.0
Log Speed (ft/min)	NA	NA	NA	NA	NA
Pre-Verification	C9514FTb20160 411AV00CAB1	C9514FTb20160 411AV00CAB1	C9514FTb20160 411AV00CAB1	C9514FTb20160 411AV00CAB1	C9514FTb20160 725AV00CAB1
Start File	AD000000	BD002100	CD002900	DD003900	AD004200
Finish File	AD002401	BD003002	CD004300	DD004200	AD012601
Post-Verification	EV00CAA1	EV00CAA1	EV00CAA1	EV00CAA1	BV00caa1
Depth Return Error (in.)	NA	NA	NA	high 2 1/2	NA
Comments	No fine gain adjustments made				

Log Run	12 Repeat				
HEIS Number	1019663				
Date	07/25/16				
Logging Engineer	Felt				
Start Depth (ft)	91.0				
Finish Depth (ft)	100.01				
Count Time (sec)	200				
Live/Real	R				
Shield (Y/N)	N				
MSA Interval (ft)	1.0				
Log Speed (ft/min)	NA				
Pre-Verification	C9514FTb20160 725AV00CAB1				
Start File	BD009100				
Finish File	BD010001				
Post-Verification	BV00CAA1				
Depth Return Error (in.)	high 3				
Comments	No fine gain adjustments made				


Stoller Newport News Nuclear
NMLS Log Run Information

Log Run	5	6 Repeat	9	10 Repeat	
HEIS Number	1019656	1019657	1019660	1019661	
Date	04/11/16	04/11/16	07/21/16	07/21/16	
Logging Engineer	Spatz	Spatz	Meisner/ McClellan/Felt	Felt	
Start Depth (ft)	0.0	37.0	42.0	111.0	
Finish Depth (ft)	43.25	42.0	127.26	120.0	
Count Time (sec)	15	15	15	15	
Live/Real	R	R	R	R	
Shield (Y/N)	NA	NA	NA	NA	
MSA Interval (ft)	0.25	0.25	0.25	0.25	
Log Speed (ft/min)	NA	NA	NA	NA	
Pre-Verification	C9514FPb20160 411AV00CAB1	C9514FPb20160 411AV00CAB1	C9514FPb20160 721AV00CAB1	C9514FPb20160 721AV00CAB1	
Start File	AD000000	BD003700	AD004200	BD011100	
Finish File	AD004325	BD004200	AD012726	BD012000	
Post-Verification	BV00CAA1	BV00CAA1	BV00caa1	BV00caa1	
Depth Return Error (in.)	NA	high 1/2	NA	high 2	
Comments	None	None	None	None	

HRLS Log Run Information

Log Run	7	8 Repeat			
HEIS Number	1019658	1019659			
Date	04/11/16	04/11/16			
Logging Engineer	Spatz/Felt	Spatz/Felt			
Start Depth (ft)	22.0	23.0			
Finish Depth (ft)	29.0	24.0			
Count Time (sec)	300	300			
Live/Real	R	R			
Shield (Y/N)	NA	NA			
MSA Interval (ft)	1.0	1.0			
Log Speed (ft/min)	NA	NA			
Pre-Verification	C9514FTb20160 411AV00CAB1	C9514FTb20160 411AV00CAB1			
Start File	AD002200	BD002300			
Finish File	AD002900	BD002400			
Post-Verification	BV00CAA1	BV00CAA1			
Depth Return Error (in.)	NA	high 1/2			
Comments	No fine gain adjustments made	No fine gain adjustments made			



Stoller Newport News Nuclear

Logging Operation Notes

A centralizer was installed on the sondes during logging of the first casing string. No centralizer was used during logging of the second casing string due to the smaller internal diameter of the casing. The sondes were sleeved in 4 mil plastic during each log run of the second casing string in order to prevent potential contamination of equipment.

Pre- and post-survey verification measurements met the acceptance criteria for the established systems.

Analysis Notes

Analyst	K. J. Felt	Date	09/16/16
Reference(s)	SGRP-PRO-OP-53040, Rev. 0; SGRP-PRO-OP-53051, Rev. 0		

SGLS spectra were processed in batch mode in APTEC SUPERVISOR to identify individual energy peaks and determine count rates. Concentrations were calculated in an EXCEL template identified as ftb_20160223_CC136, using an efficiency function and corrections for casing and dead time as determined during annual response checks.

A casing correction for a 5/8-in. thick casing was applied for the first Becker Hammer push to 43 ft. A correction for a 1/2-in. thick casing was applied for the remainder of the borehole drilled by the Sonic drill.

NMLS data are reported in counts per second.

An interpreted data set was created for this borehole. Log run 2 was not used due to the shorter count times associated with the log run as well as the availability of HRLS data in that depth interval. Generally, 20 second count times with the SGLS are used to define an interval of high activity that will be subsequently logged with the HRLS. Where two casings and depth overlaps occur at 42 and 43 ft, values collected during logging of the first casing string have been retained and data from the second casing string have been removed from the final interpreted data set.

The HGU⁶ is an empirical unit of gamma activity proposed as a means to standardize gamma log response across multiple logging systems with different response characteristics. The HGU is defined in terms of measurements in the Hanford Borehole Model Facility, and the magnitude is selected such that 1 HGU is approximately equivalent to typical Hanford background activity, based on data from background samples as reported in *Hanford Site Background Part 2, Soil Background for Radionuclides* (DOE/RL-96-12).

Results and Interpretations

Cs-137 was detected at 1, 14, and 16 ft, as well as nearly continuously from 21 to 56 ft. A maximum concentration of approximately 37,500 pCi/g was measured at 24 ft. Though not detected, MDLs are plotted for processed uranium (Pa-234m [U-238] and U-235).

Casing joints are evident by reduced count rates for the moisture and gamma measurements at 10-ft intervals beginning at 47 ft.

The neutron moisture log primarily responds to moisture present in the surrounding formation. In general, an increase in count rate reflects an increase in moisture content. Moisture content may increase in sediments of relatively high silt or clay content.

The manmade, KUT, and moisture repeat plots indicate that the respective systems were working properly.

⁶Hanford Gamma Unit



Stoller Newport News Nuclear

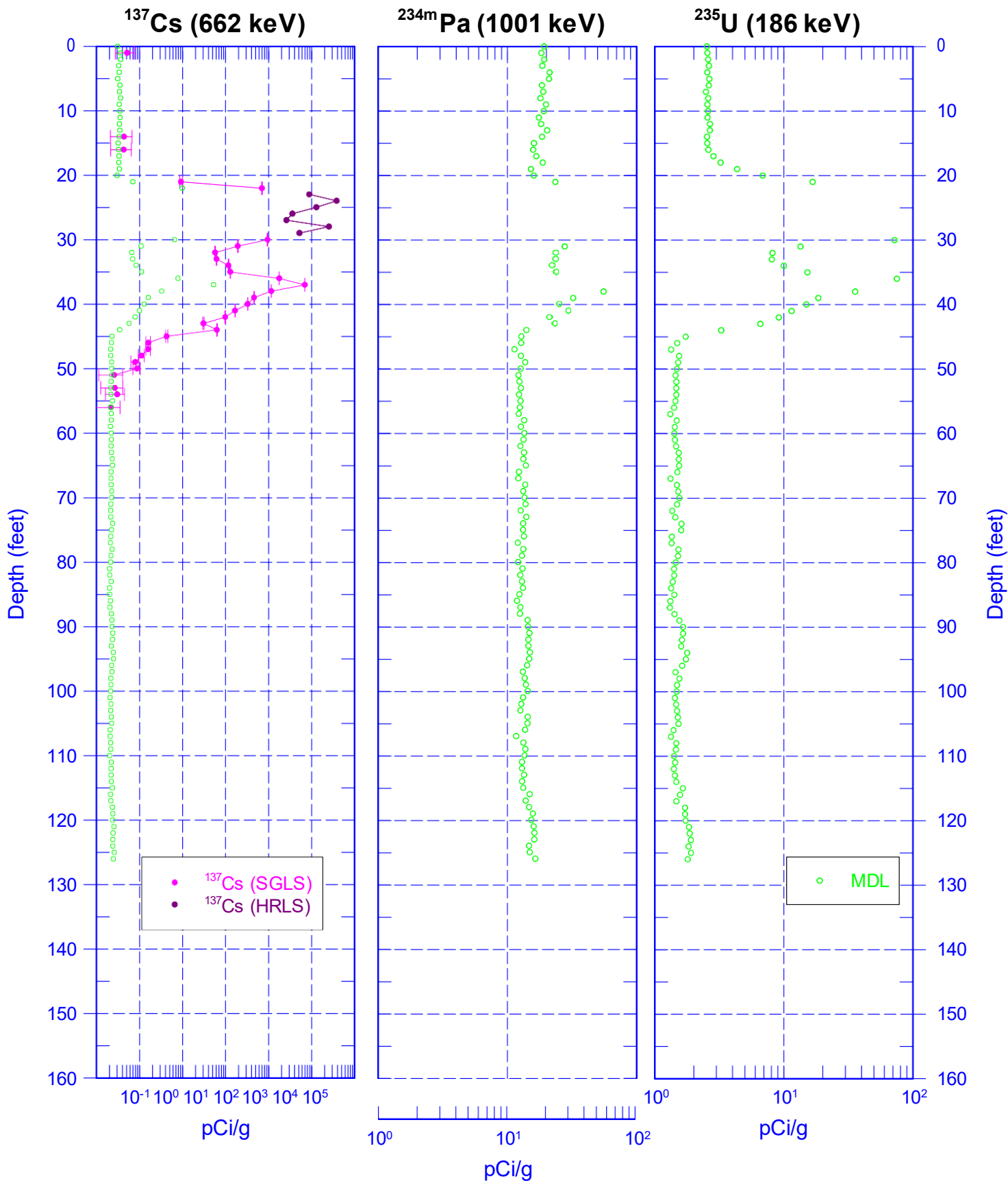
List of Log Plots

Depth Reference is ground surface.

- Manmade Radionuclides (0-160 ft)
- Natural Gamma Logs (0-160 ft)
- Combination Plot (0-120 ft)
- Combination Plot (110-230 ft)
- Combination Plot (0-130 ft)
- Total Gamma & Moisture (0-160 ft)
- Total Gamma & Hanford Gamma Unit (0-160 ft)
- Repeat Section of Manmade Radionuclides (38-43 ft)
- Repeat Section of Natural Gamma Logs (38-43 ft)
- Repeat Section of Natural Gamma Logs (90-101 ft)
- Moisture Repeat Section (36-43 ft)
- Moisture Repeat Section (110-121 ft)



C9514 Manmade Radionuclides

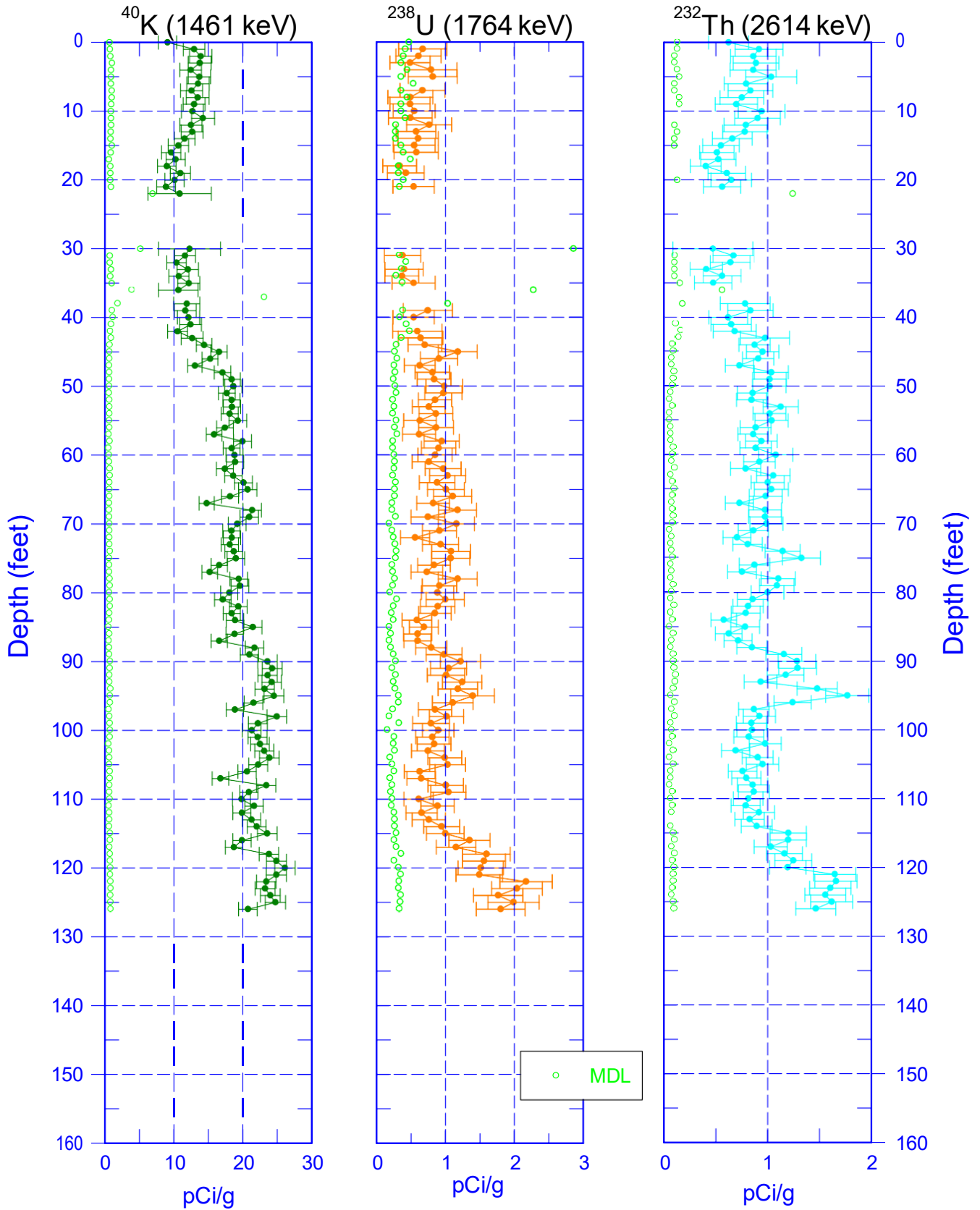


Zero Reference - Ground Surface



Stoller Newport News Nuclear
A Subsidiary of Huntington Ingalls Industries

C9514 Natural Gamma Logs



Zero Reference - Ground Surface

Depth (feet)

C9514 Combination Plot



Stoller Newport News Nuclear
A Subsidiary of Huntington Ingalls Industries

Man-Made
Radionuclides

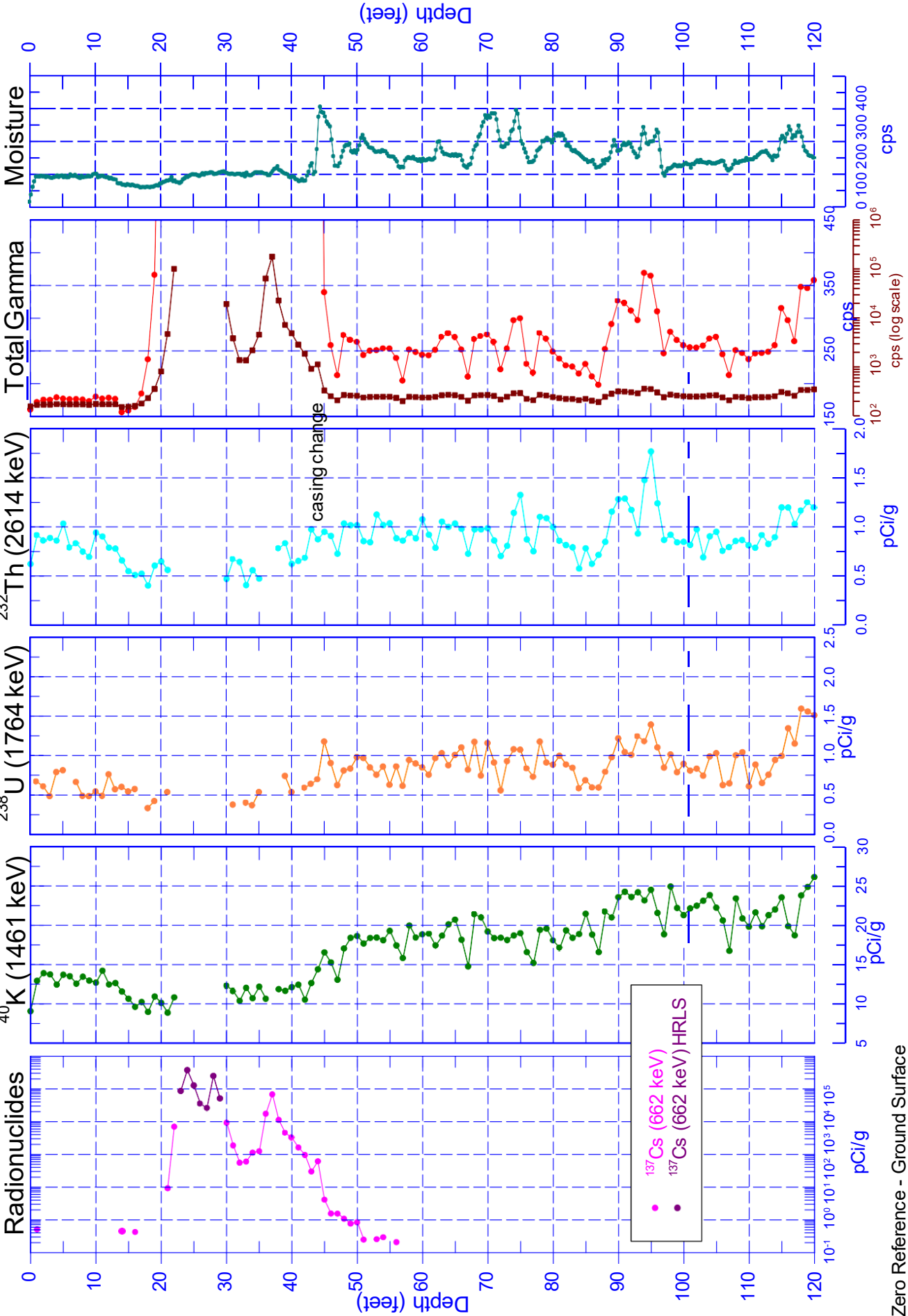
⁴⁰K (1461 keV)

²³⁸U (1764 keV)

²³²Th (2614 keV)

Total Gamma

Moisture

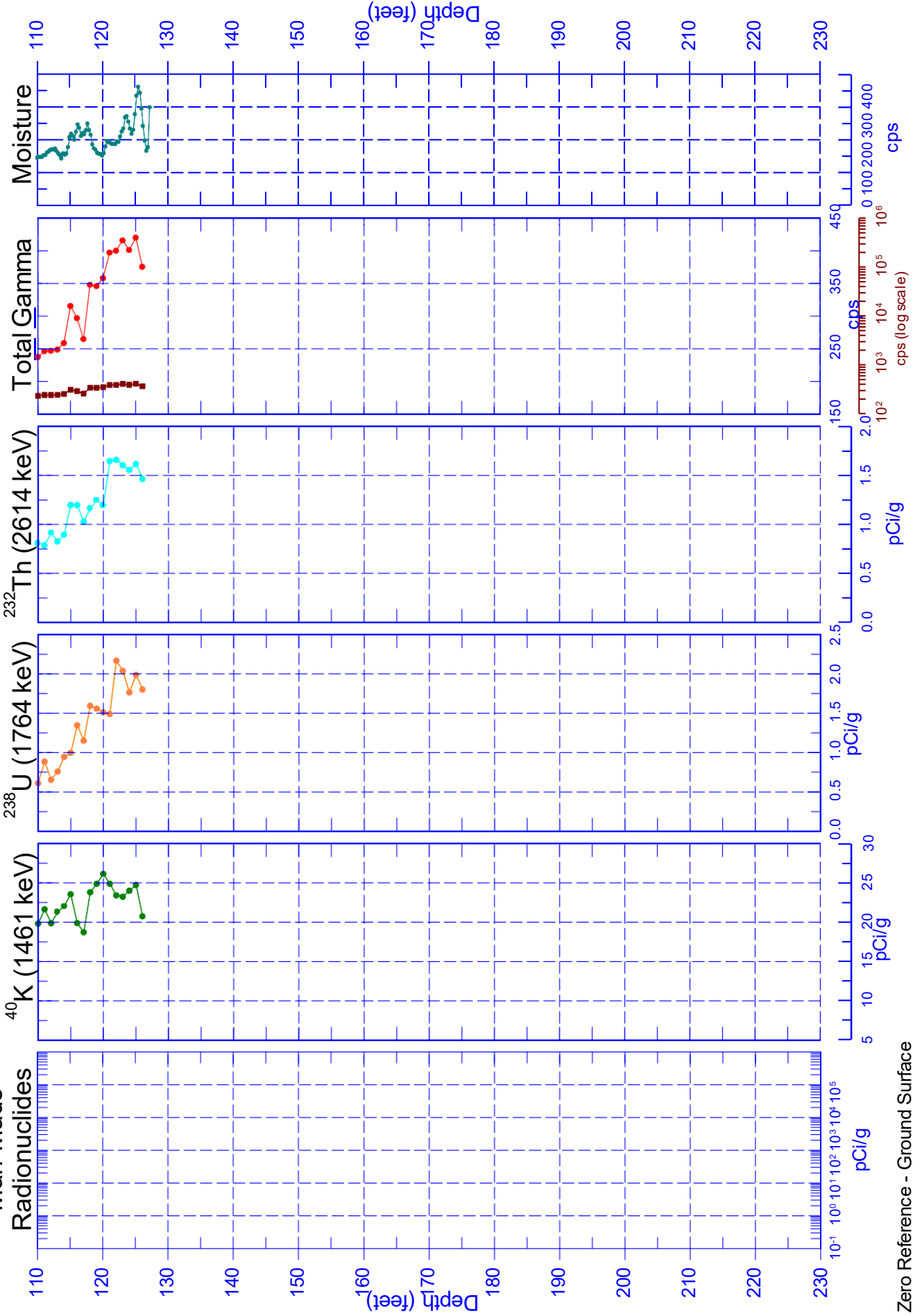




Stoller Newport News Nuclear
A Subsidiary of Huntington Ingalls Industries

C9514 Combination Plot

Man-Made
Radionuclides



Zero Reference - Ground Surface

Depth (feet)

C9514 Combination Plot



Stoller Newport News Nuclear
A Subsidiary of Huntington Ingalls Industries

Man-Made
Radionuclides

¹³⁷Cs (662 keV) HRLS
¹³⁷Cs (662 keV) HRLS

⁴⁰K (1461 keV)
²³⁸U (1764 keV)
²³²Th (2614 keV)
Total Gamma
Moisture

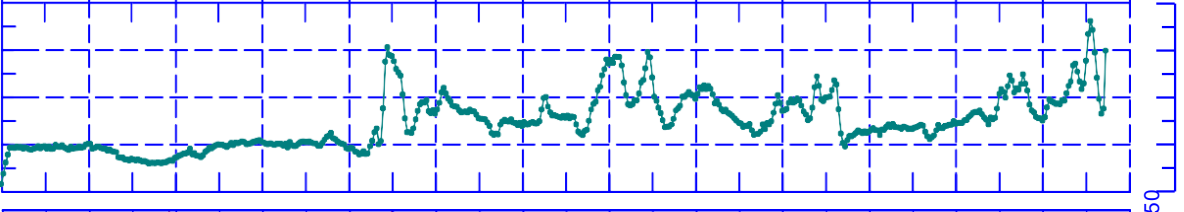
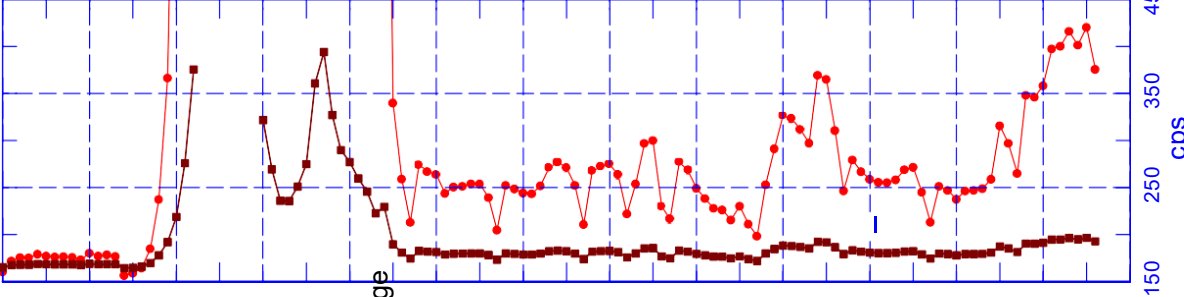
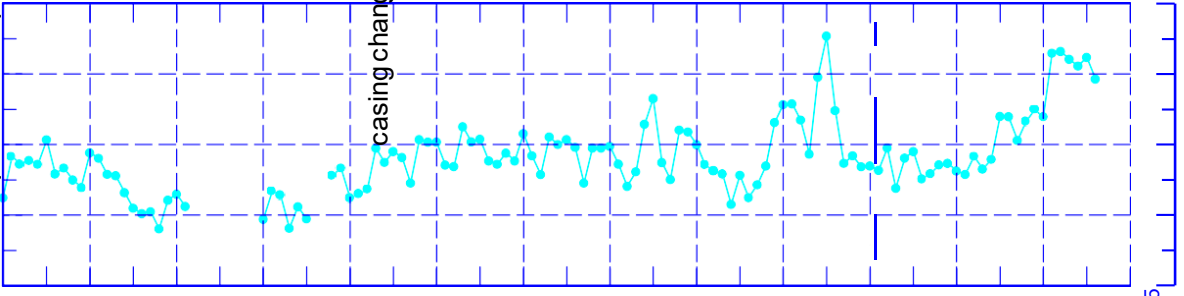
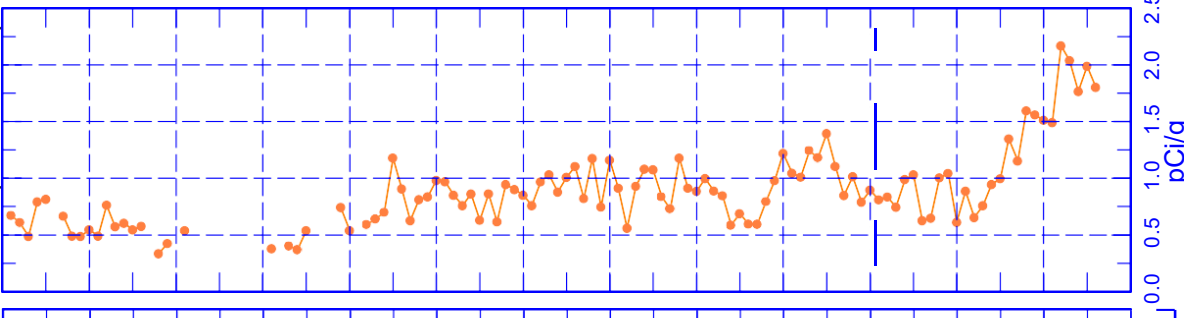
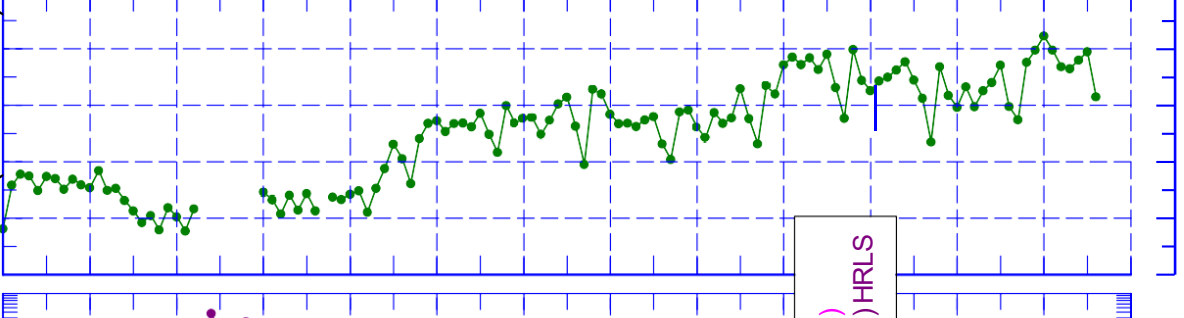
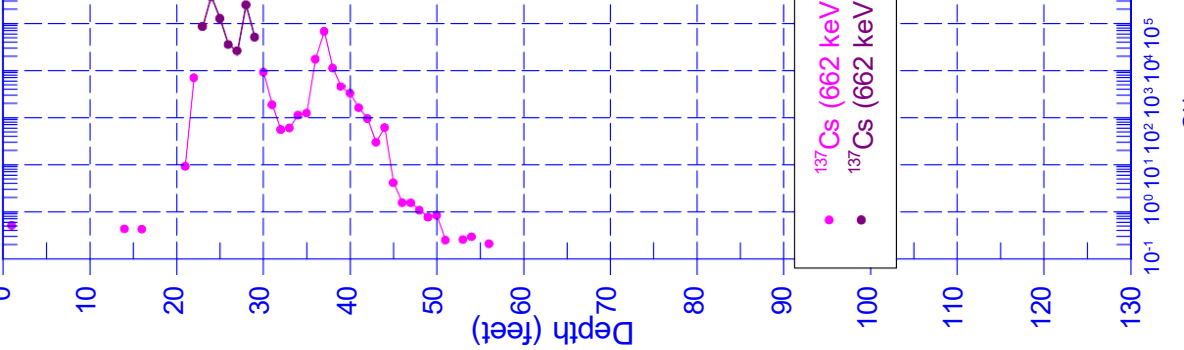
Depth (feet)

0 10 20 30 40 50 60 70 80 90 100 110 120 130

0 5 10 15 20 25 30 35 40 45 50 55 60 65 70 75 80 85 90 95 100 105 110 115 120 125 130

0 10² 10³ 10⁴ 10⁵ 10⁶ 2.0 450

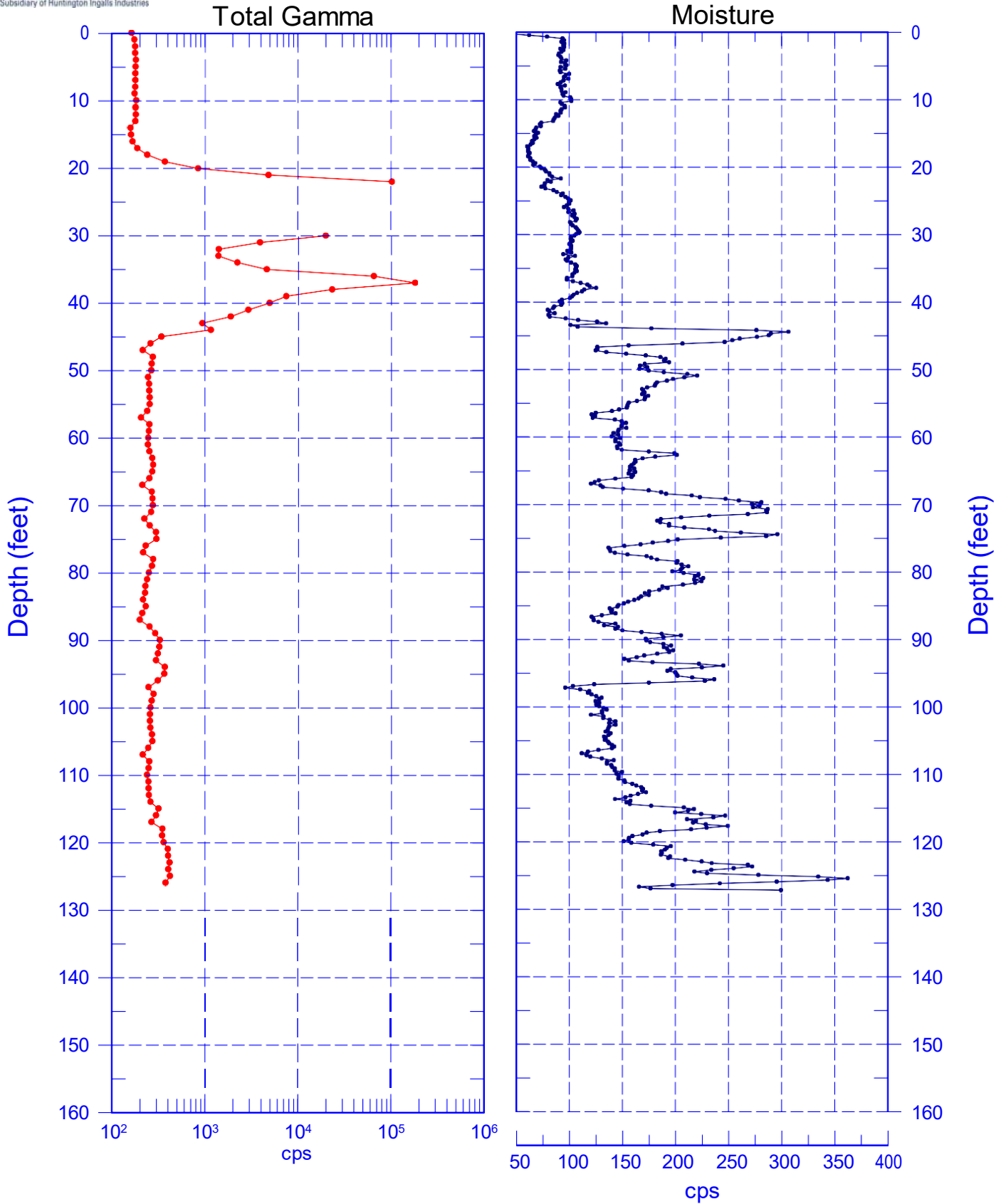
0 100 200 300 400 cps





C9514

Total Gamma & Moisture



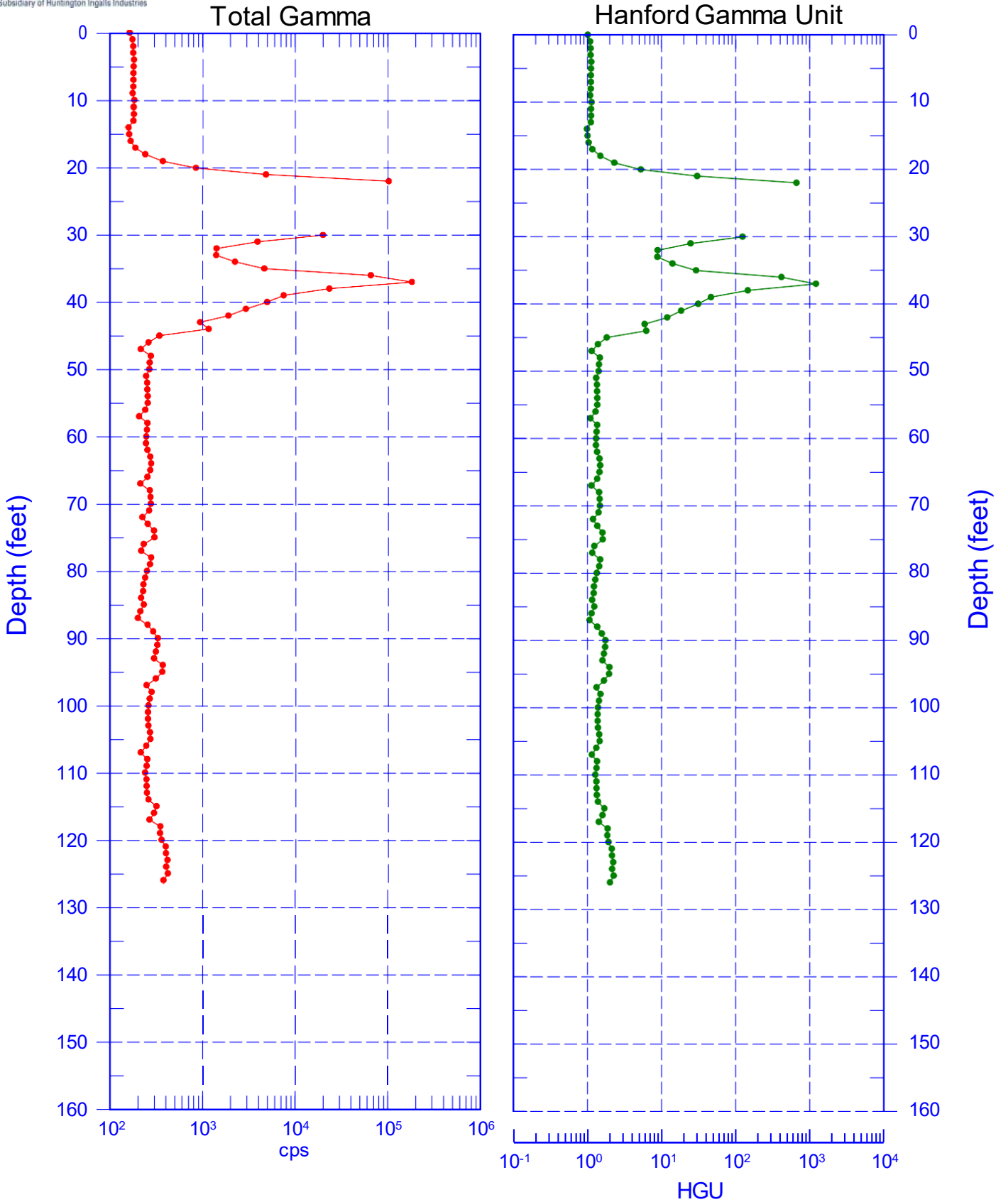
Zero Reference - Ground Surface



Stoller Newport News Nuclear
A Subsidiary of Huntington Ingalls Industries

C9514

Total Gamma & Hanford Gamma Unit



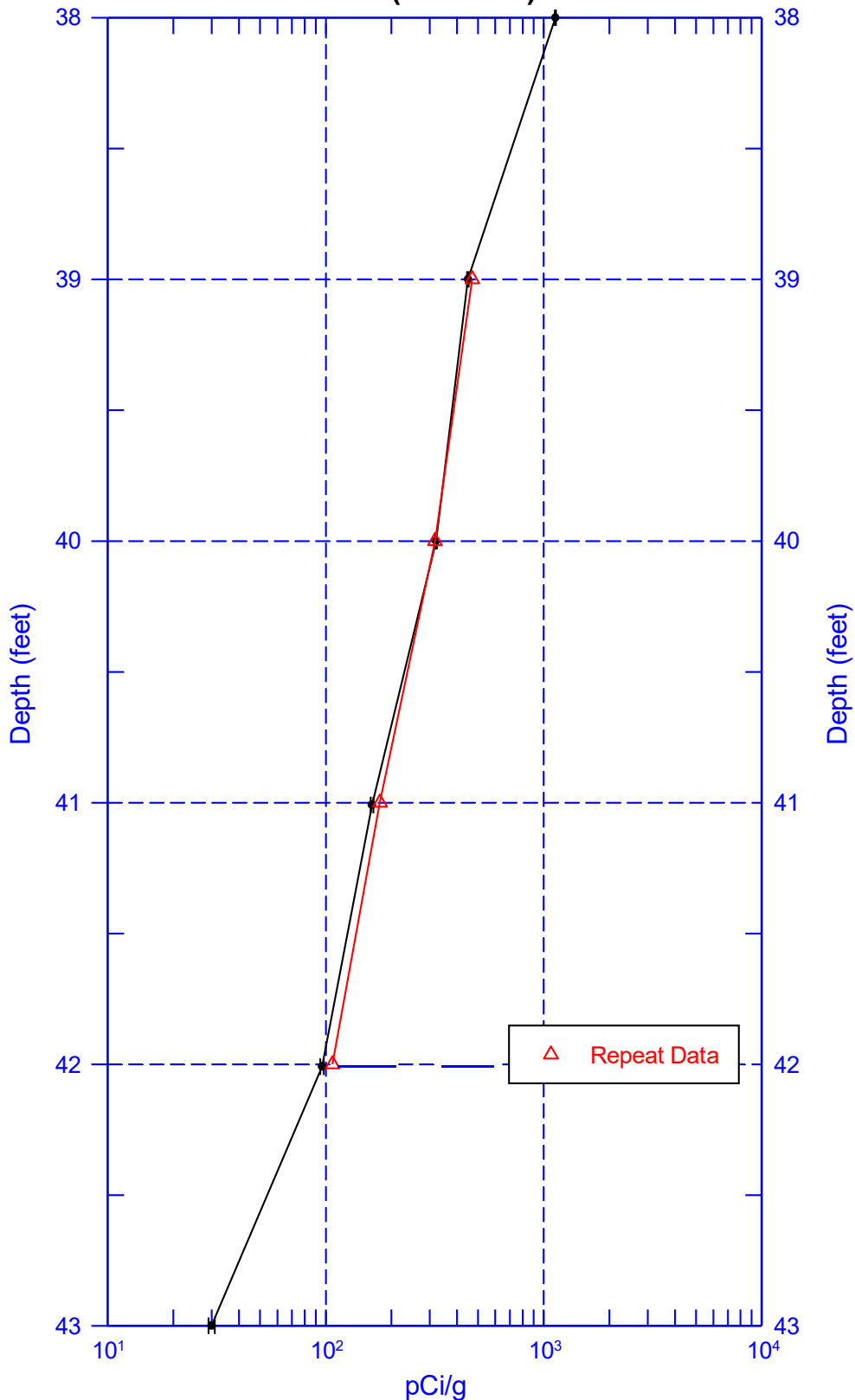
Zero Reference - Ground Surface



C9514

Repeat Section of Manmade Radionuclides

¹³⁷Cs (662 keV)

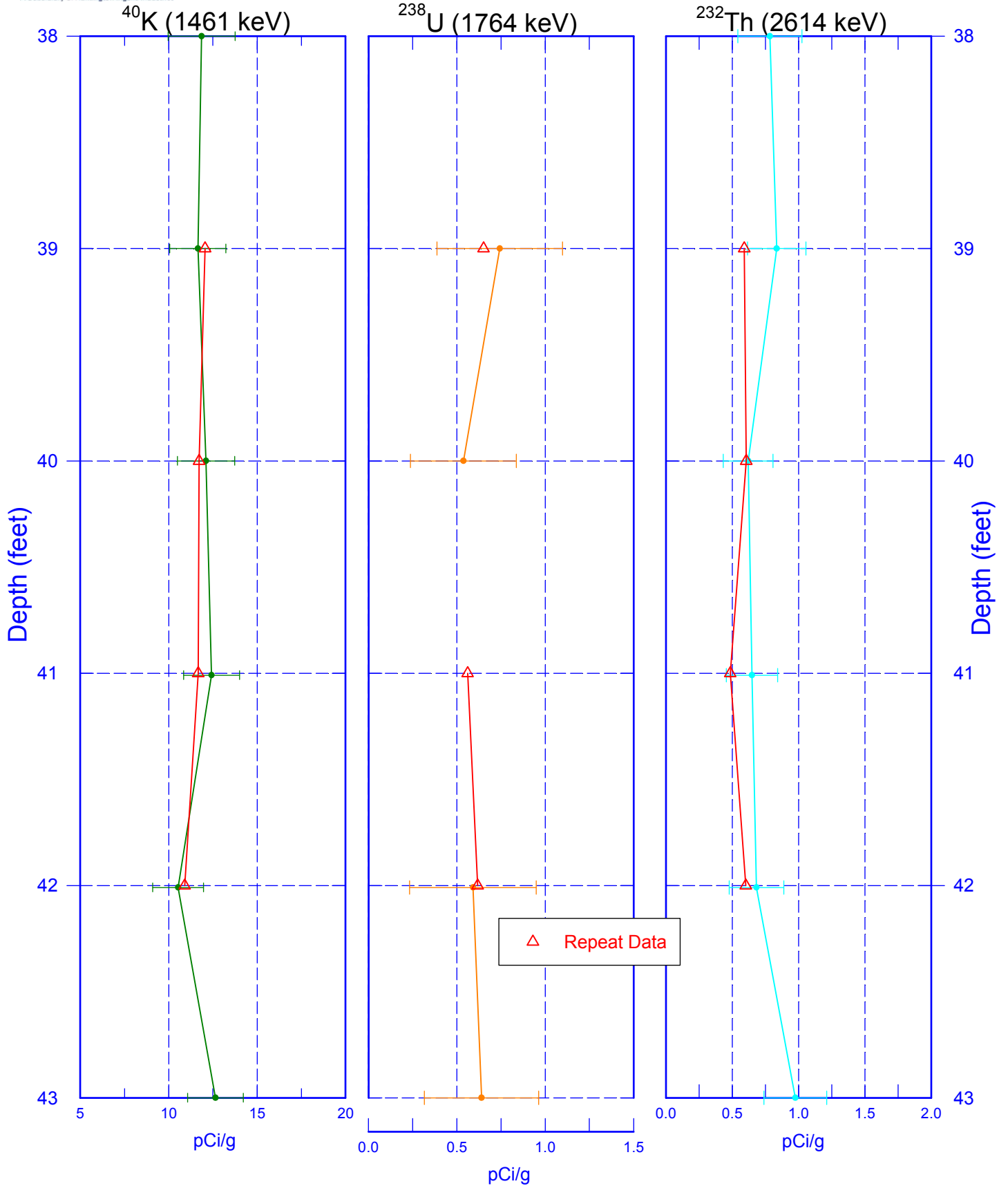




Stoller Newport News Nuclear
A Subsidiary of Huntington Ingalls Industries

C9514

Repeat Section of Natural Gamma Logs

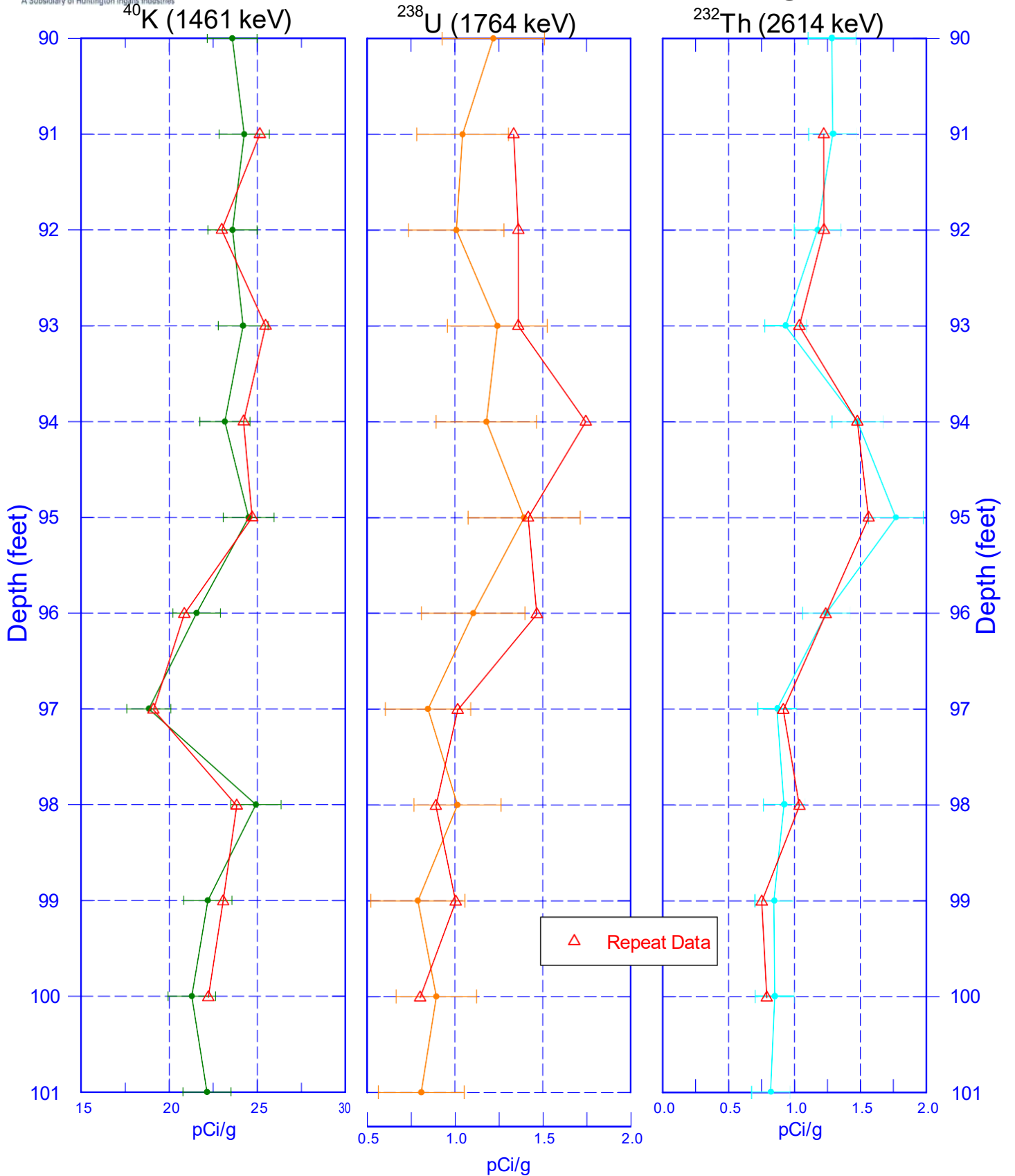




Stoller Newport News Nuclear
A Subsidiary of Huntington Ingalls Industries

C9514

Repeat Section of Natural Gamma Logs



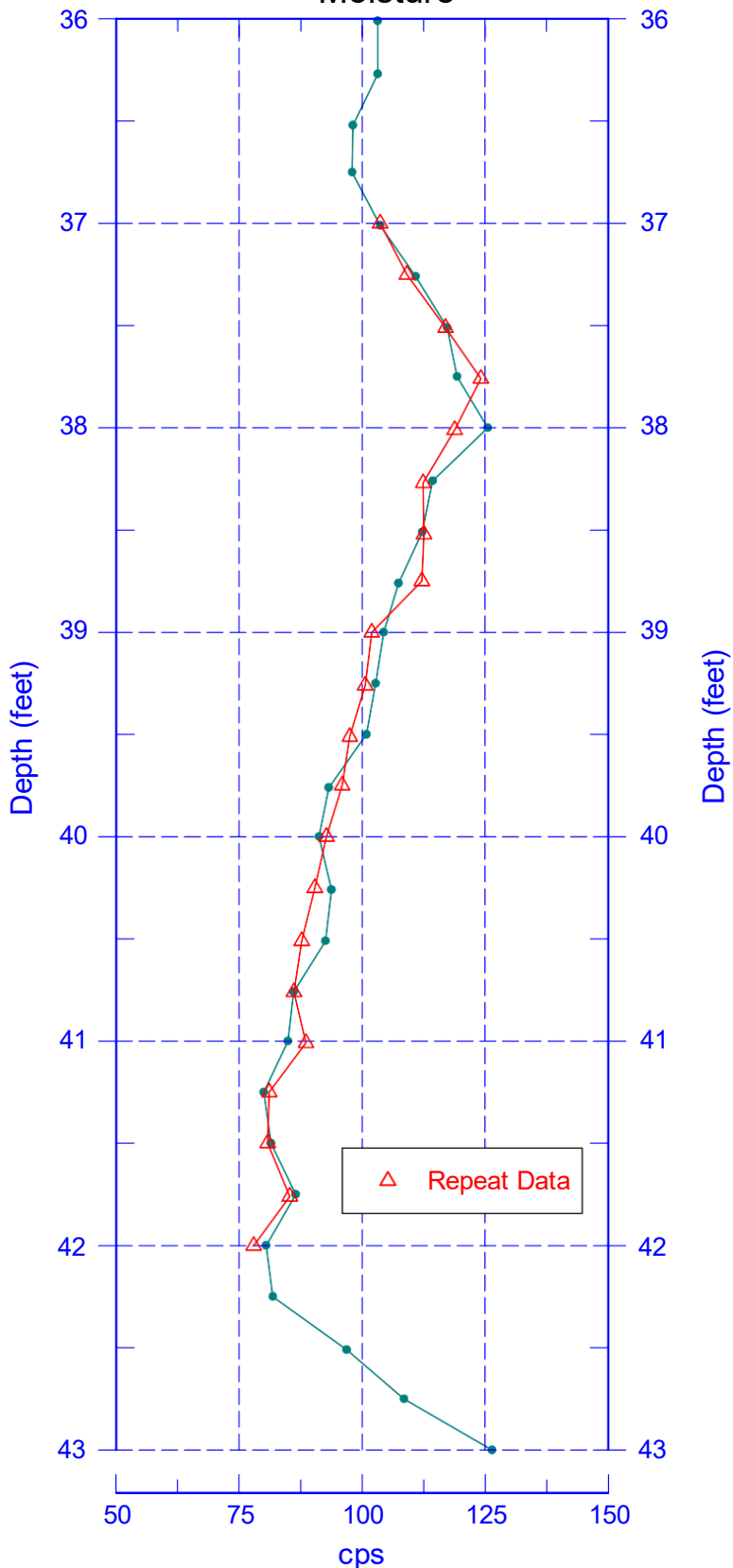
Zero Reference - Ground Surface



C9514

Moisture Repeat Section

Moisture

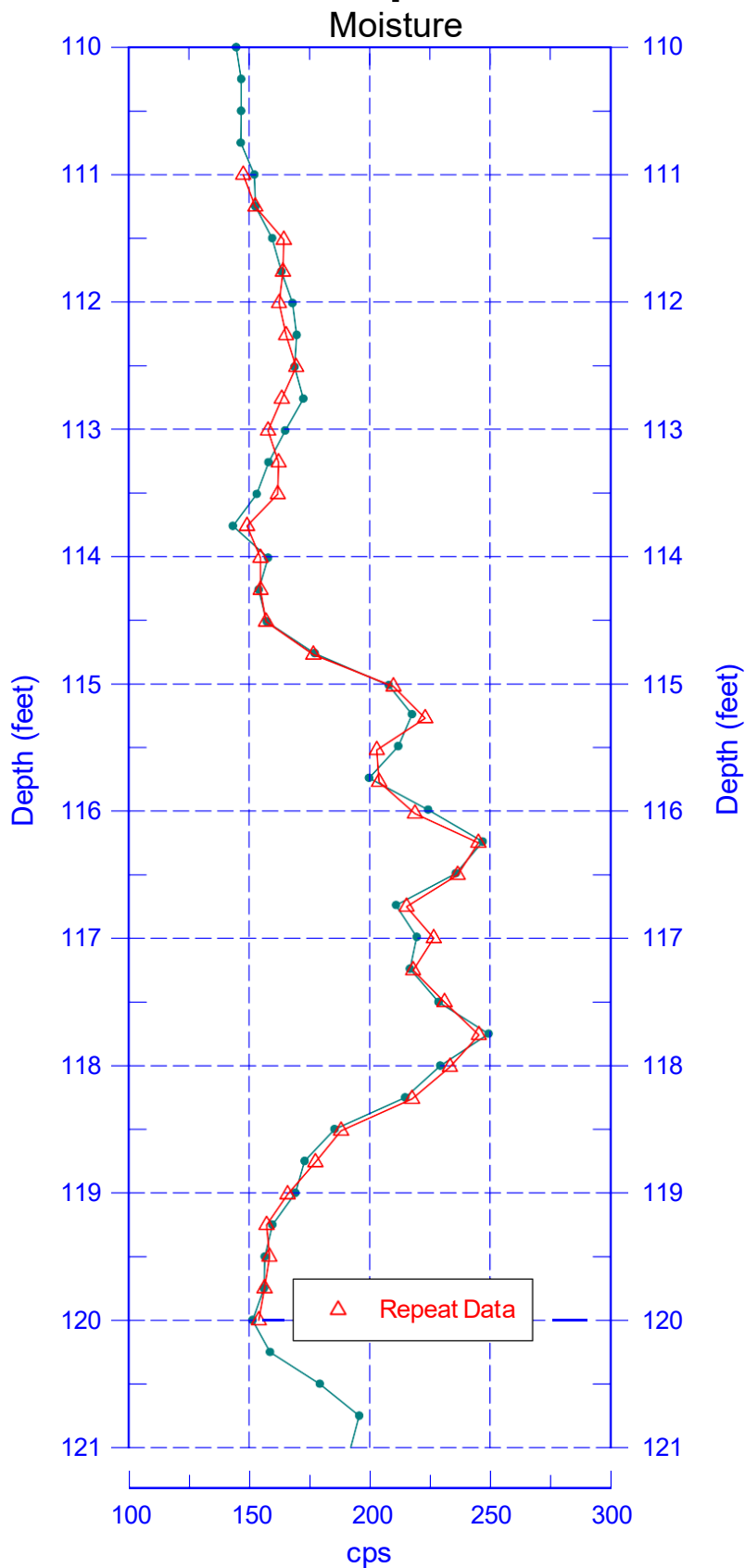


Zero Reference - Ground Surface



C9514

Moisture Repeat Section



Zero Reference - Ground Surface

This page intentionally left blank.

Appendix C

Borehole Core Log Reports and Photographs

This page intentionally left blank.

Contents

C9512 (216-S-9 Crib) Core Log Report & Photographs.....	C-1
C9513 (216-S-13 Crib) Core Log Report & Photographs.....	C-12
C9514 (216-S-21 Crib) Core Log Report & Photographs.....	C-31

This page intentionally left blank.

BOREHOLE LOG			Page <u>1</u> of <u>6</u>
Well ID: C9512		Well Name: NA	Date: <u>10/6/16</u>
Project: 200 DV-1 OU Characterization Phase 3		Location: 216-S-9 Crib	
Reference Measure Point: Ground Surface			
Depth (ft)	Sample	Graphic Log	Sample Description: Sediment Classification, Grain Size Distribution, Color, Moisture Content, Sorting, Angularity, Mineralogy, Particle Size, Reaction to HCl, Other
			Comments: Depth of Casing, Drilling Method, Sampling Method, Sampler Size, Water Level, Other
30			Sonic Core
32.5			
35			35.5-36.2: Slough Sand <u>10/12/16</u>
	Core 1		36.2-37.0: Sandy Gravel (SG): 60% Gravel, 40% Sand; Gravel: vf-pcb - 2cm, predom vf-pcb, 80% Mafic, 20% Felsic, SA; dry, no rxn w/HCl, PS, 2.5Y4/2 dk grayish brn, gravel size increases w/depth
			37.0-40.7: Sandy Gravel (SG): 60% Gravel, 40% Sand; Gravel: f-pcb - 3cm, predom f-pcb, 70% mafic, 30% felsic; Sand: 70% felsic, 30% mafic, vf-vc, predom vc, SA; dry, CaCO ₃ nodules (strong rxn w/HCl), iron staining, stratified bedding
37.5			40.7-40.9: Silt (M) 100% dry, no rxn w/HCl, non-plastic, 2.5Y4/4 light yellowish brn, grades to vf sand
40	Core 2		40.9-42.0: Sand (S) 95% Sand, 5% Silt; dry, no rxn w/HCl, 2.5Y4/2 light brownish gray, coarsening downward, vf-c
			
42.5	Core 3		44.6-45.2: Gravelly Sand (GS): 80% Gravel, 20% Sand; Gravel (G): 1-3cm, predom 2cm, SR-R, 90% mafic, 10% felsic; Sand: vf-vc, predom c, 70% felsic, 30% mafic, SA; dry, no rxn w/HCl, PS, 2.5Y4/1 gray
45			45.2-47.2: Silty Gravel (mG): 60% Gravel, 10% Sand, 30% Silt; Gravel: 1cm-7cm, predom 5cm, SR-R, 70% mafic, 30% felsic w/ quartzite; Sand: vf; dry-moist, mod rxn w/HCl, PS, suspect contaminant (dk gray/black), no odor; color varies from 2.5Y4/1 light gray to 2.5Y4/2 dk grayish brn, chalcocite in silt.
			

Reported By: Jen Russell Geologist Jen Russell 10/6/16
 Print Name Title Signature Date

Reviewed By: Tessa Clark Geologist Tessa Clark 10/20/16
 Print Name Title Signature Date

For Office Use Only

OR Doc Type: _____ WMU Code(s): _____

BOREHOLE LOG (Cont.)

Date: 10/6/16

Well ID: C9512

Well Name: NA

Location: 216-S-9 Crib

Depth (ft)	Sample	Graphic Log	Sample Description: Sediment Classification, Grain Size Distribution, Color, Moisture Content, Sorting, Angularity, Mineralogy, Particle Size, Reaction to HCl, Other	Comments: Depth of Casing, Drilling Method, Sampling Method, Sampler Size, Water Level, Other
47.5	Core 4		47.2-47.8: No core	Sonic Core
50			47.8-52.2: Silty Gravel (mG): 60% Gravel, 10% Sand, 30% Silt; Gravel: 1-7cm, predom 5cm, SR-R, 70% Mafic, 30% Felsic w/ quartzite; Sand: vf-f, predom vf; dry-moist mod-strong rxn w/ HCl, PS, no odor, 2.5Y 4/2 dk grayish brn	Core 4 B36165 47.2-52.2
52.5	Core 5		52.4-56.2: Silty Gravel (mG): 60% Gravel, 10% Sand, 30% Silt; Gravel: 1-10cm, predom 5cm, SR-R, 60% Mafic, 40% Felsic; Sand: vf-f, predom vf; moist, chalcopirite throughout silt, mod rxn w/ HCl, 2.5Y 4/2 dk grayish brn, PS, CaCO3 nodules throughout - Strong rxn w/ HCl.	Core 5 B36167 52.4-57.4
55			56.2-57.4: Sand (S) 100%: Dry, vf-c, predom med., 70% Felsic qtz, 30% Mafic basalt, iron staining, SA, MS, no rxn w/ HCl, massive, 2.5Y 4/3 light yellowish brn	
57.5	Core 6		57.5-62.5: Sand (S) 100%: Dry, vf-c, predom medium, 80% Felsic qtz, 20% Mafic, trace mica, SA	2.5Y 4/3 light yellowish brn, norm w/ HCl Core 6 B36169 57.5-62.5
60			57.5-58.9: m-c sand	
			58.9-59.6: vf-f sand grades to m-c @	
			59.6-60.9: m-c	
62.5			60.9-61.9: 70% Silt 5%, Sand 95%	Aliquot 40.8-62.0
			silt beds at 61.4 and 61.6, ~1.5cm thick	
			61.9-62.5: m sand	
65			Cores from 62.2 - 77.3 (per supporting documentation provided by EHPRC) TO PNNL NOT LOGGED	

Reported By:

Jen Russell

Geologist

Jen Russell

10/12/16

Print Name

Title

Signature

Date

BOREHOLE LOG (Cont.)

Date: 10/12/16

Well ID: C9512

Well Name: NA

Location: 216-S-9 Crib

Depth (ft)	Sample	Graphic Log	Sample Description: Sediment Classification, Grain Size Distribution, Color, Moisture Content, Sorting, Angularity, Mineralogy, Particle Size, Reaction to HCl, Other	Comments: Depth of Casing, Drilling Method, Sampling Method, Sampler Size, Water Level, Other
67.5				
70			Cores from 62.2 - 77.3 (per Supporting documentation provided by CHPRC)	
			10 PNNL	
72.5			NOT LOGGED	
75				
77.5			76.9 - 78.4: Sandy silt (sM): 80% Silt, 20% Sand; Sand: vf-f, predom. vf, 95% Felsic, 5% Mafic, SA; dry, non-plastic, strong rxn w/ HCl, 2.5% 1/2 light gray, mod sorted, grades to silty sand	Core 11 B361B3 76.9 - 81.9
80			78.4 - 79.7: Silty Sand (mS): 75% Sand, 25% Silt; Sand: vf-m, predom. med, 80% Felsic, 20% Mafic, trace mica, SA; rhythmites throughout (not well defined), dry, PS, no rxn w/ HCl, 2.5% 1/2 light brownish gray	Aliquot 78.5 - 79.8
80.5			79.7 - 80.9: Sand (S) 95% Sand, 5% Silt; Sand: vf, 90% Felsic, 10% Mafic, SA; no rxn w/ HCl, WS, dry, laminated, 2.5% 1/3 light yellowish brn	
			80.9 - 81.9: Silty Sand (mS): 70% Sand, 30% Silt; Sand: 70% Felsic, 30% Mafic, vf-c, predom. med.; moist, laminae/rhythmites (f), fining downward, PS, no rxn w/ HCl, 2.5% 1/2 light grayish brn	
85			82.9 - 86.3: Silty Sand (mS): 70% Sand, 30% Silt; vf-f sand, 90% Felsic, 10% Mafic, SA, rhythmites, no rxn w/ HCl, WS, 2.5% 1/3 Pale brn	Core 12 B361B5 82.9 - 87.9
			86.3 - 87.9: Sandy Silt (sM): 30% Sand, 70% Silt; vf-f sand, predom vf, 90% Felsic, 10% Mafic, SA, MS, wk rxn w/ HCl, platy structure, dry, non-plastic, 2.5% 1/3 light yellowish brn	

Reported By:

Jen Russell

Geologist

Jen Russell

10/12/16

Print Name

Title

Signature

Date

BOREHOLE LOG (Cont.)

Date: 10/12/16

Well ID: C9512

Well Name: NA

Location: 216-S-9 Crib

Depth (ft)	Sample	Graphic Log	Sample Description: Sediment Classification, Grain Size Distribution, Color, Moisture Content, Sorting, Angularity, Mineralogy, Particle Size, Reaction to HCl, Other	Comments: Depth of Casing, Drilling Method, Sampling Method, Sampler Size, Water Level, Other
97.5	Core 13		87.0-90.5: Silty Sand (mS): 70% Sand, 30% Silt; vf-f sand, 90% Felsic, 10% Mafic, SA, laminated, no rxn w/HCl, WS, 2.5Y 7/3 Pale brn, dry	Sonic Core
90			90.5: Sand grain size increases to m-c, 2.5Y 7/2 light gray, mod rxn w/HCl, 80% Sand, 20% Silt	Core 13 B361B7 87.0-92.0
92.5	Core 14		92.5-97.5 Sand (S) 95% Sand, 5% Silt; sand: vf-c, predom med, 80% Felsic, quartzose, 20% Mafic; dry, rhythmites interbedded, 2.5Y 4/2 light brnish gray, no rxn w/HCl, PS, iron staining	Core 14 B361B9 92.5-97.5
95			97.1: 2cm silt bed, wk rxn w/HCl	
97.5	Core 15		97.1: 2cm silt bed, wk rxn w/HCl	
100			97.0-99.2: Sand (S) 95% Sand, 5% Silt; sand: vf-f, predom. fine, 95% Felsic, 5% Mafic, moist, rhythmites and laminae, 2.5Y 4/2 light brnish gray, no rxn w/HCl, MS	Core 15 B361C1 97.0-102.0
102.5			99.2-102.0: Silty Sand (mS): 75% Sand, 25% Silt; Sand: vf-c, predom fine, fining downward fining downward (vf @ 100.9), 20% Felsic, 20% Mafic; laminae throughout & vf very thin bedding (1cm), moist, no rxn w/HCl, mod sorted, 2.5Y 4/2 grayish brn	
102.5	Core 16		102.6-103.9: Sandy silt (sM): 70% Silt, 30% Sand; Sand: vf, 95% Felsic, 5% Mafic, SA; dry, laminated	Core 16 B361C3 102.6-107.6
105			from 103.6-103.9, no rxn w/HCl, WS, 2.5Y 4/3 light yellowish brn, w/ mica	
			103.9-104.0: Silty sand w/ wood bits up to 0.5cm long	
			104.0-107.6: Silty sand (mS): slightly silty sand (mS): Sand (S): 90% Sand, 10% Silt; Sand: vf-f from 104.0-104.6, WS, SA	Aliquot
			f-c, predom. med from 104.6-107.6, massive, 45% Felsic, 35% Mafic, trace mica ; no rxn w/HCl to 106.6, wk rxn from 106.6-107.6	103.1-104.1e
			2.5Y 4/2 light brnish gray 104.0-104.6, 2.5Y 4/1 gray from 104.6-107.6, MS, moist	

Reported By: Jen Russell Geologist Jen Russell Signature 10/13/16 Date

Print Name Title Signature Date

BOREHOLE LOG (Cont.)

Page 5 of 6

Date: 10/13/16

Well ID: C9512

Well Name: NA

Location: 216-S-9 Crib

Depth (ft)	Sample	Graphic Log	Sample Description: Sediment Classification, Grain Size Distribution, Color, Moisture Content, Sorting, Angularity, Mineralogy, Particle Size, Reaction to HCl, Other	Comments: Depth of Casing, Drilling Method, Sampling Method, Sampler Size, Water Level, Other
107.5	Core 17		107.0-112.0: ^{JE 10/13/16} Slightly Silty Sand (ms) 90% Sand, 10% Silt; dry, no rxn w/ HCl, SA, 80% Felsic, 20% Mafic	Sonic Core
110			107.0-109.7: vf-f sand interbedded rhythmites, 25% ^{JE 10/13/16} light yellowish brn, laminae throughout	Core 17 B361C5 107.0-112.0
112.5			109.7-110.2: f-vc sand, coarsening downward, silty and iron stain (no lateral) @ 109.8, trace mica, 2.5Y 5/2 grayish brn	
115	Core 18		112.0-117.0: ^{JE 10/13/16} Slightly (m) S: Silty Sand (ms): 80% Sand, 20% Silt; Sand: vf-med, 80% Felsic, 20% Mafic, trace mica; dry, no rxn w/ HCl, med-WS, 2.5Y 4/2 light brnish gray	Core 18 B361C7 112.0-117.0
117.5			112.4-113.0: vf sand / silt, rhythmites	
120			113.0-114.5: f-med sand, massive	
122.5			114.5-115.2: vf sand / silt, lamina @ 114.9	
125			115.2-117.0: f-med sand rhythmites throughout	
<p>Cores from 117.0 - 127.0 (no recovery from 127.0-127.2) TO PNNL</p> <p>NOT LOGGED</p>				

Reported By:

Jen Russell

Geologist

Jen Russell

Signature

10/13/16

Date

Print Name

Title

BOREHOLE LOG (Cont.)

Date: 10/17/14

Well ID: C9512

Well Name: NA

Location: 216-S-9 Crib

Depth (ft)	Sample	Graphic Log	Sample Description: Sediment Classification, Grain Size Distribution, Color, Moisture Content, Sorting, Angularity, Mineralogy, Particle Size, Reaction to HCl, Other	Comments: Depth of Casing, Drilling Method, Sampling Method, Sampler Size, Water Level, Other
127.5	Optional 21		127.2 - 130.7: Silt (M) 90% Silt, 10% Sand; Sand: wf - f, 80% Felsic, 20% Mafic, SA, wf throughout, fine grained sand beds from at 127.6 and 128.0, 2 cm thick; moist, laminated, wk rxn w/ HCl, WS, 2.5Y 1/2 light brnsh gray, 2.5Y 5/3 light olive brn 129.2 - 129.4, grades to (m) S.	Sonic Core Optional 21 B361F9 127.2 - 132.2
130			130.7 - 132.2: Slightly Silty Sand (m) S: 85% Sand, 15% Silt; Sand: wf - m, predom f, trace mica, 90% Felsic, 10% Mafic, SA, MS; no rxn w/ HCl, massive, dry, 2.5Y 1/2 light brnsh gray.	Aliquot 129.2 - 130.2
132.5			132.0 - 137.0: Silt (M) 100%; moist, laminated, wk - mod rxn w/ HCl, non-plastic, 2.5Y 1/4 light yellowish brn.	Optional 22 B361H1 132.0 - 137.0
135			134.7 - 135.1: 90% Silt, 10% Clay, low plasticity 135.9 - 137.0: 90% Silt, 10% very fine sand.	Aliquot
137.5	Optional 23		137.0 - 142.0: Silt (M) 100%; moist, non-plastic wk - mod rxn w/ HCl, platy structure, 2.5Y 5/3 light olive brn, iron staining 141.5 - 142.0.	Optional 23 137.0 - 142.0
140			138.8 - 140.9: Silt 90%, Clay 10%, low plasticity, wk rxn w/ HCl - mod rxn w/ HCl, 2.5Y 4/4 olive brn, moist	Aliquot 139.0 - 140.5
142.5	Total Depth: 142.0 ft			
145	JR 10/13/14			

Reported By:

Jen Russell

Geologist

Print Name

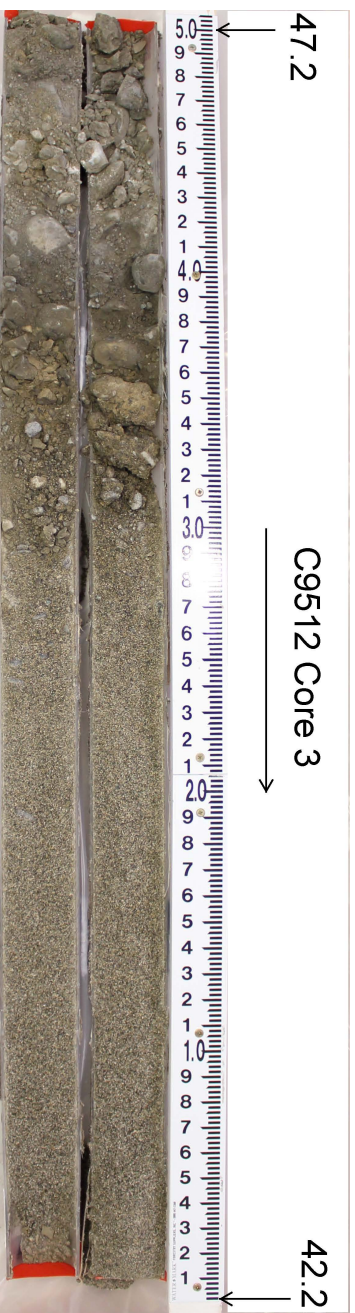
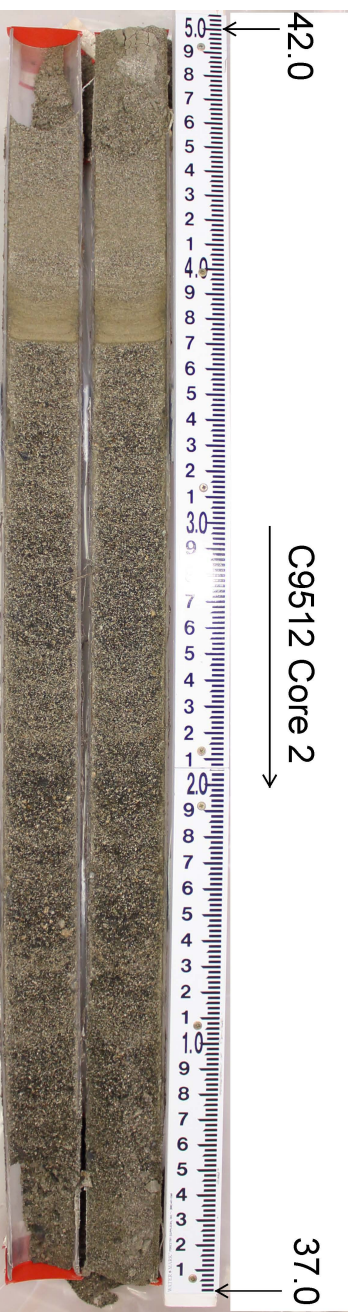
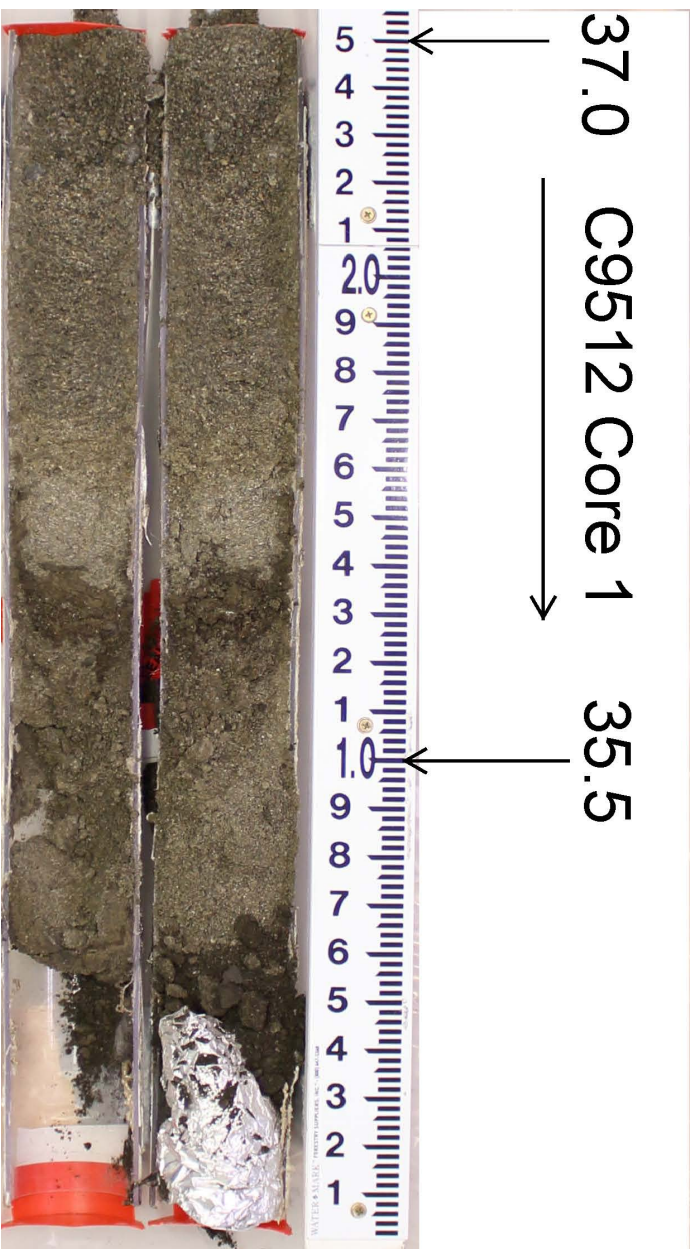
Title

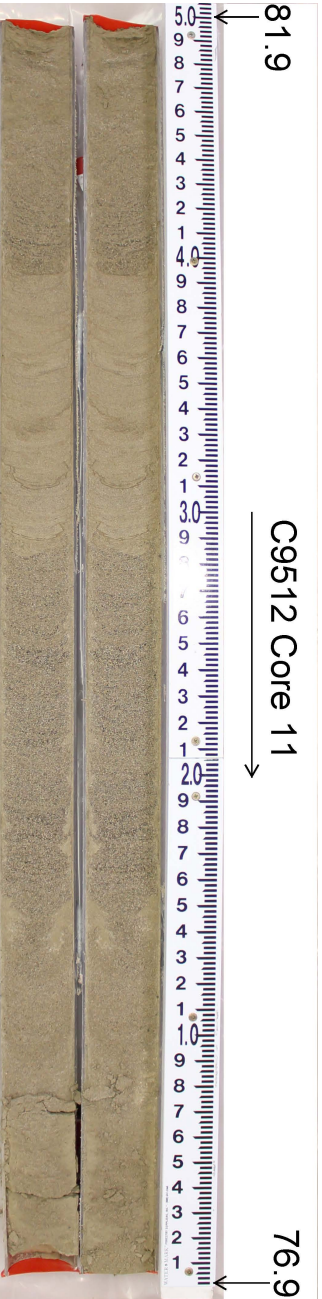
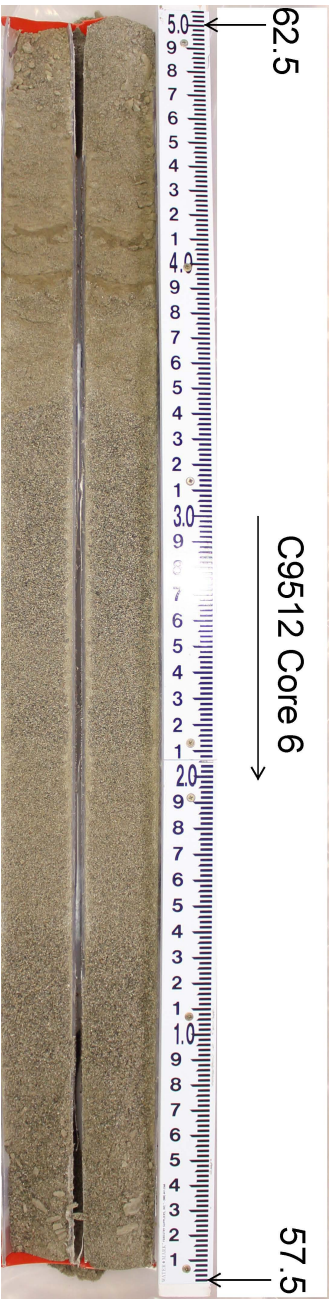
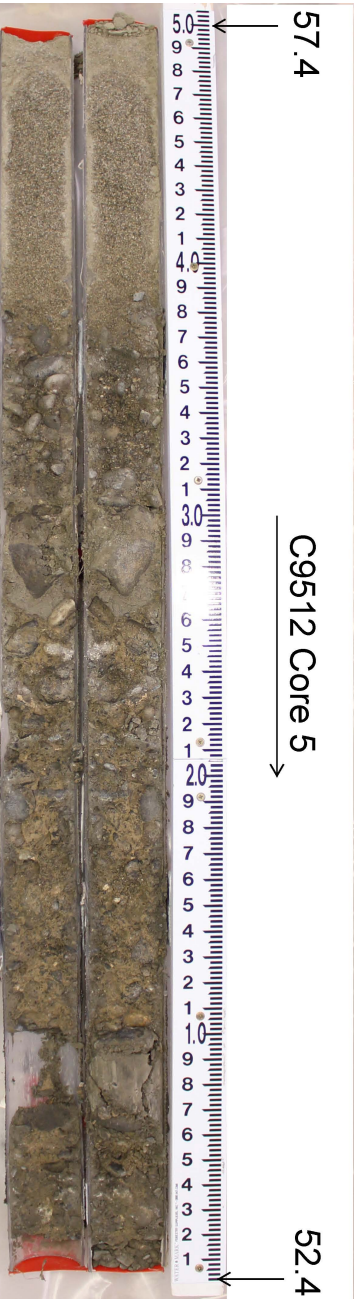
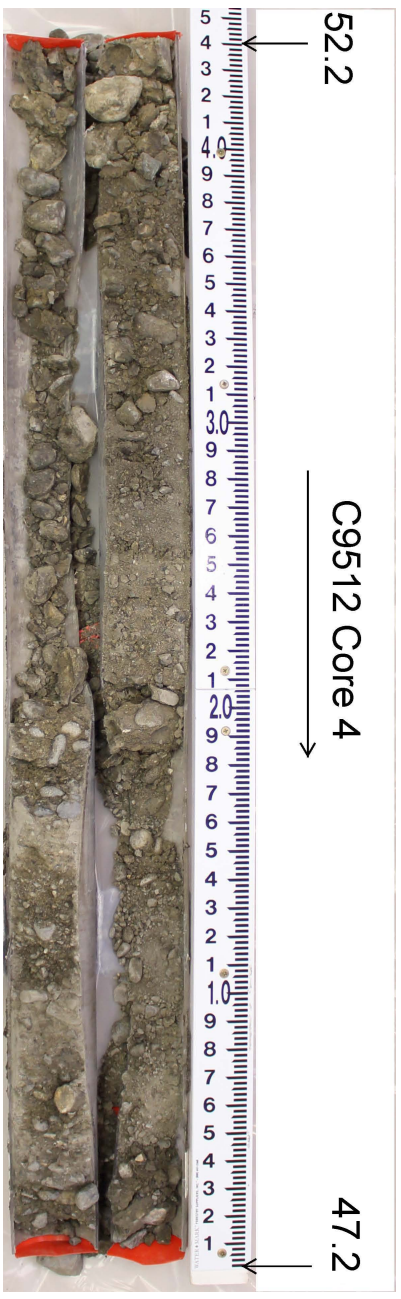
Jen Russell

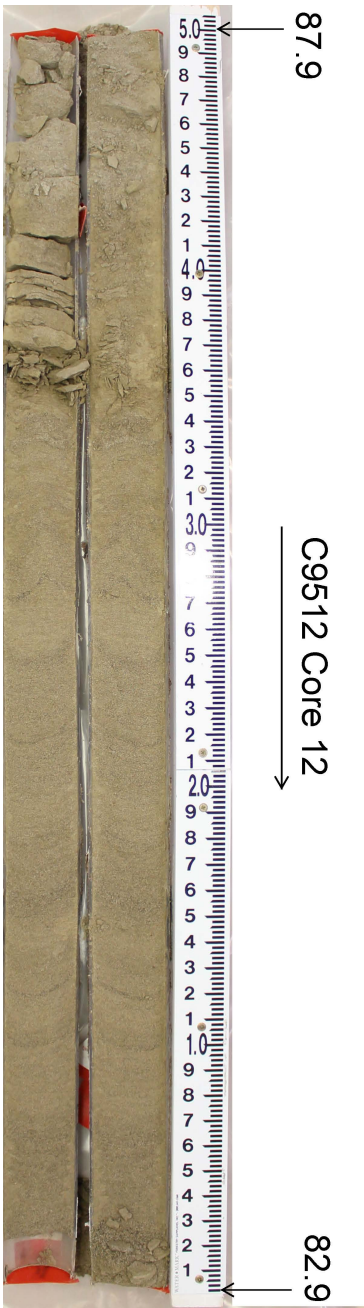
Signature

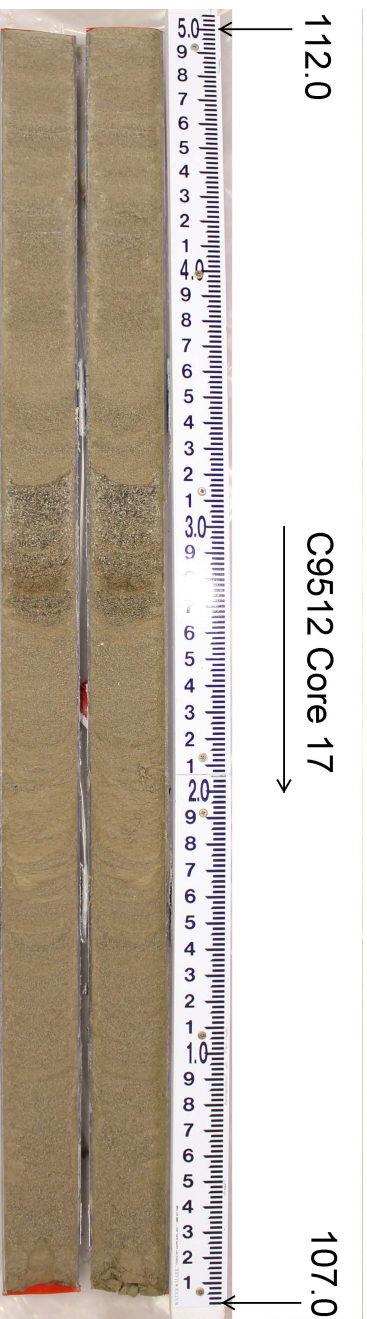
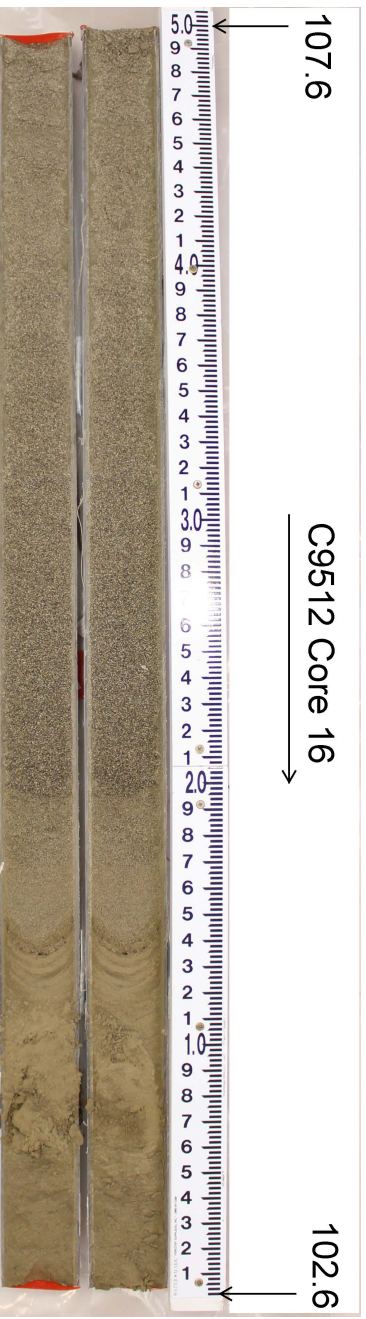
10/12/14

Date











BOREHOLE LOG

Page 1 of 10
Date: 9/21/17

Well ID: C9513 Well Name: NA Location: 216-S-13 Crib
Project: 200-DV-1 Operable Unit Reference Measure Point: Ground Surface

Depth (ft)	Sample	Graphic Log	Sample Description:		Comments:
			Sediment Classification, Grain Size Distribution, Color, Moisture Content, Sorting, Angularity, Mineralogy, Particle Size, Reaction to HCl, Other		Depth of Casing, Drilling Method, Sampling Method, Sampler Size, Water Level, Other
45	Core 1		45.0-45.2: Sandy Gravel (sG): 30%og, 60%os, 10%om; Griv. fn		Core 1 B39WVA 45.0-47.5
			to coarse pebbles (2cm), A-SR, 70%om, 30%os Sand: vfn-vc, 60%of, 40%of		
	Core 2		45.2-46.4: Sand (s): 95%os, 5%og; Griv. fn pebs, A-SA, 50%om, 50%of; sand: fn lev. coarse, 50%om, 50%of		Core 2 B39WV4 47.5-50.0
47.5			SA-SR, 2.5 1/3 dk. brn, no rxn w/HCl; PS, massive; vfn-m s. interbed (1.0-1.5cm) @ 45.5, 45.6, 45.9, 46.1, + 46.3; v. crs s. fn peb. interbed (1.5cm) @ 46.0.		
	Core 3		46.4-47.5: Slightly Silty Sand (mS): 80%os, 20%om; S: vfn-cr, 75%of, 25%om; SA-SR, 2.5 1/2, grayish brn, dry		Core 3 B39WV6 50-55
50			no rxn w/HCl; PS, interbedded/coarsens downward; rhythmites & vfn s/m interbeds (~1mm);		
	Core 4		47.5-48.8: Gravelly Sand (gS): 10%og, 90%os; Griv. fn pebs (10mm max)		Core 4 B39WV8 55-60
52.5			A-SA, 80%om, 20%of; S: vfn-vc, 50%om, 50%of; SR-A, 2.5 1/2, dark grayish brn, dry, no rxn w/HCl; WS, massive; fn sand interbed @ 48.3' (3cm)		
	Core 5		50.0-50.2: Silty Sand (mS): 50%os, 50%om; S: vfn-m, 50%om, 50%of		Core 5 B39WV0 60-65'
55			SA-SR, m; non-plastic; 2.5 1/2 dk. gray brown; moist, comp, massive; mod rxn w/HCl.		
	Core 5		50.2-54.5: Sand (s): 5%og, 95%os; Griv. fn-m pebs (max 9mm); A-SA, 60%om, 40%of; S: vfn-vc, 50%om, 50%of		Core 5 B39WV0 61.0-63.0'
57.5			SR-A, 2.5 1/2, dark gray, dry, no rxn w/HCl; WS, massive; fn: fn-s. interbeds @ 50.3 (1mm), 50.4 (3cm) + 50.5 (2cm); Fe staining @ s. interbeds; gnd. contact @ 54.5.		
57.2	Core 5		54.5-55.0: Sand (s): 5%og, 95%os; Griv. fn-m pebs (max 9mm); A-SA, 60%om, 40%of; S: vfn-vc, 50%om, 50%of; SR-A, 2.5 1/2, dark gray, dry, strong rxn w/HCl; WS, mass; Ca-cementation.		Core 5 B39WV0 61.0-63.0'
60			55-57.8: Sand (s): 5%og, 95%os; Griv. fn-m pebs; A-SA, 60%om, 40%of; S: vfn-vc, 50%om, 50%of; SR-A, 2.5 1/2, dark gray, dry, no rxn w/HCl; WS, massive; micas; gnd. contact @ 57.8.		
	Core 5		57.8-58.3: Silty Sand (mS): 75%os, 25%om; S: vfn-c, predom vfn-m, 60%om, 40%of; SR-A, m; non-p. cementation; 2.5 1/2 dk. brown, gray, dry, strong rxn w/HCl; minor rhythmites; cemented; PS.		Core 5 B39WV0 61.0-63.0'
			58.3-59: Sand (s): 5%og, 95%os; Griv. fn-m pebs (9mm); A-SA, 60%om, 40%of; S: vfn-vc, 50%om, 50%of; SR-A, 2.5 1/2, dark gray, dry, no rxn w/HCl (mod @ 58.3 + 59 contacts); WS, massive; micas; gnd. contact @ 59'.		
	Core 5		59.0-60.0: Silty Sand (mS): 50%os, 50%om; S: vfn-vc, 70%of, 30%om; SA, m; non-plast; 2.5 1/2, gray, dry, strong rxn w/HCl; silt (80%om, 15% vfn-matic s.) dike end @ 59.6; silt interbeds and nodules present throughout; all silt = v. strong rxn w/HCl; lower 2" of liner = melted/warped.		Core 5 B39WV0 61.0-63.0'
			60.0-61.1: Sandy Silt (SM): 30% Sand, 70% Silt; Sand: vfn-vc, predom vfn; SA, 30%om, 70%of; Silt lamina @ 60.5', Sand rhythmites 60.7-61.1, Silt dike (1cm), nonplastic, moist, no rxn w/HCl, 2.5 1/2 grayish brn		
	Core 5		61.1-63.3: Sand (s): 100% vfn-m, 30%om, 70%of; trace mica, WS, SA, 2.5 1/2, grayish brn, massive w/ 1 cm silt dike, no rxn w/HCl		Core 5 B39WV0 61.0-63.0'
			63.3-63.8: Silt (M) 100% non-plastic, dry, 2.5 1/3 pale brn, strong rxn w/HCl		

Reported By: T. Clark / Jen Russell Geologist / Jen Russell T. Clark / Jen Russell 10.26.17 / 10.27.17
Print Name Title Signature Date

Reviewed By: Sarah Springer geologist (PG) Sarah Springer 10-31-17
Print Name Title Signature Date

For Office Use Only
OR Doc Type: WMU Code(s):

BOREHOLE LOG (Cont.)

Page 2 of 10

Date: 9/21/17

Well ID: C9513

Well Name: NA

Location: 216-S-13 Crib

Depth (ft)	Sample	Graphic Log	Sample Description: Sediment Classification, Grain Size Distribution, Color, Moisture Content, Sorting, Angularity, Mineralogy, Particle Size, Reaction to HCl, Other	Comments: Depth of Casing, Drilling Method, Sampling Method, Sampler Size, Water Level, Other
62.5	Core 5		62.8-65.0: Sand (S) 100% m-c, 10% M, 90% F, no rxn w/HCl dry, SA, WS, 4cm silt dike - strong rxn w/HCl	Core 5 B39WWD 60-65' Aliquot 61.0-63.0'
65	Core 6		65-65.4: Sand (S): 90% S, 10% m; v. fn-c, predom vf-m; SA, 70% fct, 30% maf, PS, dry, 2.5Y 5/2 grayish brn, no rxn w/HCl, massive; silt nodules @ corners @ 65' top of core (strong rxn w/HCl) ~1cm. 65.4-69.0: Slightly Silty Sand (mS): 80% S, 20% m; S: v. fn-m, 30% maf, 70% fct, trace mica, WS, SA, 2.5Y 5/3, lt. olive brn; no rxn w/HCl, dry; rhythmites throughout; grad. contact @ 69.	Core 6 B39WW2 65-70
67.5				
70	Core 7		69.8-73.1: Slightly Silty Sand (mS): 80% S, 20% m; S: v. fn-m, 30% maf, 70% fct, mica, WS, SA, 2.5Y 5/3 lt. olive brn, dry, no rxn w/HCl; massive; dark gray silty sand interbed (0.6cm) @ 69.3; lt. olive brn (mS) interbed (2.5cm) @ 69.6, 1.0cm @ 69.7; strong rxn w/HCl.	Core 7 B39WW4 70-75 No Core 8 or 9.
72.5				
75	Core 10		75.0-80.0: Sandy Silt (SM): 30% S, 70% m; S: v. f-c, predom vf, 90% F, 10% m; SA; m; non-plastic, wk-str rxn w/HCl; moist, massive; 2.5Y 4/3 olive brn, MS (minor rhythmites 73.1-73.3; grad contact @ 74.5) 75.0-76.5: 2.5Y 4/3 olive brn 75.9-76.2: c. sand 76.4-76.5: c. sand 75.8-76.5: iron staining, prominent @ 76.2 76.5-79.0: 2.5Y 4/2 light brownish gray w/f sand laminae throughout 79.0-80.0: 2.5Y 4/2 grayish brn, decreased sand content	Core 10 B39WXD 75-80' Aliquot 76-79.0'
77.5	Core 10			
80	Core 11		80.0-85.0: Silty Sand (mS): 50% S, 50% m; Sand: v. f-c, predom vf, 75% fct, 25% maf, SA; m; non-plastic; no rxn w/HCl; dry; platy structure (80.0-80.4) (80.4-81.6) (82.7-85.0), laminae throughout (80.4-82.7); MS, 2.5Y 5/3 light olive brn; Fe staining on laminae (80.4-81.6); silt laminae @ 81.1, 81.3, 81.4, 81.6; Fe-stained m.	Core 11 80.0-85.0'

Reported By: T. Clark / Jen Russell Geologist / Geologist T. Clark / Jen Russell 10-26-17 / 10-27-17
 Print Name Title Signature Date

BOREHOLE LOG (Cont.)

Date:

Well ID: C9513

Well Name: NA

Location: 216-S-13 Crib

Depth (ft)	Sample	Graphic Log	Sample Description: Sediment Classification, Grain Size Distribution, Color, Moisture Content, Sorting, Angularity, Mineralogy, Particle Size, Reaction to HCl, Other	Comments: Depth of Casing, Drilling Method, Sampling Method, Sampler Size, Water Level, Other
82.5	Core 11		80.0-85.0: Silty Sand (MS): 50% m, 30% s; sand: v-f-c, predom v-f-f, 75% fcls, 25% m, SA; m: non-plast; no rxn w/HCl; dry; platy structure @ 80.0-85.0'	Core 11 80.0-85.0'
85			80-80.4 + 82.7-85.0: laminae @ 80.4-82.7; MS; 2.5Y 5/3 light olive brn; Fe staining on laminae (80.4-81.6); silt laminae @ 81.1, 81.3, 81.6 (+Fe stained). 85.0-88.1: Silty Sand (MS): 75% s, 25% m; S: v-f-m, SA, 75% fcls, 25% mafic m; non-plast; no rxn w/HCl; dry; mass; MS; 2.5Y 7/3 olive brn, mica present. → 87.1-87.6: s. coarsens downward to vfn-v-crse (to 2.5Y 4/2 H-brnsh gray). → 87.6-88.1: s. coarsens down from v-f-m to vfn-v-crse (to 2.5Y 6/2).	Core 12 85.0-90.0
87.5	Core 12		88.1-88.9: Silt (m): 90% m, 10% s; S: 75% m, 25% f, v-f-f; m: non-plast; wk rxn w/HCl; dry; cross-bedded; silt lamina dipping 20° from 88.1-88.3, lateral beds 88.3-88.6, massive; 2.5Y 4/3 olive brn; 88.6-88.9: → lateral beds 88.3-88.6; 2.5Y 5/3 lt. olive brn, inc. sand % to 20%; m: 80%. → massive 88.6-88.9; 2.5Y 4/3 olive brn; graded contact @ 88.9.	
90			88.9-90: Silty Sand (MS): 70% s, 30% m; S: v-fn-vc, 70% fcls, 30% maf; SA; m: non-plast; no rxn w/HCl; dry, massive to 89.3; WS; 2.5Y 6/2 H-brnsh gray. → 89.3-90: interbedded (1.5-2cm) sand beds w/silt (2-5mm) laminae; silt: strong rxn w/HCl; 2.5Y 4/3 olive brn.	
90	Core 13		90.0-90.4: Sand (S): 100% v-f, WS, SA, 90% fcls, 10% mafic, small rhythmites moist, no rxn w/HCl, 2.5Y 4/2 light brn gray, strong MIBK odor (MIBK)	
92.5			90.4-91.9: Silt (M) 100% m; non-plastic, wk rxn w/HCl, moist, 2.5Y 5/4 light olive brn from 90.4-90.8, 2.5Y 5/1 gray from 90.8-91.9, clay nodules (5cm diameter) @ 90.9, strong MIBK odor Core 13 B39WX9 90.0-95.0'	
95	Core 14 A		91.9-93.3: Sand (S): 100% v-f-m, predom f, trace mica, 25% mafic, 75% fcls, WS, silt cross bedding from 92.5-92.7; strong MIBK odor, 2.5Y 6/2 light brnsh gray, no rxn w/HCl	
97.5			93.3-95.0: Silty Sand (MS): 60% s, 40% silt; Sand: v-f-f, 90% fcls, 10% mafic, trace mica, SA, WS; v. wk rxn w/HCl, laminae throughout, med. gr. sand sand 93.8-94.1, 2.5Y 5/1 gray, strong MIBK odor Core 14 B 97.5-100'	
97.5	Core 14 B		95.0-97.5: Silty Sand (MS): 75% s, 25% m; S: v-f-c, predom v-f-m, 80% fcls, 20% maf; SA; trace mica; PS; no rxn w/HCl; dry; 2.5Y 5/1 gray, minor silt laminae @ 97.4-97.5 (poss. altered by drilling), rhythmites @ 95.0-95.3; strong MIBK odor.	Core 14 A 95.0-97.5
100			97.5-99.7: Silty Sand (MS): 50% s, 50% m; S: v-f-f, 85% fcls, 15% maf; trace mica, SA, WS; m: non-plast; no rxn w/HCl; dry to moist; laminae throughout (silt); 5Y 5/1 gray; v. strong MIBK odor. Core 14 B 97.5-100'	
100	Core 15		99.7-100: Silty Sand (MS): 60% s, 40% m; S: v-f-m, 75% f, 25% maf; SA, WS; massive; m: non-plast; no rxn w/HCl; dry; 2.5Y 5/2 grayish brn; strong MIBK odor.	
100			100-101.9: Silty Sand (MS): 70% s, 30% m; S: v-f-crse, 70% f, 30% m; SA, MS; m: non-plast; no rxn w/HCl; dry; 2.5Y 5/2 grayish brn; strong MIBK odor. Core 15 100-105 → Interbeds of predom. m-crse sand @ 100.4, 100.6, 100.7, 100.9, + 101.1 (1.5-2cm thick) → Silt lamina (4mm) @ 101.7'	

Reported By:

T. Clark / J. en Russell
Print Name

Geologist / Geologist
Title

T. Clark / J. en Russell
Signature

10-26-17 / 10-27-17
Date

BOREHOLE LOG (Cont.)

Date:

Well ID: C9513

Well Name: NA

Location: 216-S-13 Crib

Depth (ft)	Sample	Graphic Log	Sample Description: Sediment Classification, Grain Size Distribution, Color, Moisture Content, Sorting, Angularity, Mineralogy, Particle Size, Reaction to HCl, Other	Comments: Depth of Casing, Drilling Method, Sampling Method, Sampler Size, Water Level, Other
102.5	Core 15		101.9-103.9: Slightly Silty Sand (MS): 80% s, 20% m; S: vfn-v.crsz (predom m.crsz); 60% f, 40% m; SA: 5R; no rxn w/HCl; dry; 2.54% light gray; mIBK odc; 100-105 (massive);	Core 15
			103.9-105: Silty Sand (MS): 60% s, 40% m; S: vfn-crsz (predom. f.m.); 70% f, 30% m; SA, WS; m: non-plast/consolidation; wk-mod rxn w/HCl; dry; 2.54% light gray; mIBK odc; massive;	
105	Core 16		105.5-110.5: Silty Sand (MS): 70% s, 30% m; S: vfn-crsz, predom. vfn-med; SA, 70% f, 30% m; MS; m: non-plast; no rxn w/HCl; dry; 2.54% light olive brown; strong mIBK odc; rhc fines throughout; mica present; -> silt laminae (1mm) @ 109.4-109.5.	Core 16 105.5-110.5
107.5				
110				
112.5				
115				
117.5				
120				

CORES TO PNNL

NR 10/27/17

Reported By: T. Clark Ken Russell Geologist Geologist JK Ken Russell 10-26-17 - 10-27-17
 Print Name Title Signature Date

BOREHOLE LOG (Cont.)

Date:

Well ID: C9513

Well Name: NA

Location: 216-S-13 Crib

Depth (ft)	Sample	Graphic Log	Sample Description: Sediment Classification, Grain Size Distribution, Color, Moisture Content, Sorting, Angularity, Mineralogy, Particle Size, Reaction to HCl, Other	Comments: Depth of Casing, Drilling Method, Sampling Method, Sampler Size, Water Level, Other
122.5			124.8-125.3: Sandy Silt (SM): 60%om, 40%os; s: v.f. f. Total 30%om, 70%os, SA; m: non-plastic; no rxn w/HCl; dry; clay @ 10-26-17 2.51 1/2 lt. brownish gray; platy structure; strong MIBK odor; silt nodules @ 125.3; v. sharp contact @ 125.3'	
			125.3-125.8: Silt (M): 90%om, 10%os; s: v.f. f. (too small to determine mod/fels %); m: non-plastic; wk-mod rxn w/HCl; dry; bedded @ 10-26-17 2.51 3/4 light olive brn; MIBK odor; silt; silt beds/laminated p/w contact @ 125.3+125.8 (v. sharp); laminar dip @ 125.6'	
125			125.8-126.1: Sandy Silt (SM): 80%om, 20%os; s: v.f. f. m; 80%of, 20%om; SA; m: non-plastic; no rxn w/HCl; dry; 2.51 5/3 lt. olive brn; MIBK odor; platy structure; grad. contact @ 126.1; v-shaped.	Core 20 B 124.8-127.3
			126.1-127.3: Silty Sand (MS): 60%os, 40%om; s: v.f. f. m; 80%of, 20%om; SA; SR; m: non-plast; no rxn w/HCl; dry; platy; 2.51 5/3 lt. olive brn; MIBK odor; sand fines downward to v.f. f. @ 127.3. 1 → med. sand interbed (2cm) @ 127.0, angles 10°	
127.5			127.3-127.7: Sand Silt (SM): 80%om, 20%os; s: v.f. f. m; 80%of, 20%om; SA; m: non-plast; no rxn w/HCl; dry; 2.51 5/3 lt. olive brn; PS; platy structure; strong MIBK odor; sand lens (2cm) @ 127.6	Core 20 A
			127.7-128.5: Silty Sand (MS): 50%os, 50%om; s: v.f. f. c; 70%of, 30%om; SA; PS; no rxn w/HCl; dry; 2.51 5/3 grayish brn; massive; MIBK odor; silt lens @ 127.7' contact.	127.3-129.8
			128.5-129.8: Sand Silt (SM): 80%om, 20%os; s: v.f. f. m; 80%of, 20%om; SA; m: non-plast; no rxn w/HCl to mod @ depth; dry; 2.51 5/3 lt. olive brn; PS; platy structure; MIBK odor; silt laminae (1mm) @ 128.6'	increase @ 10-26-14
130			130.5-135.5: Sandy Silt (SM): 25% Sand, 75% Silt; Sand: v.f. f, 90% felsic, 10% mafic, SA; PS; no rxn w/HCl; Silt: non-plastic, mod-strong rxn w/HCl; 2.51 3/4 light yellowish brn, moist, MS, platy structure, iron staining from 131.8-132.6; strong acetone odor; interbedded silt and sand laminae; v. thin beds	Core 21 B39X41 130.5-135.3 Aliquot 131.5-133.5
132.5			135.2-136.0: Sand Silt (SM): 25% s, 75%om; s: v.f. f, 90%of, 10%om; SA; dry; wk to strong rxn w/HCl; Silt: low plat; 2.51 3/4 lt. yellowish brn; platy structure; MIBK odor; silt + sand interbedded laminae + v. thin beds.	wk to strong rxn w/HCl @ 10-27-17
			136.0-138.8: Silty Sand (MS): 60%os, 40%om; s: v.f. f, SA; 70%of, 30%om; m: non-plastic; dry; no rxn w/HCl; 2.51 3/4 lt. yellowish brn; MS; platy structure; MIBK odor; → 5% increases w/ depth to 75%os, 25%om @ 138.8.	→ folded silt lamina @ 135.5 @ 10-27-17
135			→ 37.2-138.8: silt/clay nodules + deformities; rip-up clasts(?); match unit from 138.8-140.2: banded/bedded silt; 2.51 3/4 lt. olive brn; strong rxn w/HCl.	Core 22 135.2-140.2
137.5			138.8-140.2: Sandy Silt (SM): 80%om, 20%os; s: v.f. f, 90%of, 10%om; SA; s: inc. w/ depth to 40%os, 60%om; PS; m: clay nodule @ 138.8 (and plat); silt is low plat; wk to strong rxn w/HCl (dec. w/ depth); dry; 2.51 5/3 lt. olive brn to 2.51 1/2 lt. brownish gray w/ depth; interbedded silt + sand laminae + v. thin beds.	
140			140.5-140.9: Silt/Clay (M): 100%om; high plasticity; massive; dry; strong rxn w/HCl; 2.51 1/3 olive brn; strong MIBK odor.	10-27-17 Core 23 B
			140.9-142.0: Sandy Silt (SM): 70%om, 30%os; s: v.f. f, SA; 80%of, 20%om; m: low plat; platy; dry; no rxn w/HCl; 2.51 5/3 lt. olive brn; MIBK odor. → silt laminae (1mm) @ 141.9.	140.5-143.0

Reported By:

T. Clark / Jen Russell
Print Name

Geologist / Geologist
Title

Jen Russell
Signature

10-26-17 / 10-27-17
Date

BOREHOLE LOG (Cont.)

Date: _____

Well ID: C9513

Well Name: NA

Location: 216-S-13 Crib

Depth (ft)	Sample	Graphic Log	Sample Description: Sediment Classification, Grain Size Distribution, Color, Moisture Content, Sorting, Angularity, Mineralogy, Particle Size, Reaction to HCl, Other	Comments: Depth of Casing, Drilling Method, Sampling Method, Sampler Size, Water Level, Other
142.5	Core 23B		142.0-143.0: Silt(m): 90% s, 10% f; s: v-fn (too small to determine distribution); m: low plast; platy structure; dry; mod. rxn w/HCl	Core 23B 140.5-143.0
	Core 23A		2.5 1/3 lt. olive brn; mIBK odor; clay nodule (2.5 1/3 lb. du. brn) @ 142.6 (2cm).	
			143.0-145.5: Sandy Silt(sm): 20% s, 80% m; s: v-f, 90% f, 10% m; SA; PS; m: non-plast.	Core 23A 143.0-145.5
145	Core 24		145.1-145.5: 20% s, 80% m Sandy Silt(sm): 20% s, 80% m; Sand: v-f, 90% f, 10% m; SA; Silt: non-plastic; mod rxn w/HCl; 2.5 1/3 lt. olive brn; dry; MS; platy structure; strong mIBK odor. Trace mica in sand.	Core 24 B39 X50 145.1-150.1 Alignot
			145.5-148.8: Silt(m): 10% s, 90% s; sand: v-f	146.1-148.8
147.5			predom v-f, 90% f, 10% m, SA; Silt: non-plastic, MS; mod rxn w/HCl; 2.5 1/3 olive brn; dry; platy structure; strong mIBK odor; Fe-staining @ 148.7-148.8.	Clastic sand dike (2cm max) from 143.0-145.0: 100% s, v-f, 80% f, 20% m; SA-SR; 2.5 1/2 lb. brownish gray; PS; brown clay btw sand and sandy silt unit.
			→ 2cm sandy silt (20% s, 80% m) interbeds @ 146.9 + 148.3; 2.5 1/3 lt. olive brn	→ clay lamina (4mm) @ 145.2, 10-27-17 → nodule @ 145.3.
150			148.8-150.1: Sandy Silt(sm): 20% s, 80% m; Sand: v-f; predom v-f, 90% f, 10% m, SA-SR; Silt: non-plastic; no rxn w/HCl; 2.5 1/2 grayish brn; dry, MS; platy structure; strong mIBK odor; → @ 149.5: 3cm interbed silt (100% s), non-plastic, 2.5 1/2 dk grayish brn.	
152.5	Cores to PNAK @ 10-27-17			
155	Cores to PNAK @ 10-27-17			
157.5	Cores to PNAK @ 10-27-17			
160	Cores to PNAK @ 10-27-17			

Reported By:

T. Clark / Jen Russell
Print Name

Geologist / Geologist
Title

Jen Russell
Signature

10-5-17 / 10-27-17
Date

BOREHOLE LOG (Cont.)

Date:

Well ID: C9513

Well Name: NA

Location: 216-S-13 Crib

Depth (ft)	Sample	Graphic Log	Sample Description: Sediment Classification, Grain Size Distribution, Color, Moisture Content, Sorting, Angularity, Mineralogy, Particle Size, Reaction to HCl, Other	Comments: Depth of Casing, Drilling Method, Sampling Method, Sampler Size, Water Level, Other
162.5				
165			165.3-167.0: Sandy Silt (SM): 80%om, 20%os; s: vfn-fn; 80%of, 20%om; SA, PS, m; low plast; dry; mod. rxn w/HCl; platy structure; 2.51 ^{1/3} lt. yellowish brn; strong MIBK odor. → Sand dike @ 165.7-167.0: 100% s (vf-m; 90%of, 20%om, SA, trace mica, no rxn w/HCl) with sandy silt rip-up clasts throughout; 2.51 ^{1/3} lt. yellowish brn.	
			167.0-167.8: Sandy Silt (SM): 60%om, 40%os; s: vfn-fn, 90%of, 10%om; SA, PS (Core 28) m; low plast; no rxn w/HCl; platy; 2.51 ^{5/4} lt. olive brn; dry; MIBK odor.	165.3-170.3
			167.8-170.3: 100% silt/clay (M): 100%om; high plasticity; strong rxn w/HCl, dry; MIBK odor; → 167.8-168.6: 2.51 ^{5/3} lt. olive brn, platy structure; clay ball (dry, v. strong HCl rxn, 2.51 ^{1/3} lt. yellowish brn @ 167.8, 7cm diameter). → 168.6-169.3: 2.51 ^{5/4} lt. olive brn, platy structure + wood(?) chips throughout. → 169.3-169.9: 2.51 ^{1/3} olive brn, massive → 169.9-170.3: 2.51 ^{5/3} lt. olive brn, platy; clay nodules (2.51 ^{1/3} lt. yell brn) @ 169.9 (5mm).	
167.5	Core 28			
170			170.5-172.0: Silt (M): 95%om, 5%os; s: vf-f, SA, 90%of, 10%om; silt: low plasticity, mod rxn w/HCl; 2.51 ^{5/4} lt. olive brn; moist, massive; MIBK odor. 172.0-173.0: Silt (M): 90%om, 10%os; s: vf-f, SA; trace mica; silt: low-plast; mod rxn w/HCl; 2.51 ^{1/2} ol. brn; moist; platy; MIBK odor; grad. contact; gray clay nodules @ 172.1; wood @ 172.2.	Core 29 B 39X76 Aliquot @ 171-172
	Core 29 B			
172.5			173.0-173.8: Silt (M): 5% 100%os silt; non-plastic, mod rxn w/HCl; 2.51 ^{1/3} olive brn; moist, massive; strong MIBK odor.	Core 29 A B39X74
	Core 29 A		173.8-173.9: Sand (S): 100%os, vf-m, predom m, WS, SA, 40%mat, 60%of, moist, no rxn w/HCl, 10YR 4/2 drk grayish brn, massive; MIBK odor. Aliquot @ 173.6-175.0	173.0-175.5
175			173.9-174.2: Silty Sand (MS): 70%os, 30%om; s: vf-f, 80%of, 20%mat (mat inc. w/ depth to 50%); trace mica, SA, WS, no rxn w/HCl; 2.51 ^{1/2} dark grayish brn, laminar throughout; s: size inc to predom f; strong MIBK odor.	Core 30
	Core 30		174.2-174.3: Silt (M): 100%om, non-plast, mod rxn w/HCl; 2.51 ^{1/2} drk grayish brn; moist, massive, strong MIBK odor. (Sandy silt (SM) @ 10.5.17)	175.1-180.1
177.5			174.3-174.5: Silt (M): 80%om, 20%os; s: vf-f, predom f, SA, 90%of, 10%om; silt: non-plast; no rxn w/HCl; 2.51 ^{1/3} lt. olive brn; moist; platy; strong MIBK odor.	
	Core 31		174.5-174.7: Sand (S): 90%os, 10%om; s: vf-m, predom f, WS, SA, 40%mat, 60%of, moist, no rxn w/HCl, 10YR 4/2 dark grayish brn, laminar; MIBK odor.	
			174.7-175.5: Sandy Silt (SM): 70%om, 30%os; Sand: vf-f, 80%of, 10%mat, SA; size inc to predom m. w/ depth. silt: non-plastic; no rxn w/HCl; 2.51 ^{5/3} lt. olive brn; dry; platy; strong MIBK odor.	
180			→ clay nodules (0.5cm) @ 174.7, 174.9, 175.0 + 175.3; mod rxn w/HCl.	
	Core 31		175.1-175.9: Silt/clay (M): 100%om; high plasticity; strong rxn w/HCl; moist; platy; 2.51 ^{1/3} olive brown; no odor.	
			175.9-176.9: Sandy Silt (SM): 70%om, 30%os; s: vf-f, 90%of, 10%om; SA, PS, m; mod plast; mod rxn w/HCl; 2.51 ^{5/3} lt. olive brown; platy; moist; no odor. @ 176-176.4: 100% s dike (3cm), 60%of, 40%om, vf-m; 2.51 ^{1/3} olive brn, no rxn w/HCl; → 176.6-176.7: silty sand dike (nodules), 2.51 ^{5/3} lt. olive brn; silt laminar betw sand dikes. @ 10.5.17	
			→ unconformity @ 175.9 contact.	

Reported By:

T. Clark / Jan Russell
Print Name

Geologist / Geologist
Title

T. Clark / Jan Russell
Signature

10.5.17 10.27.17
Date

BOREHOLE LOG (Cont.)

Page 8 of 10

Date: 10/12/17

Well ID: C9513

Well Name: NA

Location: 216-S-13 Crib

Depth (ft)	Sample	Graphic Log	Sample Description: Sediment Classification, Grain Size Distribution, Color, Moisture Content, Sorting, Angularity, Mineralogy, Particle Size, Reaction to HCl, Other	Comments: Depth of Casing, Drilling Method, Sampling Method, Sampler Size, Water Level, Other
182.5	Core 31		176.9-180.1: Sand(s): 11(SM): 60% m, 40% s; v.f. f; SA, PS, 70% of 30cm; m: low plat; platy; dry; 2.54% olive brn; ^{10/27/17} non-rxn w/ HCl	Core 31 180.6-185.6
			→ 100% sand lens (8cm) bed @ 170.7-171.3; 30% of: sandy siltine grain size to v.f.-m; s=50% to 178.3'. → Platy, sandy silt to 180.1 (60% m, 40% s).	
185	Core 32		180.6-185.6: Sand(s): 90% s, 10% m; sand: v.f.-med; 60% fcls, 40% mat	Core 32 184.9-189.9
			SA, trace mica; m: non-plastic; moist; no rxn w/ HCl; 2.54% olive brn, no odor; minor rhythmites throughout	
187.5	Core 32		184.9-189.9: Sand(s): 90% s, 10% m; sand: v.f.-med, 60% fcls, 40% mat, SA, PS; trace mica; m: non-plastic; moist; no rxn w/ HCl; 2.54% olive brn; slight ^{10/27/17} m/BK odor; rhythmites throughout.	Core 32 184.9-189.9
			→ Top 3" altered by drilling ^{10/27/17} (184.9-185.2). → @ 188.8-189.9: silt bedding (1cm) + laminae (2mm) present: 100% m, wk rxn w/ HCl; 2.54% dark gray; trace gravels in sand interbeds (felsic, SA-SR, v.f.n pebbles)	
190	Core 33 B		190.4-192.9: Slightly silty sand (mS): 80% s, 20% m; sand: v.f.-m;	Core 33 B 190.4-192.9; aliquot @ 190.9-192.5 ^{10/5/17}
			predom v.f. f; 60% fcls, 40% mat, SA, trace mica; m: non-plast; trace gravels (v.f.n pebbles); dry to silt. moist; no rxn w/ HCl; 2.54% olive brn, no odor; minor rhythmites @ ~191.2'	
192.5	Core 33 A		192.9-194.9: Sand(s): 100% s; 60% of 40% m, v.f.-c, predom f-m, c-grains = mica; ^{10/5/17} no rxn w/ HCl; moist 192.9-193.4; dry 193.4-194.9; 2.54% grayish brn; mod m/BK odor; small rhythmites throughout.	Core 33 A 192.9-195.4; aliquot @ 193.4-194.7
			194.9-195.2: Sandy Gravel (sG): 50% g, 40% s, 10% m; gravel: v.f.n. peb-4cm; SR: 60% m, 40% fcls; sand: v.f.-v.c, predom f-m; 70% of 30% fcls, SR, SA, mica; m: non-plast; 2.54% olive brn; dry; PS; no rxn w/ HCl; consolidated/semi-cem.	
195	Core 34		194.7-195.7: Slightly silty sand (mS): 5% Gravel, 80% sand, 15% silt; Gravel: m peb-5 cm, 75% felsic, 25% mafic; SK; Sand: f-m, 70% ^{10/12/17} mafic, 20% felsic, SA, trace mica, quartz; Silt: non-plastic; 2.54% 1/2 H brownish gray, dry, no rxn w/ HCl, PS, ^{10/12/17} fines downward, v. thin laminae of silt throughout and increasing in number toward contact at 195.7; silt laminae somewhat deformed.	Core 34 - B39X90 194.7 - 199.7
			195.7-199.7: Sandy Gravel (sG): ^{10/12/17} 50% Gravel, 50% Sand; Gravel: v.f. peb-10 cm, 70% felsic, 30% mafic, SR-R, dom. quartz; Sand: f-vc, 70% felsic, 30% mafic, SA, qtz, trace mica; 2.54% 1/3 H olive brown, dry, no rxn w/ HCl, PS, massive, Fe staining throughout, dark blackish staining around cobbles at ^{10/12/17} 196.2-196.4; 196.2-196.4.	
200	Core 35		200.5-205.5: Sandy Gravel (sG): 40% gravel, 60%	Core 35 - B39X92 200.5-205.5

Reported By: T. Clark / A. McGuire Geologist / Geologist AM / Angela McGuire 10/5/17 / 10/27/17
 Print Name Title Signature Date

BOREHOLE LOG (Cont.)

Page 9 of 10

Date: 10/12/17

Well ID: C9513

Well Name: NA

Location: 216-S-13 Crib

Depth (ft)	Sample	Graphic Log	Sample Description: Sediment Classification, Grain Size Distribution, Color, Moisture Content, Sorting, Angularity, Mineralogy, Particle Size, Reaction to HCl, Other	Comments: Depth of Casing, Drilling Method, Sampling Method, Sampler Size, Water Level, Other
202.5	Core 35		200.5-205.5-Sandy Gravel (SG): 40% Gravel, 60% Sand; Gravel: f-peb-10 cm, 70% felsic, 30% mafic, SR, med-coarse peb dominate especially through 202.0-209.5 bgs;	Core 35 - B39X92 200.5 - 205.5
205			205.5-208.8: Sandy Gravel (SG): 50% Gravel, 50% Sand; Gravel: f-peb-9 cm, 90% felsic, 10% mafic, quartzite, SR; Sand: vf-c, dom-med, 85% felsic, 15% mafic, SA; 2.546/2 H brownish grey, dry, massive, PS, Fe staining around pebbles/cobbles	Core 36 - B39X94 205.5 - 210.5
207.5	Core 36		208.8-210.5: Sandy Gravel (SG): 30% Gravel, 70% Sand; Gravel: f-peb-4 cm, 75% felsic, 25% mafic, SA-SR, dom-SR; Sand: 80% felsic, 20% mafic, vf-m, trace mica, SA; 2.546/2 H brownish grey, dry, massive, PS, Fe staining at 209.2, Fe staining at transitional contact at 208.8 bgs.	
210			layer of pink gravel (f. peb) size at 210.2 bgs.	
212.5				
215				
217.5				
220				

Cores to PNNL (10-27-17)

Reported By:

A. McGuire
Print Name

Geologist
Title

Angela McGuire
Signature

10-27-17
Date

BOREHOLE LOG (Cont.)

Date:

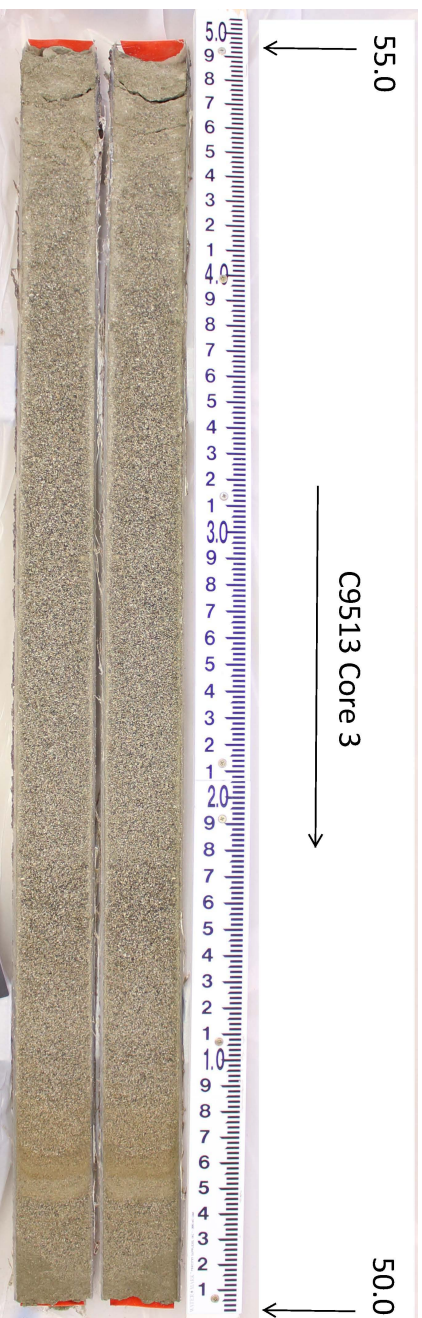
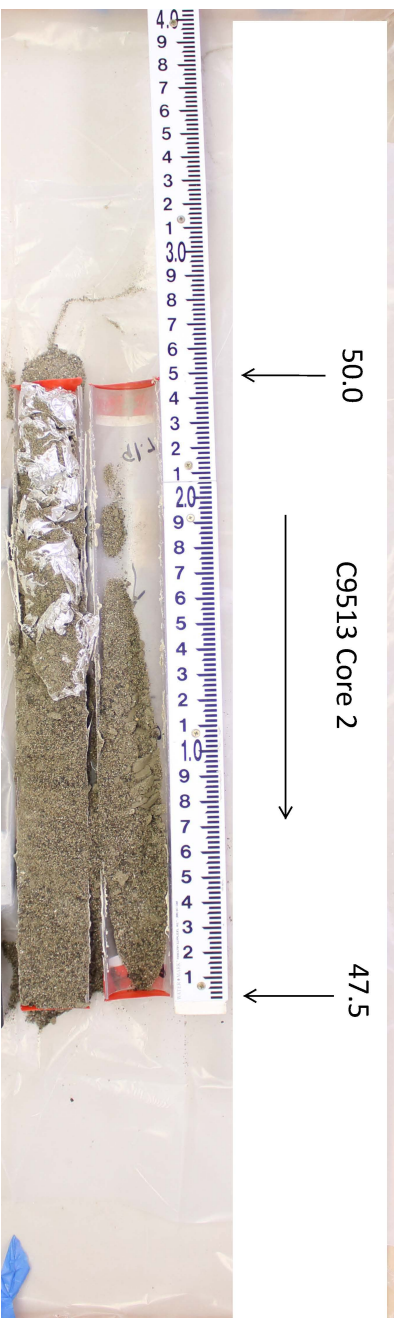
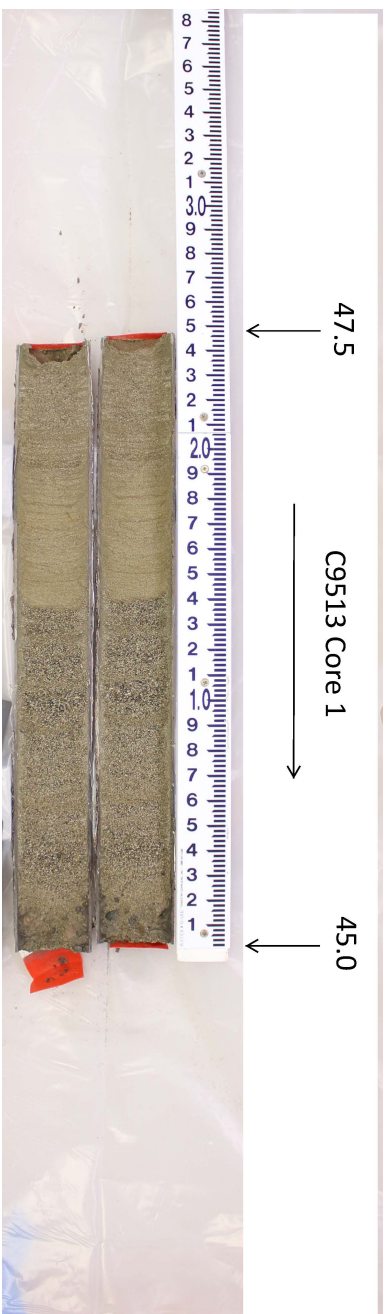
Well ID: C9513

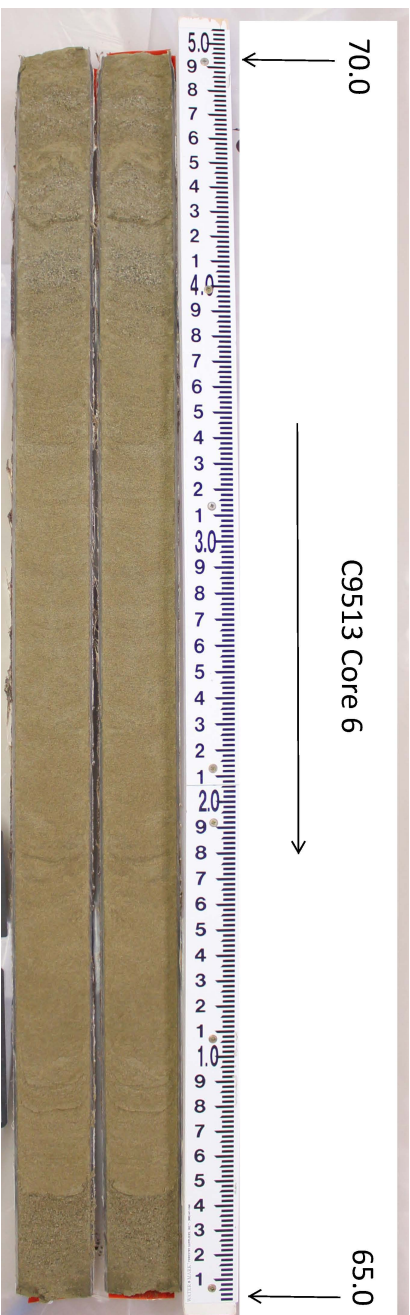
Well Name: NA

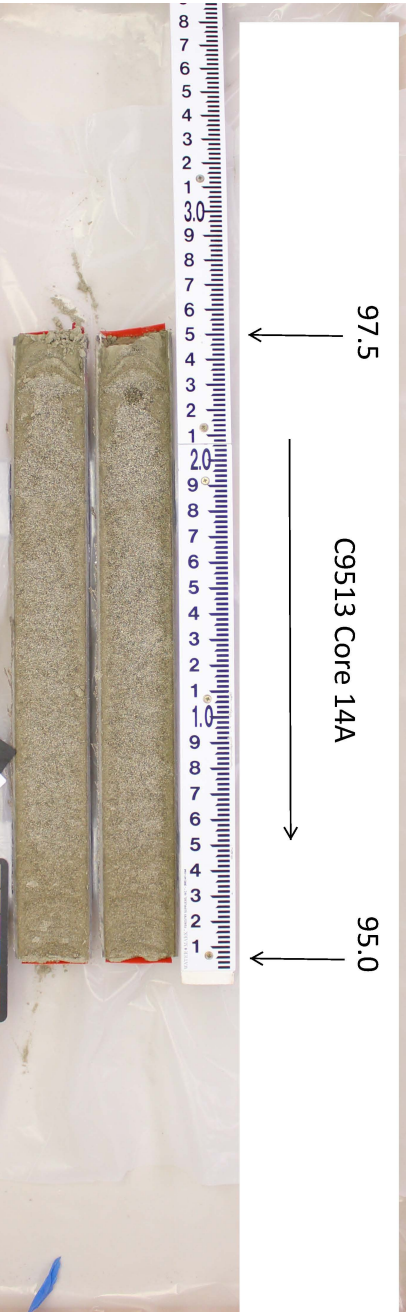
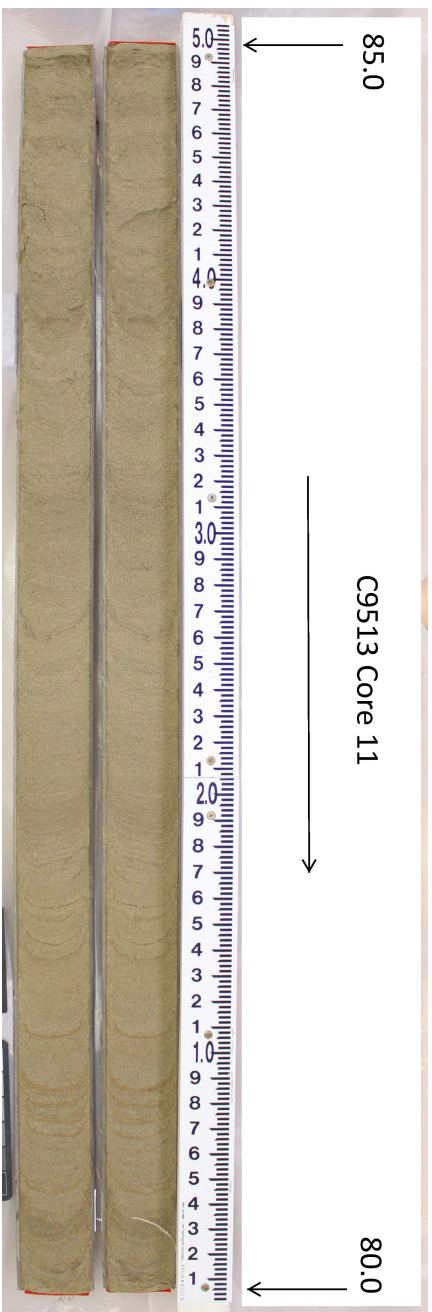
Location: 216-S-13 Crib

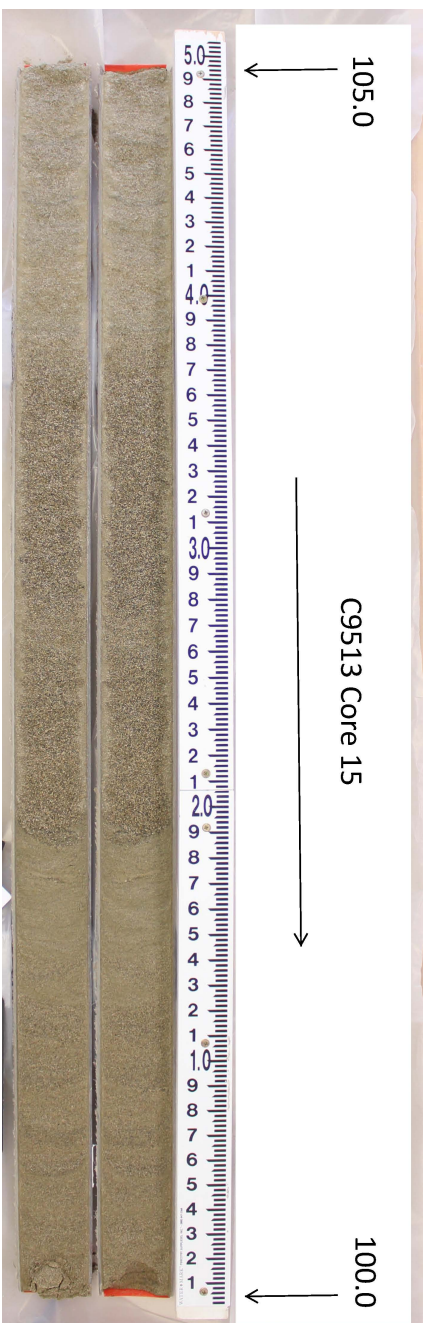
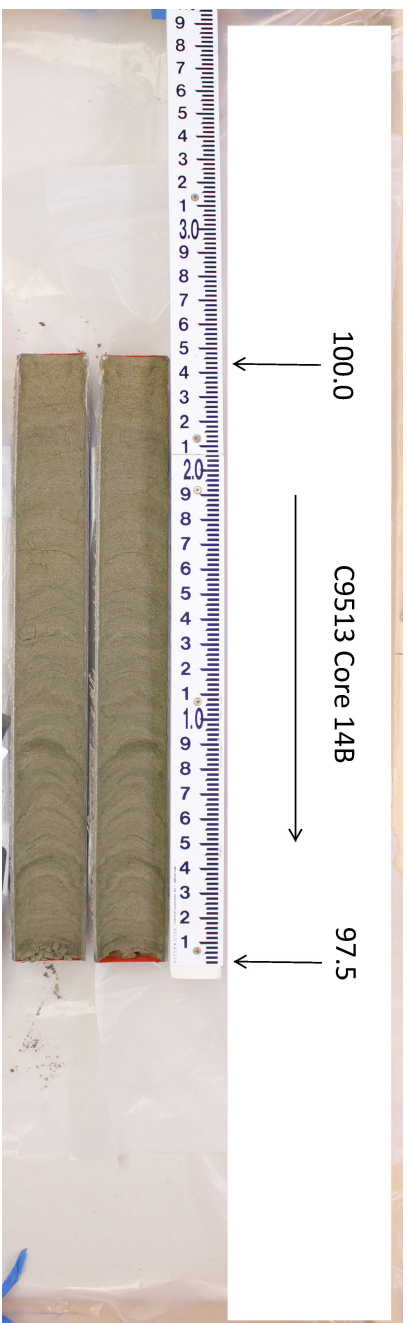
Depth (ft)	Sample	Graphic Log	Sample Description: Sediment Classification, Grain Size Distribution, Color, Moisture Content, Sorting, Angularity, Mineralogy, Particle Size, Reaction to HCl, Other	Comments: Depth of Casing, Drilling Method, Sampling Method, Sampler Size, Water Level, Other
222.5			<i>Cores to PNAAL @ 10-27-17</i>	
225	Core 40		224.7-226.6: Sand(s): 100% s, vfn-m, predom f; 70% of 30% WS, SA, 2.5 1/2 ft. brush gray, dry, no rxn w/ HCl, rhythmites from 225.5-226.6.	Core 40 224.7-229.7; aliquot @ 225.0-227.0
227.5			226.6-229.7: Silty Sandy Gravel (msG): 40% g, 30% s, 30% m; Gravel: vfn prb-10cm SR-A, 50% felsic, 50% mafic (qtz, basal); sand: vfn-vc, predom 60% of 40% m, SA, PS; m: non-plast; dry; no rxn w/ HCl; 2.5 1/3 ft. yel. brn; v. consolidated. → @ 227.2-227.3: thin sand bed (5cm); 70% of 30% m, vfn-m, 2.5 1/2 ft. brush gray, dry, rhythmites	
230	Core 41		230.4-235.4: Silty Sand, Gravel (mSG): 40% g, 30% s, 30% m; Gravel: vfn prb-10cm SR-A, 50% felsic (qtz, 50% mafic (bas)); sand: vfn-vc, SA, PS, 60% of 40% m; m: non-plast; dry, no rxn w/ HCl; 2.5 1/3 ft. yel brn; v. consolidated; minor Fe-staining. → @ 232.1-232.3: thin (bcm) sand interbed: 100% s, 70% of 30% m, vfn-m, 2.5 1/2 ft. brush gray; dry; massive.	Core 41 230.4-235.4 Aliquot @ 231.4-234.4
232.5				
235	Core 42		235.5-240.5: Sandy Gravel (SG): 40% gravel, 55% sand, 5% silt; Gravel: fpeb-7cm, 70% felsic, 30% mafic, SR, qtz, basalt; Sand: f-c, 75% felsic, 25% mafic, SA, qtz, trace mica; silt: non-plastic, present at lens at 237.5 bgs: 2.5 yel 3 ft yellowish brown, dry, massive, no rxn w/ HCl, PS, Fe staining throughout especially around cobbles 235.5-236.2 and 235.10/12/17 ADM 238.5-240.5 bgs.	Core 42 - B39 X D0 235.5-240.5
237.5				
240			Total Depth 240.5 bgs	

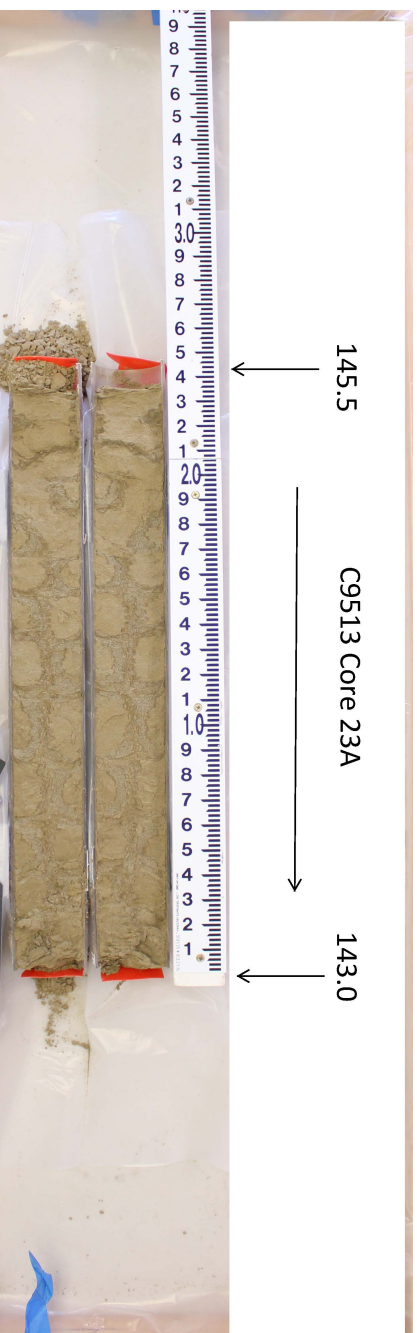
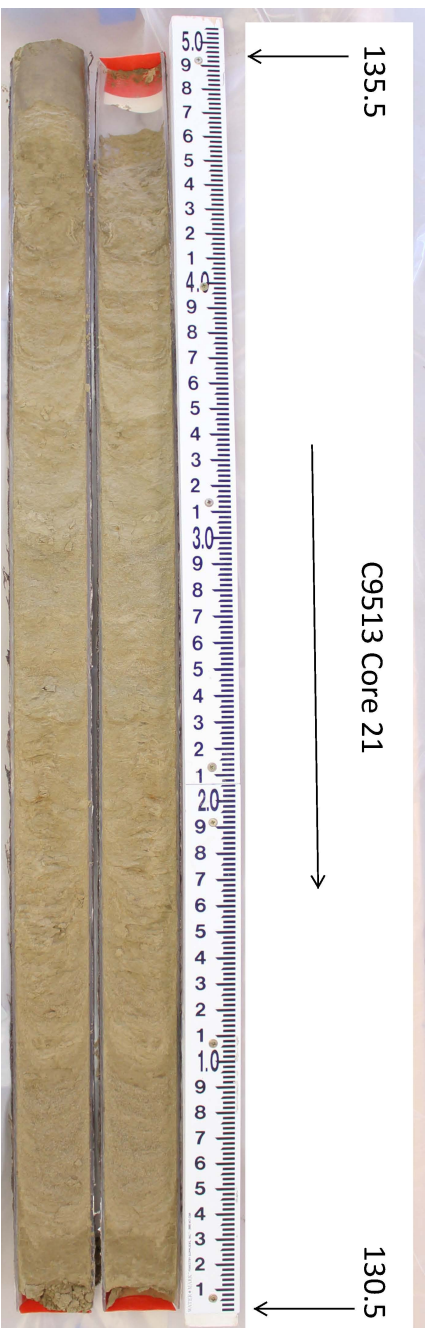
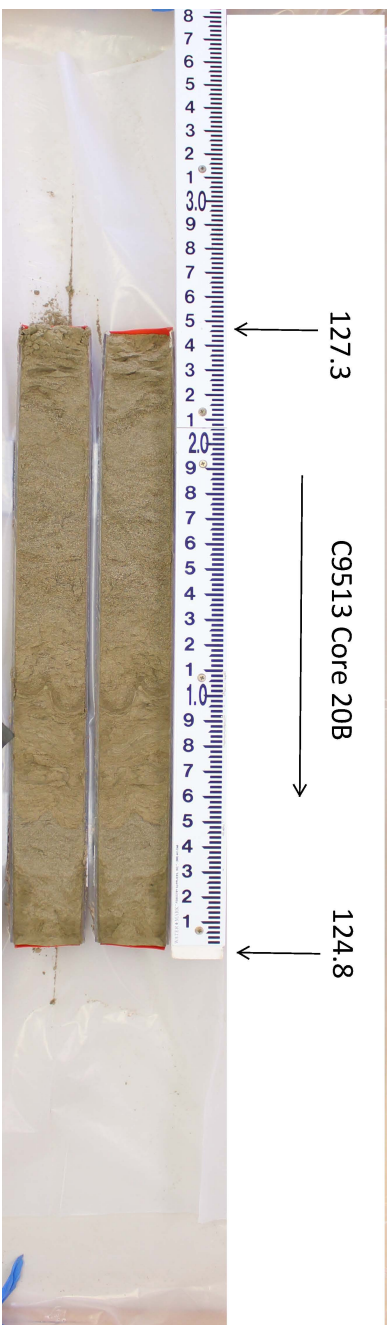
Reported By: T. Clark / A. McGuire Geologist / Geologist Z. Z. / Angela Nelson 10-6-17 / 10-27-17
 Print Name Title Signature Date

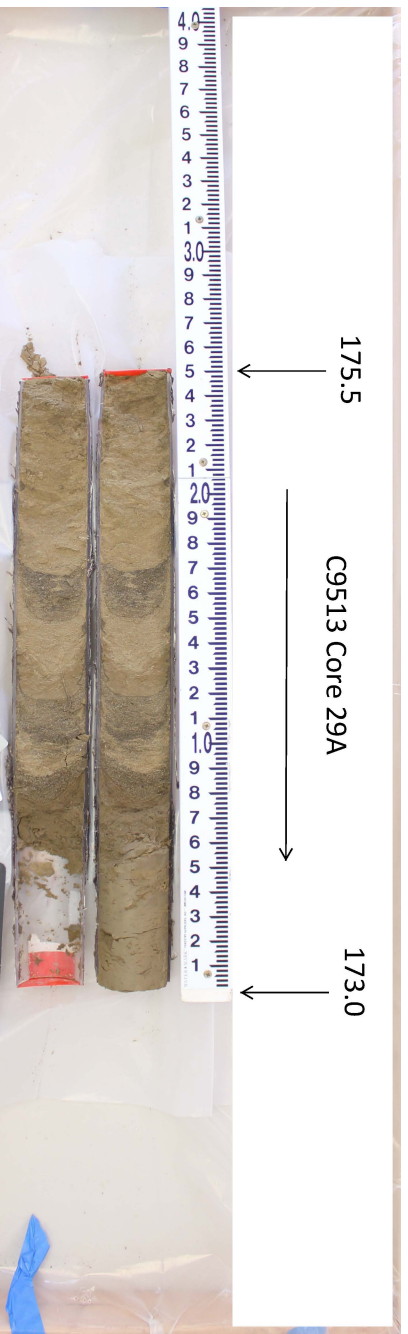
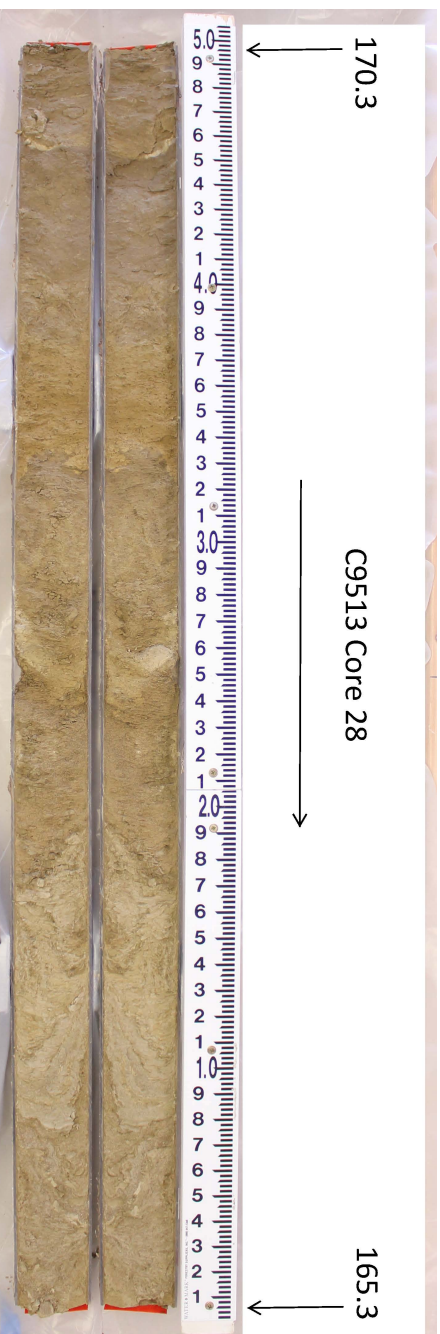


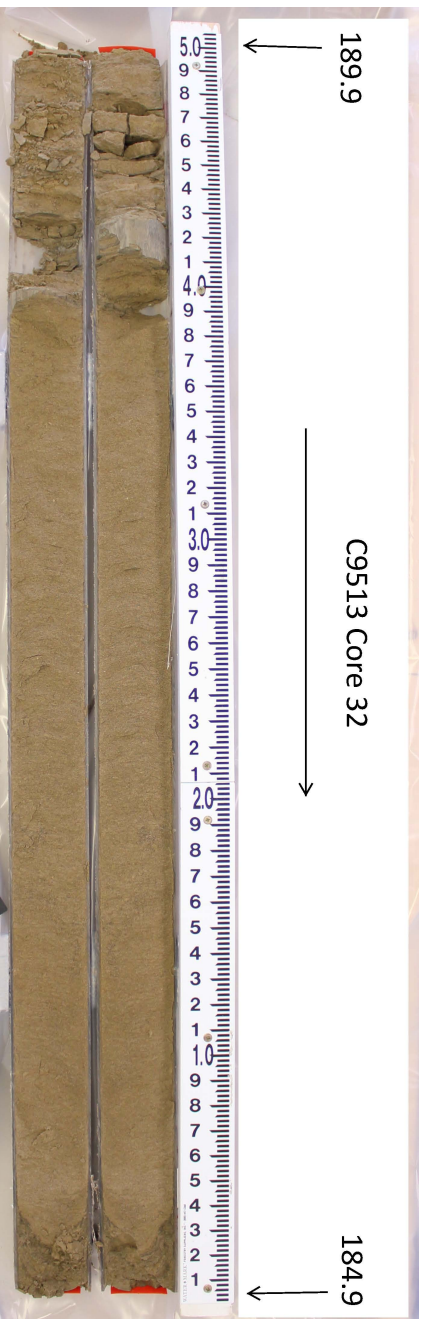
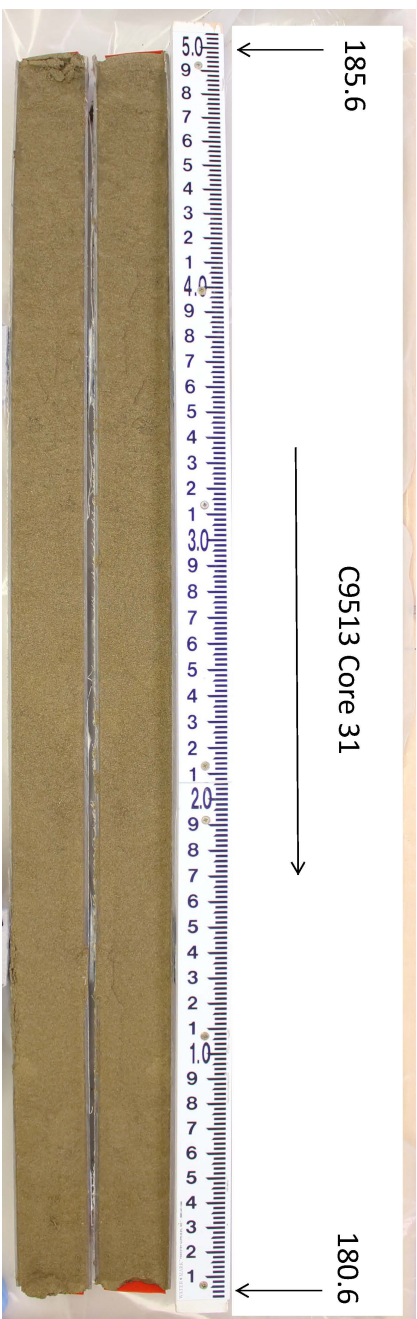
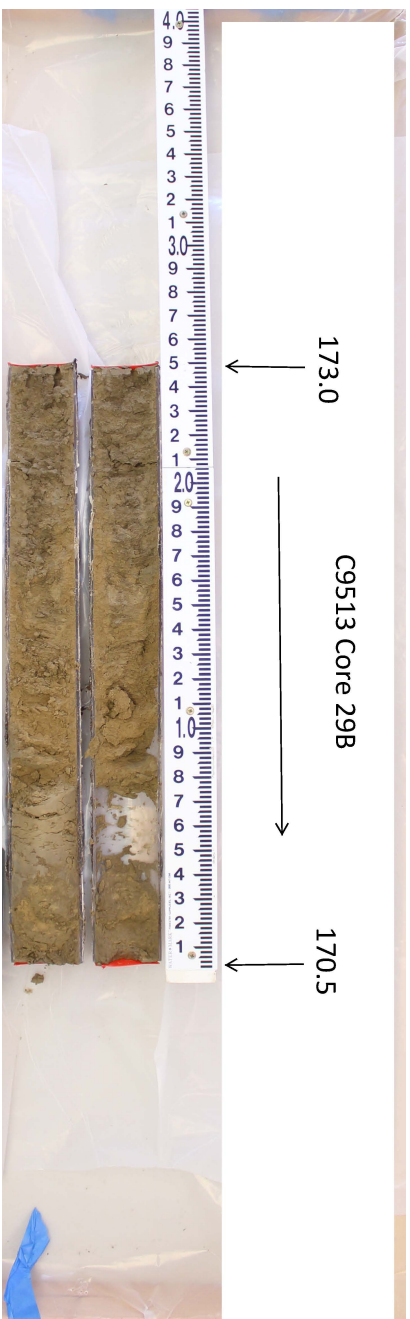


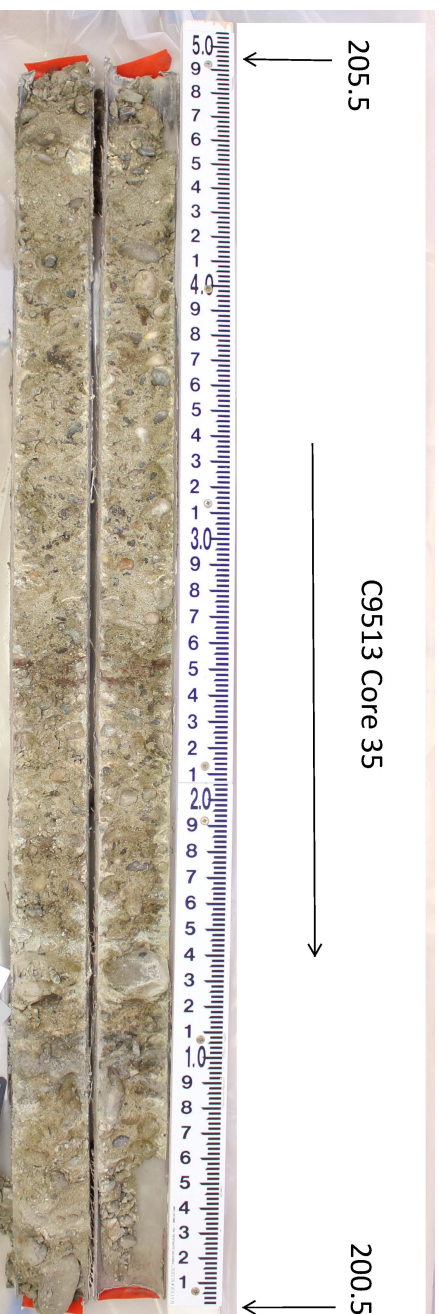
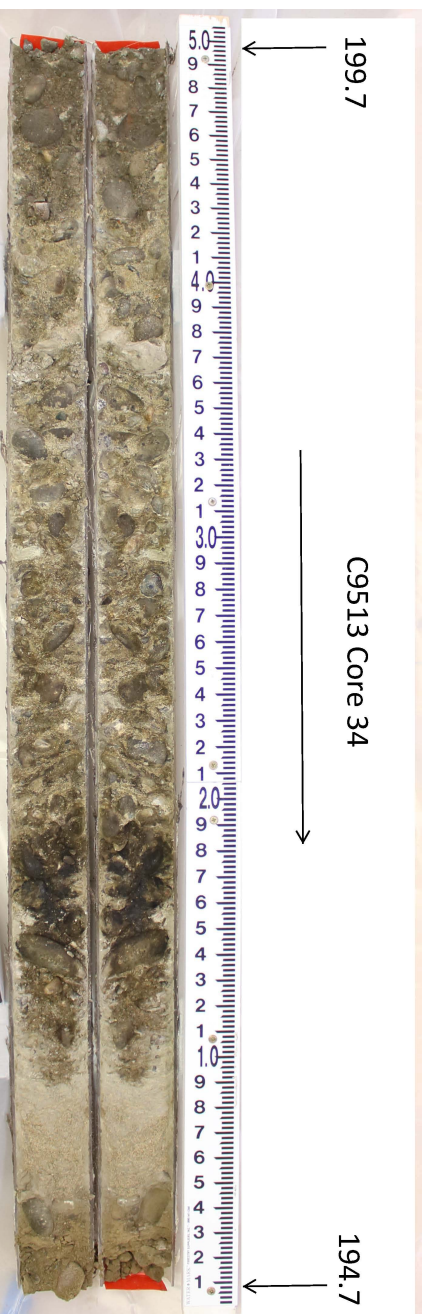
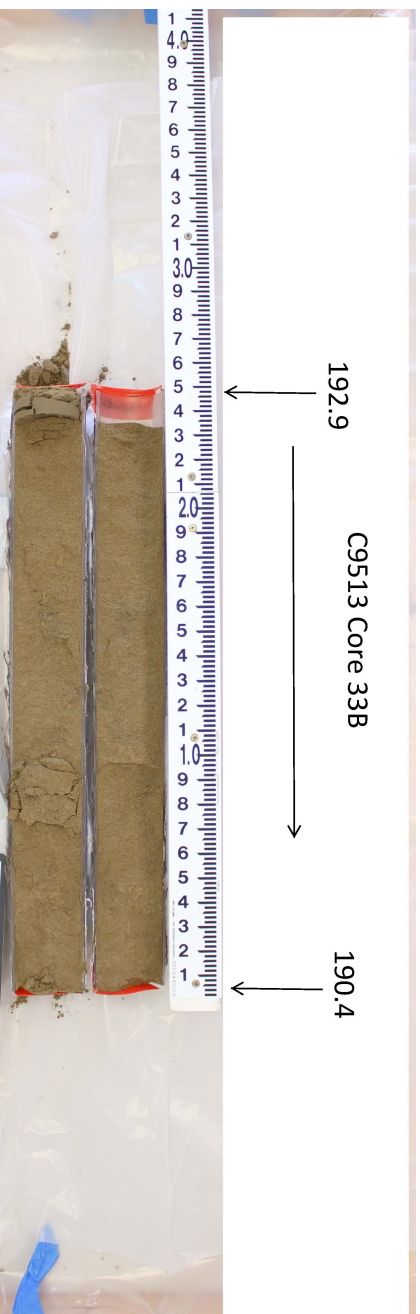
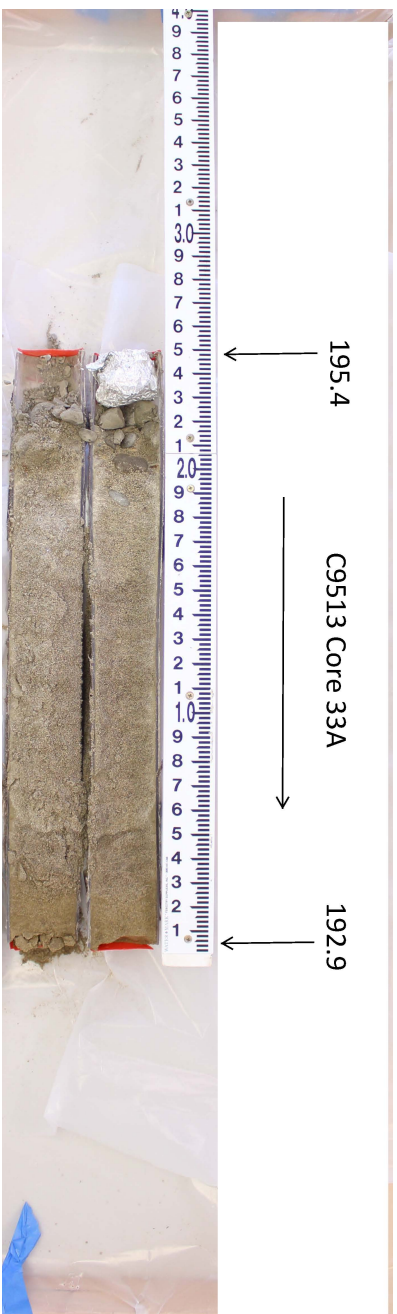


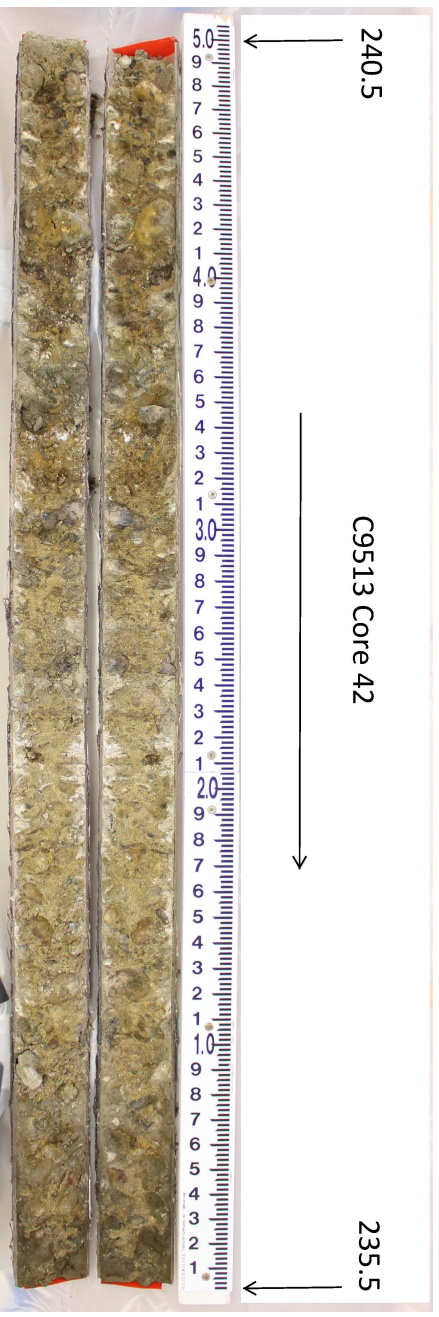
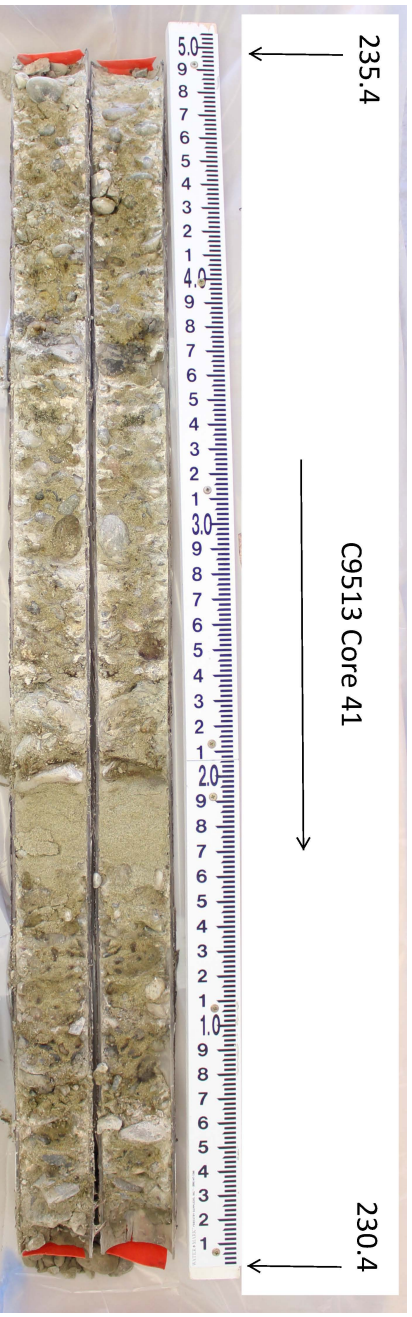
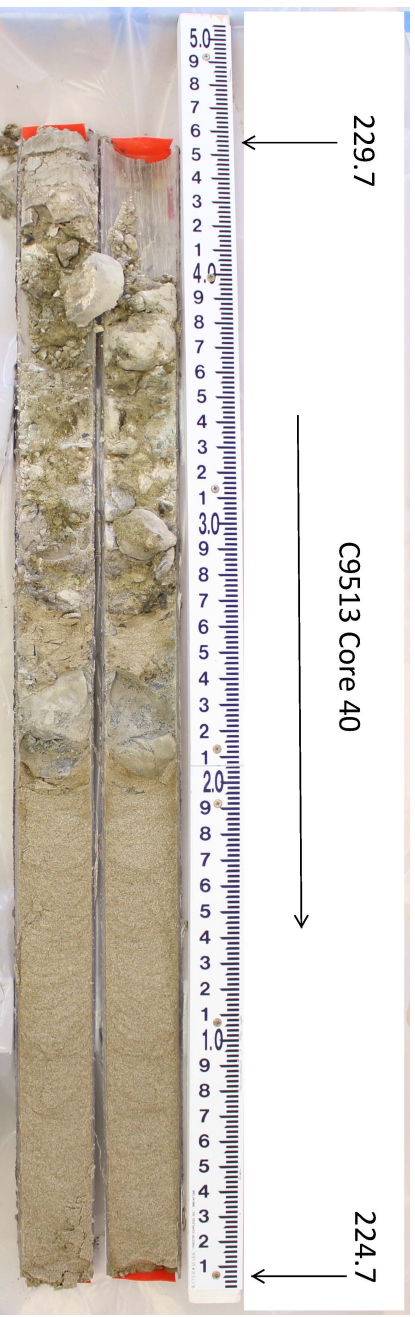
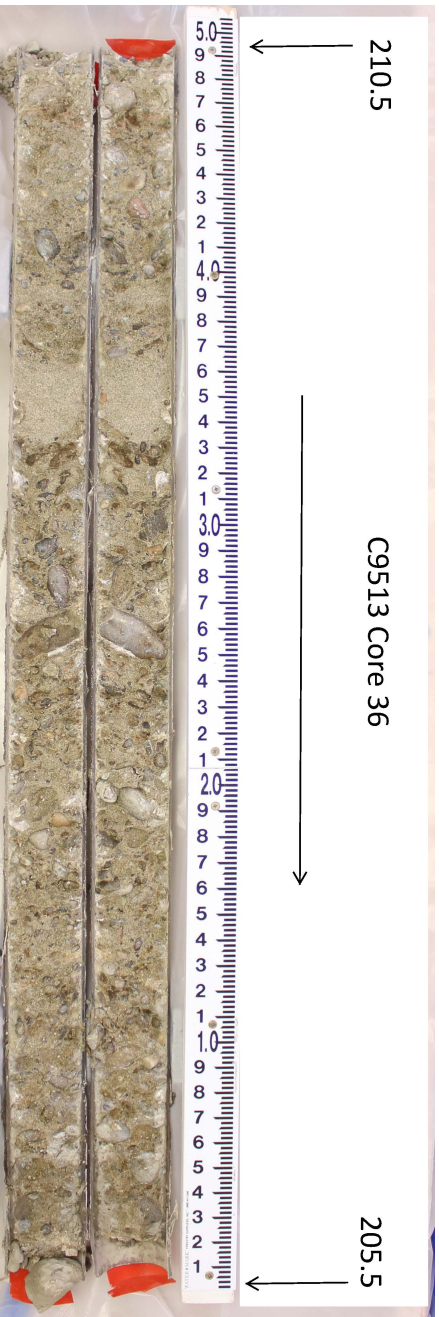












BOREHOLE LOG				Page <u>1</u> of <u>6</u>
Well ID: C9514		Well Name: NA		Date: <u>9/14/16</u>
Project: 200 DV-1 OU Characterization Phase 3			Location: 216-S-21 Crib	
Reference Measure Point: Ground Surface				
Depth (ft)	Sample	Graphic Log	Sample Description: Sediment Classification, Grain Size Distribution, Color, Moisture Content, Sorting, Angularity, Mineralogy, Particle Size, Reaction to HCl, Other	Comments: Depth of Casing, Drilling Method, Sampling Method, Sampler Size, Water Level, Other
40				Sonic Core RS = Rad. Screen
42.5				
45	Core 1		44.1 - 46.6: Sandy Silt; Sand 40%, Silt 60% (SM) vf-f sand, moist, 2.5Y4/3 olive brn, non-plastic, platy structure, trace mica, no rxn w/ HCl, MS	Core 1 B36107 (RS - B36106) 44.1 - 46.6 Aliquot 44.6 - 45.6
47.5	Core 2		47.4 - 49.9: Silty Sand (MS): 70% Sand, 30% Silt; Sand: vf-f, SA, 95% Felsic, 5% Mafic, predom vf; moist, no rxn w/ HCl, 2.5Y5/4 light olive brn, massive, WS, trace mica, iron staining	GM: 51/42/53 cpm PAM: 2 cpm Core 2 B36109 47.4 - 49.9
50	Core 3		49.6 - 52.1: Silty Sand (MS): 70% Sand, 30% Silt; Sand: vf-f, SA, 95% Felsic, 5% Mafic, predom vf; moist, no rxn w/ HCl, 2.5Y5/4 light olive brn, massive, WS, trace mica, iron staining	Core 3 B36111 49.6 - 52.1
52.5	Core 4		52.5 - 55.0: Sand (S): 90% Sand, 10% Silt; Sand: vf-f, 70% Felsic, 30% Mafic, SA; dry, WS, no rxn w/ HCl, trace mica, iron staining, massive, predom. f 2.5Y5/2 grayish brn	Core 4 B36113 52.5 - 55.0
55	Core 5		54.7 - 57.2: Sand (S): 100%, vf-f, predom f, massive, 70% Felsic, 30% Mafic, SA, dry, 2.5Y5/2 grayish brn, trace mica, iron staining, WS, no rxn w/ HCl	Core 5 B36115 54.7 - 57.2
Reported By: <u>Jen Russell</u> Geologist <u>Jen Russell</u> 9/21/16				
Reviewed By: <u>Tessa Clark</u> Geologist <u>Tessa Clark</u> 10/25/16				
For Office Use Only				
OR Doc Type:		WMU Code(s):		

BOREHOLE LOG (Cont.)

Date: 10/19/16

Well ID: C9514

Well Name: NA

Location: 216-S-21 Crib

Depth (ft)	Sample	Graphic Log	Sample Description: Sediment Classification, Grain Size Distribution, Color, Moisture Content, Sorting, Angularity, Mineralogy, Particle Size, Reaction to HCl, Other	Comments: Depth of Casing, Drilling Method, Sampling Method, Sampler Size, Water Level, Other
57.5	Core 6		57.1-62.1: Sand (S) 100%: vf-f, 70% felsic, 30% mafic, trace mica, SA, WS, massive, dry, no rxn w/ HCl, 2.5Y 3/2 very dark grayish brown.	Smic Core Core 6 B36117 57.1-62.1
60				
62.5				
62.5	Core 7		62.1-62.4: Slough 62.4-62.6: JR 10/19/16 62.6-67.1: Sand (S) Slightly silty sand (m) S: Sand 85% Silt 15%; Sand: vf-f, predom vf, 90% felsic, 10% mafic, massive, trace mica; moist, 2.5Y 6/3 light yellowish brn, no rxn w/ HCl, WS.	Core 7 B36119 62.1-67.1
65				
67.5				
67.5	Core 8		67.1-67.8: Silt (M): 90% silt, 10% sand, dry, strong rxn w/ HCl, vf sand, 2.5Y 5/3 light olive brn, platy structure, WS, JR 10/19/16, non-plastic	Core 8 B36121 67.1-72.1
70				
70.2				
70.2	Core 9		67.8-70.2: Sand (S) 100%, vf-m, predom f, no rxn w/ HCl, 2.5Y 5/4 light olive brn, massive, silt bed @ 69.9 (1.5cm)	Aliquot 47.8-69.5
70.2				
70.4				
70.4	Core 9		70.2-70.4: Sandy silt bed (SM): Sand: vf, 95% felsic, 5% mafic, 60% silt, 40% sand; dry, no rxn w/ HCl, 2.5Y 7/3 pale brn	
70.4				
70.4				
70.4	Core 9		70.4-71.5: Silty sand (m) S: 60% sand, 40% silt; Sand: vf-f, 70% felsic, 30% mafic; dry, 2.5Y 4/2 dark grayish brn to 70.9, 2.5Y 4/2 light brownish gray 70.9-71.5, no rxn w/ HCl, WS-MS, JR 10/25/16, massive	
72.5				
71.5				
71.5	Core 9		71.5-72.1: Sandy silt (SM): 60% silt, 40% sand; moist, med rxn w/ HCl, 2.5Y 5/4 light olive brn, vf sand	Core 9 B36123 72.0-77.0
72.0				
72.0				
72.0	Core 9		72.0-74.7: Stratified Sand (S): 90% sand, 10% silt; dry to moist, no rxn w/ HCl, PS	
75				
72.0				
72.0	Core 9		72.0-73.5: vf-c sand, vf grading to c @ ~ 73.0, 2.5Y 4/2 light brownish gray	
73.5				
73.5				
73.5	Core 9		73.5-74.1: c grading to vf, 2.5Y 5/4 light olive brn, 85% f, 15% m, 30% felsic, 70% mafic, JR 10/19/16	
74.1				
74.1				
74.1	Core 9		74.1-74.4: m-c sand, trace mica, 30% mafic, 70% felsic, 2.5Y 4/2 light brn gray	
74.4				
74.4				
74.4	Core 9		74.4-74.7: vf, 2.5Y 5/3 light olive brn, 85% felsic, 15% mafic	

Reported By:

Jen Russell
Print Name

Geologist
Title

Jen Russell
Signature

10/19/16
Date

BOREHOLE LOG (Cont.)

Date: 10/19/16

Well ID: C9514

Well Name: NA

Location: 216-S-21 Crib

Depth (ft)	Sample	Graphic Log	Sample Description: Sediment Classification, Grain Size Distribution, Color, Moisture Content, Sorting, Angularity, Mineralogy, Particle Size, Reaction to HCl, Other	Comments: Depth of Casing, Drilling Method, Sampling Method, Sampler Size, Water Level, Other
57.5				
60				
62.5				
65				
67.5				
70				
72.5				
75				
77.5				
80				
82.5				
85				
87.5				
90				
92.5				
95				
97.5				
100				
102.5				
105				
107.5				
110				
112.5				
115				
117.5				
120				
122.5				
125				
127.5				
130				
132.5				
135				
137.5				
140				
142.5				
145				
147.5				
150				
152.5				
155				
157.5				
160				
162.5				
165				
167.5				
170				
172.5				
175				
177.5				
180				
182.5				
185				
187.5				
190				
192.5				
195				
197.5				
200				
202.5				
205				
207.5				
210				
212.5				
215				
217.5				
220				
222.5				
225				
227.5				
230				
232.5				
235				
237.5				
240				
242.5				
245				
247.5				
250				
252.5				
255				
257.5				
260				
262.5				
265				
267.5				
270				
272.5				
275				
277.5				
280				
282.5				
285				
287.5				
290				
292.5				
295				
297.5				
300				
302.5				
305				
307.5				
310				
312.5				
315				
317.5				
320				
322.5				
325				
327.5				
330				
332.5				
335				
337.5				
340				
342.5				
345				
347.5				
350				
352.5				
355				
357.5				
360				
362.5				
365				
367.5				
370				
372.5				
375				
377.5				
380				
382.5				
385				
387.5				
390				
392.5				
395				
397.5				
400				
402.5				
405				
407.5				
410				
412.5				
415				
417.5				
420				
422.5				
425				
427.5				
430				
432.5				
435				
437.5				
440				
442.5				
445				
447.5				
450				
452.5				
455				
457.5				
460				
462.5				
465				
467.5				
470				
472.5				
475				
477.5				
480				
482.5				
485				
487.5				
490				
492.5				
495				
497.5				
500				

NR 10/19/16

Core 9 (Cont.)
Slightly silty sand (m)S:

74.7-76.1: Sandy silt (sm): Sharp contact, trace wood bits noted above/at contact, 80% Sand, 20% Silt; Sand: vf; laminated in upper 0.3ft, Silt layer ~ 2cm thick w/ lenticular bed of vf sand in center @ 74.8' (strong rxn w/ HCl), strong rxn w/ HCl, 2.5% light olive brn, grades to silty sand @ 76.1
76.1-77.0: Silty sand (ms): 80% Sand, 20% Silt; Sand: vf-f, 95% FeSiC, 5% mafic, trace mica; 2.5% light brnish gray, laminated silt lens @ 76.0 (nodule), no rxn w/ HCl, dry

Core 9 B36123
72.0-77.0

Core 9

Reported By:

Jen Russell
Print Name

Geologist
Title

Jen Russell
Signature

10/19/16
Date

BOREHOLE LOG (Cont.)

Date: 10/19/16

Well ID: C9514

Well Name: NA

Location: 216-S-21 Crib

Depth (ft)	Sample	Graphic Log	Sample Description: Sediment Classification, Grain Size Distribution, Color, Moisture Content, Sorting, Angularity, Mineralogy, Particle Size, Reaction to HCl, Other	Comments: Depth of Casing, Drilling Method, Sampling Method, Sampler Size, Water Level, Other
77.5	Core 10		77.1-82.1: Sand (S): 90% Sand, 10% Silt; Interbedded vf - c. Sand beds, dry, no rxn w/ HCl, vf/f beds laminated, m-c sand 20% Mafic, 80% Felsic, 77.8: 4 mm silt lamina, 2.5Y 5/6 light olive brn	Some Core
80			80.2-82.1: vf sand/silt laminae	Core 10 B36125 77.1-82.1
82.5				Aliquot 78.3-79.8'
85	Core 11		82.5-87.5: Sand (S): 100%; vf - c, dry, trace mica, 80% Felsic, 20% Mafic, no rxn w/ HCl, 2.5Y 4/6 light brownish gray, PS, vf sand lamina @ 83.0 ~3mm thick	Core 11 B36127 82.5-87.5
87.5			86.2-87.5: massive sharp contact @ 83.0 between grain size (vf/c) JR 10/20/16	
90	Core 12		87.2-91.1: Sand (S) 100%; vf - c, dry, 80% Felsic, 20% Mafic, no rxn w/ HCl	
90			87.2-89.4: Massive, 2.5Y 4/2 light brownish gray, WS, trace mica, m-c, predom c	
90			89.4-91.1: rhythmites, laminae, vf, 2.5Y 4/3 light yellowish brn, WS	Core 12 B36129 87.5 - JR 10/20/18 87.2 - 92.2
92.5	Core 13		91.1-92.2: Sandy Silt (SM): 75% Silt, 25% Sand; sand: vf, 90% Felsic, 10% Mafic, SA; dry, no rxn w/ HCl, 2.5Y 4/4 light yellowish brn, WS	
92.5			92.2-93.5: Sand (S) 90% Sand to 94.1: 95% Sand 5% Gravel; Sand: m-c, 80% Felsic, 20% Mafic, SA, WS Gravel: 3 cm cobble, basalt, A; dry, trace mica; no rxn w/ HCl, 2.5Y 5/2 grayish brn	Core 13 B36131 92.2-97.2
95			93.5-94.1: Silt (M) 100% moist, 2.5Y 5/6 light olive brn, wk rxn w/ HCl, non-plastic	
95			94.1-97.2: Sand (S): 95% Sand, 5% Silt; interbedded vf - med sand beds/rhythmites, no rxn w/ HCl, 2.5Y 4/4 light yellowish brn - 2.5Y 4/4 light olive brn, Iron staining from 93.7-95.7	Aliquot 93.7-95.7
			94.4-94.7, laminae from 95.8-97.2, 80% Felsic, 20% Mafic	

Reported By:

Jen Russell
Print Name

Geologist
Title

Jen Russell
Signature

10/20/16
Date

BOREHOLE LOG (Cont.)

Page 5 of 6

Date: 10/20/16

Well ID: C9514

Well Name: NA

Location: 216-S-21 Crib

Depth (ft)	Sample	Graphic Log	Sample Description: Sediment Classification, Grain Size Distribution, Color, Moisture Content, Sorting, Angularity, Mineralogy, Particle Size, Reaction to HCl, Other	Comments: Depth of Casing, Drilling Method, Sampling Method, Sampler Size, Water Level, Other
97.5	Core 14		97.1 - 99.4: Sand (S) 100%: vf-vc, predom m-c, 65% Felsic, 35% Mafic, trace mica SA rhythmites through out, grades to gravelly Sand iron staining, 2.5Y 4/2 light brownish gray, dry, no rxn w/HCl	Sonic Core Core 14 B36133 97.1 - 102.1
100			99.4 - 102.1: Gravelly Sand (gS): Gravel 20%, 80% Sand; Gravel: vf peb - 4cm, SR-R, 50% Mafic, 50% Felsic, gravel size increases w/depth, Felsic content increases w/depth; Sand: vf-vc, 60% Felsic, 40% Mafic, SA; rhythmites 99.4-101.2, massive from 101.2 to 102.1, dry, iron staining, med rxn w/HCl @ 101.2-102.1, no rxn w/HCl from 97.1-101.2,	
102.5	Core 15		102.0 - 107.0: 2.5Y 5/2 grayish brn, PS, f-m sand from 100.3-100.9. 2.5Y 4/2 light grayish brn w/pebbles	Core 15 B36135 102.0 - 107.0
105			102.0 - 102.8: Gravelly Sand (gS): 75% Sand, 25% Gravel; Gravel: f peb - 9cm, SR-R, 60% Felsic w/granite, 40% Mafic; Sand: f-c, predom med., 70% Felsic, 30% Mafic, SA; dry, PS, no-wk rxn w/HCl, 2.5Y 4/3 light yellowish brn	
107.5	Core 16		107.2 - 112.2: Gravelly Sand (gS): 85% Sand, 15% Gravel; Gravel: vf peb - 3cm, 60% Felsic, 40% Mafic, pebbles predom. mafic, cobbles predom felsic; Sand: vf-c, predom c, 60% Felsic, 40% Mafic, trace mica, SA, no rxn w/HCl, 2.5Y 4/2 light brownish gray	Core 16 B36137 107.2 - 112.2 SR-R # 107.2-112.2
110				
112.5	Core Opt. 17		112.2 - 114.8: Sand (S) 100%: vf-vc, predom. f-medium, trace mica, 70% Felsic, 30% Mafic, dry, no rxn w/HCl, coarse-grained layers 113.2-113.5, iron staining	Core Optional 17 112.2 - 117.2 B36139 Aliquid
115			114.8 - 115.9: Silty sand (mS): 60% Sand, 40% Silt; Interbedded sand & silt beds/laminae, Sand: vf-f, 80% Felsic, 20% Mafic, trace mica, moist, no rxn w/HCl, 2.5Y 4/3 light yellowish brown, suspect charcoal fragments & iron staining @ contact (114.8)	114.8 - 115.8 or wood bits
			115.9 - 117.2: Silt (M): 100%, moist, 2.5Y 4/2 light brownish gray, wk rxn w/HCl, vf laminae (crossbedded), non-plastic	

Reported By:

Jen Russell
Print Name

Geologist
Title

Jen Russell
Signature

10/20/16
Date

BOREHOLE LOG (Cont.)

Page 6 of 6

Date: 10/20/16

Well ID: C9514

Well Name: NA

Location: 216-S-21 Crib

Depth (ft)	Sample # <i>10/20/16</i>	Graphic Log	Sample Description: Sediment Classification, Grain Size Distribution, Color, Moisture Content, Sorting, Angularity, Mineralogy, Particle Size, Reaction to HCl, Other	Comments: Depth of Casing, Drilling Method, Sampling Method, Sampler Size, Water Level, Other
117.5	<i>Core Optional 18</i>		117.4-117.7: Silt (M) 100%, moist, 2.5 ^{1/2} light brn sh gray, wk rxn w/HCl, vf laminae (crossbedded)	Sonic Core
120			117.7-120.9: Sand (S) 100%; vf-med, dry, 95% felsic, 5% mafic, SA, WS, iron staining (ferric) horizontal, rhythmites through to 120.2, no rxn w/HCl linear	Core Optional 18 117.4 - 122.4
			120.2-120.9: massive (gradational contact)	B36141
			120.9-122.4: Interbedded silt and sand layers Sand: vf-f, 90% felsic, 10% mafic, no rxn w/HCl, SA, 2.5 ^{1/2} light gray, MS, 0.5-3cm thick Silt: 2.5 ^{5/8} light olive brn, strong rxn w/HCl, non-plastic, 0.5-2cm thick, laminated; dry rhythmites and/or graded beds within sand layers, silt lenses 120.9-121.1	
122.5	<i>Core Optional 19</i>		122.0-124.3: Silt (M): moist, 2.5 ^{5/8} light olive brn, vf laminae, no rxn w/HCl, 100% silt, non-plastic	Core Optional 19 122.0 - 127.0
125			124.3-125.3: Sandy silt (SM): 60% silt, 40% sand Sand: vf, 95% felsic, 5% mafic, trace mica; dry, 2.5 ^{1/2} light yellowish brn, laminae & very fin beds throughout, platy structure	B36143 Aliquot 123.5 - 125.0
			125.3-127.0: Silt (M): 70% silt, 30% clay, moist, low plasticity, wk-mod rxn w/HCl, 2.5 ^{5/8} light olive brn	
127.5			Total Depth 127.0	
130				
132.5				
135				

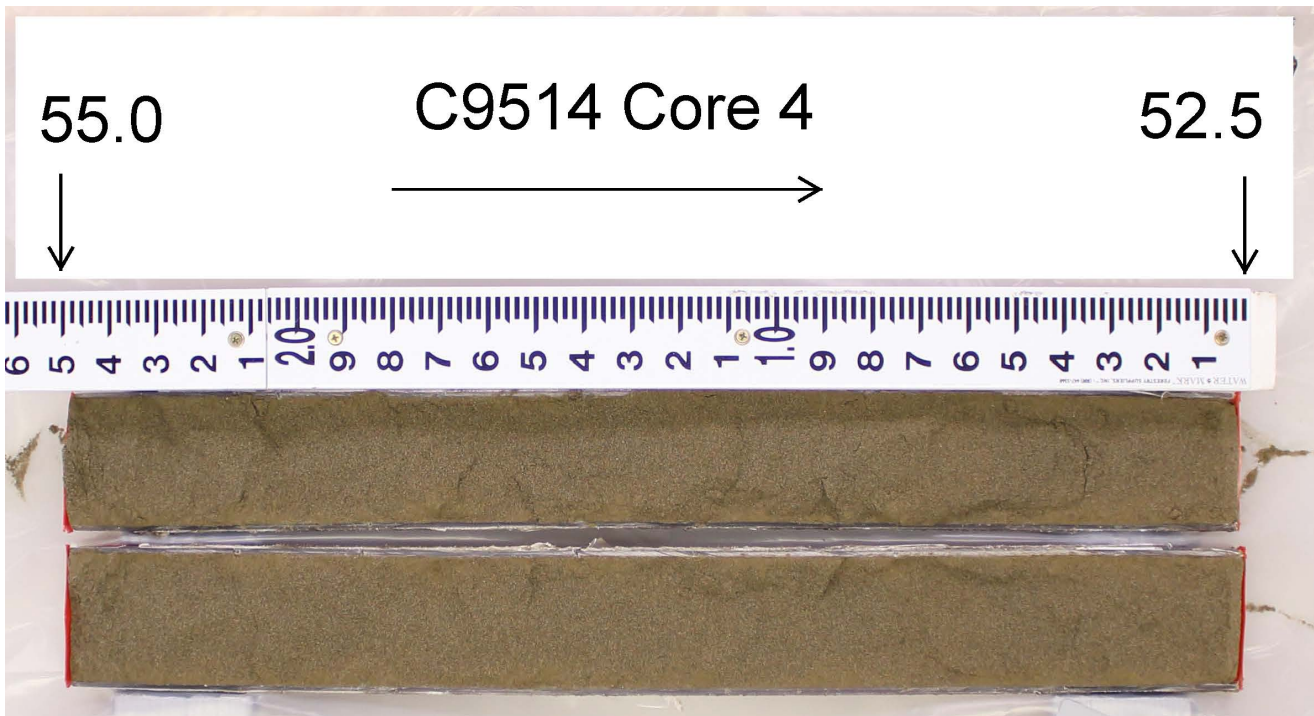
Reported By:

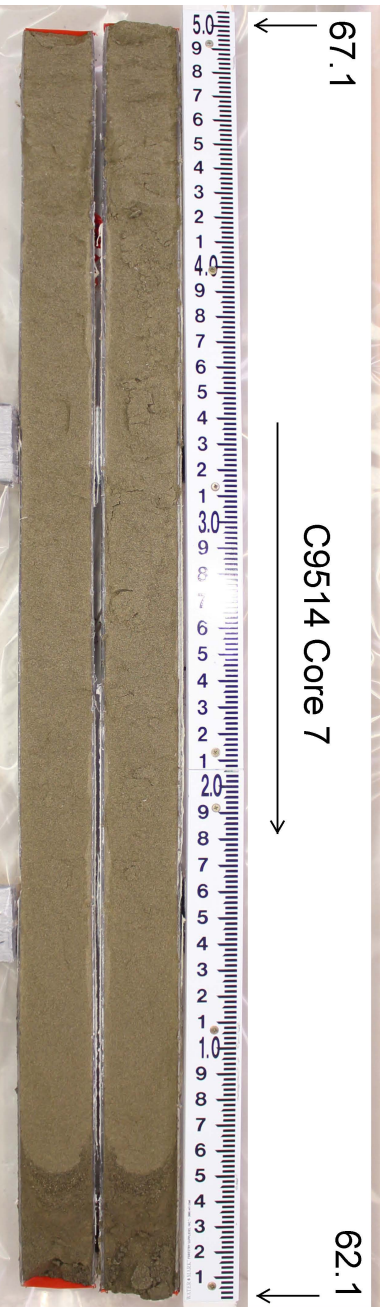
Jen Russell
Print Name

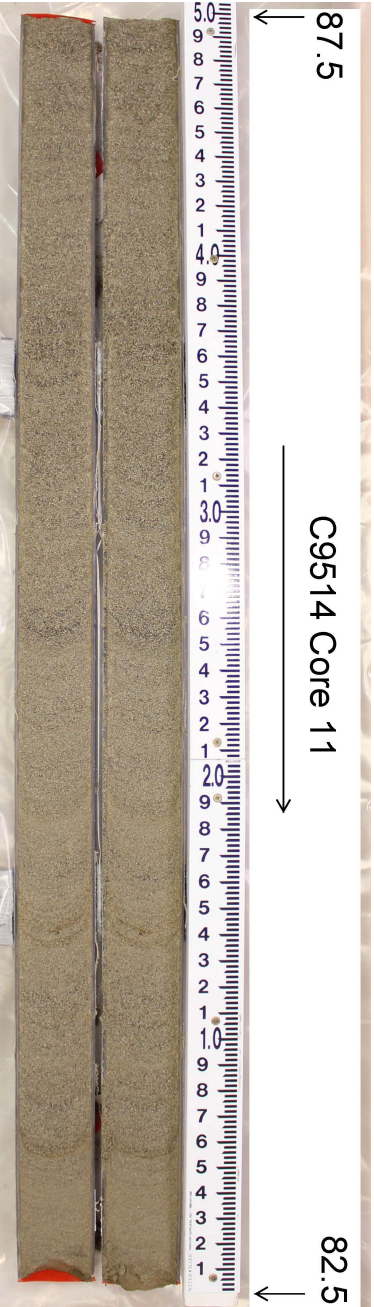
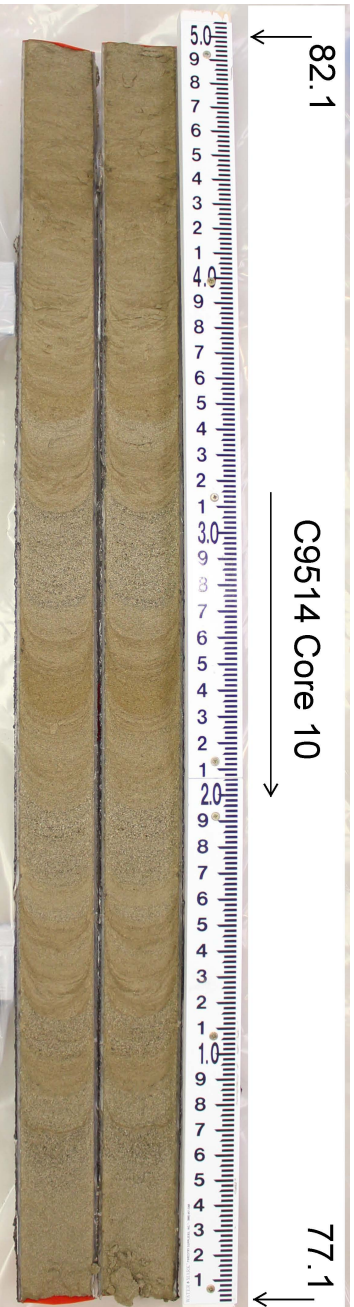
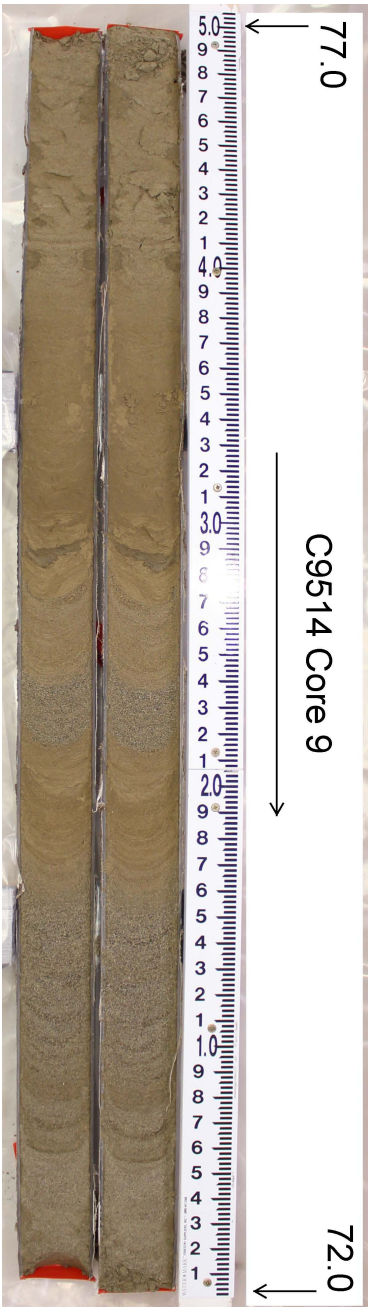
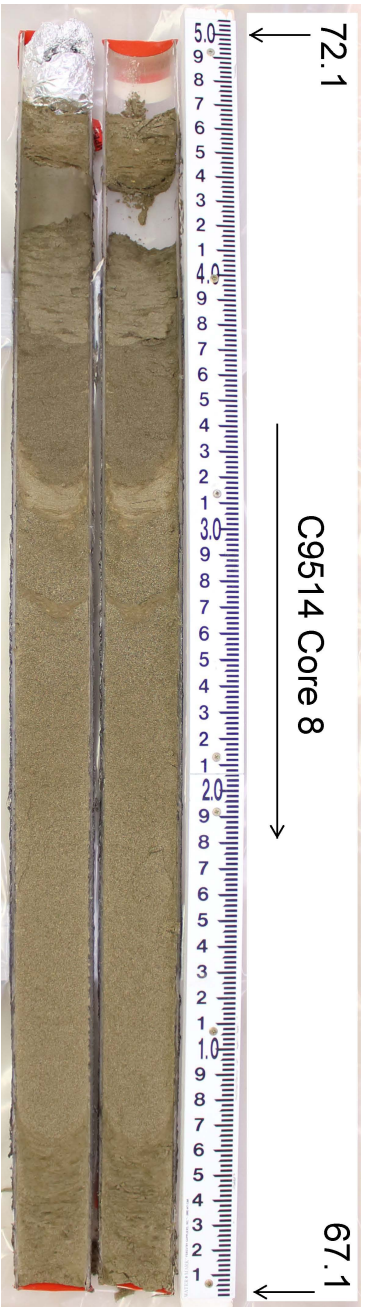
Geologist
Title

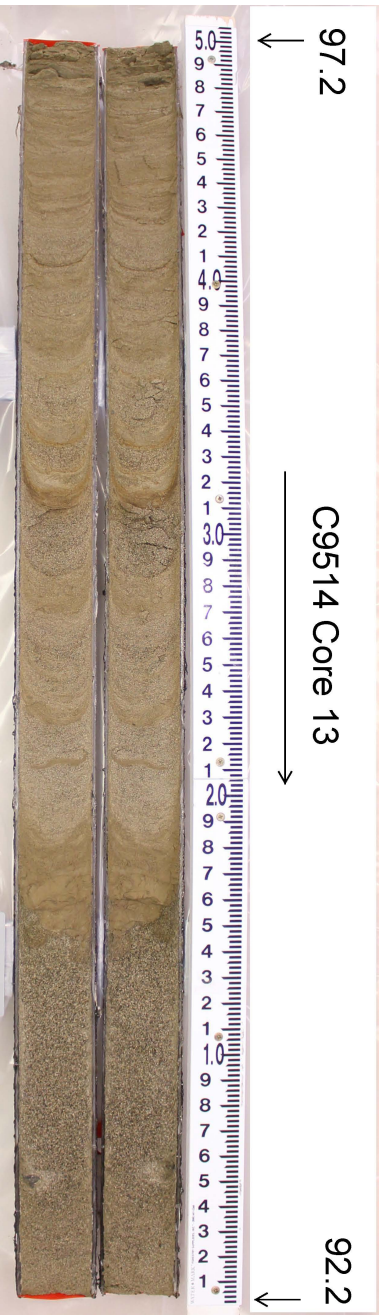
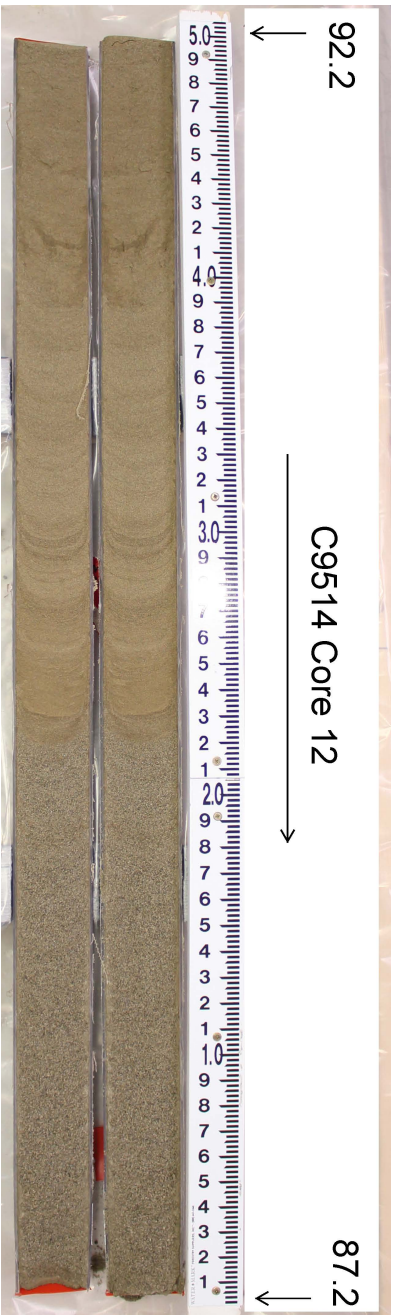
Jen Russell
Signature

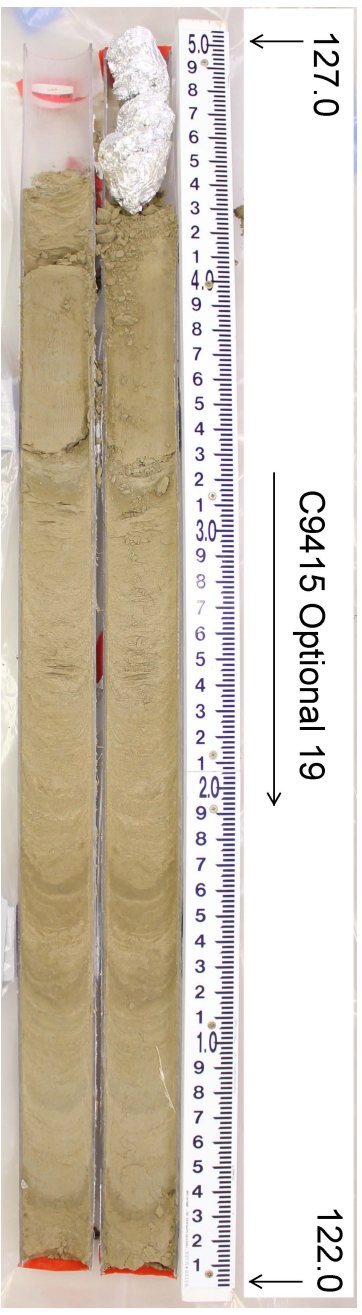
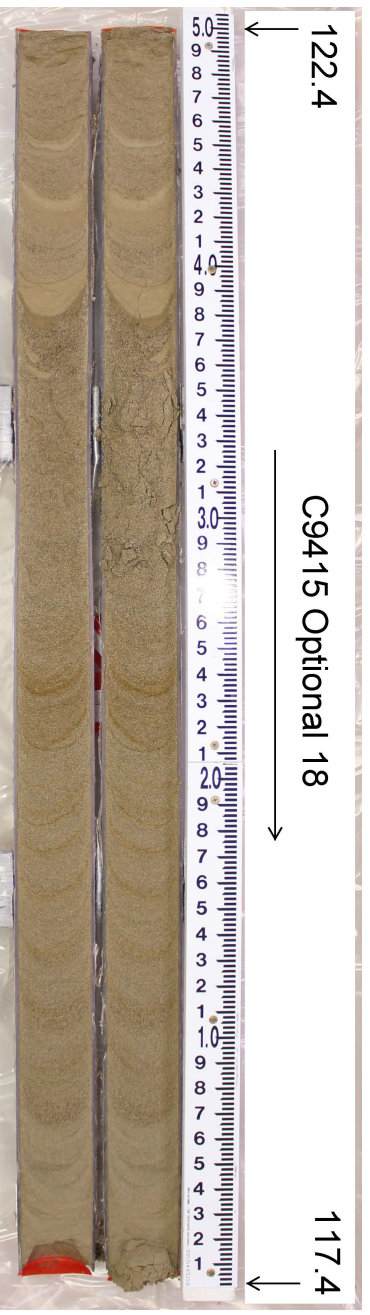
9/21/16
Date











This page intentionally left blank.

Appendix D

Contaminant Attenuation and Transport Characterization of 200-DV-1 Operable Unit Sediment Samples (PNNL-26208)

This page intentionally left blank.



Proudly Operated by Battelle Since 1965

Contaminant Attenuation and Transport Characterization of 200-DV-1 Operable Unit Sediment Samples

May 2017

MJ Truex
JE Szecsody
NP Qafoku
CE Strickland
JJ Moran
BD Lee
MM Snyder
AR Lawter

CT Resch
BN Gartman
L Zhong
MK Nims
DL Saunders
BD Williams
JA Horner
II Leavy

SR Baum
BB Christiansen
RE Clayton
EM McElroy
D Appriou
KJ Tyrrell
ML Striluk



Prepared for the U.S. Department of Energy
under Contract DE-AC05-76RL01830

DISCLAIMER

This report was prepared as an account of work sponsored by an agency of the United States Government. Neither the United States Government nor any agency thereof, nor Battelle Memorial Institute, nor any of their employees, makes **any warranty, express or implied, or assumes any legal liability or responsibility for the accuracy, completeness, or usefulness of any information, apparatus, product, or process disclosed, or represents that its use would not infringe privately owned rights.** Reference herein to any specific commercial product, process, or service by trade name, trademark, manufacturer, or otherwise does not necessarily constitute or imply its endorsement, recommendation, or favoring by the United States Government or any agency thereof, or Battelle Memorial Institute. The views and opinions of authors expressed herein do not necessarily state or reflect those of the United States Government or any agency thereof.

PACIFIC NORTHWEST NATIONAL LABORATORY
operated by
BATTELLE
for the
UNITED STATES DEPARTMENT OF ENERGY
under Contract DE-AC05-76RL01830

Printed in the United States of America

Available to DOE and DOE contractors from the
Office of Scientific and Technical Information,
P.O. Box 62, Oak Ridge, TN 37831-0062;
ph: (865) 576-8401
fax: (865) 576-5728
email: reports@adonis.osti.gov

Available to the public from the National Technical Information Service
5301 Shawnee Rd., Alexandria, VA 22312
ph: (800) 553-NTIS (6847)
email: orders@ntis.gov <<http://www.ntis.gov/about/form.aspx>>
Online ordering: <http://www.ntis.gov>



This document was printed on recycled paper.

(8/2010)

Contaminant Attenuation and Transport Characterization of 200- DV-1 Operable Unit Sediment Samples

MJ Truex	CT Resch	SR Baum
JE Szecsody	BN Gartman	BB Christiansen
NP Qafoku	L Zhong	RE Clayton
CE Strickand	MK Nims	EM McElroy
JJ Moran	DL Saunders	D Appriou
BD Lee	BD Williams	KJ Tyrrell
MM Snyder	JA Horner	ML Striluk
AR Lawter	II Leavy	

May 2017

Prepared for
the U.S. Department of Energy
under Contract DE-AC05-76RL01830

Pacific Northwest National Laboratory
Richland, Washington 99352

Summary

Contaminants disposed of at the land surface must migrate through the vadose zone before entering groundwater. Processes that occur in the vadose zone can attenuate contaminant concentrations during transport through the vadose zone. Thus, quantifying contaminant attenuation and contaminant transport processes in the vadose zone, in support of the conceptual site model (CSM) and fate and transport assessments, is important for assessing the need for, and type of, remediation in the vadose zone and groundwater. The framework to characterize attenuation and transport processes provided in U.S. Environmental Protection Agency (EPA) guidance documents was used to guide the laboratory effort reported herein.

The 200-DV-1 Operable Unit (OU) is in the process of characterizing the vadose zone to support a remedial investigation and feasibility study. Through a data quality objectives process, specific 200-DV-1 waste sites were selected for evaluation of attenuation and transport processes for mobile uranium, technetium-99 (Tc-99), iodine-129 (I-129), chromium, and nitrate contaminants. The specific elements of the laboratory effort were selected to provide data and associated interpretation to support the following three objectives:

- Define the contaminant distribution and the hydrologic and biogeochemical setting
- Identify attenuation processes and describe the associated attenuation mechanisms
- Quantify attenuation and transport parameters for use in evaluating remedies

These objectives are elements of the framework identified in EPA guidance for evaluating Monitored Natural Attenuation (MNA) of inorganic contaminants, and they directly support updating the CSM for these waste sites (and generally for the Hanford Central Plateau). Importantly, the information supports defining suitable contaminant transport parameters that are needed to evaluate transport of contaminants through the vadose zone and to the groundwater. This type of transport assessment supports a coupled analysis of groundwater and vadose zone contamination. The laboratory study information, in conjunction with transport analyses, can be used as input to evaluate the feasibility of remedies for the 200-DV-1 OU. This remedy evaluation will be enhanced by considering these study results that improve the understanding of controlling features and processes for transport of contaminants through the vadose zone to the groundwater.

The laboratory study described in this report was conducted using the samples shown in Table ES-1 for the selected waste sites in the S- and T-Complexes of the 200-DV-1 OU. The laboratory study included categories of individual analysis and experiments derived from EPA guidance for MNA of inorganic contaminants. Sediment characterization included determining contaminant concentrations (and oxidation state for some contaminants), concentrations of important geochemical constituents, microbial ecology relevant to contaminant attenuation, physical properties, and pore-water oxygen and hydrogen isotopes. Additional information to help assess attenuation processes included sequentially applying increasingly harsh extraction solutions to the sediment and measuring contaminants and geochemical constituents in the extractions (sequential-extraction analysis). This technique helps interpret the distribution of contaminants among mobile, partially mobile, and functionally immobile phases in the sediments. The character of iron and manganese phases in the sediments was also determined in relation to their role in redox reactions. Several types of methods were applied to evaluate

transport characteristics and to develop transport parameters for contaminants. Where existing contaminant concentrations were high enough to enable testing, batch and soil-column leaching experiments were conducted that are used to evaluate and quantify contaminant release rates. Because several samples had low existing contaminant concentrations, spiked-contaminant experiments were used in batch and soil-column tests to estimate the linear equilibrium partitioning coefficient (K_d), an important parameter for transport assessments.

Table ES.1. Samples included in the laboratory study.

Waste Site	Borehole	Geologic Unit	Nominal Depth Interval (ft bgs)
216-T-19 (T-19)	C9507	Cold Creek Unit silt	92-96
216-T-19 (T-19)	C9507	Cold Creek Unit caliche (high carbonate)	102-106
216-T-19 (T-19)	C9507	Ringold formation	137-140
216-T-25 (T-25)	C9510	Hanford Formation/Cold Creek Unit silt transition	112-115
216-S-9 (S-9)	C9512	Hanford Formation	62-65
216-S-9 (S-9)	C9512	Hanford Formation/Cold Creek Unit silt transition	122-125

Interpretation of this laboratory study can be considered from several perspectives relevant to supporting 200-DV-1 OU activities. Results for each contaminant were evaluated across all of the samples to identify contaminant-specific conclusions and to enable consideration of how results from this study may be relevant to other waste sites. Results were also evaluated with respect to conclusions relevant to the specific waste sites included in the study. Lastly, study results were evaluated with respect to updating CSMs and future evaluation of remedies, including the associated fate and transport assessment needed as a basis for remedy evaluation.

The data and information from this laboratory study were interpreted to support the following conclusions for each contaminant included in the study.

- Uranium
 - Uranium concentrations were low in most samples; therefore, a significant fraction of the uranium may be associated with natural background concentrations.
 - The dominant form of uranium was as U(VI), supporting the conclusion that little uranium reduction has occurred in these samples.
 - For samples where uranium concentrations were elevated, only a small fraction of the uranium was present in the aqueous phase or in a form that would be transported in the aqueous phase under equilibrium partitioning conditions. Most of the uranium was associated with precipitates, and transport of uranium would be controlled by dissolution processes. This type of slow-release transport behavior was observed in the batch and soil-column leaching experiments for samples with higher uranium concentration.
 - Uranium K_d values were varied across the different samples tested, with the highest K_d value associated with the sample of the high carbonate Cold Creek Unit (CCU) material. Thus, in transport assessments, selection of a K_d value for uranium should consider spatial variation of the K_d value based on lithologic units and carbonate content. The CCU samples show the highest K_d values for uranium. Thus, carbonate content and smaller particle sizes are important to consider for uranium K_d . Organic carbon content did not appear to be important, but was generally low in

all samples. In terms of desorption versus adsorption K_d values, there was no clear trend across all of the samples.

- Iodine

- I-129 concentrations in the vadose zone were non-detect for all samples. Total iodine concentrations were moderate and suitable for conducting attenuation and transport studies. Because total iodine and I-129 form the same chemical species, attenuation and transport behavior for total iodine and I-129 will be the same.
- Total iodine speciation in the aqueous phase was mostly dominated by iodide. However, sequential extractions showed only a small fraction of the iodine was present in the aqueous phase or in a form that would be transported in the aqueous phase under equilibrium partitioning conditions. Most of the iodine was associated with precipitates (likely carbonates), and transport of iodine in these precipitates would be controlled by dissolution processes. Speciation was not possible in the carbonate precipitate extractions for the sequential extraction procedure, but it is likely that the iodine present in these extractions was iodate because scientific literature has shown co-precipitation of iodate and carbonates. The leaching experiments showed some slow-release behavior of iodine that may be associated with these carbonate precipitates.
- Total iodine K_d values show minimal sorption of iodide and moderate sorption of iodate. Iodate K_d values varied across the different samples tested, with the highest K_d values associated with the samples with high carbonate concentrations. Thus, in transport assessments, selection of a K_d value for iodate should consider spatial variation of the K_d value based on carbonate content. Unlike uranium, the higher iodate K_d values are not all associated with CCU material (smaller particle sizes). Organic carbon content did not appear to be important, but was generally low in all samples. Transport of iodide and iodate through the vadose zone will be different, and speciation should be considered when conducting transport assessments. Desorption K_d values were mostly higher than adsorption K_d values in the batch experiments that were conducted.

- Tc-99

- Tc-99 was not detected in any of the samples.
- Tc-99 K_d values determined in spiked-contaminant tests were minimal to low, and values varied slightly across the different samples tested. However, the nominal retardation value for Tc-99 from these data would be close to 1. In batch testing, some of the desorption K_d values for Tc-99 were higher than the corresponding adsorption K_d values. Chemical reduction during the experimental timeframe (up to 56 days total) may have contributed to the higher apparent desorption K_d values, noting that reduction of Tc-99 by Hanford sediments has been observed in the laboratory.

- Chromium

- Cr(VI) was not detected in most samples and, when detected, was present at a low concentration. Total chromium measured in acid extractions was likely from natural background.
- Cr(VI) K_d values determined in spiked-contaminant tests were low, and values varied slightly across the different samples tested. The measured K_d values generally increased with experiment time (from 1 to 28 days). It is possible that all or some of this increase was due to Cr(VI) reduction, which has been observed in laboratory experiments with Hanford sediment. Desorption K_d values from batch experiments were all higher than adsorption values. However,

some of the concentration changes in the batch desorption experiments (up to 56-day duration) may have been due to some Cr(VI) reduction.

- Nitrate
 - Nitrate concentrations were high in all of the samples. Two samples showed very low nitrite concentrations as a potential indicator of denitrification. However, nitrite concentrations were 4 to 5 orders-of-magnitude lower than nitrate concentrations, indicating that minimal reduction had occurred.
 - Nitrate behavior in leaching experiments showed rapid elution, consistent with a minimal K_d value. The nominal retardation value for nitrate from these data would be close to 1.

The following conclusions were developed for the specific boreholes/waste sites analyzed in this study.

- T-19
 - Samples for the laboratory study from the T-19 waste site (borehole C9507) were of CCU silt, CCU caliche, and Ringold (silty, sandy gravel) materials. These samples were from locations well below the historical waste discharge and did not show signs of altered biogeochemistry induced by the waste discharge, other than the presence of contaminants. Nitrate concentrations were similar in all of the samples, indicating that waste fluids had penetrated to at least the depth of the lowest sample. The pore-water pH was consistent with a carbonate-saturated system. The highest uranium and (total) iodine concentrations were in the CCU caliche (high carbonate) material, suggesting that uranium and iodine accumulated in this zone as the waste solution passed through. Accumulation could be expected based on the observed high K_d value in this unit and the potential formation of uranium- and iodine-carbonate precipitates. Thus, the CCU is an important unit at this waste site for controlling contaminant transport. Tc-99 was not detected in any of these samples. Cr(VI) was only detected at a very low concentration near the detection limit in the CCU caliche sample.
 - Based on the data collected in this laboratory study, the following attenuation processes are important at this waste site. Sorption processes are important for uranium and iodate, and to a lesser extent for chromate and Tc-99. Formation of uranium- and iodate-carbonate precipitates also appears to be an attenuation mechanism in T-19 borehole samples. Minor indications of reduction were observed in one T-19 sample, and the potential for reduction through biotic or abiotic (e.g., ferrous iron) mechanisms is present, though it would likely have limited effect on future contaminant migration.
- T-25
 - The sample for the laboratory study from the T-25 waste site (borehole C9510) was of CCU silt materials. The sample was from a location well below the historical waste discharge and did not show signs of altered biogeochemistry induced by the waste discharge, other than the presence of contaminants. The presence of high nitrate concentration indicates that waste fluids had penetrated to at least the depth of the sample. The pore-water pH was consistent with a carbonate-saturated system. The CCU silt had high carbonate content, though not as high as the CCU caliche sample from the T-19 site. Uranium and total iodine were present at low concentrations, though concentrations were sufficient for assessment of leachability. High K_d values were measured for uranium and iodine, similar to the high K_d values measured for the T-

19 CCU caliche sample that also had a large fraction of carbonate. Accumulation could be expected based on the high observed K_d value in this unit and the potential formation of uranium- and iodine-carbonate precipitates. Thus, the CCU silt is an important unit at this waste site controlling contaminant transport. Tc-99 and Cr(VI) were not detected in any of the samples.

- Based on the data collected in this laboratory study, the following attenuation processes are important at this waste site. Sorption processes are important for uranium and iodate, and to a lesser extent for chromate and Tc-99. Formation of uranium- and iodate-carbonate precipitates also appears to be an attenuation mechanism in T-25 borehole samples. The potential for reduction through biotic or abiotic (e.g., ferrous iron) mechanisms is present, though it would likely have limited effect on future contaminant migration.
- S-9
 - Samples for the laboratory study from the S-9 waste site (borehole C9512) were of sandy Hanford Formation and transition from Hanford to CCU silt materials. These samples were deep below the historical waste discharge and did not show significant signs of altered biogeochemistry induced by the waste discharge, other than the presence of contaminants. However, the upper sample showed indication of potential reductive activity that, along with the very high nitrate concentration, may indicate some waste solution effects at this depth. Nitrate concentration was very high in the upper sample (the highest concentration of all samples in the laboratory study), and was at a moderately high concentration in the lower sample, indicating that waste fluids had penetrated to at least the depth of the lowest sample. The pore-water pH was consistent with a carbonate-saturated system. The uranium concentration in the lower sample was low, but was an order of magnitude higher than the uranium concentration in the upper sample. Neither sample appeared to be elevated in carbonate. Tc-99 and Cr(VI) were not detected in any of the samples.
 - Based on the data collected in this laboratory study, the following attenuation processes are important at this waste site. Sorption processes are important for uranium and iodate, and to a lesser extent for chromate and Tc-99. Formation of uranium- and iodate-carbonate precipitates also appears to be an attenuation mechanism in S-9 borehole samples. Minor indications of reduction were observed in one S-9 sample and the potential for reduction through biotic or abiotic (e.g., ferrous iron) is present, though it would likely have limited effect on future contaminant migration.

The study provided a set of data that addressed the study objectives and can support future evaluation of remedies, including MNA, and the associated fate and transport assessment that is needed as a basis for remedy evaluations. The first objective was to jointly evaluate contaminant concentrations and the biogeochemical and hydrologic setting for these data. This information provides a baseline for interpreting attenuation and transport studies. As noted, there were significant variations in transport parameter values and some attenuation mechanisms linked to specific sediment characteristics (e.g., carbonate content). For scaling and use of this information in fate and transport assessments, these variations should be considered in light of the sample properties. For this study, the sample properties were strongly linked to the sediment units sampled rather than waste stream properties. Thus, scaling and use in future efforts can translate the attenuation and transport information from this laboratory study to other waste sites based on the distribution of similar sediment units (e.g., the CCU silt and CCU caliche).

Another objective of the study was to identify attenuation processes that appear to be active in these samples and that will affect contaminant transport through the vadose zone. Sorption processes are important for uranium and iodate, and to a lesser extent for chromate and Tc-99. Carbonate content appeared to be important for uranium and iodate K_d . Accumulation in carbonate precipitates was identified as an attenuation mechanism for uranium and iodate. Slow release of uranium and total iodine was evident in leaching experiments. Geochemical signatures of reducing conditions were minimal or non-existent in the samples. However, there was indication of potential catalysts for reductive processes, including the presence of microbes and reduced iron and manganese phases. These reductive catalysts may be responsible for some of the difficult-to-extract contaminant phases (e.g., precipitated phases) observed in sequential extraction analysis. Attenuation mechanisms relevant to chromium and Tc-99 (other than sorption) could not be fully assessed because of the low/non-detect concentrations of these contaminants.

A key objective of the study was to quantify attenuation and transport parameters to support parameterization of fate and transport assessments. This type of assessment will be needed to evaluate transport of contaminants through the vadose zone, to evaluate the coupled vadose zone-groundwater system, and to assess the need for, magnitude of, and/or design of remediation. The contaminant- and sample-specific values from stop-flow portions of soil-column experiments, batch leaching, and K_d experiments provide a set of information that can be directly used to develop transport parameters. Soil-column effluent concentration data can also be compared to one-dimensional simulations to assess fate and transport model configurations for K_d or for surface complexation models.

Collectively, the information from this laboratory study can be considered in terms of updating the CSM for contaminants in the vadose zone. It can also provide input to describing the coupled vadose zone-groundwater system that needs to be considered for remedy determinations. CSM elements from this laboratory study are listed below. These elements will need to be incorporated with other data collected during the 200-DV-1 OU remedial investigation as part of updating the CSMs for the 200-DV-1 OU component waste sites.

- Sequential extraction experiments (and more coarsely indicated by comparison of water- and acid-extraction contaminant data) show that only a small fraction of the uranium and iodine mass in samples is in a mobile form that would transport under equilibrium-partitioning conditions. Leaching experiment results confirmed that slow-release processes affect the transport of these contaminants. The relative amount of uranium and iodine mass in the mobile versus functionally immobile phases affects the potential for future mass discharge from the vadose zone to the groundwater.
- Laboratory data suggest that formation and dissolution of uranium- and iodate-carbonate precipitates is a potential attenuation mechanism affecting the relative mobile and immobile mass fractions and the transport characteristics of uranium and iodine.
- Attenuation and sorption are not uniform in the vadose zone, especially for uranium and the iodate form of iodine. Lithology (e.g., the presence and extent of layers such as the CCU) and carbonate content affected the transport parameter values for these contaminants.
- For the waste sites included in this study, the effects of waste chemistry (e.g., altered sediment pH or biogeochemistry), other than contaminant concentrations, did not penetrate deep into the vadose zone. The biogeochemical signature of samples shows that transport evaluation at these waste sites will not need to include properties modified by waste chemistry for the deep portion of the vadose zone.

- While the CSM should acknowledge the potential for transformation processes (e.g., biotic or abiotic reduction), minimal evidence was observed that these processes are active. However, biotic and abiotic transformation may have occurred in the past and contributed to the currently observed contaminant distribution within the sediment and pore water.
- Oxygen and hydrogen isotope data were collected and primarily show correlation to regional precipitation with some variations from evaporative and condensation processes.
- It will be important to incorporate variations in physical property data into the CSM to augment existing data and correlate to indirect measures of lithology (e.g., geophysical logging). Some additional hydraulic property data were collected for this laboratory study and will be documented in a separate report.

This laboratory study extended the characterization of the 200-DV-1 OU to include identification and quantification of contaminant attenuation processes and parameters that will be needed to evaluate transport of contaminants through the vadose zone into the groundwater. The data generated in this laboratory study enable the site CSMs and transport analyses to be updated to reflect the observed contaminant behavior. In addition, the laboratory study was structured to address the information requirements for considering MNA as all or part of a remedy (i.e., EPA's guidance document *Use of Monitored Natural Attenuation for Inorganic Contaminants in Groundwater at Superfund Sites*¹) and can be used as part of the technical defensibility for identifying attenuated transport through the vadose zone within the remedial investigation and feasibility study for the 200-DV-1 OU.

¹ EPA. 2015. *Use of Monitored Natural Attenuation for Inorganic Contaminants in Groundwater at Superfund Sites*. OSWER Directive 9283.1-36, U.S. Environmental Protection Agency, Office of Solid Waste and Emergency Response, Washington, D.C.

Acknowledgments

This work was funded by the CH2M Hill Plateau Remediation Company as part of the 200-DV-1 Operable Unit activities at the Hanford Site. The Pacific Northwest National Laboratory is operated by Battelle Memorial Institute for the DOE under Contract DE-AC05-76RL01830.

Acronyms and Abbreviations

CAWSRP	<i>Conducting Analytical Work in Support of Regulatory Programs</i>
CCU	Cold Creek Unit
CHPRC	CH2M Hill Plateau Remediation Company
CSM	conceptual site model
DI	deionized
EPA	U.S. Environmental Protection Agency
ESL	Environmental Sciences Laboratory
MNA	Monitored Natural Attenuation
MPN	most probable number
OU	operable unit
PNNL	Pacific Northwest National Laboratory
QA	quality assurance

Contents

Summary	iii
Acknowledgments.....	xi
Acronyms and Abbreviations	xiii
1.0 Introduction	1.1
2.0 Objectives	2.1
3.0 Approach	3.1
3.1 Sample Handling and Selection of Samples Intervals and Associated Analyses.....	3.1
3.2 Laboratory Methods	3.3
3.2.1 Analysis Objective 1: Physical Characterization	3.3
3.2.2 Analysis Objective 2: Microbial Ecology	3.4
3.2.3 Analysis Objective 3: Contaminant Concentration, Distribution and Oxidation- Reduction State	3.5
3.2.4 Analysis Objective 4: Geochemical Conditions.....	3.6
3.2.5 Analysis Objective 5: Contaminant Release Rate from Sediment and Mobility	3.8
3.2.6 Objective 6: Oxygen and Hydrogen Isotopic Signature of the Pore Water.....	3.11
3.2.7 Chemical Analysis Methods.....	3.12
4.0 Results	4.1
4.1 Contaminant Concentrations and Hydrologic and Biogeochemical Setting	4.1
4.1.1 Contaminants and Geochemical Constituents	4.2
4.1.2 Microbial Ecology.....	4.5
4.1.3 Iron and Manganese Characterization	4.8
4.1.4 Oxygen and Hydrogen Isotopes	4.11
4.1.5 Sediment Physical Characterization	4.18
4.2 Observation of Attenuation Processes.....	4.24
4.3 Quantification of Attenuation and Transport Parameters.....	4.41
5.0 Recommendations	5.1
6.0 Quality Assurance.....	6.1
7.0 Conclusions	7.1
8.0 References	8.1
Appendix A Geologist Descriptions of Samples	A.1
Appendix B Spiked-Contaminant Batch Experiments Individual Treatment Results	B.1

Figures

Figure 1. Attenuation mechanisms (green font) for inorganic contaminants in the vadose zone and factors that can impact attenuation (black font) (Truex et al. 2015a).	1.1
Figure 2. Location of waste sites and boreholes where samples were obtained for this laboratory study (adapted from DOE 2012).	1.3
Figure 3. Nominal schematic of analysis on specific core intervals.	3.2
Figure 4. Relative abundance of bacterial phyla based on the 16S rRNA gene.	4.7
Figure 5. Iron (a) and manganese (b) surface phase distributions in sediments, based on liquid extractions.	4.10
Figure 6. Isotope data for vadose zone sediment and perched water analyses. (A) Data resulting from the full data set. (B) Data refined by a Modified Thompson Tau test to remove outlier points (continued on next page). Depiction of winter precipitation is after DePaolo et al. (2004) with a nominal value of $\delta^{18}\text{O}$ of $\sim -18\text{‰}$ and $\delta^2\text{H}$ of $\sim -138\text{‰}$	4.15
Figure 7. $\delta^{18}\text{O}$ relating to sample depth, average local winter precipitation, and local shallow groundwater within the Hanford Site: (A) sample data from the T- and S-Complexes, and (B) sample data from the B-Complex.	4.17
Figure 8. Correlation of isotopic ($\delta^2\text{H}$ and $\delta^{18}\text{O}$) analysis and measured nitrate concentration from T- and S-Complex samples.	4.18
Figure 9. Photograph of sample B35442 (Core C9507, liner 16B, CCUc sediment sample).	4.19
Figure 10. Photograph of sample B35461 (Core C9507, Ringold sediment sample).	4.19
Figure 11. Photograph of sample B361M9 (Core C9510, liner 14B, H2/CCUz sample).	4.20
Figure 12. Photograph of sample B36175 (Core C9512, liner 8B, H1/H2 sample).	4.20
Figure 13. Photograph of sample B361F1 (Core C9512, liner 20B, H2/CCUz sample).	4.21
Figure 14. Particle size distribution of sample B35442 (Core C9507, liner 16B, CCUc sediment sample).	4.22
Figure 15. Particle size distribution of sample B35461 (Core C9507, Ringold sediment sample).	4.22
Figure 16. Particle size distribution of sample B361M9 (Core C9510, liner 14B, H2/CCUz sample).	4.23
Figure 17. Particle size distribution of sample B36175 (Core C9512, liner 8B, H1/H2 sample).	4.23
Figure 18. Particle size distribution of sample B361F1 (Core C9512, liner 20B, H2/CCUz sample).	4.24
Figure 19. Uranium sequential extraction results. Note that leaching experiments were not conducted for samples T-19 Ringold (C9507-B35461), S-9 8C (C9512-B36177), or S-9 20C (C9512-B361F3).	4.27
Figure 20. Iodine sequential extraction results. Note that leaching experiments were not conducted for samples T-19 Ringold (C9507-B35461), S-9 8C (C9512-B36177), or S-9 20C (C9512-B361F3).	4.28
Figure 21. Chromium sequential extraction results.	4.29
Figure 22. Cations measured in sequential extraction solutions. Note that metals are not reported if the extraction solution contained that metal (Ca for extraction 4, Mg for extractions 2 and 3, and Na in extractions 3 and 4).	4.30
Figure 23. Major and trace cations/metals measured in sequential extractions: (a) Ca, (b) Mg, (c) Sr, (d) Na, (e) K, (f) Ba, (g) Fe, (h) Mn, (i) Si, (j) Al, and (k) Si/Al ratio. The sediment sample codes are F41 = C9507-B35434, T19 14C; F42 = C9507-B35443, T19 16C; F43 =	

C9507-B35461, T19 138'; F44 = C9510-B361N1, T25 14C; F45 = C9512-B36177, S9 8C; and F46 = F47 = C9512-B361F3, S9 20C.	4.31
Figure 24. Aqueous uranium concentration in long-term batch leaching experiment.	4.33
Figure 25. Aqueous total iodine concentration in long-term batch leaching experiment: (a) total iodine for all sediments, (b) iodine species for C9507-B35443, T-19 16C, (c) iodine species for C9507-B35461, T-19 138', and (d) iodine species for C9510-B361N1, T-25 14C. Iodine speciation for other sediments was below detection limits.	4.34
Figure 26. Artificial groundwater leaching of the C9507-B35434, T19 14C sample for (a) uranium, and (b) total iodine effluent concentrations. Most iodate and iodide concentrations were below detection limits.	4.35
Figure 27. Artificial groundwater leaching of the C9507-B35434, T19 14C sample for (a) cation and (b) anion effluent concentrations for selected samples.	4.36
Figure 28. Artificial groundwater leaching of the C9507-B35434, T19 14C sample for tracer (bromide) effluent concentration.	4.36
Figure 29. Artificial groundwater leaching of the C9507-B35443, T19 16C sample for (a) uranium and (b) tracer (bromide) effluent concentrations.	4.37
Figure 30. Artificial groundwater leaching of the C9507-B35443, T19 16C sample for total iodine data.	4.37
Figure 31. Artificial groundwater leaching of the C9507-B35443, T19 16C sample for (a) cation and (b) anion effluent concentrations for selected samples.	4.38
Figure 32. Artificial groundwater leaching of the C9510, T25 14C sample for (a) uranium and (b) tracer (bromide) effluent concentrations.	4.38
Figure 33. Artificial groundwater leaching of the C9510, T25 14C sample for total iodine data.	4.39
Figure 34. Artificial groundwater leaching of the C9510, T25 14C sample for (a) cation and (b) anion effluent concentrations for selected samples.	4.39
Figure 35. Artificial groundwater leaching of the C9510, T25 14C sample (duplicate sample) for (a) uranium and (b) tracer (bromide) effluent concentrations.	4.40
Figure 36. Artificial groundwater leaching of the C9510, T25 14C sample (duplicate sample) for total iodine data.	4.40
Figure 37. Artificial groundwater leaching of the C9510, T25 14C sample (duplicate sample) for (a) cation and (b) anion effluent concentrations for selected samples.	4.41
Figure 38. Breakthrough and elution responses for spiked-contaminant soil-column experiments with the C9507-B35434, T19 14C sample for (a) bromide (tracer) and chromate, (b) bromide and pertechnetate, and (c) bromide and iodate.	4.48
Figure 39. Breakthrough and elution responses for spiked-contaminant soil-column experiments with the C9507-B35461, T19 138' sample for (a) bromide (tracer) and chromate, (b) bromide and pertechnetate, and (c) bromide and iodate.	4.49
Figure 40. Breakthrough and elution responses for spiked-contaminant soil-column experiments with the C9510-B361F3, S-9 20C sample for (a) bromide (tracer) and chromate, (b) bromide and pertechnetate, and (c) bromide and iodate.	4.50

Tables

Table 1. Sediment samples selected for analyses.....	3.2
Table 2. Physical sediment analysis methods.....	3.4
Table 3. Microbiological and molecular methods.....	3.4
Table 4. Extraction methods for contaminant analysis.....	3.5
Table 5. Extraction methods for geochemical analysis.....	3.7
Table 6. Contaminant mobility tests.....	3.8
Table 7. Samples selected for spiked-contaminant analyses.....	3.9
Table 8. Vadose zone pore-water simulant recipe (from Serne et al. 2015). Adjust pH to 7.0 to 7.2 with sodium hydroxide or sulfuric acid.....	3.10
Table 9. Artificial (Hanford) groundwater.....	3.10
Table 10. Contaminants and spike concentrations.....	3.10
Table 11. Batch test supernatant analyses (specific methods per Table 12, Section 3.2.7).....	3.11
Table 12. Chemical analyses.....	3.12
Table 13. Baseline contaminant concentrations.....	4.2
Table 14. Contaminant data.....	4.3
Table 15. Geochemical constituents.....	4.4
Table 16. Microbial phenotype results showing ability of bacteria to grow on a variety of electron acceptors. Values indicate number of cells/g of sediment tested.....	4.6
Table 17. Ferrous and ferric iron phases in sediments based on liquid extractions.....	4.9
Table 18. Manganese phases in sediments based on liquid extractions.....	4.9
Table 19. Summary of Hanford mineralogy (after Xue et al. 2003).....	4.11
Table 20. Sediment samples selected for analyses and isotope data values (outliers removed).....	4.12
Table 21. Summary of measured physical properties.....	4.21
Table 22. Sequential extraction of contaminants from sediment samples.....	4.25
Table 23. Tabulated sequential extraction results for uranium, iodine, and chromium.....	4.26
Table 24. Iodine speciation.....	4.29
Table 25. Post-sorption contaminant release rates calculated for batch leaching experiments.....	4.42
Table 26. Contaminant release rates calculated for stop-flow events during soil-column leaching experiments.....	4.42
Table 27. Calculated partitioning coefficients for spiked-contaminant experiments using the pore-water recipe (Table 8).....	4.43
Table 28. Calculated partitioning coefficients for spiked-contaminant experiments using the artificial groundwater recipe (Table 9).....	4.44
Table 29. Calculated partitioning coefficients for spiked-contaminant experiments using the pore-water recipe (Table 8) for samples B35434 and B35461 with multiple spiked- contaminant concentrations.....	4.45
Table 30. Calculated partitioning coefficients for spiked-contaminant experiments using the artificial groundwater recipe (Table 9) for samples B35434 and B35461 with multiple spiked-contaminant concentrations.....	4.46
Table 31. Calculated partitioning coefficients for spiked-contaminant column experiments.....	4.47

1.0 Introduction

Contaminants disposed of at the land surface must migrate through the vadose zone before entering groundwater. Processes that occur in the vadose zone can attenuate contaminant concentrations during transport through the vadose zone. Thus, quantifying contaminant attenuation and contaminant transport processes in the vadose zone, and the resulting temporal profile of contaminant discharge to the underlying groundwater, are important for assessing the need for, and type of, remediation in the vadose zone and groundwater. This type of information will enhance the existing conceptual site models (CSMs) for the 200-DV-1 Operable Unit (OU) (Serne et al. 2010; CHPRC 2015a,b) in support of fate and transport analysis and remedy evaluation.

Contaminant transport through the vadose zone beneath aqueous waste disposal sites is affected by two types of attenuation processes: (1) attenuation caused by advective and dispersive factors related to unsaturated water flow and (2) attenuation caused by biogeochemical reactions and/or physical/chemical interaction with sediments (e.g., phenomena such as sorption, solubility control, and decay/degradation that slow contaminant movement relative to water movement). Figure 1 summarizes the types of attenuation mechanisms that may affect contaminant transport in the vadose zone. Note that Figure 1 includes waste fluid properties and chemistry because wastes at Hanford were typically released directly to the vadose zone and attenuation may be affected by the nature of the waste material (e.g., Szecsody et al. 2013; Truex et al. 2014).

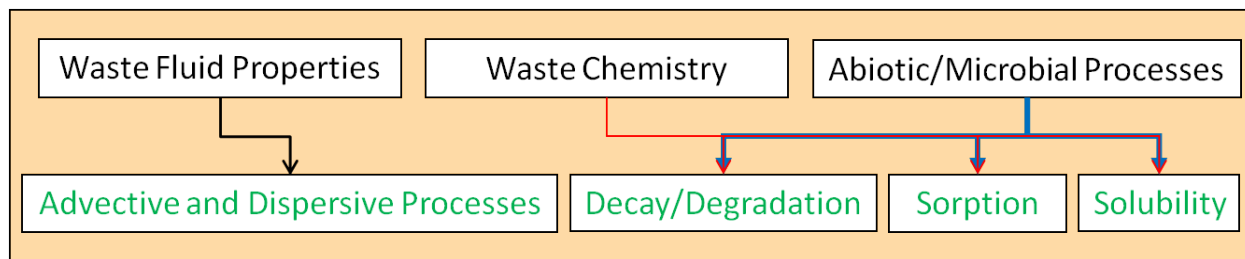


Figure 1. Attenuation mechanisms (green font) for inorganic contaminants in the vadose zone and factors that can impact attenuation (black font) (Truex et al. 2015a).

A framework to characterize these attenuation and transport processes is provided by U.S. Environmental Protection Agency (EPA) guidance document *Use of Monitored Natural Attenuation for Inorganic Contaminants in Groundwater at Superfund Sites* (EPA 2015). Additional information about vadose zone attenuation processes reported by Truex and Carroll (2013) and Truex et al. (2015a) is also relevant for characterization of the vadose zone. These documents point to approaches that can be applied to identify and describe transport parameters for a vadose zone site.

The 200-DV-1 OU project is in the process of characterizing the vadose zone to support a remedial investigation and feasibility study (DOE 2012, 2016). Through a data quality objectives process, specific 200-DV-1 waste sites were selected for evaluation of attenuation and transport processes for mobile uranium, technetium-99 (Tc-99), iodine-129 (I-129), chromium, and nitrate contaminants. These waste sites were selected based on the following factors:

- Waste stream inventory (radiological and/or chemical component)
- Waste stream differentiation (acid/base, volume, unique characteristics)

- Disposal type (crib, trench, french drain, reverse well, etc.)
- Potential to obtain parameters from significant (site-specific) geologic units to fill data gaps in transport parameters

The data quality objectives process also identified that the characterization of attenuation and transport processes needed to include the following activities:

- Evaluate contaminant and geochemical constituents in the samples
- Identify interactions of contaminants with sediments
- Quantify contaminant mobility
- Evaluate factors controlling contaminant mobility

This report provides information for analyses on sediment samples from the S-Complex and T-Complex portions of the 200-DV-1 OU. The samples were collected from the three borehole locations depicted in Figure 2. Detailed description of these waste sites and boreholes is contained in the 200-DV-1 OU characterization planning documents (DOE 2012, 2016) and will be compiled in future 200-DV-1 characterization reports. This report focuses only on description of the analyses conducted on the samples selected to assess attenuation and transport processes.

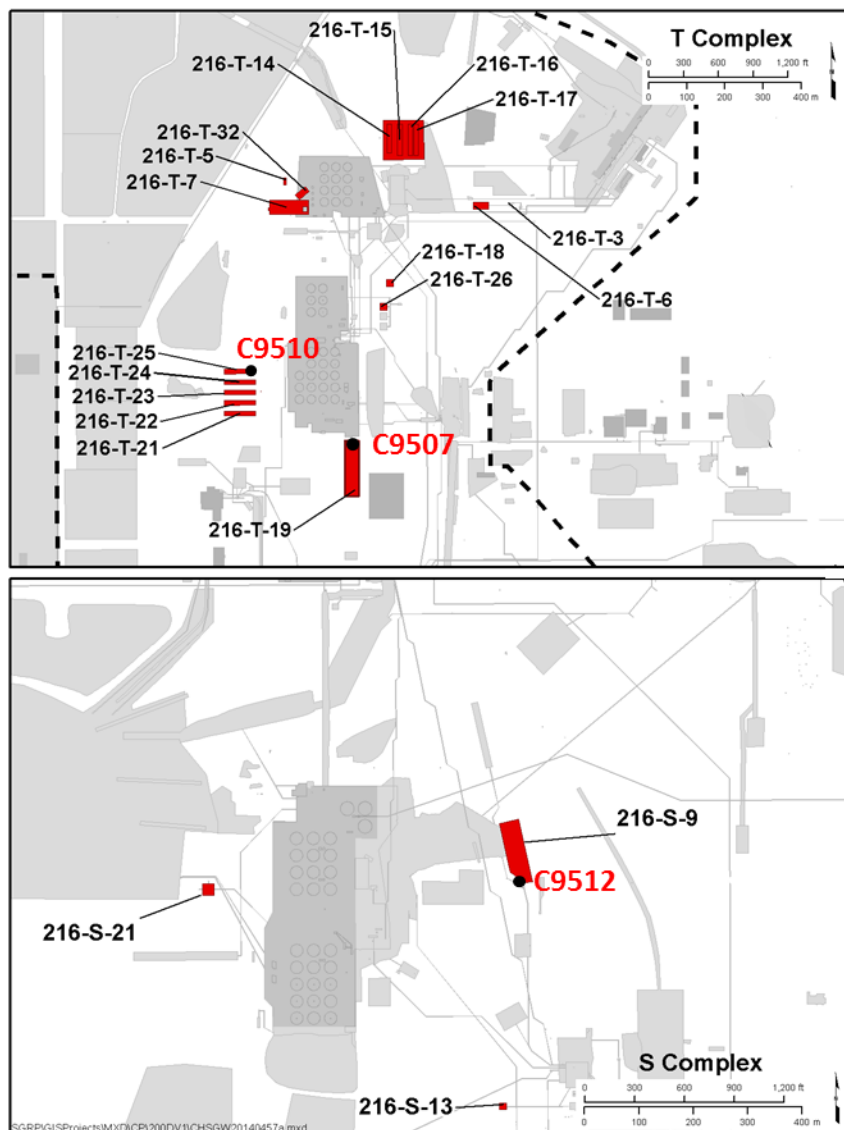


Figure 2. Location of waste sites and boreholes where samples were obtained for this laboratory study (adapted from DOE 2012).

This characterization information will be used to refine CSMs by enhancing the understanding of controlling features and processes for transport of contaminants through the vadose zone to the groundwater. The characterization approach was developed based on EPA (2015) guidance, identifying specific objectives (Section 2.0) and types of laboratory analyses (Section 3.0) to conduct on sediment samples. This report provides results and interpretation of these laboratory analyses from analysis of samples collected in fiscal year 2016 (Section 4.0), recommendations for future analyses on these and other samples (Section 5.0), and conclusions with respect to how these results are important for the remedial investigation/feasibility study for the 200-DV-1 OU and associated contaminant fate and transport assessment (Section 7.0). Quality assurance applied for this work is described in Section 6.0.

2.0 Objectives

The specific types of data identified for inclusion in the laboratory study reported herein will provide data and associated interpretation to support the following three objectives. These objectives are elements of the framework identified in the EPA guidance (EPA 2015) for evaluating Monitored Natural Attenuation (MNA) of inorganic contaminants, which directly supports development of suitable contaminant transport parameters.

- Define the contaminant distribution and the hydrologic and biogeochemical setting
- Identify attenuation processes and describe the associated attenuation mechanisms
- Quantify attenuation and transport parameters for use in evaluating remedies

These overall objectives led to a series of laboratory analyses designed to provide suitable data and information. A phased approach was used for this effort to progressively gather more detailed information based on initial results. This progressive/tiered approach is consistent with EPA MNA guidance.

The information from these analyses will be used as input to evaluate the feasibility of MNA and other remedies for the 200-DV-1 OU. The information from these analyses will also be used as input to refine the CSM for the targeted vadose zone sites.

3.0 Approach

Samples for the laboratory analyses were collected by CH2M Hill Plateau Remediation Company (CHPRC) as part of the drilling campaign for the 200-DV-1 OU remedial investigation. Sets of samples for each borehole included multiple sample intervals as potential targets for the analyses. The sample handling procedures used upon sample delivery to the laboratory are described in Section 3.1. This section also describes the selection of the specific sample intervals and the analyses selected for these sample intervals. Laboratory and experimental methods were derived from the approaches described in *Use of Monitored Natural Attenuation for Inorganic Contaminants in Groundwater at Superfund Sites* (EPA 2015). The laboratory analysis methods are presented in Section 3.2.

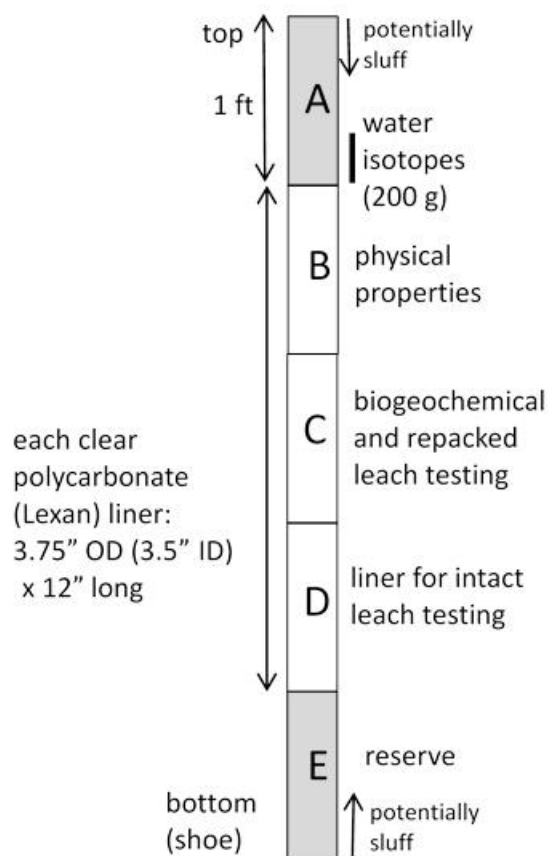
3.1 Sample Handling and Selection of Samples Intervals and Associated Analyses

Pacific Northwest National Laboratory (PNNL) and CHPRC jointly selected samples for testing through meetings that were held after all of the samples for a borehole were collected. The selected samples from boreholes C9507, C9510, and C9512 are listed in Table 1. The samples were in 12-inch-long liners within a 5-ft-long sonic core, except for samples B35461 and B35463 from the C9507 borehole (at the T-19 waste site). Sample B35461 was from the Ringold unit, where the sample recovery was poor. CHPRC and PNNL identified a 5-ft liner with approximately 2 ft of the liner containing sample material suitable for the laboratory analyses. The 2-ft section of this liner was received by PNNL. This 2-ft-long portion of liner was cut into four 6-in. lengths and distributed for different types of analyses. CHPRC and PNNL identified another 5-ft liner, sample B35461, with approximately 2 ft of the liner containing an apparently intact sample suitable for intact hydraulic property measurement. The 5-ft liner was received by PNNL. This liner was processed for intact hydraulic property assessment (along with another sample), which will be described in a separate report.

The liner samples were shipped from the drilling site to the PNNL 331 Building, where they were inspected, the chain of custodies were completed, and the samples were placed in a refrigerator (4°C). Once selected, the sample liner for use in isotopic analyses was frozen, except as noted in Table 1 where a subsample of liquid from a liner containing saturated sediment and free liquid was collected and frozen as the sample for isotopic analysis. The nominal liner sample disposition plan within a 5-ft core sample is shown in Figure 3. Target 5-ft cores selected for testing generally divide liners for specific types of tests according to this plan. However, the plan was modified in some cases depending on the observed sample recovery and initial inspection of material type within the liners by the PNNL-CHPRC technical team.

Table 1. Sediment samples selected for analyses.

Borehole and Liner Designation	Borehole ID	Sample ID	Nominal Geologic Unit	Depth Interval (ft bgs)	Analysis (report section)
T19 core 14A	C9507	B35432	CCUz	92.1-93.1	3.2.6
T19 core 14C	C9507	B35434	CCUz	94.1-95.1	3.2.2, 3.2.3, 3.2.4, 3.2.5
T19 core 14D	C9507	B35435	CCUz	95.1-96.1	3.2.1 (intact analysis, separate report)
T19 core 16A	C9507	B35441	CCUc	102.4-103.4	3.2.6
T19 core 16B	C9507	B35442	CCUc	103.4-104.4	3.2.1
T19 core 16C	C9507	B35443	CCUc	104.4-105.4	3.2.2, 3.2.3, 3.2.4, 3.2.5
T-19 Ringold	C9507	B35461/B36H08	Ringold	137.6-138.1	3.2.3, 3.2.4, 3.2.5
T-19 Ringold	C9507	B35461/B36H08	Ringold	138.1-138.6	3.2.3, 3.2.4, 3.2.5
T-19 Ringold	C9507	B35461/B36H08	Ringold	138.6-139.1	3.2.1
T-19 Ringold	C9507	B35461/B36H08	Ringold	139.1-139.6	3.2.2, 3.2.6
T-19 Ringold	C9507	B35463	Ringold	142.6-147.7	3.2.1 (intact analysis, separate report)
T-25 core 14A	C9510	B361M7	H2/CCUz transition	112.3-113.3	3.2.6
T-25 core 14B	C9510	B361M9	H2/CCUz transition	113.3-114.3	3.2.1
T-25 core 14C	C9510	B361N1	H2/CCUz transition	114.3-115.3	3.2.2, 3.2.3, 3.2.4, 3.2.5
S-9 core 8A	C9512	B36173	H1/H2	62.2-63.2	3.2.6
S-9 core 8B	C9512	B36175	H1/H2	63.2-64.2	3.2.1
S-9 core 8C	C9512	B36177	H1/H2	64.2-65.2	3.2.2, 3.2.3, 3.2.4, 3.2.5
S-9 core 20A	C9512	B361D9	H2/CCUz transition	122-123	3.2.6
S-9 core 20B	C9512	B361F1	H2/CCUz transition	123-124	3.2.1
S-9 core 20C	C9512	B361F3	H2/CCUz transition	124-125	3.2.2, 3.2.3, 3.2.4, 3.2.5

**Figure 3.** Nominal schematic of analysis on specific core intervals.

3.2 Laboratory Methods

Laboratory analyses were selected to evaluate attenuation processes and other factors affecting fate and transport of contaminants in the vadose zone. These analyses were based on the characterization approaches described for evaluating MNA of inorganic contaminants (EPA 2007a,b, 2010, 2015). The analyses were selected to provide data to support interpretation of contaminant behavior in the vadose zone, and will be used in conjunction with additional information produced by CHPRC as part of their related characterization efforts at these and other vadose zone boreholes. The laboratory experimental effort was organized using the following specific analysis objectives, which are related to the overall objectives described in Section 2.0. The subsequent sections describe the laboratory methods applied for each of the analysis objectives.

Analysis Objectives

1. Characterize the physical aspects of the sample that are used to evaluate pore water flow and provide the sediment information needed to interpret and scale biogeochemical analysis results.
2. Characterize the microbial ecology in the samples, focusing on identification of the microbial phenotypes that are present. This information will be used to interpret (1) microbial processes that can directly affect the chemical form of the contaminant, (2) the microbial community's relation to geochemical processes affecting sediment surface phases and contaminant chemical form, and (3) microbial processes related to sequestration or accumulation of contaminants.
3. Characterize the contaminant concentration, distribution, and, where appropriate, the oxidation-reduction state and chemical form in the pore water and on sediment surfaces. This information allows interpretation of contaminant mobility in the context of the biogeochemical system data.
4. Characterize the geochemical conditions in the pore water and on sediment surfaces to facilitate interpretation of attenuation and transport processes. Information about elements and compounds in the samples enables evaluation of biogeochemical processes related to the contaminant chemical form and mobility.
5. Characterize the contaminant mobility using tests that impose specific conditions, and collect temporal data for interpreting the mobility of the contaminant (e.g., by quantifying the rate of contaminant transfer to the aqueous phase).
6. Determine the oxygen and hydrogen isotopic signature of the pore water for use in comparing to existing data that may enable the source of the pore water within the sample to be evaluated.

3.2.1 Analysis Objective 1: Physical Characterization

Standard physical sediment analysis methods shown in Table 2 were applied as needed to meet analysis objective number 1. Because of the long duration required for determining unsaturated hydraulic properties, results of the hydraulic property evaluation will be presented in a separate report.

Table 2. Physical sediment analysis methods.

Required Data	Method Basis
Moisture content	ASTM D2216-10
Intact-core dry bulk density, particle density and porosity	ASTM D7263-09, D854-14
Intact-core air permeability	ASTM D6539-13
Core particle size by sieve (4, 2, 1, 0.5 mm sieves)	ASTM D6913-04
Core particle size by laser diffraction (< 0.5 mm)	ASTM D4464-15
Lithology, texture, petrologic composition (sand, gravel, basalt, quartz) and photos	Geologist inspection of borehole samples

3.2.2 Analysis Objective 2: Microbial Ecology

Microbiological and molecular analyses performed on the soil samples are listed in Table 3. Two categories of analyses were applied to evaluate the microbial ecology of the samples. The first category is based on applying an extract of the sample to different types of microbial culturing media. Microbial growth for these culturing media is measured and used to interpret the phenotypes of microbes present in the sample. The second category is based on extracting genetic material from the sample, identifying the genetic sequences present, and comparing these sequences to sequences in published databases to identify the microbes present at the genus or species level.

Methods for enumeration of total microbial numbers, bacterial density, and total heterotrophs were based on methods contained in the *Standard Methods for the Examination of Water and Wastewater*, 22nd Edition (Rice et al. 2012). Modifications for methods included verification of electron acceptor utilization using methods from the literature. The quality approach used for gene quantification was based on a guidance document from the EPA (2004).

Table 3. Microbiological and molecular methods.

Required Data	Method Basis
Total microbial numbers	APHA SM 9216A
Total heterotrophs	APHA SM 9221C Nitrate – Callos et al. 1999 Iron – Gould et al. 2003 Manganese – Grebel et al. 2016
Bacterial density	APHA SM 9215A
Total heterotrophs	
Anaerobic heterotrophs	
Nitrate-reducing bacteria	
Iron-reducing bacteria	
Manganese-reducing bacteria	
Overall phylogenetic diversity	Argonne National Lab Next Generation Sequencing Core
Gene sequence information	Facility Quality Assurance Policy
Bacterial identification	Benson et al. 2015; Rehm et al. 2013; O’Leary et al. 2015; Cole et al. 2013

APHA is American Public Health Association.

3.2.3 Analysis Objective 3: Contaminant Concentration, Distribution and Oxidation-Reduction State

Contaminant data were interpreted based on the elements and compounds present in the sample pore water or on sediment surfaces. Contaminant information was obtained by the analyses listed in Table 12 (Section 3.2.7). However, specific types of extractions were applied to provide material for analysis. The type of extraction and the concentration of the contaminant were both needed to interpret the contaminant conditions. Extractions applied to evaluate the contaminant conditions are listed in Table 4. In addition, alkaline extraction was conducted on sediment samples by EPA Method 3060A to provide material for analysis of chromium.

Table 4. Extraction methods for contaminant analysis.

Required Data	Method Basis
Water extraction (1:1 sediment:H ₂ O)	Um et al. 2009 and Zachara et al. 2007
Acid extraction (1:3 sediment:H ₂ O, 8M HNO ₃)	Um et al. 2009 and Zachara et al. 2007
Sequential extractions: Artificial groundwater Ion exchangeable pH 5.0 acetate pH 2.3 acetic acid Oxalate, oxalic acid 8M HNO ₃ , 95°C	Gleyzes et al. 2002; Beckett 1989; Larner et al. 2006; Sutherland and Tack 2002; Section 3.2.3.1
1000-hour carbonate extraction	Zachara et al. 2007; Kohler et al. 2004; Section 3.2.3.2

3.2.3.1 Sequential Extractions

Six sequential liquid extractions were conducted on a sediment sample. Extraction 1 is the aqueous contaminant fraction, extraction 2 is the adsorbed contaminant fraction (ion exchangeable), extraction 3 is the “rind-carbonate” contaminant fraction, extraction 4 is the total carbonate contaminant extraction fraction, extraction 5 is the Fe-oxide contaminant fraction, and extraction 6 is defined as the hard-to-extract contaminant fraction. These sequential extractions were conducted at a 1:2 sediment:liquid ratio at room temperature (20°C to 25°C). The extractions used reagents 1 through 6 defined below.

- **Reagent 1 - Artificial groundwater:**

Constituent	Concentration (mM)
H ₂ SiO ₃ *nH ₂ O, silicic acid	0.2
KCl, potassium chloride	0.11
MgCO ₃ , magnesium carbonate	0.15
NaCl, sodium chloride	0.26
CaSO ₄ , calcium sulfate	0.49
CaCO ₃ , calcium carbonate	1.5

Once the chemicals dissolved, an excess of calcium carbonate (CaCO₃) was added to the solution and allowed to mix. After approximately 1 week, excess CaCO₃ was filtered out using a 0.45-µm filter.

- **Reagent 2 - 0.5 mol/L Mg(NO₃)₂:** 128.2 g Mg(NO₃)₂•6H₂O + 30 µL 2 mol/L NaOH to pH 8.0, balance deionized (DI) H₂O to 1.0 liter

- **Reagent 3 - Acetate solution:** 136.1 g sodium acetate•3H₂O + 30 mL glacial acetic acid (17.4 mol/L), pH 5.0, balance DI H₂O to 2.0 liters
- **Reagent 4 - Acetic acid solution:** concentrated glacial acetic acid, pH 2.3; 50.66 mL glacial acetic acid (17.4 mol/L) + 47.2 g Ca(NO₃)₂•4H₂O, pH 2.3, balance DI H₂O to 2.0 liters
- **Reagent 5 - Oxalate solution:** 0.1 mol/L ammonium oxalate, 0.1 mol/L oxalic acid; 9.03 g anhydrous oxalic acid + 14.2 g ammonium oxalate•H₂O, balance DI H₂O to 1.0 liter
- **Reagent 6 - 8.0 mol/L HNO₃:** 502 mL conc. HNO₃ (15.9 mol/L) + 498 mL DI H₂O

In the first extraction, 6 mL of artificial groundwater (reagent 1) is mixed with 3.0 (±0.5) g of sediment for 50 minutes in a centrifuge tube. The tube is then centrifuged at 3000 rpm for 10 minutes, and liquid is drawn off the top of the sediment and filtered (0.45 μm) for analysis. Extractions 2 and 3 are conducted with the same procedure except using reagents 2 and 3, respectively. The fourth extraction uses the same procedure except with a contact time of 5 days and with use of reagent 4. The fifth extraction is conducted the same as extraction 1 except using reagent 5. In the sixth extraction, 6 mL of nitric acid (reagent 6) is added to the sediment and mixed for 2 hours at 95°C. The tube is then centrifuged at 3000 rpm for 10 minutes, and liquid is drawn off the top of the sediment and filtered (0.45 μm) for analysis.

3.2.3.2 1000-hour Carbonate Extraction

A carbonate solution (0.0144M NaHCO₃ + 0.0028M Na₂CO₃ (pH 9.3); 2.42 g NaHCO₃ + 0.592 g Na₂CO₃ + balance DI H₂O to 2.0 liters) is used for the 1000-hour carbonate extractions (Kohler et al. 2004). Sediment (3.0 ± 0.5 g) and 6.0 mL of the carbonate solution were placed in 45-mL Teflon or polycarbonate centrifuge tubes, mixed for 1000 hours at 6 rpm, and centrifuged at 3000 rpm for 10 minutes, and liquid was drawn off the top of the sediment and filtered (0.45 μm) for analysis.

3.2.4 Analysis Objective 4: Geochemical Conditions

Geochemical conditions were interpreted based on the elements and compounds present in the sample pore water or on sediment surfaces. The geochemical information was obtained by the analyses listed in Table 12 (Section 3.2.7). However, specific types of extractions are applied to provide material for analysis. The type of extraction and the concentration of the element/compound were both needed to interpret the data in terms of the geochemical conditions. Extractions applied to evaluate the geochemical conditions are listed in Table 5.

Table 5. Extraction methods for geochemical analysis.

Required Data	Method Basis
Water extraction (1:1 sediment:H ₂ O)	Um et al. 2009 and Zachara et al. 2007
Acid extraction (1:3 sediment:H ₂ O, 8M HNO ₃)	Um et al. 2009 and Zachara et al. 2007
Sequential extractions: Artificial groundwater Ion exchangeable pH 5.0 acetate pH 2.3 acetic acid Oxalate, oxalic acid 8M HNO ₃ , 95°C	Gleyzes et al. 2002; Beckett 1989; Larner et al. 2006; Sutherland and Tack 2002; Section 3.2.3.1
1000 h carbonate extraction	Zachara et al. 2007; Kohler et al. 2004; Section 3.2.3.2
Iron/Mn phase extractions: Ion exchangeable Fe(II), Mn, Oxide/sulfide, Total Fe(II), Fe(III), Mn, Amorphous- Fe(III), Mn-oxides, Crys.-Fe(III), Mn-oxides	Heron et al. 1994; Chao and Zhou 1983; and Hall et al. 1996; Section 3.2.4.1

3.2.4.1 Iron and Manganese Extractions

Iron extractions were conducted to quantify ferrous iron, ferric iron, and manganese, which are solubilized by different solutions. These extractions were conducted in an anoxic chamber.

- For the first extraction, sediment samples (2.0 ± 0.5 g) were mixed with 10.0 mL of ion exchange (1.0 M CaCl₂) solution for 50 minutes at 6 rpm, centrifuged (3000 rpm, 10 minutes), and filtered (0.45 μm). The solution was then analyzed for Fe(II) and Mn.
- For the second extraction, sediment samples (2.0 ± 0.5 g) were mixed with 10.0 mL of 0.5M HCl for 24 hours at 6 rpm, centrifuged (3000 rpm, 10 minutes), and filtered (0.45 μm). The solution was then analyzed for Fe(II) and Mn.
- For the third extraction, sediment samples (2.0 ± 0.5 g) were mixed with 10.0 mL of 5M HCl for 24 hours at 6 rpm, centrifuged (3000 rpm, 10 minutes), and filtered (0.45 μm). The solution was then analyzed for Fe(II) and Mn. The solution was also analyzed for total Fe.
- For the fourth extraction, sediment samples (2.0 ± 0.5 g) were mixed with 10.0 mL of 0.25M NH₂OH•HCl solution for 30 minutes at 50°C, centrifuged (3000 rpm, 10 minutes), and filtered (0.45 μm). The solution was then analyzed for total Fe and Mn.
- For the fifth extraction, sediment samples (2.0 ± 0.5 g) were mixed with 10.0 mL of dithionite-citrate-bicarbonate solution (0.3 mol/L Na-citrate, 1.0 mol/L NaHCO₃, and 0.06 mol/L sodium dithionite), mixed for 30 minutes at 80°C, centrifuged (3000 rpm, 10 minutes), and filtered (0.45 μm). The solution was then analyzed for total Fe and Mn.

3.2.5 Analysis Objective 5: Contaminant Release Rate from Sediment and Mobility

Contaminant mobility was evaluated for some sediment samples (B35434, B35443, and B361N1; Table 1) in batch and soil-column leaching tests that impose specific conditions and collect temporal data. These tests expose contaminated sediment to an aqueous solution (simulated groundwater) and measure changes in contaminant concentration over time under flowing or quiescent (batch) conditions (Table 6). For the column tests, sequential extractions for contaminants (Section 3.2.3) were conducted on the post-test sediments from the column for comparison to the pre-leaching results obtained on the sediments. Because contaminant concentrations in some of the samples were low, and to augment the batch and column leaching data, spiked contaminant experiments (batch and column) were also conducted for all of the samples (Table 6). Contaminant and other geochemical constituent information from samples collected during the tests were obtained by the analyses listed in Table 12 (Section 3.2.7).

Table 6. Contaminant mobility tests.

Required Data	Method Basis
Batch-leaching test	Szecsody et al. 1994; Section 3.2.5.1
1-D soil-column test	Qafoku et al. 2004; Szecsody et al. 2013; Section 3.2.5.2
Spiked-contaminant tests	Section 3.2.5.3

3.2.5.1 Batch-Leaching Test

Batch experiments used 50 g of sediment and 200 mL of air-saturated artificial groundwater placed in a 250-mL polyethylene centrifuge bottle. The bottle was placed on a slow (12-rpm) linear mixer with supernatant samples taken at 1, 10, 30, 100, 300, 1000 hours for analysis of the target contaminants. Sampling consisted of (a) centrifuging the bottle at 3000 rpm for 10 minutes, (b) removing 5.0 mL from the bottle, and (c) filtering the liquid (0.45 μm).

3.2.5.2 Soil-Column Test

Soil-column experiments were conducted with one-dimensional, vertical, bottom-up flow of injected simulated groundwater solution through contaminated sediment. The concentration of contaminant in the effluent was measured. A non-sorbing, non-reactive tracer (bromide ion) was included in the injection solution and its breakthrough was measured to assess column flow dynamics. The flow rate was set to achieve a residence time of between 1 and 4 hours. Sampling frequency in the effluent was varied based on typical contaminant elution dynamics with more dynamics present at earlier times (fewer pore volumes).

Stop-flow events ranging from 10 to 1000 hours were conducted, during which the flow rate of solution through the column was stopped to provide time for contaminants present in one or more surface phases on the sediment surface to partition into pore water (i.e., diffusion from intraparticle pore space, or time-dependent dissolution of precipitated phases, and/or desorption). Operationally, initiating a stop-flow event involves turning off the pump and plugging both ends of the column (to prevent water movement out of the sediment column). Ending a stop-flow event involves reconnecting the column to the pump, turning on the effluent sample collector, and then turning on the pump. The calculation of the

contaminant release rate from sediment (μg contaminant/g of sediment/day) uses the contaminant effluent concentration before and after the stop-flow event, and the duration of the stop-flow event.

3.2.5.3 Spiked-Contaminant Tests

One objective of the 200-DV-1 OU vadose zone characterization program is to determine the attenuation/transport parameters that can be used to evaluate contaminant transport. In some cases, contaminants were present in samples in sufficient concentration that batch and column leaching experiments (Sections 3.2.5.1 and 3.2.5.2) could be used to estimate transport parameters such as the linear equilibrium partitioning coefficient (K_d) or other types of parameters that describe contaminant transport behavior (e.g., based on modeling analysis of the results). However, some samples lacked sufficient contaminant concentrations to conduct these leaching tests. For this reason, PNNL and CHPRC determined that batch and column tests using samples spiked with contaminants should be conducted on all of the sediment samples to provide a dataset useful for estimating the K_d value or other types of parameters that describe contaminant transport behavior (e.g., based on modeling analysis of the results). Samples selected for the spiked-contaminant tests are listed in Table 7.

Table 7. Samples selected for spiked-contaminant analyses.

Borehole and Liner Designation	Borehole ID	Sample ID	Geologic Unit	Depth Interval (ft bgs)
Spiked-Contaminant Batch Testing				
T19 core 14C	C9507	B35434	CCUz	94.1-95.1
T19 core 16C	C9507	B35443	CCUc	104.4-105.4
T-19 137-139	C9507	B35461/B36H08	Ringold	137.6-138.6
T-25 core 14C	C9510	B361N1	H2/CCUz transition	114.3-115.3
S-9 core 8C	C9512	B36177	H1/H2	64.2-65.2
S-9 core 20C	C9512	B361F3	H2/CCUz transition	124-125
Spiked-Contaminant Soil-Column Testing				
T19 core 14C	C9507	B35434	CCUz	94.1-95.1
T-19 137-139	C9507	B35461/B36H08	Ringold	137.6-138.6
S-9 core 20C	C9512	B361F3	H2/CCUz transition	124-125

Specific chemical species of the contaminants were used in the adsorption/desorption K_d measurements. For Tc-99, TcO_4^- was used. For iodine, both I^- and IO_3^- were used. Uranyl nitrate was added to provide uranium. For Cr, CrO_4^{2-} was used. Stable I-127 at low concentrations was used as a surrogate for I-129 in these experiments.

Batch experiments used the solutions listed in Table 8 and Table 9.

Table 8. Vadose zone pore-water simulant recipe (from Serne et al. 2015). Adjust pH to 7.0 to 7.2 with sodium hydroxide or sulfuric acid.

Constituent	Concentration (mM)
CaSO ₄ *2H ₂ O	12
NaCl	1.7
NaHCO ₃	0.4
NaNO ₃	3.4
MgSO ₄	2.6
MgCl ₂ *6H ₂ O	2.4
KCl	0.7
Adjust pH to 7.0 to 7.2 with sodium hydroxide or sulfuric acid	

Table 9. Artificial (Hanford) groundwater.

Constituent	Conc. (mM)
H ₂ SiO ₃ *nH ₂ O, silicic acid	0.20
KCl, potassium chloride	0.11
MgCO ₃ , magnesium carbonate	0.15
NaCl, sodium chloride	0.26
CaSO ₄ , calcium sulfate	0.49
CaCO ₃ , calcium carbonate	1.50

For the Table 9 solution, the reagents were added to DI water. Once the chemicals dissolved, an excess of calcium carbonate (CaCO₃) was added to the solution to equilibrate with calcite while stirring. After approximately 1 week, excess CaCO₃ was filtered out using a 0.45- μ m filter. The final pH was 7.5. 85,000, 170,000, and 850,000

After the solutions are prepared, they were spiked to reach targeted concentrations of contaminants (Table 10). Additional concentrations were tested for sediments B35434 and B35461 (see parentheses, Table 10). For Tc-99, 5, 10, and 50 μ g/L equate to 85,000, 170,000, and 850,000 pCi/L, respectively.

Table 10. Contaminants and spike concentrations.

Contaminant	Contaminant Concentration in Simulated Pore Water	Contaminant Concentration in Simulated Groundwater
Tc-99	50 μ g/L (5, 10 μ g/L)	50 μ g/L (5, 10 μ g/L)
Cr	500 μ g/L (100, 1000 μ g/L)	500 μ g/L (100, 1000 μ g/L)
U	500 μ g/L (100, 1000 μ g/L)	500 μ g/L (100, 1000 μ g/L)
I ⁻	100 μ g/L (500, 1000 μ g/L)	100 μ g/L (500, 1000 μ g/L)
IO ₃ ⁻	100 μ g/L (500, 1000 μ g/L)	100 μ g/L (500, 1000 μ g/L)

Spiked-contaminant batch adsorption/desorption experiments were conducted in 50-mL polypropylene centrifuge tubes at room temperature (~22°C). The experiments were performed at a solid-to-solution ratio of 2:3. The supernatant was sampled (filtered through a 0.45- μm filter membrane) for contaminant analysis (Table 11) at 1, 7, and 28 days of equilibration, with the experimental tubes mounted horizontally on an orbital shaker at the slowest rotation speed possible. Batch experiments were conducted in duplicate for each sampling time, each contaminant ($^{99}\text{TcO}_4^-$, I, IO_3^- , U, and CrO_4^{2-}), and each of the two solutions.

Table 11. Batch test supernatant analyses (specific methods per Table 12, Section 3.2.7).

Data and Instrumentation	Constituents Analyzed
Metals by ICP-OES	Al, Ba, Ca, Fe, K, Mg, Mn, Na, Si, Sr, Cr
U, Tc-99 by ICP-MS	U, Tc-99
Iodine by ICP-MS	Iodide, iodate, and total iodine
Anions by ion chromatography	Br^- , Cl^- , F^- , NO_3^- , NO_2^- , PO_4^{3-} , SO_4^{2-}
Aqueous pH by electrode	pH

ICP is inductively coupled plasma; MS is mass spectrometry; OES is optical emission spectroscopy.

The desorption portion of the experiment was conducted by adding an amount of unspiked solution to each of the centrifuge tubes that was equal to the amount of supernatant removed. The tube was vortexed to mix well, equilibrated on an orbital shaker, and resampled at 28 days.

Soil-column experiments were conducted with one-dimensional, vertical, bottom-up flow of injected simulated groundwater solution through the sediment. The breakthrough of contaminant concentration at the effluent was compared to the influent contaminant concentration and the breakthrough of a non-sorbing, non-reactive tracer (bromide ion). These data can be analyzed by one-dimensional flow analysis to estimate an adsorption K_d . After contaminant breakthrough, the influent solution was switched to contaminant-free solution. The subsequent elution of contaminant and decrease of the contaminant concentrations in the effluent were then tracked. These data can be analyzed by one-dimensional flow analysis to estimate a desorption K_d . One duplicate column experiment (using the same sediment) was conducted for each batch of 20 samples.

3.2.6 Objective 6: Oxygen and Hydrogen Isotopic Signature of the Pore Water

Isotopic analysis for oxygen and hydrogen can be applied for water samples. Within the vadose zone, however, much of a sample's water remains bound to the surfaces of soil particles or contained within pore spaces, making isotope measurement challenging. An extraction procedure was used to quantitatively remove water from solid soil samples and ensure minimal isotopic fractionation during the extraction and collection process.

A vacuum distillation apparatus was applied for extraction. This apparatus was constructed based on slightly modified versions of those discussed in West et al. (2006) and Goebel and Lascano (2012). In brief, a soil sample is added to one end of the system and then frozen to prevent water migration out of the material. Once a vacuum is established, the sample is heated to drive off the native water, which is collected into a cryogen trap cooled by liquid nitrogen. Once the extraction is complete, the water is removed from this cryogen trap and its isotopic content can be analyzed on a separate instrument, offline

from the extraction system. Extracted water extracted was analyzed for isotopic ratios using a PNNL operating procedure (OP-DVZ-AFRI-002) for the analytical instrument.

3.2.7 Chemical Analysis Methods

Standard chemical analytical methods were applied to quantify elements and compounds that are present in extraction solutions and temporal samples from the tests described in Section 3.2, as shown in Table 12.

Table 12. Chemical analyses.

Analysis ^(a)	Hold Time	Constituents Analyzed	Method Basis
Metals by ICP-OES	6 months	Al, Ba, Ca, Fe, K, Mg, Mn, Na, Si, Sr, Cr	EPA 6010D
U, Tc-99 by ICP-MS	6 months	U, Tc-99	EPA 6020B
Iodine species by ICP-MS	6 months	Iodide, iodate	PNNL-ESL-ICPMS-iodine
Kinetic phosphorescence analysis	6 months	U(VI)	Brina and Miller 1992
Cr(VI)	24 hrs	Cr(VI)	Hach 8023
Fe(II)	24 hrs	Fe(II)	Hach 8147
Br ⁻ by electrode	28 days	Br ⁻	EPA 9211
Anions by ion chromatography	Nitrate, nitrite: each 48 hr; PO ₄ : 48 hr	Cl ⁻ , F ⁻ , Br ⁻ , NO ₃ ⁻ , NO ₂ ⁻ , PO ₄ ³⁻ , SO ₄ ²⁻	EPA 9056A
pH by electrode	Immediate (12 hr)	pH	EPA 9040C
Specific conductance (SpC) by electrode	Immediate (12 hr)	SpC	EPA 9050A
Total carbon (TC) and total inorganic carbon (TIC) ^(b)	28 days	TC and TIC	EPA 9060A

(a) Analyses were for aqueous samples except as noted footnote b.

(b) TC and TIC were also analyzed directly on sediment samples as an information-only analysis using manufacturer procedures (SHIMADZU SSM-5000A procedure).

4.0 Results

The laboratory analysis data are described below and interpreted in relation to the three main objectives of the work (Section 2.0). These objectives were developed to be consistent with EPA guidance for evaluating natural attenuation of contaminants, and to provide data and parameters that support contaminant fate and transport assessments. The sections below present the data for each of the three objectives. Quantification of hydraulic properties for selected samples is also being conducted to support these objectives. However, because of the long-term nature of those tests, results of hydraulic property evaluation will be provided in a separate report.

In Section 4.1, contaminant distribution data are presented in the context of the hydrologic and biogeochemical setting. This information enables the data collected in this effort to be linked with the 200-DV-1 OU characterization data compiled by CHPRC. Collectively, this information is a foundation for interpreting contaminant distribution, correlations between contaminant data and other types of data, and the sediment conditions relevant for interpreting attenuation and transport parameters.

Section 4.2 presents and interprets data in terms of identifying contaminant attenuation processes and the types of attenuation mechanisms that are suggested by these data. Some of these data quantify how contaminants are distributed in different phases within the vadose zone. This distribution provides input to interpretation of attenuation processes and contaminant mobility. Other data quantify contaminant mobility based on batch or column experiments that measure the release rate of contaminants from a sediment sample. Data quantifying the type and content of iron and manganese in the sediment are also provided because several of the targeted contaminants are sensitive to redox reactions and iron oxides are important for contaminant sorption.

Section 4.3 presents data and interpretations that support quantification of attenuation and transport parameters. Batch and column experimental data provide information to estimate contaminant partitioning and kinetically controlled release rates from sediments. Because contaminant concentrations were low in many of the sediment samples, results of spiked-contaminant experiments (batch and column tests) are presented with quantification of contaminant partitioning from these tests. This report provides an initial interpretation of attenuation and transport parameters. The data will also be useful for additional interpretation by others through modeling of the results.

4.1 Contaminant Concentrations and Hydrologic and Biogeochemical Setting

Several types of data provide information about the contaminant concentrations and the hydrologic and biogeochemical setting for the sediment samples. Contaminant and geochemical constituent concentrations were measured for sediments using water, acid, and/or alkaline extractions, where appropriate. Microbial ecology was evaluated to identify the number and types of organisms present and to provide information about the types of reactions they may catalyze. Characterization of iron and manganese was conducted to assess the potential for redox reactions and iron-oxide sorption. Oxygen and hydrogen isotopes were measured as a potential means to distinguish different sources of pore water. Sediment physical properties were measured, photographs of the sediments were taken, and geologic

material was classified. Collectively, this information defines the foundation for scaling and interpreting attenuation and transport parameters for field applications.

4.1.1 Contaminants and Geochemical Constituents

Baseline analyses and associated sediment extractions are shown in Table 13. In these samples, analyses for Tc-99 and I-129 were all non-detect with nominal detection limits of 17 and 1.25 pCi/g, respectively. The full set of contaminant data collected for the sediment samples is shown in Table 14. Note that for the purpose of evaluating iodine attenuation and transport behavior, this project used total iodine data because its concentration is above the method detection limit. The samples were also analyzed to determine the iodide and iodate concentrations in the sample because the transport properties of iodide and iodate are different (e.g., Zhang et al. 2013; Truex et al. 2016). Unfortunately, matrix interferences rendered determination of the speciation difficult, with results only reportable for two of the samples. Chromium concentrations as measured by alkaline extraction or water extraction were low. Only one sample had detectable Cr(VI) in the water extract and this value was near the detection limit. Total chromium measurements for the water extract were non-detect for this same sample, although the detection limit was higher than for the Cr(VI) measurement; dilution had to be applied for total chromium measurement because of the high nitrate concentration in the samples. Data for geochemical constituents are listed in Table 15.

Table 13. Baseline contaminant concentrations.

Sample Name	Sample Location	Technetium-99 pCi/g dry (acid)	Uranium ug/kg dry (acid)	Iodine-129 pCi/g dry (water)	Chromium ug/kg dry (alkaline)	Nitrate ug/kg dry (water)
C9507-B35434	T19 14C (CCUz)	ND	784	ND	848	77,200
C9507-B35443	T19 16C (CCUc)	ND	3890	ND	ND	83,600
C9507-B35461	T19 138' (Ringold)	ND	320	ND	ND	95,800
C9510-B361N1	T25 14C (H2/CCU)	ND	490	ND	ND	6330
C9512-B36177	S-9 8C (H1/2)	ND	268	ND	657	235,000
C9512-B361F3	S-9 20C (H2)	ND	293	ND	ND	9350

Table 14. Contaminant data.

Water Extracts										
Sample Name	Sample Location	Technetium-99 pCi/g dry	Uranium ug/kg dry	U(VI) ug/kg dry	Total Iodine ug/kg dry	Iodate ug/kg dry	Iodide ug/kg dry	Chromium ug/kg dry	Cr(VI) ug/kg dry	Nitrate ug/kg dry
C9507-B35434	T19 14C (CCUz)	ND	5.78	6.14	2	1.09	1.07	ND	ND	77,200
C9507-B35443	T19 16C (CCUc)	ND	114	98.57	42.5	NR	NR	ND	14.20	83,600
C9507-B35461	T19 138' (Ringold)	ND	0.15	0.22	7.88	NR	NR	ND	ND	95,800
C9510-B361N1	T25 14C (H2/CCU)	ND	3.57	4.26	10.2	NR	NR	ND	ND	6330
C9512-B36177	S-9 8C (H1/2)	ND	0.0568	ND	2.21	ND	ND	ND	ND	235,000
C9512-B361F3	S-9 20C (H2)	ND	0.461	0.63	2.17	1.09	1.04	ND	ND	9350
Acid Extracts										
Sample Name	Sample Location	Technetium-99 pCi/g dry	Uranium ug/kg dry	U(VI) ug/kg dry	Chromium ug/kg dry					
C9507-B35434	T19 14C (CCUz)	ND	784	946	5640	--	--	--	--	--
C9507-B35443	T19 16C (CCUc)	ND	3890	3335	5920	--	--	--	--	--
C9507-B35461	T19 138' (Ringold)	ND	320	310	3650	--	--	--	--	--
C9510-B361N1	T25 14C (H2/CCU)	ND	490	420	4020	--	--	--	--	--
C9512-B36177	S-9 8C (H1/2)	ND	268	279	4520	--	--	--	--	--
C9512-B361F3	S-9 20C (H2)	ND	293	302	7130	--	--	--	--	--
Alkaline Extraction										
Sample Name	Sample Location	Chromium ug/kg dry								
C9507-B35434	T19 14C (CCUz)	848	--	--	--	--	--	--	--	--
C9507-B35443	T19 16C (CCUc)	ND	--	--	--	--	--	--	--	--
C9507-B35461	T19 138' (Ringold)	ND	--	--	--	--	--	--	--	--
C9510-B361N1	T25 14C (H2/CCU)	ND	--	--	--	--	--	--	--	--
C9512-B36177	S-9 8C (H1/2)	657	--	--	--	--	--	--	--	--
C9512-B361F3	S-9 20C (H2)	ND	--	--	--	--	--	--	--	--

Table 15. Geochemical constituents.

		Water Extracts																			
Sample Name	Sample Location	pH	SpC mS/cm	Al ug/g dry	Ba ug/g dry	Ca ug/g dry	Fe ug/g dry	Mg ug/g dry	Mn ug/g dry	K ug/g dry	Si ug/g dry	Na ug/g dry	Sr ug/g dry	Cl ug/g dry	Fl ug/g dry	Nitrite ug/g dry	PO4 ug/g dry	SO4 ug/g dry	TOC ug/g dry	TIC ug/g dry	
C9507-B35434	T19 14C (CCUz)	8.6	0.257	ND	4.19	ND	0.652	ND	ND	3.02	17.5	ND	ND	ND	ND	5.52	ND	ND	ND	11.2	
C9507-B35443	T19 16C (CCUc)	9.36	0.699	ND	0.862	ND	0.461	ND	ND	12.2	64.5	ND	ND	ND	4.68	ND	ND	12.1	ND	55.1	
C9507-B35461	T19 138' (Ringold)	8.13	0.288	ND	4.97	ND	1.68	ND	ND	4.13	19.5	ND	ND	ND	1.4	ND	ND	10.2	ND	9.4	
C9510-B361N1	T25 14C (H2/CCU)	8.38	0.124	ND	6.28	ND	1.51	ND	ND	4.05	3.51	ND	ND	0.544	0.506	ND	ND	6.02	ND	11.8	
C9512-B36177	S-9 8C (H1/2)	8.3	0.516	ND	8.92	ND	1.7	ND	4.11	4.49	88.7	ND	ND	ND	9.73	ND	ND	ND	ND	10.8	
C9512-B361F3	S-9 20C (H2)	8.39	0.126	ND	4.32	ND	1.35	ND	2.24	7.43	20.1	ND	ND	0.798	ND	ND	ND	4.45	ND	7.6	
		Acid Extracts																			
Sample Name	Sample Location	Al ug/g dry	Ba ug/g dry	Ca ug/g dry	Fe ug/g dry	Mg ug/g dry	Mn ug/g dry	K ug/g dry	Si ug/g dry	Na ug/g dry	Sr ug/g dry										
C9507-B35434	T19 14C (CCUz)	3600	36.2	8740	6560	2900	176	829 J	ND	132	21.9										
C9507-B35443	T19 16C (CCUc)	5530	75.7	142,000	6020	15,000	112	655 J	ND	1040	200										
C9507-B35461	T19 138' (Ringold)	3200	38.4	2810	8340	2050	136	400 J	ND	447	16.2										
C9510-B361N1	T25 14C (H2/CCU)	3460	53.6	42,200	5690	2670	125	452 J	27.9	136	52.9										
C9512-B36177	S-9 8C (H1/2)	3030	33.9	7920	6020	2880	160	654	ND	209	21.4										
C9512-B361F3	S-9 20C (H2)	3760	36.9	6830	6490	2920	142	1020	ND	118	22.1										
		TOC Sediment and Water Extract																			
Sample Name	Sample Location	TC-sed ug/g dry	TIC-sed ug/g dry	TOC-sed ug/g dry	TOC-WE ug/g dry	TIC-WE ug/g dry	Moisture wt%														
C9507-B35434	T19 14C (CCUz)	3400	3220	ND	11.2	5.79															
C9507-B35443	T19 16C (CCUc)	50900	49100	1740	55.1	15.7															
C9507-B35461	T19 138' (Ringold)	287	ND	ND	9.4	4.3															
C9510-B361N1	T25 14C (H2/CCU)	16100	16200	ND	11.8	6.49															
C9512-B36177	S-9 8C (H1/2)	2960	2710	249	10.8	2.69															
C9512-B361F3	S-9 20C (H2)	2750	2350	402	7.6	5.8															

Note: J flag for potassium acid extract results denotes an estimated value because the blank spike recovery was 78.2%, which is outside the target range of 80-120%.

Contaminant concentrations in all of the samples were low except for moderate uranium concentrations in one sample and high nitrate concentrations in all samples (although some samples had much higher nitrate concentrations than other samples). Total iodine concentrations were moderate. Although total iodine is not an identified contaminant of potential concern, its transport behavior is expected to be the same as I-129 and was of interest to enable evaluation of transport behavior and parameters in these samples. Cr(VI) concentrations were low or not detectable. Chromium (total) was measured in acid extractions and is likely natural chromium present in the sediment.

Because of the very low contaminant levels in three of the samples (B35461, B361F3, and B36177), soil-column leaching studies were not conducted on these samples. Even though it was determined that soil-column leaching could provide useful information for the other three samples (B35434, B35443, and B361N1), contaminant concentrations in these samples were low to moderate. Thus, spiked-contaminant studies were conducted for all of the samples. The sample with moderate uranium concentration was from a portion of the CCU with a high carbonate concentration. High carbonate concentration may have acted to retain uranium contamination as it migrated into this unit through formation of uranium carbonate compounds. Sequential extraction tests described in Section 4.2 provide more information in relation to the phase distribution of uranium contamination and other contaminants.

Geochemical indicators identified by the EPA MNA guidance are those associated with formation of categories of precipitates that may affect contaminants, those associated with contaminant sorption (e.g., iron oxides), and those associated with redox processes. Geochemical indicators are also used for joint interpretation with biological characterization data (see Section 4.1.2). Geochemical data show similar conditions in all samples except for higher carbonate content in samples B35443 (the highest content by a significant amount) and B361N1, as indicated by high calcium concentrations in the acid extractions (and high magnesium for B35443) and by the high total inorganic carbon in the sediment analyses. Contaminants affected by carbonate concentration include uranium, iodine (iodate species), and Cr(VI) (in the form of chromate). Two of the samples (B35434 and B36177) showed minor indications of geochemically reduced conditions due to low sulfate concentrations and the presence of nitrite. Iron and manganese concentrations in the water extracted for these samples were non-detect, although iron and manganese could have been oxidized and precipitated as oxides during sample collection and handling. Nitrite and sulfides would be more resistant to oxidation and may be remnant indicators of geochemically reduced conditions in these samples. Reductive processes affect the fate and transport of uranium, Tc-99, Cr(VI), iodine, and nitrate. Organic carbon was present in samples B35443, B361F3, and B36177, though at generally low concentration. Organic carbon is important to consider in conjunction with the biological system. These geochemical data will be considered with respect to interpreting the other types of characterization data discussed below.

4.1.2 Microbial Ecology

The microbial ecology in the samples was evaluated using several types of analyses. Culturing techniques provide information about the phenotype of microbes that are present and able to actively use specific types of electron acceptors when electron donors are present. The data provide an estimate of the population of each phenotype (i.e., nitrate reducers). However, the data do not indicate how active the microbes are in situ, but indicate what types and existing populations of microbes can be active (i.e., are present and alive). This information is important because use of electron acceptors such as nitrate, iron,

and manganese by microbes changes the redox state and related chemical form of these materials. These changes affect how these chemicals interact with contaminants or, in the case of nitrate, reduce its concentration as a contaminant. Many microbes capable of using these electron acceptors have also been shown to transform radionuclides, such as TC-99, uranium, and iodate. Genetic evaluation tools were also applied. These tools compare genetic material from the sample to known bacterial phyla to identify the microbes in the samples. By knowing the microbial phyla, literature information can be used to assess what general type of reactions these microbes may catalyze.

Table 16 shows the results of sediment characterization using culturing techniques. Overall distribution of phyla within four of the samples is shown in Figure 4. Two of the samples, both from borehole S-9, did not show a response in the genetic analysis.

Table 16. Microbial phenotype results showing ability of bacteria to grow on a variety of electron acceptors. Values indicate number of cells/g of sediment tested.

Sample ID	Borehole Designation	Depth (ft bgs)	Oxygen	Nitrate	Iron	Manganese	Colony Forming Units
C9507-B35434	T19 14C (CCUz)	94.1-95.1	1,100	> 1,100,000	> 1,100,000	460	0
C9507-B35443	T19 16C (CCUc)	104.4-105.4	460,000	> 1,100,000	1,100,000	20,000	4,100,000
C9507-B35461	T19 138' (Ringold)	138	240	11,000	> 1,100,000	> 1,100	0
C9510-B361N1	T25 14C (H2/CCU)	114.3-115.3	> 1,100	> 1,100,000	1,100,000	> 1,100	172,667
C9512-B36177	S-9 8C (H1/2)	64.2-65.2	> 1,100,000	210,000	1,100,000	240	117,000
C9512-B361F3	S-9 20C (H2)	124-125	2,100	240,000	21,000	43,000	1,776,667

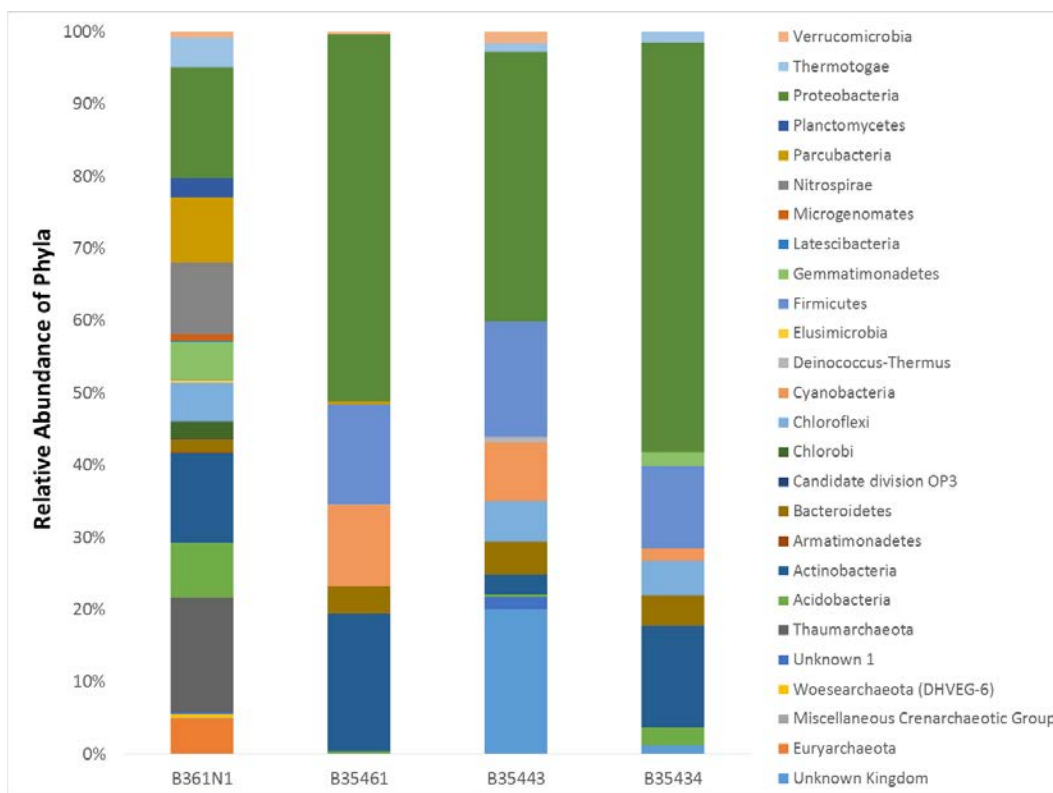


Figure 4. Relative abundance of bacterial phyla based on the 16S rRNA gene.

Most probable number (MPN) analysis was performed using a range of common electron acceptors that may be found in the Hanford vadose zone, either as natural constituents of the minerals present (e.g., iron and manganese) or as contaminants (nitrate) introduced to the environment during waste disposal activities. Total heterotrophs (provided as colony forming units) are another measure of aerobic bacteria that may grow better on a solid surface. Bacteria in sediment from sample B35434 showed low numbers, while in sample B35443, numbers of aerobic bacteria were high (4×10^5 to 4×10^6). Number of aerobic heterotrophs in the Ringold sediments (sample B35461) dropped to zero for total heterotrophs and 2.4×10^2 for MPN. Bacterial numbers in sample B35434 and sample B35461 may be low compared to the number in sample B35443 because more moisture was present in sample B35443 (see Table 16). In addition, TOC was highest in sample B35443, indicating bacteria may have had a potential carbon source or that bacteria may have already grown on these sediments. Low bacterial numbers in sample B35461 may have also been affected by the non-standard core handling (e.g., storage at room temperature for a period before shipment to the laboratory).

When compared to negative controls to which no sediment was added, sediment samples from boreholes T19 (B35434 and B35443) and T25 (B361N1) showed cell densities for bacteria using nitrate as the electron acceptor in numbers greater than 1×10^6 bacteria/g of sediment. Samples from the S9 borehole (B36177 and B361F3) showed slightly lower cell density at $\sim 2.3 \times 10^5$ cells/g of sediment. High numbers of bacteria able to grow in the presence of nitrate as a potential electron acceptor is not surprising because high concentrations of nitrate were found in the sediments when extracted with water (Table 14).

In addition, growth was noted in treatments containing ferric iron as the electron acceptor, with bacterial numbers exceeding 1×10^6 cells/g of sediment in most cores. Numbers of bacteria were only 2.1×10^4 for sample B361F3. Chemical analysis used to determine whether growth was associated with reduction of the electron acceptor present indicated that bacteria were able to grow using nitrate as an electron acceptor, but reduction to ferrous iron did not occur during growth on ferric iron with the exception of sample B361F3, indicating that the bacteria may have been growing under fermentative conditions. Extraction of ferrous and ferric iron (Table 17) showed higher levels of ferrous iron, indicating that reduction events may have occurred previously. These results may explain why iron reduction was not noted in most of the MPN tests containing ferric iron. Of the electron acceptors tested, treatments with manganese showed the least growth, but the number of manganese reducers was the highest in sample B35443, which also showed the highest moisture. In addition, this sample contained the most Mn(IV) (Table 18), compared to the other samples tested.

Figure 4 shows that samples from all depths for borehole T19 (samples B35434, B35443, and B35461) show a microbial community dominated by Proteobacteria, indicating that there is likely a range of facultative anaerobes that should have the ability to use various inorganic, metal, and radionuclides as electron acceptors. There are also significant numbers of *Actinobacteria* and *Firmicutes*, which also contain facultative members. These phyla are also significant because when adverse conditions such as decreased water are encountered, they can form spores that allow for survival for long periods. Facultative anaerobes are able to grow in oxic as well as anoxic environments using alternate electron acceptors such as nitrate. Phyla found in the samples also contain many bacterial species that are capable of contaminant transformation, which ultimately could affect fate and transport. A diverse, more evenly distributed community was present in the sample analyzed from borehole T25 (sample B361N1). This sample also had Proteobacteria, which represented approximately 15% of the total community. Interestingly, the T25 sample (B361N1) also contained a significant percentage of Archaea, which have not commonly been encountered in Hanford sediments.

4.1.3 Iron and Manganese Characterization

Iron and manganese exist in multiple redox states and chemical forms in the subsurface. The relative distribution of iron and manganese in different forms provides insight into the sorptive and reactive capacity of the sediments. A series of extractions with measurement of iron and manganese was conducted to characterize the sediments using extraction techniques identified in scientific literature (and referred to in EPA MNA guidance [EPA 2015]).

Table 17 and Table 18 show the results of the extractions and iron and manganese analyses, respectively. For context, the information is also plotted, showing the relative portions of different iron forms and the relative amount of redox-active iron and ferrous iron phases (Figure 5a) and Mn phases (Figure 5b).

Table 17. Ferrous and ferric iron phases in sediments based on liquid extractions.

Sample Name	Sample Location	ads. Fe ^{II} (mg/g)	Fe ^{II} CO ₃ ,		am. Fe ^{III} (mg/g)	crys. Fe ^{III} (mg/g)	Other Fe ^{III} (mg/g)	Total Fe ^{II+III} (mg/g)
			FeS (mg/g)	Other Fe ^{II} (mg/g)				
C9507-B35434	T19 14C (CCUz)	< 1.20E-3	0.316	5.25	0.0195	0.549	13.8	19.4
C9507-B35443	T19 16C (CCUc)	< 1.20E-3	< 1.20E-3	7.24	< 1.20E-3	0.061	6.90	14.1
C9507-B35461	T19 138' (Ringold)	< 1.20E-3	3.92	5.50	0.1852	0.327	19.2	28.6
C9510-B361N1	T25 14C (H2/CCU)	< 1.20E-3	< 1.20E-3	9.57	0.0086	0.286	13.8	23.4
C9512-B36177	S-9 8C (H1/2)	< 1.20E-3	0.991	4.18	0.0414	0.228	11.1	16.3
C9512-B361F3	S-9 20C (H2)	< 1.20E-3	1.22	4.98	0.0382	0.640	14.6	20.8
C9512-B361F3	S-9 20C (H2)	< 1.20E-3	1.22	4.80	0.0351	0.632	13.9	19.9

ads. = adsorbed, am. = amorphous, crys. = crystalline

Table 18. Manganese phases in sediments based on liquid extractions.

Sample Name	Sample Location	ads. Mn ^{II} (mg/g)	Mn ^{II} CO ₃ (mg/g)	am. Mn ^{II+IV} (mg/g)	crys. Mn ^{II+IV} (mg/g)	Other Mn ^{II+IV} (mg/g)	Total Mn ^{II+IV} (mg/g)
C9507-B35443	T19 16C (CCUc)	< 1.20E-3	2.78E-03	1.93E-03	5.66E-03	0.153	0.163
C9507-B35461	T19 138' (Ringold)	1.86E-03	0.133	7.89E-02	< 1.20E-3	0.117	0.328
C9510-B361N1	T25 14C (H2/CCU)	< 1.20E-3	3.07E-02	6.02E-02	1.91E-03	0.140	0.232
C9512-B36177	S-9 8C (H1/2)	< 1.20E-3	0.145	1.52E-01	< 1.20E-3	< 1.20E-3	0.246
C9512-B361F3	S-9 20C (H2)	< 1.20E-3	0.120	7.02E-02	< 1.20E-3	0.077	0.267
C9512-B361F3	S-9 20C (H2)	< 1.20E-3	0.116	6.73E-02	< 1.20E-3	0.072	0.255

ads. = adsorbed, am. = amorphous, crys. = crystalline

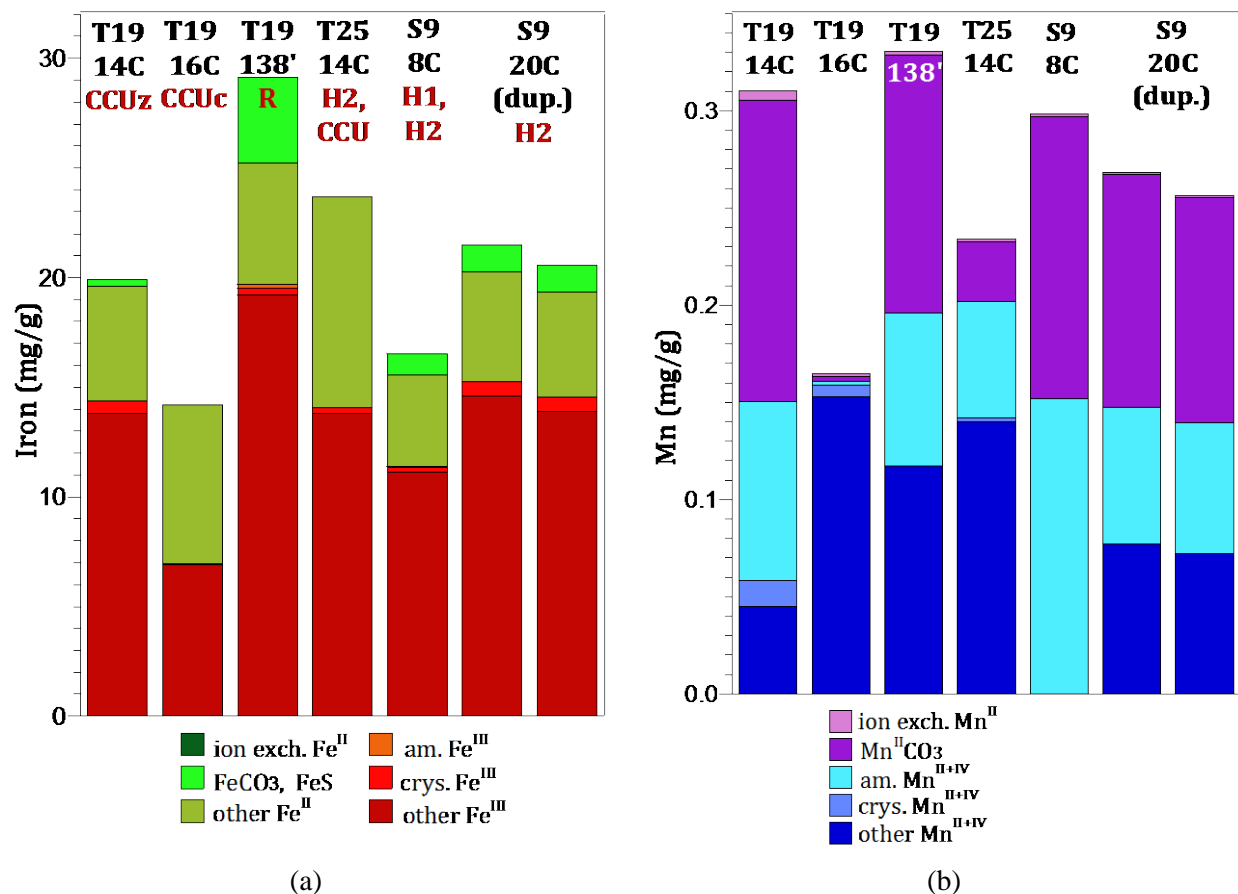


Figure 5. Iron (a) and manganese (b) surface phase distributions in sediments, based on liquid extractions.

Iron and manganese extractions were conducted to characterize the potential for contaminant redox reactions in the sediments. Sediments contained a total of 14 to 28 mg/g extractable iron, based on a 3-week 5M HCl extraction. Hanford, Ringold, and Cold Creek formation sediments contain a mixture of mafic (i.e., sediments derived from basalt) and granitic minerals, with mafic minerals (pyroxenes, amphiboles) and clay minerals containing significant Fe and Mn phases (Table 19). The amorphous and crystalline ferric iron oxide extractions (orange and light red, Figure 5a) show that a small fraction of the total ferrous iron in the sediment is more readily dissolved oxides (and available for microbial iron reduction), whereas the majority of ferrous iron was likely in pyroxene and amphibole phases. Ferrous phases accounted for 25% to 40% of the total iron (green bars in Figure 5a), with little adsorbed ferrous iron (dark green, see Table 17), minor ferrous iron in carbonates/sulfides (light green), some of which is redox reactive, and the remaining ferrous iron in unidentified phases (likely in clays). Although all of these sediments are from the vadose zone, some abiotic reduction can occur under water-saturated conditions (Szecsody et al. 2014) due to the availability of ferrous iron from carbonates/sulfides.

Table 19. Summary of Hanford mineralogy (after Xue et al. 2003).

Mineral	Formula	Both Fm (% wt)	Hanford Fm (% wt)	Ringold Fm (% wt)
Quartz	SiO ₂	37.7 ± 12.4	38.4 ± 12.8	37.03 ± 12.4
Microcline	KAlSi ₃ O ₈	17.0 ± 6.7	15.3 ± 4.4	18.7 ± 8.0
Plagioclase	NaAlSi ₃ O ₈ -CaAl ₂ Si ₂ O ₈	18.7 ± 7.7	22.2 ± 7.2	15.5 ± 6.8
Pyroxenes	(Ca,Mg,Fe)Si ₂ O ₆	3.03 ± 5.99	5.01 ± 7.83	1.14 ± 2.52
Calcite	CaCO ₃	4.97 ± 7.19	1.91 ± 1.71	0.68 ± 0.92
Magnetite	Fe ₃ O ₄	5.09 ± 4.37	4.46 ± 4.12	5.68 ± 4.63
Amphiboles	Ca ₂ (Mg, Fe, Al) ₅ (Al, Si) ₈ O ₂₂ (OH) ₂	5.55 ± 5.97	5.46 ± 5.67	5.64 ± 6.40
Apatite	Ca ₁₀ (PO ₄) ₆ (OH) ₂	0.60 ± 1.04	0.52 ± 0.92	0.67 ± 1.16
Mica ^(a)	(K, Na,Ca)(Al, Mg, Fe) ₂₋₃ (Si,Al) ₄ O ₁₀ (O, F, OH) ₂	2.07 ± 4.47	2.46 ± 3.74	1.71 ± 5.15
Ilmenite	FeTiO ₃	2.51 ± 2.66	1.28 ± 1.51	3.67 ± 3.00
Epidote	{Ca ₂ }{Al ₂ Fe ³⁺ }[O OH][SiO ₄ Si ₂ O ₇]	1.65 ± 2.98	1.78 ± 3.75	1.52 ± 2.14

(a) Muscovite, biotite, phlogopite, lepidolite, clintonite, illite, phengite

Although the total manganese (II and IV) extracted from the sediment (0.16 to 0.33 mg/g) was ~1-2% of the total iron in the sediment, there was a greater fraction of potentially redox reactive Mn^{II}. The fraction of ion exchangeable Mn^{II} was small (ranging from below detection limits to 4.7 µg/g), but the Mn^{II} associated with carbonates (0.003 to 0.16 mg/g) was significant. Mn^{II} phases were 20% to 55% of the total Mn.

4.1.4 Oxygen and Hydrogen Isotopes

Isotopic analysis for oxygen and hydrogen are developed and applied for multiple purposes (Prudic et al. 1997). For instance, the stable isotopes of water ($\delta^2\text{H}$ [deuterium] and $\delta^{18}\text{O}$ [18-oxygen]) can be used to assist with tracking of underground contaminant plumes or linking a source to a measured water sample. For the 200-DV-1 OU, the pore water in the vadose zone is a mixture of water from previous natural recharge and the anthropogenic water discharges of waste streams. Isotopic data was collected to assess whether the signatures from different areas can be correlated to mixtures of different types of water sources. As shown in Table 20, this section includes data for sediment samples collected from the S- and T-Complexes (borehole C9507 [T-19 waste site], borehole C9510 [T-25 waste site], and borehole C9512 [S-9 waste site]). To assist interpretation, plots include data for sediment samples from the B-Complex (Szecsody et al. 2017, borehole C9552 [BY Cribs waste site], borehole C9487 [B7-AB waste site], and borehole C9488 [B-8 waste site]) and for water samples from the perched-water aquifer in the B-Complex (Lee et al. 2017).

Table 20. Sediment samples selected for analyses and isotope data values (outliers removed).

Borehole and Liner Designation	Borehole ID	Sample ID	Nominal Geologic Unit	Depth Interval (ft bgs)	Data Source	$\delta^{18}\text{O}$ (‰)	$\delta^2\text{H}$ (‰)
T19 14A	C9507	B35432	CCUz	92.1-93.1	This report	-19.36 (2.0)	-145.5 (7.8)
T19 16A	C9507	B35441	CCUc	102.4-103.4	This report	-17.54 (1.0)	-135.1 (6.0)
T-19 Ringold	C9507	B35461	Ringold	139.1-139.6	This report	-15.33 (0.3)	-123.9 (1.1)
T-25 14A	C9510	B361M7	H2/CCUz	112.3-113.3	This report	-17.16 (0.2)	-138.0 (0.9)
S-9 8A	C9512	B36173	H1/H2	62.2-63.2	This report	-21.05 (2.7)	-146.7 (11.5)
S-9 20A	C9512	B361D9	H2/CCUz	122-123	This report	-20.54 (1.1)	-143.5 (6.2)
BY Cribs 13A	C9552	B341B1	H2	102.2 – 103.2	Szecsody et al. (2017)	-13.48 (0.2)	-128.3 (1.0)
BY Cribs 18A	C9552	B341C1	H2	127.3 – 128.3	Szecsody et al. (2017)	-15.13 (1.1)	-134.9 (3.3)
BY Cribs 19A	C9552	B341C3	H2	132.1 – 133.1	Szecsody et al. (2017)	-14.18 (0.4)	-130.3 (0.9)
BY Cribs 30A	C9552	B34H74	CCUg	192.2 – 193.2	Szecsody et al. (2017)	-16.43 (0.9)	-145.0 (5.7)
B7-AB 17A	C9487	B34WB1	H2	132.1 – 133.1	Szecsody et al. (2017)	-19.24 (0.1)	-143.3 (0.1)
B7-AB 35D	C9487	B34WH8	H2/CCUz	220.0 – 221.0	Szecsody et al. (2017)	-18.11 (1.8)	-141.8 (9.7)
B7-AB Opt. 12C	C9487	B354L1	CCUz	227.2 – 227.7	Szecsody et al. (2017)	-16.19 (0.5)	-127.0 (1.4)
B7-AB Opt. 14C	C9487	B354M3	CCUz	232.0 – 233.0	Szecsody et al. (2017)	-17.73 (0.9)	-135.4 (3.5)
B-8 37B	C9488	B355L8	CCUz	222.5 – 225.5	Szecsody et al. (2017)	-16.09 (0.9)	-129.4 (5.6)
Perched Water	NA	NA	Well Samples	NA	Lee et al. (2017)	Lee et al. (2017)	Lee et al. (2017)

Isotopic ratios for deuterium and 18-oxygen are reported in delta (δ) notation, defined as

$$\delta = \left(\frac{R_{sa}}{R_{std}} - 1 \right) \times 1000$$

where R is the ratio of the abundance of the heavy to light isotope (i.e. $^2\text{H}/^1\text{H}$, $^{18}\text{O}/^{16}\text{O}$), *sa* denotes the sample, and *std* indicates the standard (McKinney et al. 1950). Delta values are reported in per mil (‰), with $\delta^2\text{H}$ and $\delta^{18}\text{O}$ values relative to Vienna Standard Mean Ocean Water ($\delta^2\text{H} = 0\text{‰}$, $\delta^{18}\text{O} = 0\text{‰}$).

Isotopic analysis for oxygen and hydrogen are typically plotted as shown in Figure 6, which also shows the global meteoric water line (Craig 1961), an assembled regional meteoric water line (Graham 1983), and the rough isotope region reported for Columbia River surface water at this location (Spane and Webber 1995) for comparison to the values of water extracted and measured in this study. Error bars correlate to the standard deviation resulting from a minimum of triplicate extraction replicates each isotopically analyzed using multiple analytical replicates ($n \geq 9$). All data is shown in Figure 6a while Figure 6b contains a culled data set in which a Modified Thompson Tau test was used to eliminate outliers in the data that may have resulted from a combination of inherent sample heterogeneity and/or inefficient water extraction. Note that while this statistical application may have reduced the size of associated error bars, the overall trends discussed below remain intact. As such, the additional data discussion is based on the revised data set resulting from the statistical rejection of outlier data points (at the 95% confidence interval). In addition to the vadose zone sediment samples analyzed, isotopic ratios are plotted for water extracted from the perched-water aquifer in the B-Complex (errors bars correlate to the standard deviation of the analytical replicates, $n \geq 9$).

The global meteoric water line (Craig 1961) shows the average relationship, worldwide, between $\delta^2\text{H}$ and $\delta^{18}\text{O}$ in natural terrestrial waters (e.g., rivers, lakes) and precipitation. The deviation between the local and global meteoric water lines is attributed to evaporative processes coupled to the typically short precipitation durations and semi-arid nature of the local region (Graham 1983). There is overlap between the local meteoric water correlation for each of the extracted water samples and nearly all of the perched water samples, suggesting close connection between regional precipitation and the samples. There is also an interesting relationship between the data from boreholes containing three or more data points (C9507, C9552 [Szecsody et al. 2017], and C9487 [Szecsody et al. 2017]). In each of these cases, the data show strong correlation between the two isotopes (R^2 of 1.00, 0.97, and 0.91 respectively) as would be expected, and the linear fit to each of these data sets show a show respective slopes of 5.46, 5.74, and 5.62. These relationships show strong connection to both previous measurements of vadose zone water (DePaolo et al. 2004; identified a slope of ~ 5) and to the regional meteoric precipitation line (slope of ~ 5.8). More revealing, however, is the offset between sample data sets whereby samples from C9552 (Szecsody et al. 2017) are noticeably shifted to the right in the isotope plots, likely indicating more extensive evaporation history in these samples than in the others.

A trend was observed between the measured vadose zone samples and depth (Figure 7), but there are different behaviors of this trend in different boreholes. For instance, in the T- and S-Complex samples, the total data set displayed a correlation with R^2 of only 0.42; removal of just point B361D9 increased this correlation to R^2 of 0.96 and the three samples within core C9507 T19 also showed a strong correlation with depth (R^2 of 0.96). The trend toward isotopic enrichment (less negative values) with increased sample depth apparent in the vadose zone samples is qualitatively consistent with the observations of Hearn et al. (1989), who cited upwelling of isotopically enriched deeper waters for this trend in their analyses. However, the much shallower nature of these samples (<45 m compared to >1200 m) combined with the nature of vadose versus groundwater samples make it difficult to invoke a similar mechanism here. It is possible, however, that barometric mixing effects (similar to those described by Spane [1999]) induced mixing of underlying groundwater vapor with overlaying vadose zone water.

In contrast, DePaolo et al. (2004) suggest that strong evaporative effects in upper Hanford soil columns can create significant (e.g., 2-6 ‰ shift in $\delta^{18}\text{O}$) isotopic enrichment in resulting vadose zone moisture. This mechanism likely helps explain the enriched isotope values observed in samples from C9552 and C9488 (Szecsody et al. 2017). This effect is generally confined to only the upper couple meters (or less) of soil. While slight isotopic enrichment may be expected compared to precipitation values below this surface enrichment, that process would not account for the more depleted values being found at shallow depths within the C9507 (T19) borehole. In a core exhumed from the 200 West Area in 1999, DePaolo et al. (2004) also observed a negative isotopic anomaly in water extracted from a surface to groundwater depth profile. They attributed this excursion to leaking industrial process water that subsequently focused at the boundary of a coarser grained layer underlain by a finer grained layer. While a similar mechanism considered here would be consistent with the negative isotopic values observed in sample B35432, a more continuous depth profile would be required to validate this hypothesis. Interestingly, samples B35441 (Szecsody et al. 2017), B35461/B36H08, and B361M7 (Szecsody et al. 2017) are consistent with the absolute isotopic values DePaolo et al. (2004) observed in their study, but samples including B36173 and B361D9 (both from borehole C9512 S9) are isotopically depleted in comparison to this previous study. Winter precipitation is known to have a more depleted isotopic composition but ranges around a $\delta^{18}\text{O}$ of $\sim -18\text{‰}$ and $\delta^2\text{H}$ of $\sim -138\text{‰}$ (DePaolo et al. 2004), so seasonality on its own cannot explain these data.

These observations are more confounding in that evaporative enrichment (e.g., observed by DePaolo et al. [2004] and Singleton et al. [2004]) typically propagates down core, thus isotopically enriching the entire core. Evidence of this is seen in the perched water data whereby these samples show isotopic enrichment consistent with near-surface evaporative processes (Lee et al. 2017). A potential hypothesis for explaining the depletion of the C9512 S9 samples may rest in release of industrial condensate generated from intentional evaporitic enrichment of wastes to reduce their volumes. As noted in DOE/RL-92-93 (DOE 1992), such condensate would exhibit an isotopic depletion as an inverse to the enrichment observed in residual fluid following evaporation (as would be required by conservation of mass). Discharge of industrial condensate in the vicinity of C9512 S9 could potentially explain both the inherent depleted isotopic content of these samples as well as the deviation of these samples from the more generalized correlation between $\delta^{18}\text{O}$ versus depth; large-scale release of industrial condensate would likely overprint existing isotopic trends within the vadose depth profile. In support of this, there is noted historical release of process condensate from the D-2 receiver tank within the 202-S Building that resulted from condensation of evaporate used to concentrate decontamination waste at this location (DOE 2016). The sharp negative isotope deviation in vadose zone water within this location could represent an isotopic signature of this process that may be a useful for tracking regional migration of the resulting plume. A similar process may also contribute to the most extreme isotopic signature within the C9507 T19 borehole, notably B35432, as there was noted release of process and steam condensate from the 242 T evaporator in this region but also release of additional tank waste and waste supernate (DOE 2016). It is unclear whether a similar mechanism can explain the depleted isotope signatures in C9487 (specifically B34WB1 [Szecsody et al. 2017]), but it remains a leading hypothesis regarding the extracted water in this sample having an isotopic composition more depleted than annual precipitation extremes or observed groundwater.

The isotope measurements of the S- and T-Complex samples were plotted against measured nitrate concentrations (Figure 8). Two immediate features were observed. First, there is a linear relationship between the nitrate concentration and isotope data that also correlates to increasing depth in the borehole. The patterns seen in C9507 T19 are in contrast to the data from C9512 S9, however, which shows minimal variation in isotope values or nitrate over a fairly large vertical column (~60 ft).

Taken together, the stable isotope data provide a few interesting observations on these systems. First, most boreholes having multiple data points show covariance of the two measured isotopes, suggesting strong input from regional precipitation (e.g., C9507 T19, C9487 [Szecsody et al. 2017], C9552 [Szecsody et al. 2017], and the suite of perched water samples [Lee et al. 2017]). While each of these data sets shows isotopic signatures associated with evaporation, samples from C9552 (Szecsody et al. 2017) show a significant increase in this feature, suggesting a stronger evaporative history than in the other samples. In contrast to evaporative enrichment, some samples show negative isotope excursions suggestive of inclusion of condensate-derived moisture in the vadose zone. While this is most notable in samples B36173 and B361D9, the mechanism may also help explain observations from samples from the C9507 T19 and C9487 (Szecsody et al. 2017) boreholes.

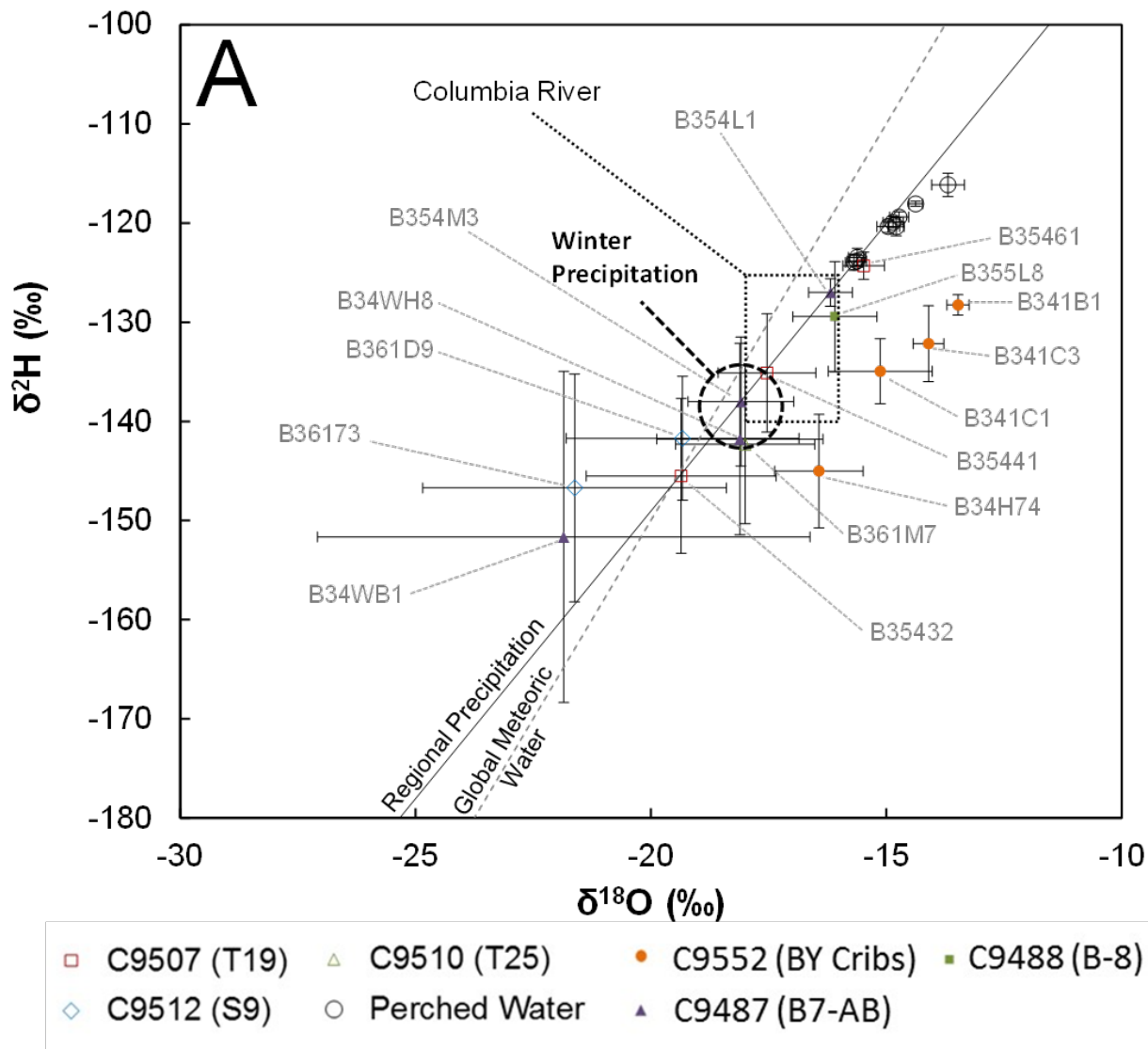


Figure 6. Isotope data for vadose zone sediment and perched water analyses. (A) Data resulting from the full data set. (B) Data refined by a Modified Thompson Tau test to remove outlier points (continued on next page). Depiction of winter precipitation is after DePaolo et al. (2004) with a nominal value of $\delta^{18}\text{O}$ of $\sim -18\text{‰}$ and $\delta^2\text{H}$ of $\sim -138\text{‰}$.

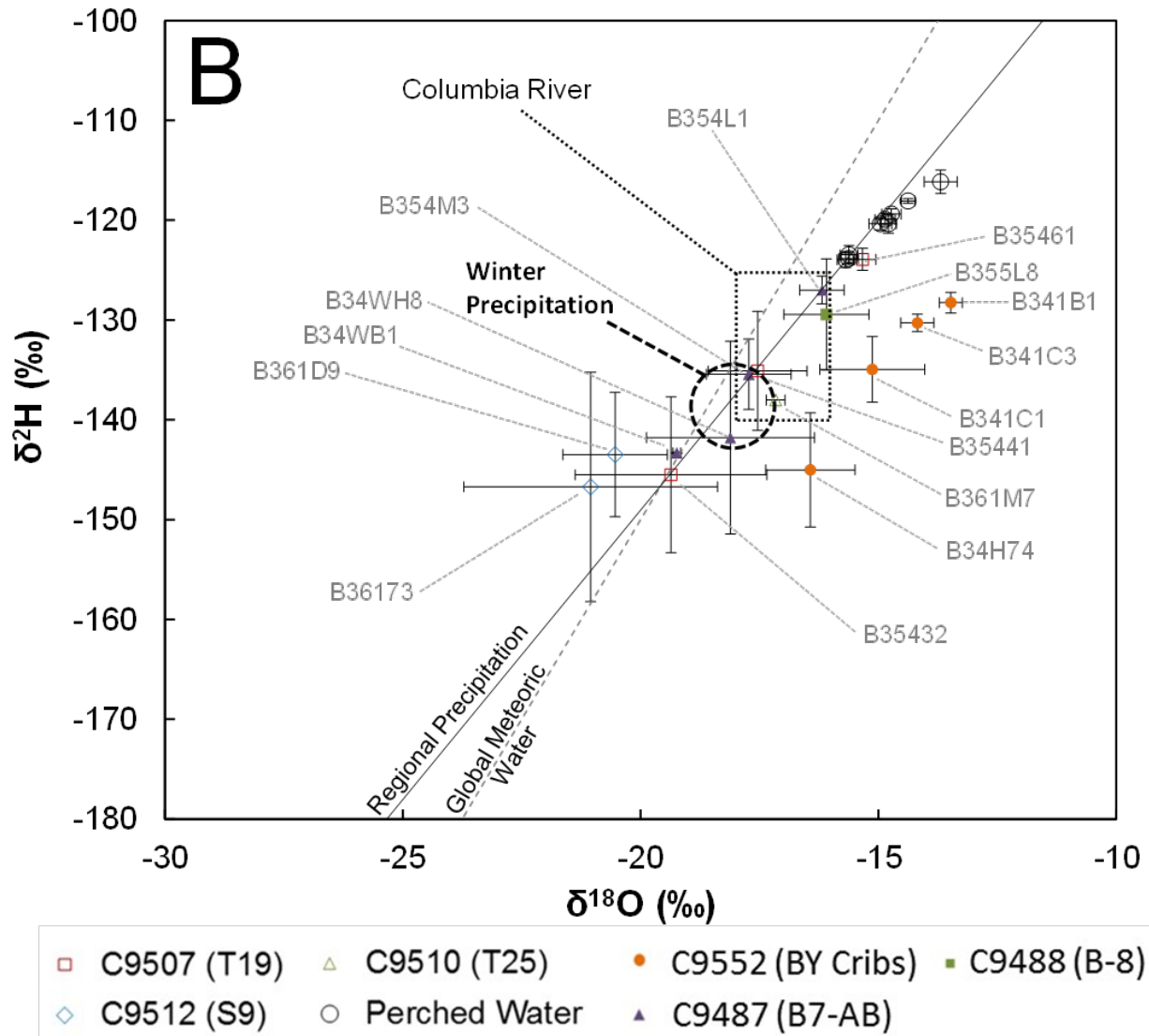


Figure 6 (continued). Isotope data for vadose zone sediment and perched water analyses. (A) Data resulting from the full data set. (B) Data refined by a Modified Thompson Tau test to remove outlier points. Depiction of winter precipitation is after DePaolo et al. (2004) with a nominal value of $\delta^{18}\text{O}$ of $\sim -18\text{‰}$ and $\delta^2\text{H}$ of $\sim -138\text{‰}$.

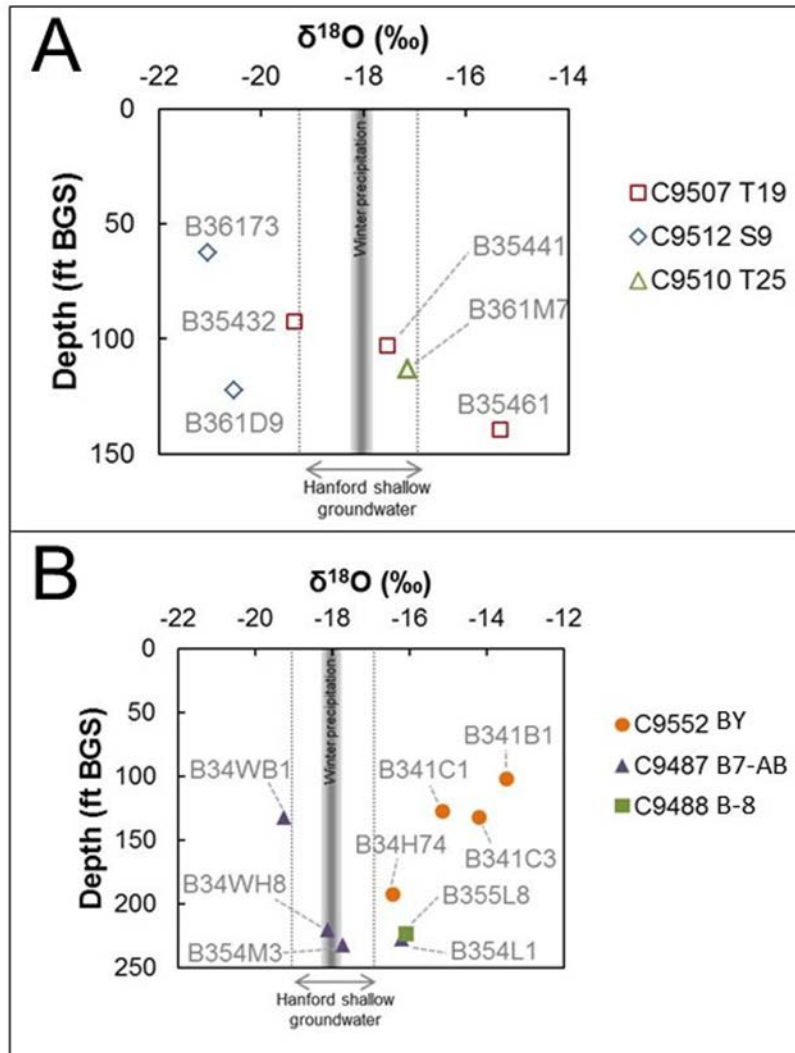


Figure 7. $\delta^{18}\text{O}$ relating to sample depth, average local winter precipitation, and local shallow groundwater within the Hanford Site: (A) sample data from the T- and S-Complexes, and (B) sample data from the B-Complex.

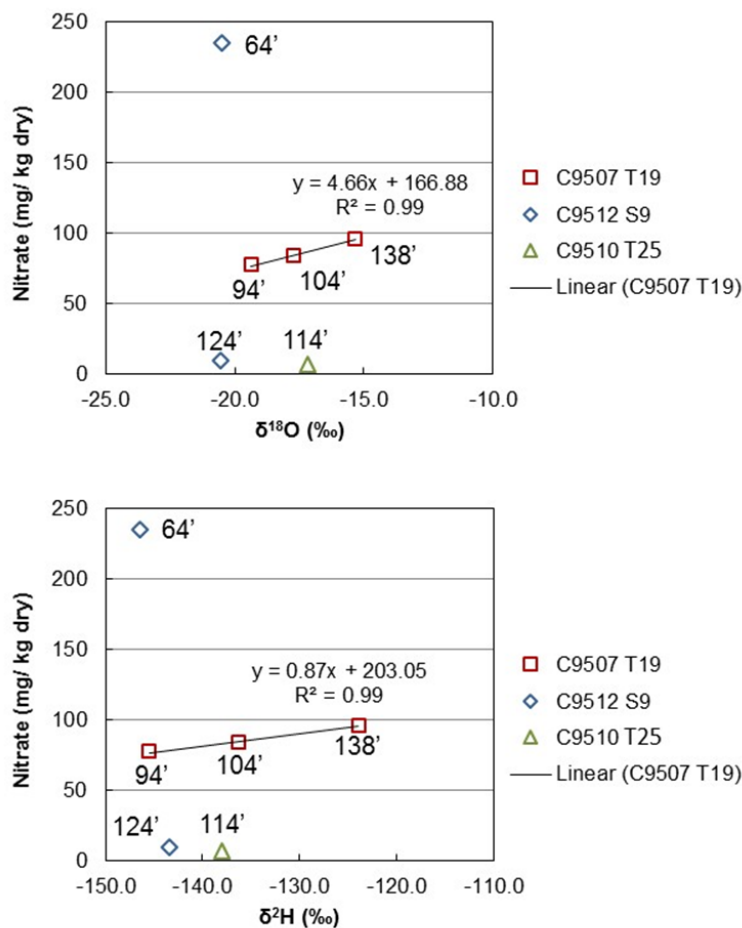


Figure 8. Correlation of isotopic ($\delta^2\text{H}$ and $\delta^{18}\text{O}$) analysis and measured nitrate concentration from T- and S-Complex samples.

4.1.5 Sediment Physical Characterization

Physical characterization was conducted to define the hydrogeologic context for the observed contaminant and biogeochemical data. Fundamental information includes a geologist log and associated core pictures, and sediment physical properties (particle size distribution, particle and bulk density, moisture content, and porosity). Air permeability was measured to provide an indication of relative differences in permeability between samples. Detailed hydraulic characterization, including saturated and unsaturated hydraulic properties, was also conducted, but will be described in a separate report. The physical data reported here are descriptive for each individual sample. However, full interpretation is best conducted by considering the data for these samples in the context of data from other samples in the vadose zone. That broader interpretation will be conducted by CHPRC as part of their overall CSM efforts for the 200-DV-1 OU.

Core pictures are shown in Figure 9 through Figure 13. The geologist logs for these samples are included in Appendix A. Table 21 is a summary of the physical sediment characterization for these samples. Plots of the particle size distributions are shown in Figure 14 through Figure 18. Note that the

physical properties for two additional samples (B35435 and B35463, Table 1) will be determined and reported as part of the hydraulic property analysis report



Figure 9. Photograph of sample B35442 (Core C9507, liner 16B, CCUc sediment sample).

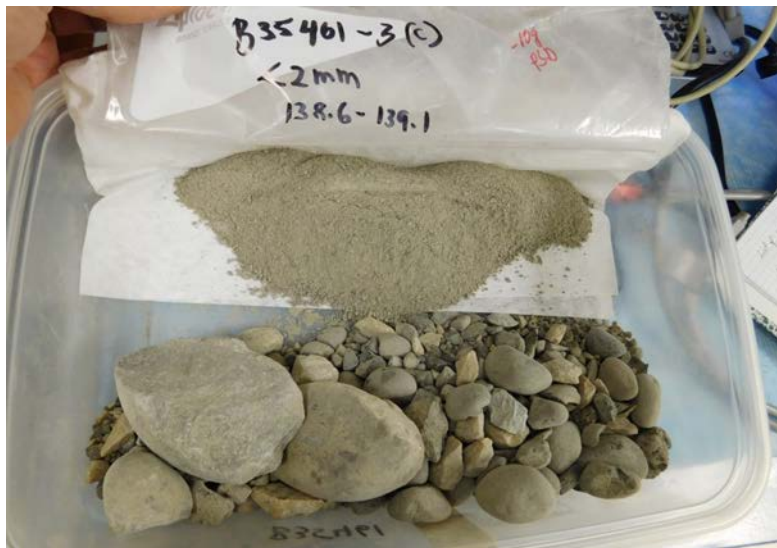


Figure 10. Photograph of sample B35461 (Core C9507, Ringold sediment sample).



Figure 11. Photograph of sample B361M9 (Core C9510, liner 14B, H2/CCUz sample).



Figure 12. Photograph of sample B36175 (Core C9512, liner 8B, H1/H2 sample).



Figure 13. Photograph of sample B361F1 (Core C9512, liner 20B, H2/CCUz sample).

Table 21. Summary of measured physical properties.

Column Parameters	Units	T19 16B	T19 138'	T25 14B	S-9 8B	S-9 20B
		(CCUc)	(Ringold)	(H2/CCU)	(H1/2)	(H2)
		C9507- B35442	C9507- B35461	C9510- B361M9	C9512- B36175	C9512- B361F1
Diameter	cm	8.89	8.89	8.89	8.89	8.89
Length	cm	30.897	15.75	30.4754	30.685	29.257
Core volume	mL	1917.833	977.631	1891.663	1904.674	1816.035
Gravimetric moisture content	g/g	0.154	0.027	0.064	0.025	0.030
Volumetric moisture content	m ³ /m ³	0.270	0.059	0.132	0.044	0.050
Bulk density	g/cm ³	1.754	2.215	2.066	1.747	1.639
Particle density	g/cm ³	2.739	2.754	2.739	2.624	2.652
Porosity	m ³ /m ³	0.360	0.196	0.246	0.334	0.382
Air permeability	darcy	0.053	----	0.059	3.935	0.779
Gravel	%	36.317	77.589	11.545	1.308	0.530
Sand	%	40.309	15.729	59.354	90.109	81.081
Silt	%	16.612	5.601	21.647	8.569	18.328
Clay/mud	%	6.763	1.082	7.456	0.015	0.062

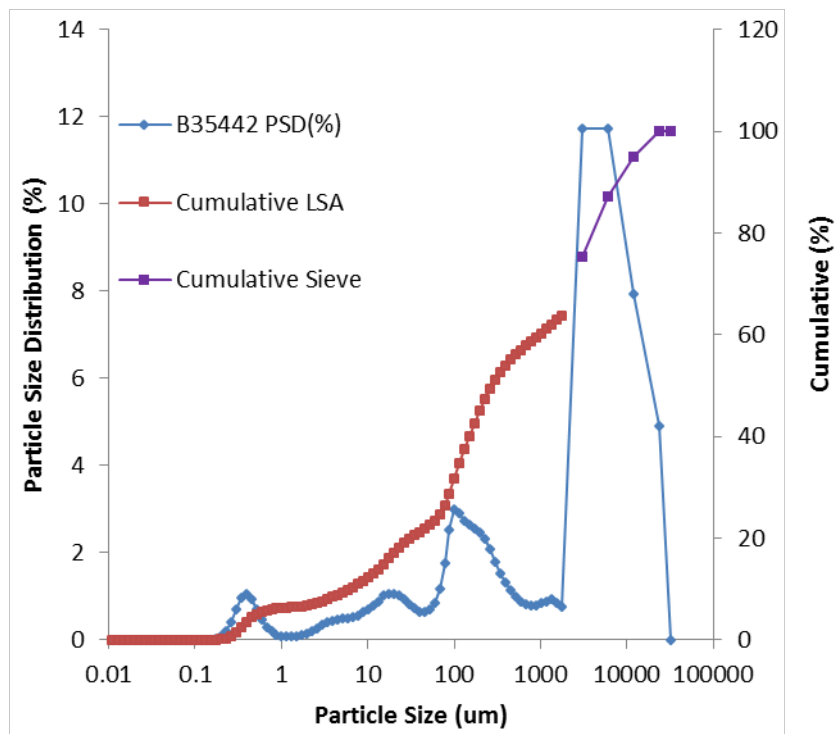


Figure 14. Particle size distribution of sample B35442 (Core C9507, liner 16B, CCUC sediment sample).

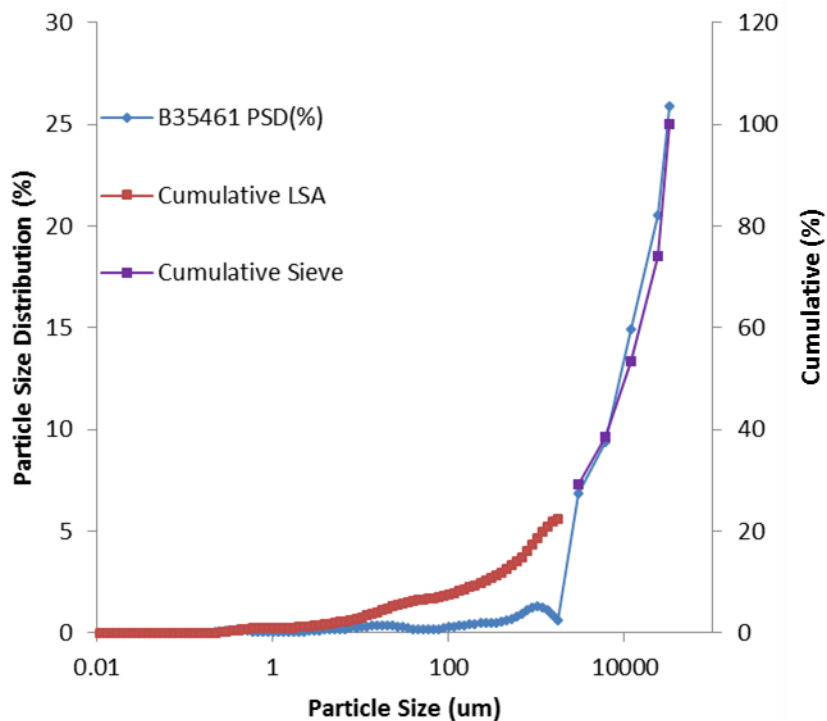


Figure 15. Particle size distribution of sample B35461 (Core C9507, Ringold sediment sample).

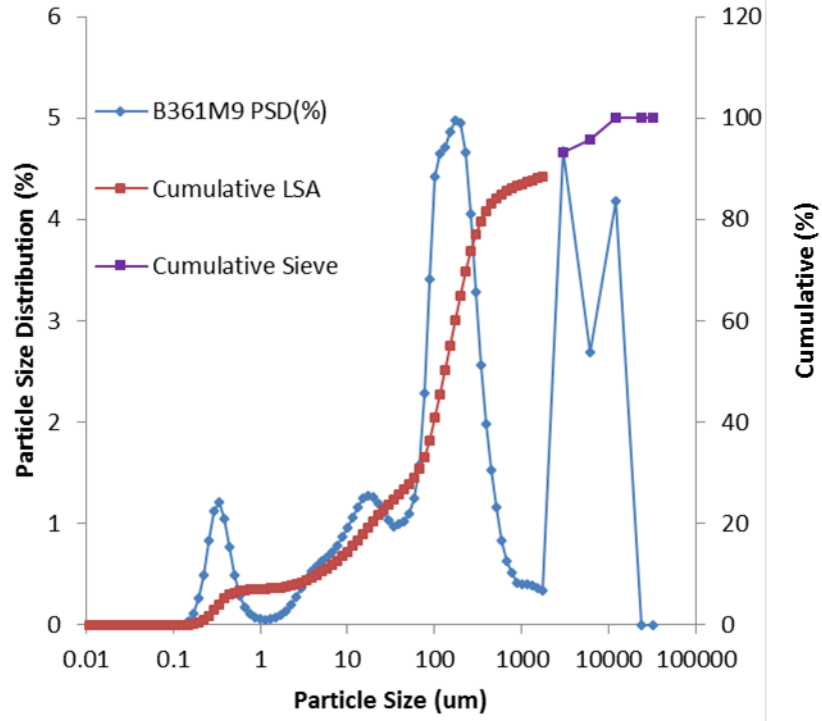


Figure 16. Particle size distribution of sample B361M9 (Core C9510, liner 14B, H2/CCUz sample).

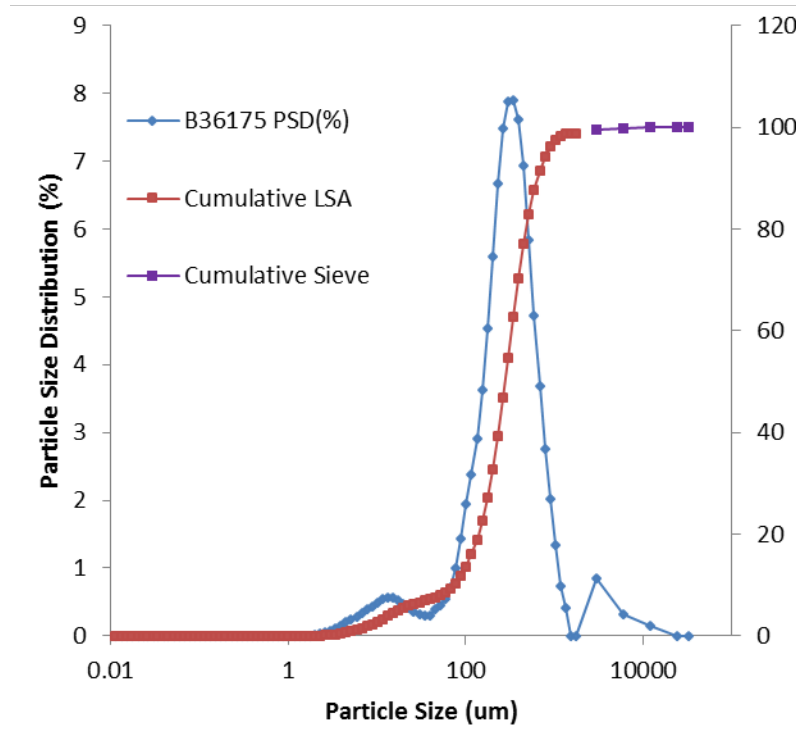


Figure 17. Particle size distribution of sample B36175 (Core C9512, liner 8B, H1/H2 sample).

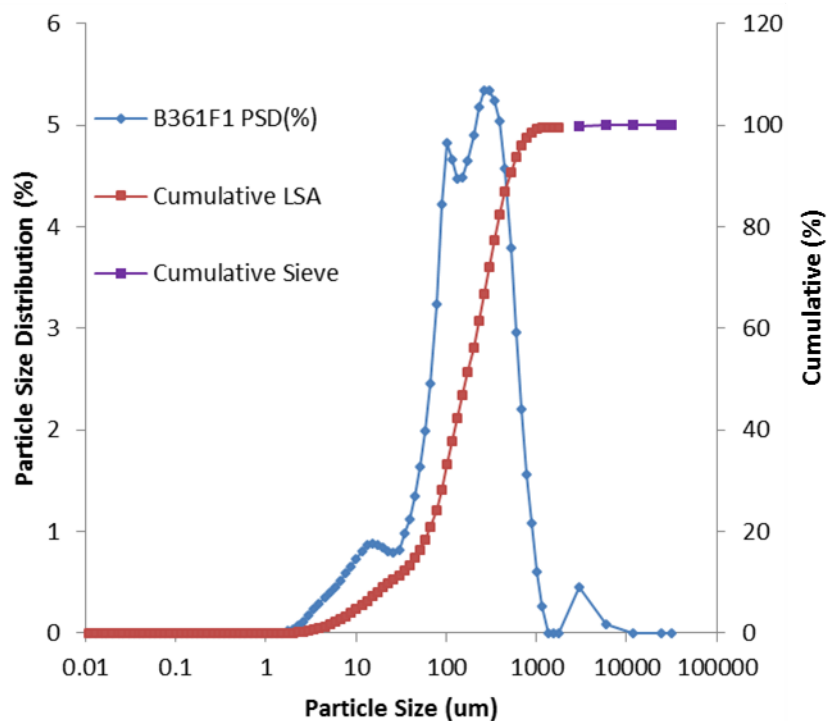


Figure 18. Particle size distribution of sample B361F1 (Core C9512, liner 20B, H2/CCUz sample).

The physical data characterize the basic hydrogeologic setting for each sample. The set of samples analyzed for this report represents a diverse set of hydrogeologic settings relevant to contaminant attenuation and transport in the Hanford Central Plateau vadose zone and important lithologic features for each targeted borehole (waste site). Additional information on hydraulic properties and physical properties for two additional samples will be reported separately.

4.2 Observation of Attenuation Processes

Identifying attenuation processes involves collecting data that can be used to demonstrate whether contaminants have interacted with sediments in a way that changes their mobility. One type of data is from sequential extractions (Table 22). In this process, a sediment sample is sequentially exposed to harsher extraction solutions and the contaminant concentration in each solution is measured. These data show how the contaminant mass in a sediment sample is distributed among water and different sediment-associated phases. Analysis for geochemical constituents was also conducted for each extraction solution to help interpret the types of sediment constituents mobilized or dissolved by each solution for the specific sediment sample. Speciation of iodine as iodide and iodate was also measured. However, interference from the matrix hindered iodine speciation analyses other than from the first extraction solution.

Table 22. Sequential extraction of contaminants from sediment samples.

Extraction Solution	Hypothesized Targeted Sediment Components	Interpreted Contaminant Mobility of Extracted Fraction	Color Code
Aqueous: artificial Hanford groundwater	Contaminants in pore water and a portion of sorbed uranium	Mobile phase	
Ion exchange: 1M Mg-nitrate	Readily desorbed contaminants	Readily mobile through equilibrium partitioning	
Acetate pH5: 1 hour in pH 5 sodium acetate solution	Contaminants associated with surface exposed carbonate precipitates and other readily dissolved precipitates	Moderately mobile through rapid dissolution processes	
Acetate pH 2.3: 1 week in pH 2.3 acetic acid	Dissolution of most carbonate compounds, and sodium boltwoodite (a hydrous uranium silicate)	Slow dissolution processes for contaminant release from this fraction; mobility is low with respect to impacting groundwater	
Oxalic acid: 1 hour	Dissolution of iron and manganese oxides	Slow dissolution processes are associated with contaminant release; mobility is very low with respect to impacting groundwater	
8M HNO ₃ : 2 hours in 8M nitric acid at 95°C	Dissolves most phases that contained anthropogenic contaminants	Very slow dissolution processes are associated with contaminant release; functionally immobile; some or all of the contaminants in this phase may be naturally occurring.	

Table 23 and associated Figure 19 through Figure 21 show the sequential extraction contaminant results for each sample for uranium, total iodine, and chromium. There was no extractable Tc-99 contamination in these samples. Iodine speciation for the first extraction is shown in Table 24. Geochemical constituents released in each extraction solution are shown in Figure 22 and in Figure 23. Interpretation of geochemical constituents accounted for the types of ions added as part of some of the extraction solutions (e.g., magnesium) and the effect of acidic conditions on some of the chemical analyses (e.g., iodine).

Table 23. Tabulated sequential extraction results for uranium, iodine, and chromium.

Sample ID	Sample	µg/g						Total	fraction					
		Ext. 1	Ext. 2	Ext. 3	Ext. 4	Ext. 5	Ext. 6		Ext. 1	Ext. 2	Ext. 3	Ext. 4	Ext. 5	Ext. 6
Uranium		Ext. 1	Ext. 2	Ext. 3	Ext. 4	Ext. 5	Ext. 6	1000h ext.	Ext. 1	Ext. 2	Ext. 3	Ext. 4	Ext. 5	Ext. 6
C9507-B35434	T19 14C (CCUz)	0.029	0.036	0.165	0.168	0.153	0.222	0.072	0.037	0.047	0.213	0.217	0.198	0.287
C9507-B35443	T19 16C (CCUc)	0.155	0.095	0.550	0.523	0.019	1.719	0.427	0.051	0.031	0.180	0.171	0.006	0.562
C9507-B35461	T19 138' (Ringold)	0.002	0.003	0.017	0.032	0.040	0.171	0.266	0.007	0.011	0.066	0.121	0.150	0.644
C9510-B361N1	T25 14C (H2/CCU)	0.007	0.023	0.099	0.082	0.029	0.163	0.403	0.017	0.057	0.245	0.203	0.071	0.406
C9512-B36177	S-9 8C (H1/2)	0.002	0.003	0.016	0.028	0.022	0.205	0.275	0.007	0.010	0.057	0.101	0.081	0.745
C9512-B361F3	S-9 20C (H2)	0.004	0.005	0.031	0.035	0.044	0.118	0.237	0.019	0.019	0.133	0.147	0.186	0.496
Iodine		Ext. 1	Ext. 2	Ext. 3	Ext. 4	Ext. 5	Ext. 6	1000h ext.	Ext. 1	Ext. 2	Ext. 3	Ext. 4	Ext. 5	Ext. 6
C9507-B35434	T19 14C (CCUz)	0.002	0.002	0.108	0.082	0.024	0	0.219	0.011	0.009	0.495	0.376	0.109	0
C9507-B35443	T19 16C (CCUc)	0.039	0.016	0.260	0.377	0.198	0	0.891	0.044	0.018	0.292	0.423	0.222	0
C9507-B35461	T19 138' (Ringold)	0.010	0.004	0.016	0.038	0.030	0	0.097	0.102	0.044	0.160	0.387	0.306	0
C9510-B361N1	T25 14C (H2/CCU)	0.012	0.017	0.217	0.292	0.196	0	0.734	0.016	0.023	0.296	0.397	0.267	0
C9512-B36177	S-9 8C (H1/2)	0.003	0.001	0.008	0.009	0.004	0	0.025	0.102	0.051	0.310	0.368	0.170	0
C9512-B361F3	S-9 20C (H2)	0.002	0.002	0.010	0.008	0.006	0	0.028	0.085	0.084	0.344	0.275	0.212	0
Chromium		Ext. 1	Ext. 2	Ext. 3	Ext. 4	Ext. 5	Ext. 6	1000h ext.	Ext. 1	Ext. 2	Ext. 3	Ext. 4	Ext. 5	Ext. 6
C9507-B35434	T19 14C (CCUz)	0.039	0	0	0	0	2.976	3.014	0.013	0	0	0	0	0.987
C9507-B35443	T19 16C (CCUc)	0.021	0	0	0	0	3.303	3.324	0.006	0	0	0	0	0.994
C9507-B35461	T19 138' (Ringold)	0.039	0	0	0.707	0.748	1.969	3.464	0.011	0	0	0.204	0.216	0.569
C9510-B361N1	T25 14C (H2/CCU)	0	0	0	0	0	2.813	2.813	0	0	0	0	0	1.000
C9512-B36177	S-9 8C (H1/2)	0	0	0	0	0	3.851	3.851	0	0	0	0	0	1.000
C9512-B361F3	S-9 20C (H2)	0	0	0	0	0	4.249	4.249	0	0	0	0	0	1.000

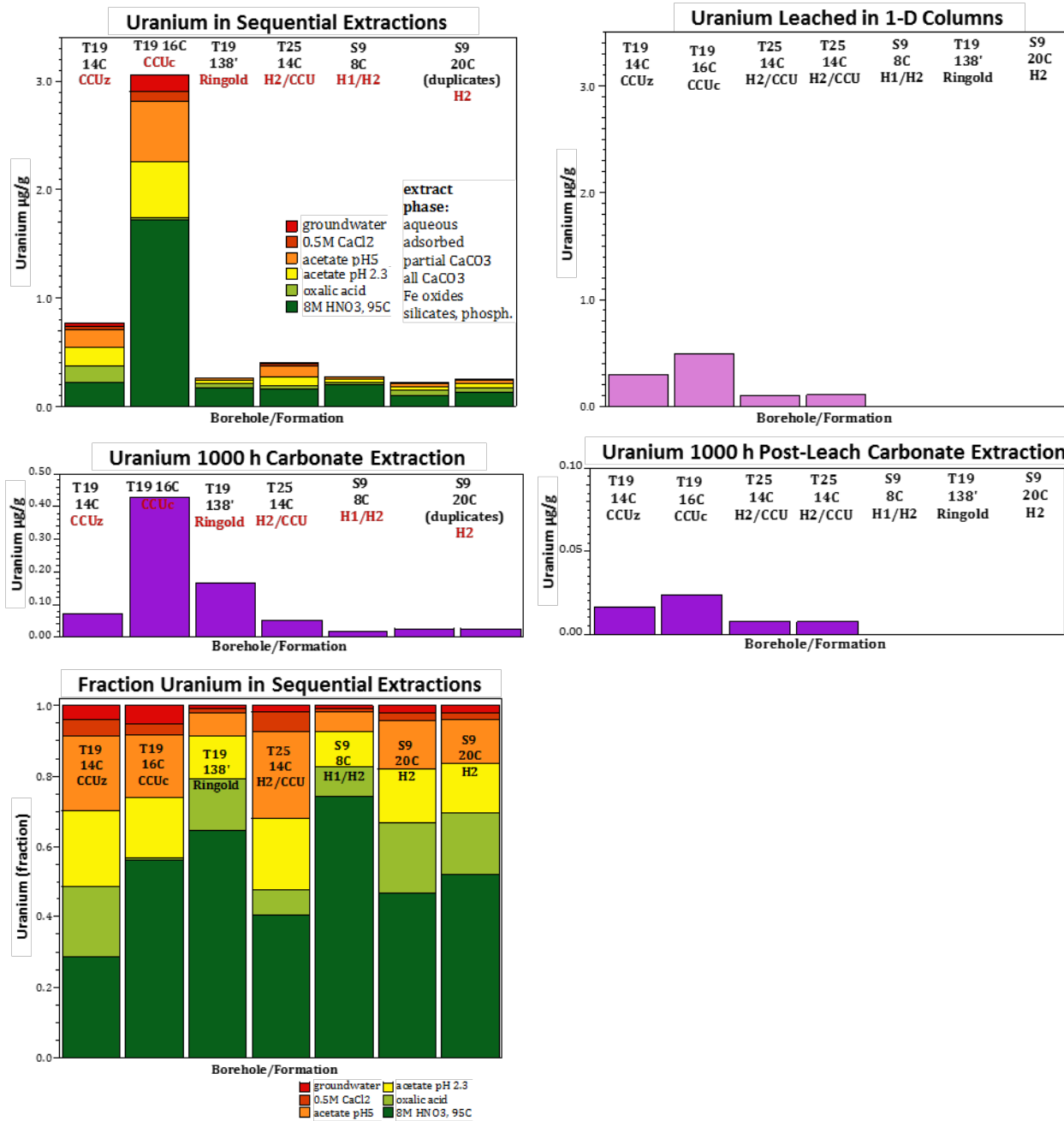


Figure 19. Uranium sequential extraction results. Note that leaching experiments were not conducted for samples T-19 Ringold (C9507-B35461), S-9 8C (C9512-B36177), or S-9 20C (C9512-B361F3).

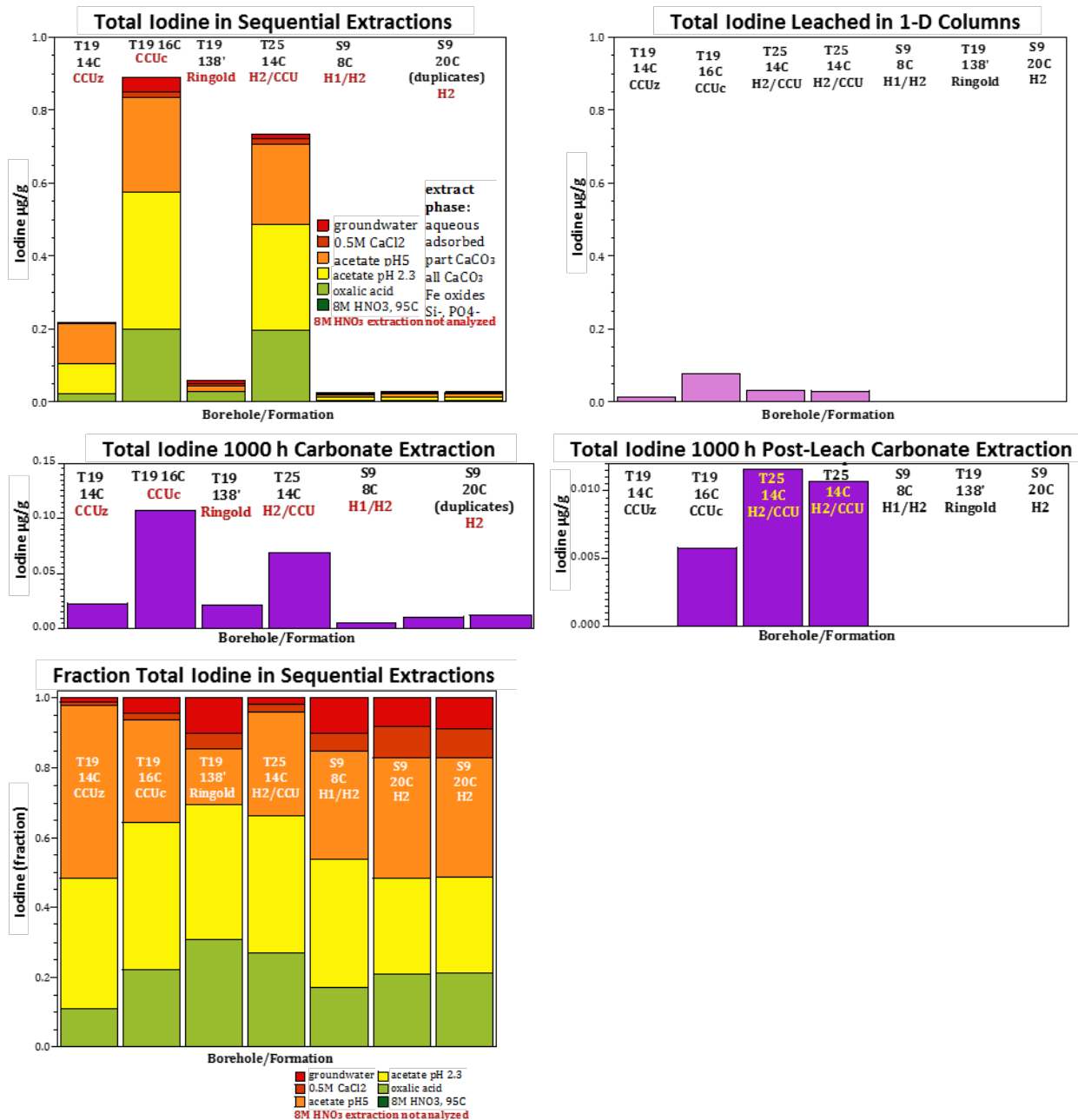


Figure 20. Iodine sequential extraction results. Note that leaching experiments were not conducted for samples T-19 Ringold (C9507-B35461), S-9 8C (C9512-B36177), or S-9 20C (C9512-B361F3).

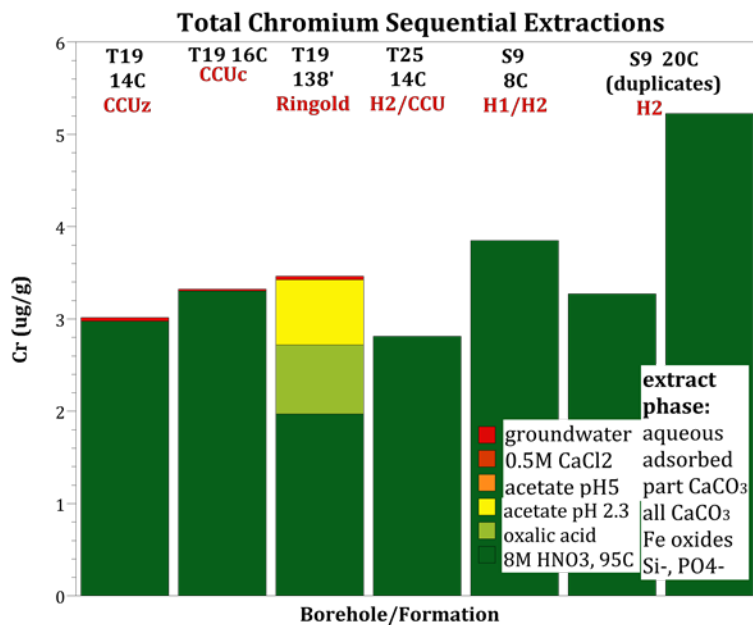


Figure 21. Chromium sequential extraction results.

Table 24. Iodine speciation.

Sample Name	Sample Location	Iodate (µg/L)	Iodide (µg/L)	Total Iodine (µg/L)
C9507-B35434	T19 14C (CCUz)	0.827	ND	1.24
C9507-B35443	T19 16C (CCUc)	3.76	13.4	18.6
C9507-B35461	T19 138' (Ringold)	0.817	4.24	5.84
C9510-B361N1	T25 14C (H2/CCU)	1.31	3.35	5.04
C9512-B36177	S-9 8C (H1/2)	ND	ND	1.19
C9512-B361F3	S-9 20C (H2)	ND	ND	1.3

ND is not detected.

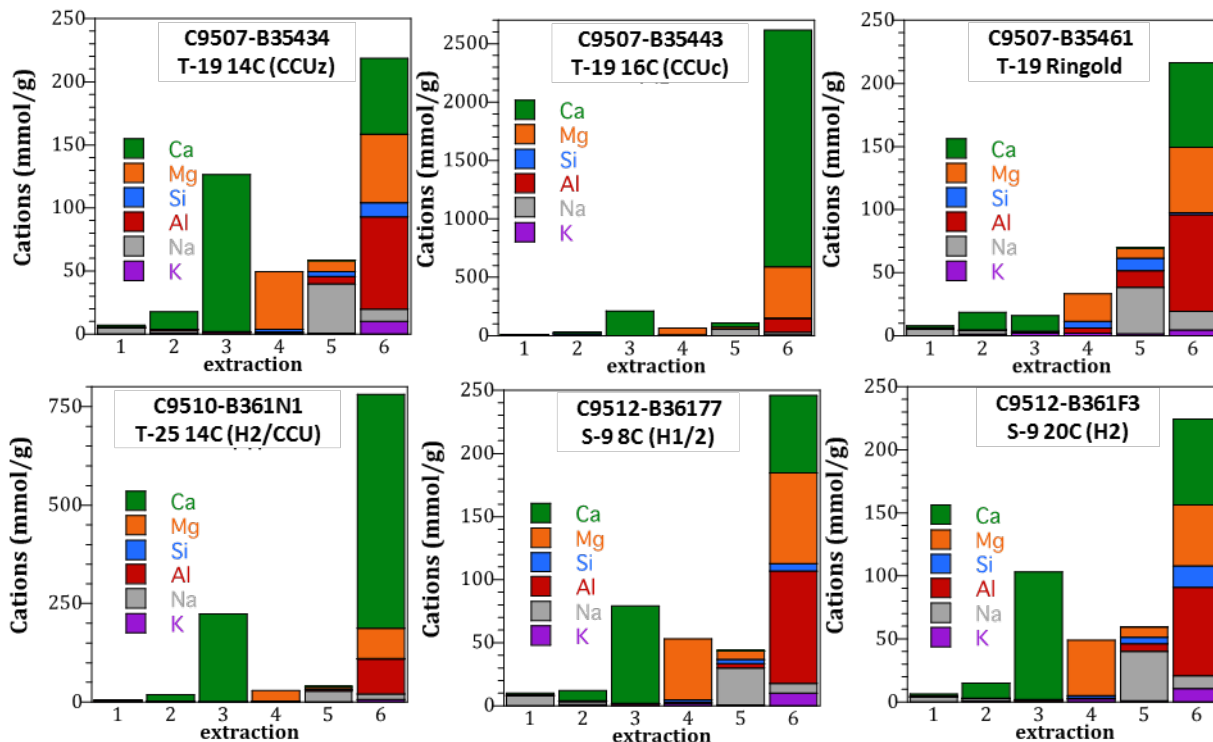


Figure 22. Cations measured in sequential extraction solutions. Note that metals are not reported if the extraction solution contained that metal (Ca for extraction 4, Mg for extractions 2 and 3, and Na in extractions 3 and 4).

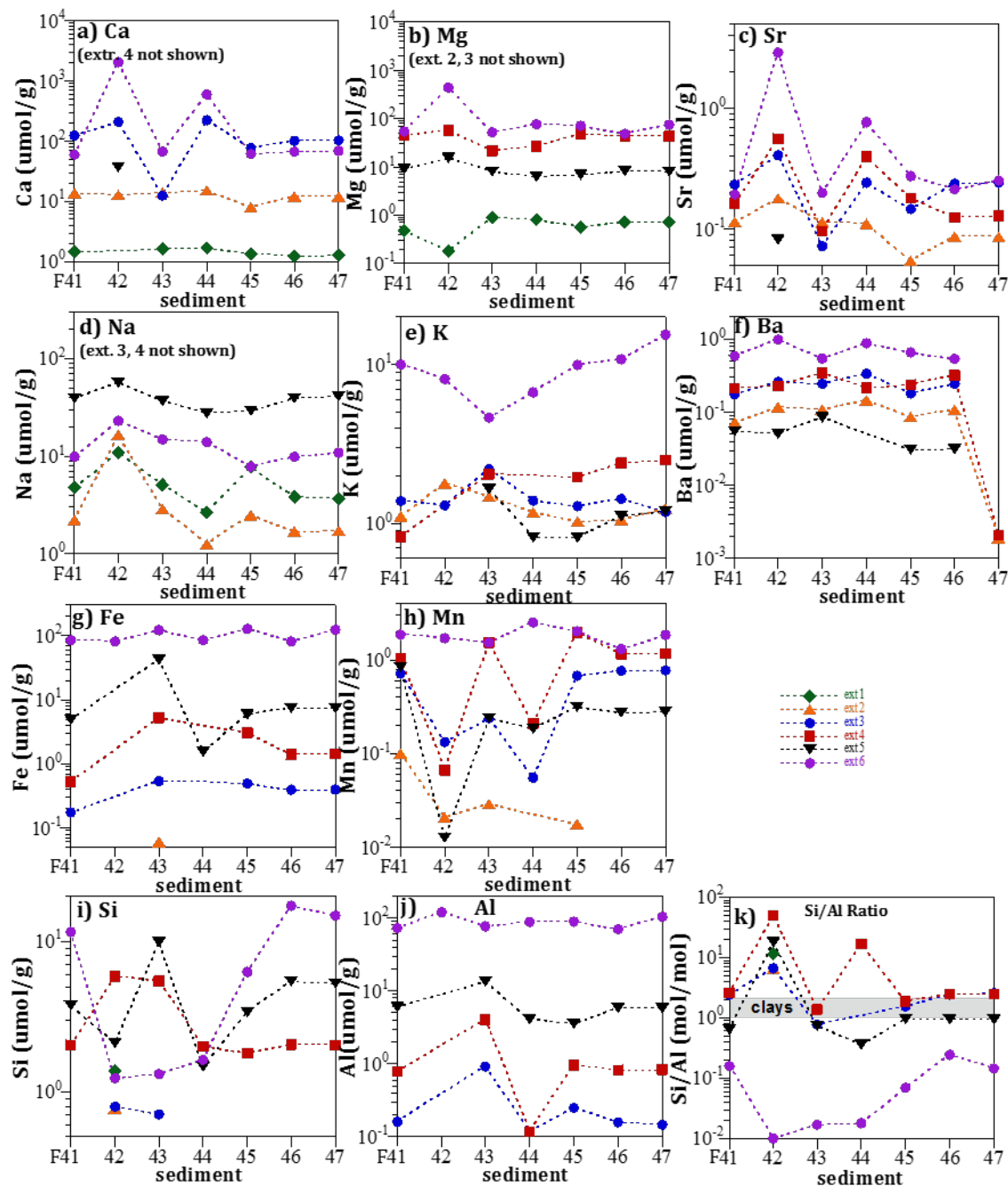


Figure 23. Major and trace cations/metals measured in sequential extractions: (a) Ca, (b) Mg, (c) Sr, (d) Na, (e) K, (f) Ba, (g) Fe, (h) Mn, (i) Si, (j) Al, and (k) Si/Al ratio. The sediment sample codes are F41 = C9507-B35434, T19 14C; F42 = C9507-B35443, T19 16C; F43 = C9507-B35461, T19 138'; F44 = C9510-B361N1, T25 14C; F45 = C9512-B36177, S9 8C; and F46 = F47 = C9512-B361F3, S9 20C.

The sequential extraction data for uranium (Table 23, Figure 19) show only a small portion of the uranium mass in the samples is present in the aqueous and sorbed (mobile) phases. In every sample, the highest fraction of uranium mass is in the sixth extraction, likely representing mostly natural uranium. For the B35443 sample of CCU high-carbonate sediment with the highest uranium concentration, the

third and fourth extractions (representing carbonate materials) show relatively high fractions of uranium. In summary, for uranium, a relatively small fraction of the uranium mass in these samples would transport under equilibrium partitioning conditions (i.e., is mobile). Thus, transport analyses should include kinetic transport processes or recognize that a portion of the uranium is functionally immobile. The 1000-hour extraction results, targeted at identifying mobile uranium, are consistent with the sequential extraction results in that the uranium mass extracted in the 1000-hour test is about the same as all of the mass in the first two sequential extractions plus a portion of the mass in the third extraction. Post-soil-column-leaching results show that the uranium mass extracted in the 1000-hour test is reduced dramatically, as expected. Soil-column effluent data analyzed as cumulative mass of uranium leached are consistent with the loss in uranium mass shown in the comparison of pre- and post-soil-column-test uranium mass in the 1000-hour extraction tests and are similar to the uranium mass present in the first two sequential extractions plus a portion of the mass in the third extraction.

The sequential extractions for total iodine (Table 23, Figure 20) also show a low fraction of the iodine in the aqueous and sorbed (mobile) phases. In every sample, the largest fraction of the iodine is in the third and fourth extractions, representing carbonate materials. Iodine is also present in the fifth extraction. Iodine determination in the sixth extractions was hindered by the acidic matrix and was not reportable. Speciation of iodine was only possible in the first extraction (Table 24). Iodide dominated the speciation in first extraction for samples B35443, B361N1, and B35461, which all had relatively high total iodine concentrations. Iodate dominated the speciation in sample B35434. Other samples were non-detect for both iodine species. A significant amount of iodine was present in the third and fourth extractions, which are targeted at determining contaminant concentrations associated with carbonate precipitates. It is most likely that carbonate-associated iodine would be in the iodate form, but speciation was not possible for these extraction solutions. As with uranium, only a small fraction of the iodine mass in these samples would transport under equilibrium partitioning conditions (i.e., is mobile). Thus, transport analyses should include kinetic transport processes or recognize that a portion of the iodine is functionally immobile. This assessment is based on total iodine (which includes both I-127 and I-129), but the behavior of I-129 is expected to be similar to total iodine. The mechanism for the relatively large portion of iodine found in the extractions not associated with equilibrium partitioning may be association of iodate with carbonate precipitates. This type of co-precipitation has been observed in the scientific literature (Zhang et al. 2013; Podder et al. 2016) and is consistent with release of iodine in the third and fourth extractions that are targeted at dissolving carbonate precipitates.

As with uranium, the iodine sequential extraction, 1000-hour extraction, and soil-column data show consistent results (Table 23, Figure 20). The 1000-hour extraction results, targeted at identifying mobile iodine, are consistent with the sequential extraction results in that the iodine mass extracted in the 1000-hour test is about the same as all of the mass in the first two sequential extractions plus a portion of the mass in the third extraction. Post-soil-column-leaching results show that the iodine mass extracted in the 1000-hour test is reduced dramatically, as expected. Soil-column effluent data analyzed as cumulative mass of iodine leached are consistent with the loss in iodine mass shown in the comparison of pre- and post-soil-column-test iodine mass in the 1000-hour extraction tests and are similar to the iodine mass that was present in the first two sequential extractions plus a portion of the mass in the third extraction.

The sequential extraction data for chromium suggest that all of the chromium is natural, as expected based on water, acid, and alkaline extraction chromium results (Section 4.1). Thus, these data are not interpreted in terms of chromium attenuation and transport processes.

Ions released from sequential extractions can be interpreted, although the interpretation must consider the ions present in the extraction solutions (Figure 22 and Figure 23). Samples B35434, B35461, B361F3, and B36177 are similar in the types and amounts of ions released in the extractions, with moderate differences in carbonate concentration (Ca and Mg released in extractions 3 and 4). Samples B35443 and B361N1 have a much higher carbonate content, as indicated by the amount of calcium released, but are otherwise similar to the other samples.

Another important category of experiment that can demonstrate contaminant mobility is a leaching test that can quantify how quickly contaminants are released into the aqueous phase. In this type of test, sediments containing contaminants are exposed to artificial pore water to quantify release of the existing contaminants into the aqueous phase. For a batch leaching test, sediments are contacted with a single aqueous solution for a long time period. Samples of the aqueous phase are analyzed for contaminant concentration. Initial, short-contact-time results are representative of equilibrium partitioning of contaminants from the sediments. Over time, if the contaminant concentration stays stable at near this initial concentration, it can be interpreted that only equilibrium partitioning is controlling contaminant release from the sediments. Concentrations rising over time indicate that some kinetically controlled process such as dissolution of precipitates or diffusion from small pores in the sediments is contributing to contaminant release from the sediments. Both partitioning and kinetically controlled contaminant release attenuate the mobility of contaminants.

Batch leaching results are shown in Figure 24 and Figure 25 for uranium and iodine, respectively. Analysis showed that Cr(VI) and Tc-99 in the artificial pore water were below detection limits in all of the sediments. The aqueous uranium concentration increased in all sediments (Figure 24), indicating slow kinetic release of uranium, likely from a combination of adsorbed U-carbonate species desorption (relatively rapid release) and exchange with uranium in solid phase carbonates (relatively slow release). Sediment uranium concentrations ranged from 0.3 to 30 $\mu\text{g/L}$ initially (at 1 hour), and increased to 0.72 to 44 $\mu\text{g/L}$ by 1000 hours.

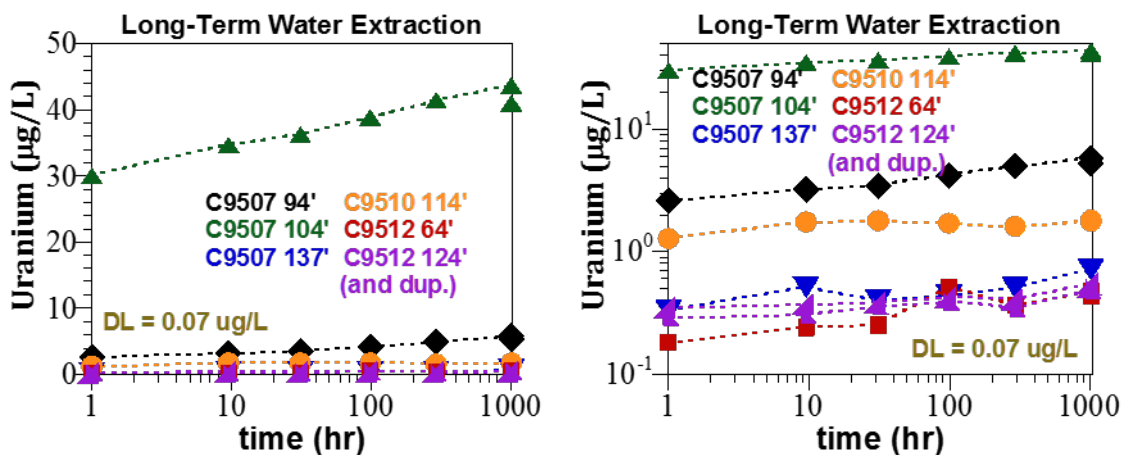


Figure 24. Aqueous uranium concentration in long-term batch leaching experiment.

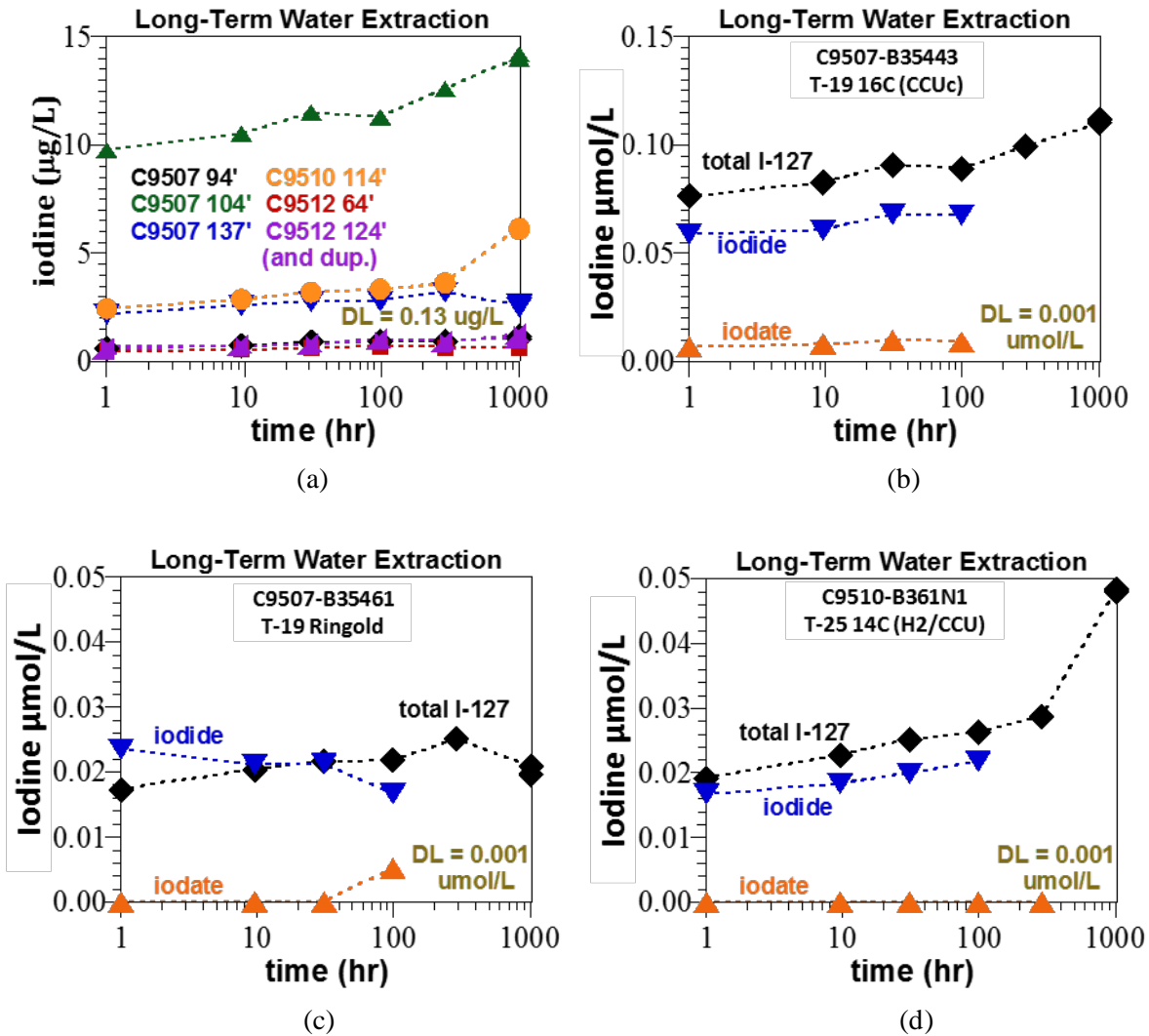


Figure 25. Aqueous total iodine concentration in long-term batch leaching experiment: (a) total iodine for all sediments, (b) iodine species for C9507-B35443, T-19 16C, (c) iodine species for C9507-B35461, T-19 138', and (d) iodine species for C9510-B361N1, T-25 14C. Iodine speciation for other sediments was below detection limits.

Release of iodine species from sediments was also kinetically controlled (Figure 25), with total iodine concentrations ranging from 0.2 to 10 $\mu\text{g/g}$ initially (at 1 hour), and increasing to 0.3 to 14 $\mu\text{g/g}$ by 1000 hours (Figure 25a). Iodine speciation was difficult to characterize in sediments at these low concentrations in a matrix of high ion concentration (i.e., mainly Na-nitrate) because the analysis relies on anion separation before iodide or iodate mass analysis. Three sediments had concentrations of iodine species (Figure 25b to d) above the detection limits, which showed that 75% to 100% of the iodine in the aqueous phase was iodide. Iodide is more mobile than iodate (about 4 times lower K_d), and iodate can be incorporated into carbonates. Thus, it is expected that iodide would be most susceptible to short-term release from sediments. Iodate, if present, may be more slowly released if it is incorporated into carbonate precipitates. Determination of iodine speciation was not possible in all of the sequential extractions. However, in samples with the highest total iodine concentration, iodide dominated the species in the first water extraction. For the sequential extractions, a significant amount of total iodine

was present in the third and fourth extractions (contaminant associated with carbonate precipitates). Dissolution rates for iodate-carbonate precipitates may be slow and may not contribute significantly to the iodine concentration in the batch leaching experiment.

Soil-column leaching tests contact sediments with a clean flowing artificial groundwater under saturated flow conditions. Contaminant concentrations in the effluent of the column are controlled by the magnitude of equilibrium partitioning and kinetically controlled contaminant release processes (e.g., dissolution of precipitates or small-pore diffusion). Soil-column tests provide data that can be interpreted in terms of modeling contaminant release and partitioning under one-dimensional transport conditions. Slower release of contaminant mass from the column (i.e., continued release over many pore volumes of water flow through the column) indicates the partitioning and/or kinetically controlled processes are attenuating the mobility of the contaminant. In addition, stop-flow events, where the water flow in the column is stopped for tens to hundreds of hours, can indicate the presence of kinetically controlled contaminant release if the contaminant concentration increases during the stop-flow event.

Soil-column leaching results are shown in Figure 26 through Figure 37. Uranium and iodine show some slow-release behavior in terms of an extended release of contaminants over time from the column. In addition, an increase in uranium and iodine concentration during stop-flow events was observed for all events, though the magnitude varied. Additional analysis of stop-flow events is provided in Section 4.3. Analysis shows that Tc-99 and Cr(VI) in effluent samples were all below detection limits, so these are not shown. Analysis of cations and anions (excluding carbonate) on selected effluent samples shows that Na and nitrate decrease rapidly to near influent artificial groundwater concentrations. Bromide breakthrough shows uniform flow in columns, with average retardation of 0.96 to 1.04. Iodine species analysis on effluent samples was difficult due to the high nitrate concentration because the analysis relies on anion separation before iodide or iodate mass analysis. Only a few samples from the first pore volume of column effluent had iodine concentrations high enough for speciation analysis. Thus, the speciation data are not of value and are not reported.

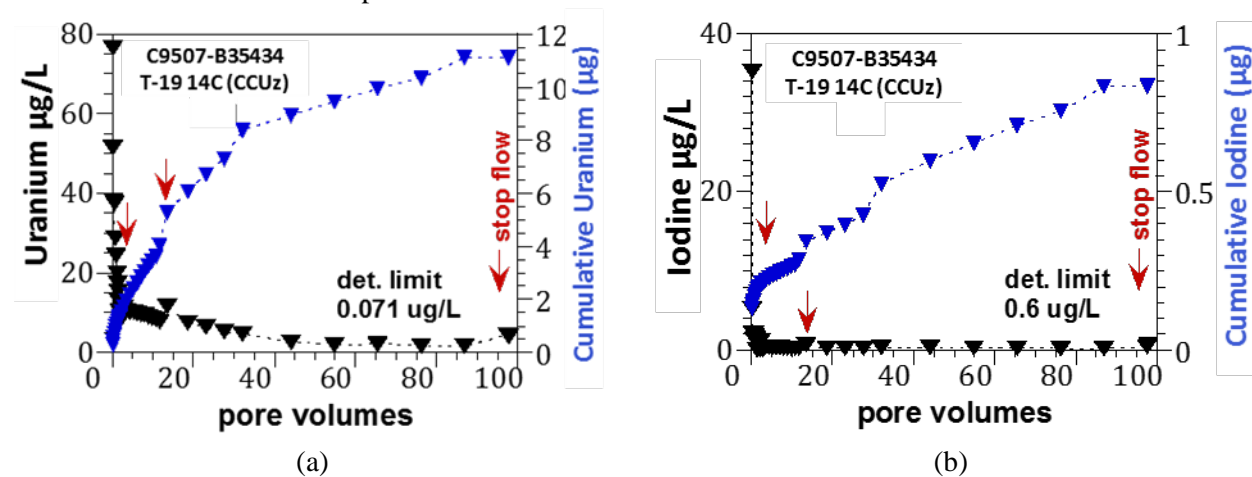


Figure 26. Artificial groundwater leaching of the C9507-B35434, T19 14C sample for (a) uranium, and (b) total iodine effluent concentrations. Most iodate and iodide concentrations were below detection limits.

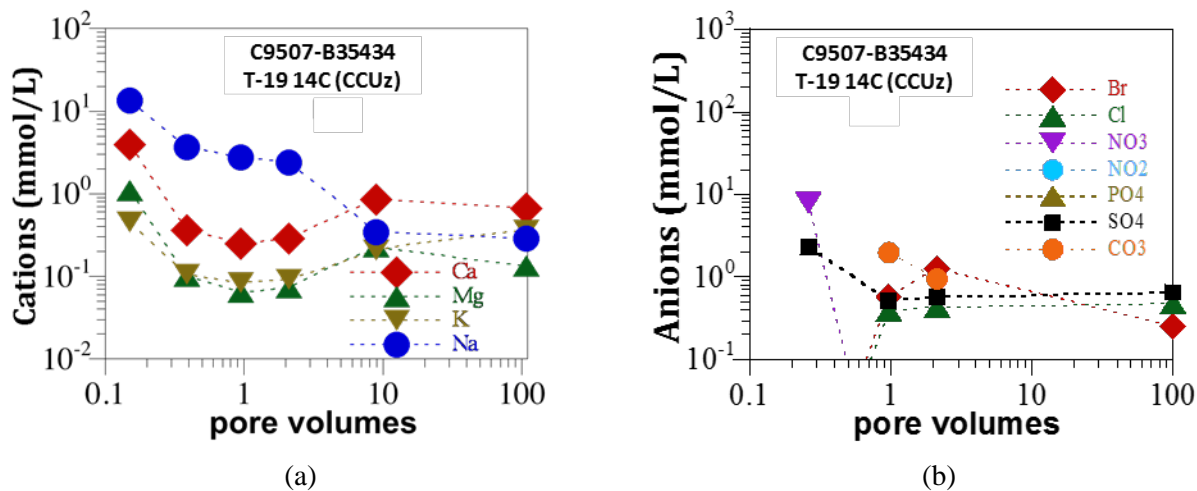


Figure 27. Artificial groundwater leaching of the C9507-B35434, T19 14C sample for (a) cation and (b) anion effluent concentrations for selected samples.

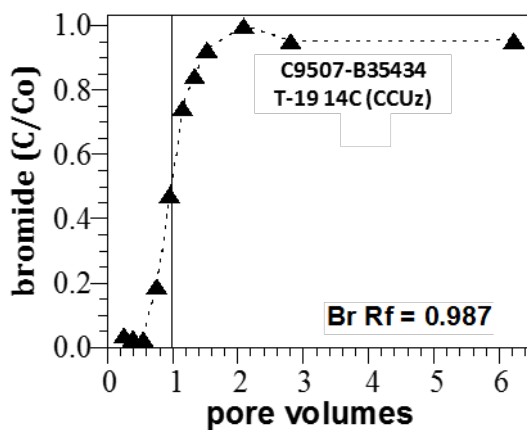


Figure 28. Artificial groundwater leaching of the C9507-B35434, T19 14C sample for tracer (bromide) effluent concentration.

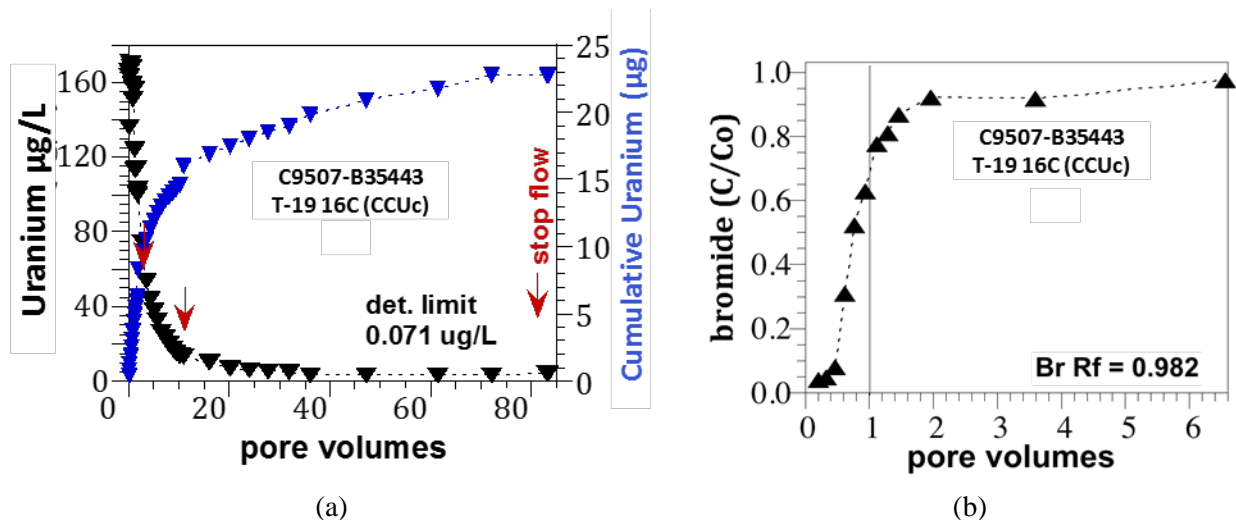


Figure 29. Artificial groundwater leaching of the C9507-B35443, T19 16C sample for (a) uranium and (b) tracer (bromide) effluent concentrations.

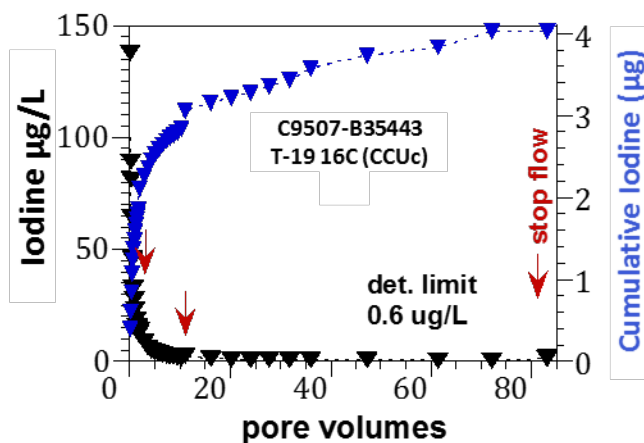


Figure 30. Artificial groundwater leaching of the C9507-B35443, T19 16C sample for total iodine data.

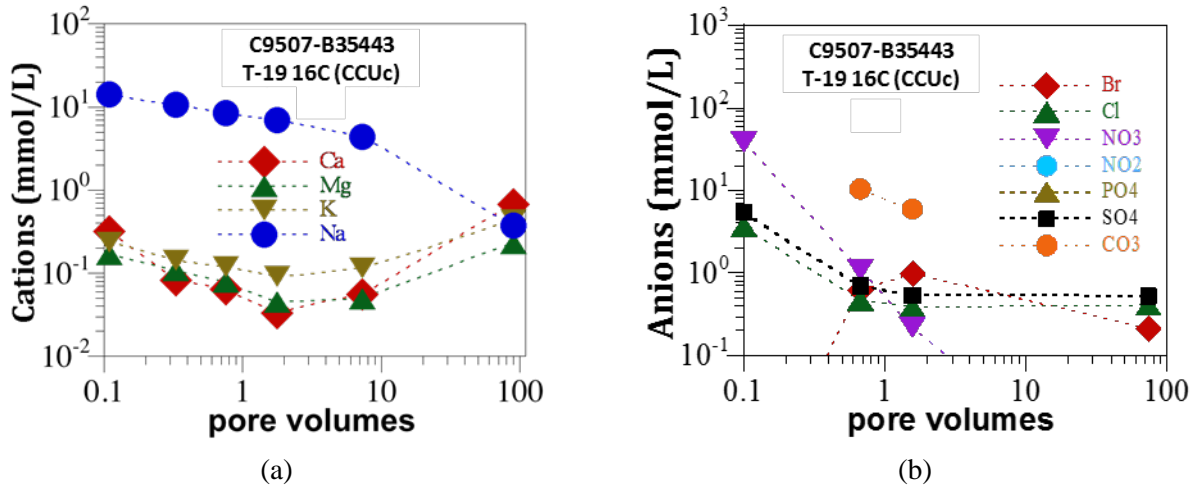


Figure 31. Artificial groundwater leaching of the C9507-B35443, T19 16C sample for (a) cation and (b) anion effluent concentrations for selected samples.

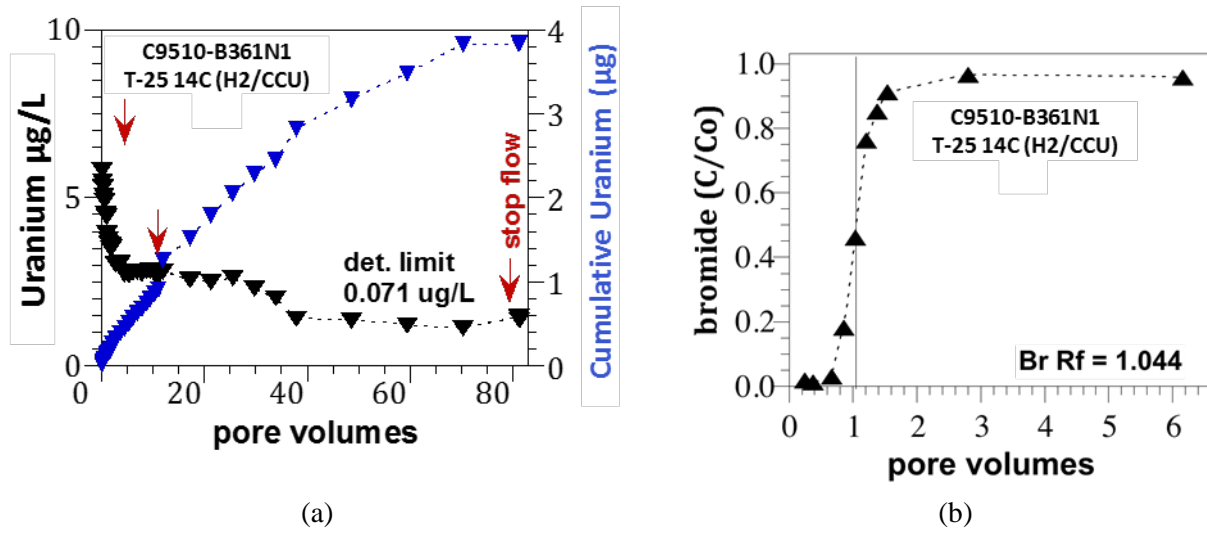


Figure 32. Artificial groundwater leaching of the C9510, T25 14C sample for (a) uranium and (b) tracer (bromide) effluent concentrations.

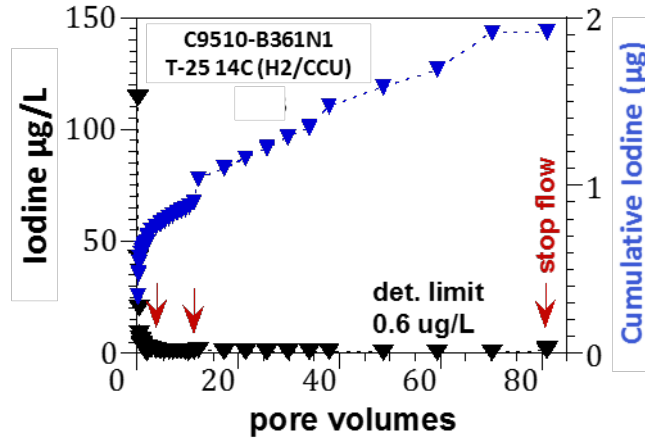


Figure 33. Artificial groundwater leaching of the C9510, T25 14C sample for total iodine data.

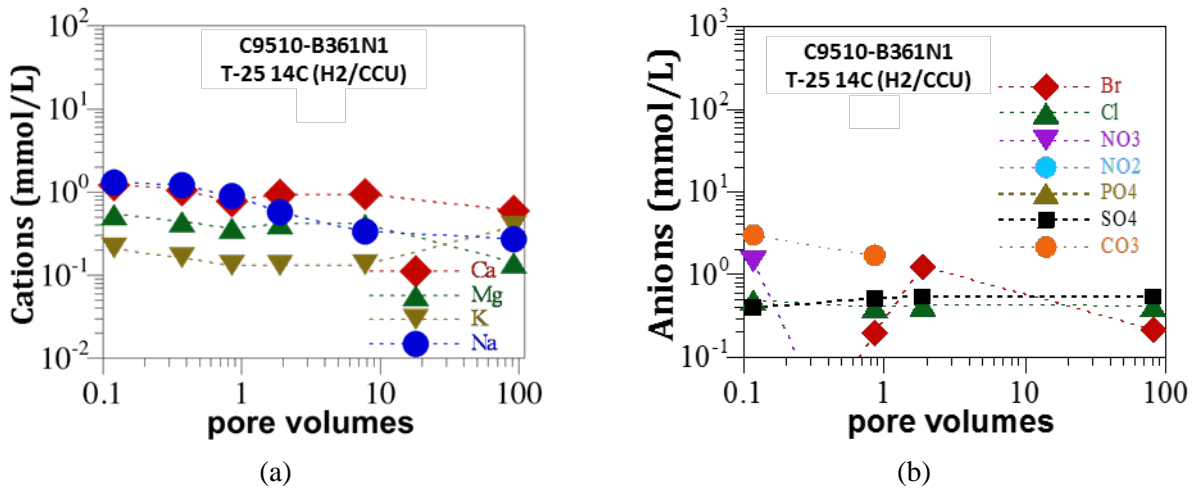


Figure 34. Artificial groundwater leaching of the C9510, T25 14C sample for (a) cation and (b) anion effluent concentrations for selected samples.

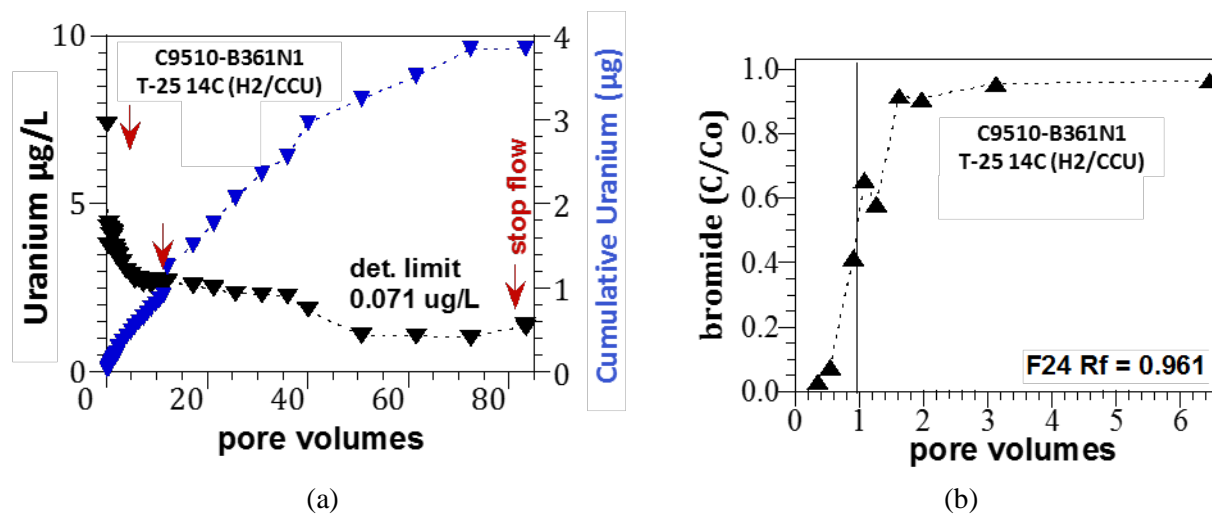


Figure 35. Artificial groundwater leaching of the C9510, T25 14C sample (duplicate sample) for (a) uranium and (b) tracer (bromide) effluent concentrations.

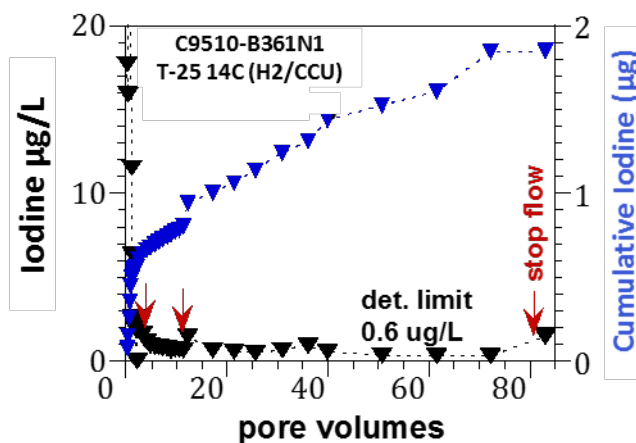


Figure 36. Artificial groundwater leaching of the C9510, T25 14C sample (duplicate sample) for total iodine data.

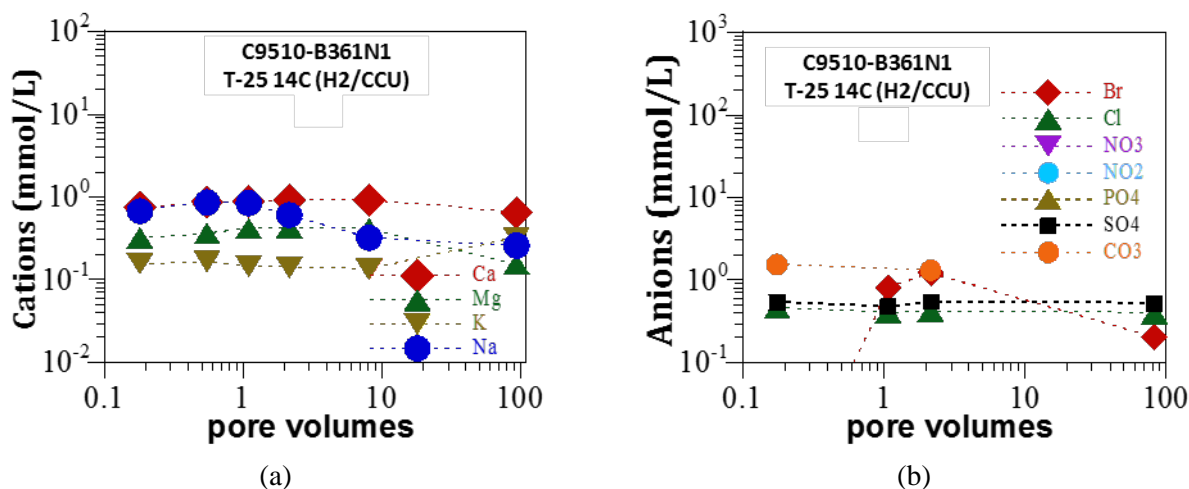


Figure 37. Artificial groundwater leaching of the C9510, T25 14C sample (duplicate sample) for (a) cation and (b) anion effluent concentrations for selected samples.

The batch and soil-column leaching tests demonstrate that there is some slow release of uranium and iodine in these samples. This type of release is consistent with attenuation mechanisms associated with sorption properties and dissolution of carbonates over time in the saturated column conditions. Nitrate was released very rapidly, confirming the low sorption properties of this contaminant. Assessment of chromium and Tc-99 was not possible with these leaching experiments due to the low/non-detect contaminant concentrations in the samples (noting that chromium in the sediments was attributed to natural chromium only extractable by acid). Interpretation of the leaching results in terms of transport parameters is provided in Section 4.3.

4.3 Quantification of Attenuation and Transport Parameters

Several types of data were collected that can be analyzed to estimate attenuation and transport parameters that are needed for fate and transport assessments. The batch leaching and soil-column leaching experiments presented in Section 4.2 can be interpreted to estimate transport parameters. The concentration trend of batch leaching data can be used to estimate a contaminant release rate. Column effluent data can be modeled to estimate transport parameters, though this type of analysis is not included in this report. Stop-flow data can be used to estimate contaminant release rates based on the observed change in concentration over the stop-flow time interval. Because some of the samples did not contain sufficient contamination for effective application of leaching experiments, spiked-contaminant tests were conducted that can be used to evaluate transport parameters. Batch experiments spiked with contaminants can be analyzed to assess both adsorption and desorption linear equilibrium partitioning coefficients (K_d) based on the observed ratio of solid- and solution-phase contaminant concentrations. Spike-contaminant soil-column tests provide breakthrough and elution curves, which, when compared to conservative tracer breakthrough and elution curves, can be used to estimate adsorption and desorption linear equilibrium partitioning coefficients (K_d).

Table 25 shows the batch leaching data interpreted as contaminant release rates from the sediment. These rates were calculated for the data collected between 100 and 1000 hours of contact time. The change in concentration from time zero, where the concentration in the aqueous phase would be zero, and the 100-hour sample was interpreted to represent sorption-related contaminant release.

Table 25. Post-sorption contaminant release rates calculated for batch leaching experiments.

Sample Name	Sample Location	Iodine (ug/kg/d)	Uranium (ug/kg/d)
C9507-B35434	T19 14C (CCUz)	0.015	0.098
C9507-B35443	T19 16C (CCUc)	0.261	0.261
C9507-B35461	T19 138' (Ringold)	-	0.024
C9510-B361N1	T25 14C (H2/CCU)	0.247	0.010
C9512-B36177	S-9 8C (H1/2)	-	-
C9512-B361F3	S-9 20C (H2)	0.022	0.010

Table 26 shows tabulated data for stop-flow events and the associated calculated contaminant release rates. The computed release rates for uranium and iodine are generally higher for samples with higher total contaminant mass leached. Over time as more pore volumes are passed through the soil-column, release rates of iodine generally declined. Note that release rates are for total iodine; the iodine speciation method was not sensitive enough to provide data during stop-flow events. For uranium, the response was mixed, with a general decline shown in the highest uranium (and carbonate) sample, B35443, but steady to increasing release rates for the other samples.

Table 26. Contaminant release rates calculated for stop-flow events during soil-column leaching experiments.

Sample Name	Sample Location	Stop Flow (pv)	Uranium Rel. Rate (ug/kg/day)	Iodine Rel. Rate (ug/kg/day)	Stop Flow (pv)	Uranium Rel. Rate (ug/kg/day)	Iodine Rel. Rate (ug/kg/day)	Stop Flow (pv)	Uranium Rel. Rate (ug/kg/day)	Iodine Rel. Rate (ug/kg/day)
C9507-B35434	T19 14C (CCUz)	2.09	1.385	0.568	11.65	1.808	0.183	86.90	1.299	0.115
C9507-B35443	T19 16C (CCUc)	1.78	1.951	1.106	10.20	0.195	0.585	83.10	0.501	0.442
C9510-B361N1	T25 14C (H2/CCU)	1.89	0.044	1.056	11.15	0.058	0.412	81.06	0.160	0.402
C9510-B361N1	T25 14C (H2/CCU)	2.15	0.023	1.017	11.65	0.042	0.366	86.90	0.178	0.553

Table 27 and Table 28 show the adsorption and desorption linear equilibrium partitioning coefficients (K_d) from spiked-contaminant batch experiments for pore water and artificial groundwater tests, respectively. Table 29 and Table 30 show the adsorption and desorption linear equilibrium partitioning coefficients (K_d) from spiked-contaminant batch experiments conducted at multiple spike concentrations for samples B35434 and B35461 for pore water and artificial groundwater tests, respectively. These results are the average of two replicate experiments. In most cases, replicate results were comparable and the average data are used to interpret the batch partitioning experiment results. Results for individual tests are shown in Appendix B.

Table 27. Calculated partitioning coefficients for spiked-contaminant experiments using the pore-water recipe (Table 8).

	Uranium			Tc-99 (pertechnetate)			Iodate			Iodide			Chromate		
	adsorption (mL/g)	desorption (mL/g)	(mL/g)	adsorption (mL/g)	desorption (mL/g)	(mL/g)	adsorption (mL/g)	desorption (mL/g)	(mL/g)	adsorption (mL/g)	desorption (mL/g)	(mL/g)	adsorption (mL/g)	desorption (mL/g)	(mL/g)
C9507-B35434 T19 14C (CCUz)	1-day	1.82	0.79	0.21	1.14	0.86	2.36	0.03	0	0.14	2.40				
	7-day	1.57	1.14	0.21	0.72	2.69	2.89	0	0	0.20	2.06				
	28-day	1.40	0.97	0.22	0.48	1.13	3.76	0	0	0.56	3.30				
C9507-B35443 T19 16C (CCUc)	1-day	9.10	6.99	0.22	13.98	3.91	5.62	0	0	0.25	2.41				
	7-day	10.49	10.24	0.31	6.12	4.03	6.36	0	0	0.28	1.71				
	28-day	8.06	10.30	0.76	9.41	3.22	NR	0	0	0.41	1.49				
C9507-B35461 T19 138' (Ringold)	1-day	1.64	0.87	0.11	0.91	0.81	1.33	0	0	0.52	NR				
	7-day	1.16	0.71	0.07	0.34	1.25	2.53	0	0	4.02	141.59				
	28-day	0.56	0.71	0.25	0.77	0.77	1.97	0	0	8.64	NR				
C9510-B361N1 T25 14C (H2/CCU)	1-day	5.21	6.26	0.20	0.65	6.59	5.92	0	0	0.18	1.81				
	7-day	5.85	5.26	0.11	0.24	6.03	7.90	0	0	0.20	1.07				
	28-day	5.42	6.63	0.17	0.27	5.13	9.06	0	0	0.65	2.52				
C9512-B36177 S-9 8C (H1/2)	1-day	0.87	0.36	0.05	0.07	1.03	2.52	0	0	0.10	11.27				
	7-day	0.75	0.44	0	0	1.33	3.16	0.04	0.16	0.24	15.66				
	28-day	0.43	0.38	0.03	0	1.06	3.83	0.00	0	0.98	11.74				
C9512-B361F3 S-9 20C (H2)	1-day	2.36	1.54	0.12	0.29	0.76	1.30	0.04	0	0.13	1.29				
	7-day	2.84	2.00	0.03	0	1.66	2.24	0.04	0.04	0.29	1.43				
	28-day	1.91	2.57	0.11	0.01	0.59	1.52	0	0	0.68	2.97				

NR is not reported because concentrations in the desorption solution were below detection.
A value of "0" was assigned to any computed K_d value of less than zero.

Table 28. Calculated partitioning coefficients for spiked-contaminant experiments using the artificial groundwater recipe (Table 9).

	Uranium			Tc-99 (pertechnetate)			Iodate			Iodide			Chromate					
	adsorption (mL/g)			desorption (mL/g)			adsorption (mL/g)			desorption (mL/g)			adsorption (mL/g)			desorption (mL/g)		
	1-day	7-day	28-day	1-day	7-day	28-day	1-day	7-day	28-day	1-day	7-day	28-day	1-day	7-day	28-day	1-day	7-day	28-day
C9507-B35434	NR	NR	NR	0.04	0.04	0.04	0.26	0.26	0.26	0.98	1.89	1.89	0	0	0	0.02	0.02	0.36
T19 14C (CCUz)	NR	NR	NR	0.04	0.04	0.04	0	0	0	1.22	1.68	1.68	0	0	0	0.05	0.05	0.33
C9507-B35443	NR	NR	NR	0.04	0.04	0.04	0	0	0	1.31	1.61	1.61	0.02	0.02	0	0.40	0.40	2.06
T19 16C (CCUc)	NR	NR	NR	0.04	0.04	0.04	1.83	1.83	1.83	2.20	4.46	4.46	0	0	0	0.09	0.09	0.88
C9507-B35461	NR	NR	NR	0.13	0.13	0.13	2.43	2.43	2.43	0.61	0.99	0.99	0	0	0	0.17	0.17	18.22
T19 138' (Ringold)	NR	NR	NR	0.27	0.27	0.27	2.35	2.35	2.35	0.80	0.95	0.95	0	0	0	0.73	0.73	18.35
C9510-B361N1	NR	NR	NR	0.14	0.14	0.14	0.40	0.40	0.40	0.70	0.96	0.96	0	0	0	4.08	4.08	36.35
T25 14C (H2/CCU)	NR	NR	NR	0.04	0.04	0.04	0.30	0.30	0.30	5.94	7.35	7.35	0	0	0	0.09	0.09	0.59
C9512-B36177	NR	NR	NR	0.07	0.07	0.07	0.07	0.07	0.07	5.10	4.03	4.03	0	0	0	0.11	0.11	0.53
S-9 8C (H1/2)	NR	NR	NR	0	0	0	0	0	0	4.89	9.09	9.09	0	0	0	0.41	0.41	1.58
C9512-B361F3	NR	NR	NR	0	0	0	0	0	0	0.68	1.31	1.31	0	0	0	0.01	0.01	0.26
S-9 20C (H2)	NR	NR	NR	0	0	0	0	0	0	0.74	1.33	1.33	0	0	0	0.15	0.15	0.79
C9512-B361F3	NR	NR	NR	0.05	0.05	0.05	0.26	0.26	0.26	0.79	1.12	1.12	0	0	0	0.06	0.06	0.26
S-9 20C (H2)	NR	NR	NR	0.07	0.07	0.07	0.28	0.28	0.28	0.94	1.14	1.14	0	0	0	0.19	0.19	0.61
C9512-B361F3	NR	NR	NR	0	0	0	0	0	0	0.87	1.22	1.22	0.001	0.001	0	0.17	0.17	0.70

NR is not reported; For uranium, the NR is because the no-sediment control showed large concentration decreases.
A value of "0" was assigned to any computed K_d value of less than zero.

Table 29. Calculated partitioning coefficients for spiked-contaminant experiments using the pore-water recipe (Table 8) for samples B35434 and B35461 with multiple spiked-contaminant concentrations.

		Uranium					
		adsorption (mL/g)	adsorption (mL/g)	adsorption (mL/g)	desorption (mL/g)	desorption (mL/g)	desorption (mL/g)
Initial Concentration		100 µg/L	500 µg/L	1000 µg/L	100 µg/L	500 µg/L	1000 µg/L
C9507-B35434	1-day	1.17	1.82	1.74	0	0.79	0.98
T19 14C (CCUz)	7-day	1.56	1.57	2.75	0.34	1.14	2.16
	28-day	1.34	1.40	2.99	0	0.97	2.58
C9507-B35461	1-day	1.57	1.64	1.58	0	0.87	0.75
T19 138' (Ringold)	7-day	1.47	1.16	2.15	0.99	0.71	1.86
	28-day	0.94	0.56	2.74	0.56	0.71	2.66
		Tc-99 (pertechnetate)					
		adsorption (mL/g)	adsorption (mL/g)	adsorption (mL/g)	desorption (mL/g)	desorption (mL/g)	desorption (mL/g)
Initial Concentration		5 µg/L	10 µg/L	50 µg/L	5 µg/L	10 µg/L	50 µg/L
C9507-B35434	1-day	0.04	0	0.21	0.80	0.43	1.14
T19 14C (CCUz)	7-day	0.55	0.45	0.21	1.16	1.61	0.72
	28-day	0.62	0.41	0.22	1.07	0.88	0.48
C9507-B35461	1-day	0.06	0	0.11	1.82	0	0.91
T19 138' (Ringold)	7-day	0.71	0.45	0.07	8.01	3.10	0.34
	28-day	0.33	0.41	0.25	1.74	5.64	0.77
		Iodate					
		adsorption (mL/g)	adsorption (mL/g)	adsorption (mL/g)	desorption (mL/g)	desorption (mL/g)	desorption (mL/g)
Initial Concentration		100 µg/L	500 µg/L	1000 µg/L	100 µg/L	500 µg/L	1000 µg/L
C9507-B35434	1-day	0.86	0.95	0.52	2.36	2.08	0.88
T19 14C (CCUz)	7-day	2.69	0.46	0.73	2.89	1.03	1.81
	28-day	1.13	0.55	0.51	3.76	0.19	0.36
C9507-B35461	1-day	0.81	0.79	0.31	1.33	2.07	0.61
T19 138' (Ringold)	7-day	1.25	0.32	0.65	2.53	0.41	1.65
	28-day	0.77	0.27	0.17	1.97	0	0
		Iodide					
		adsorption (mL/g)	adsorption (mL/g)	adsorption (mL/g)	desorption (mL/g)	desorption (mL/g)	desorption (mL/g)
Initial Concentration		100 µg/L	500 µg/L	1000 µg/L	100 µg/L	500 µg/L	1000 µg/L
C9507-B35434	1-day	0.03	0	0.08	0	0	0.17
T19 14C (CCUz)	7-day	0	0.07	0.03	0	0.09	0
	28-day	0	0.04	0.05	0	0	0.01
C9507-B35461	1-day	0	0	0	0	0	0
T19 138' (Ringold)	7-day	0	0	0	0	0	0
	28-day	0	0.02	0	0	0.01	0
		Chromate					
		adsorption (mL/g)	adsorption (mL/g)	adsorption (mL/g)	desorption (mL/g)	desorption (mL/g)	desorption (mL/g)
Initial Concentration		100 µg/L	500 µg/L	1000 µg/L	100 µg/L	500 µg/L	1000 µg/L
C9507-B35434	1-day	0.09	0.14	0.03	4.49	2.40	0.41
T19 14C (CCUz)	7-day	0.15	0.20	0.09	3.82	2.06	0.53
	28-day	0.78	0.56	0.37	2.40	3.30	2.00
C9507-B35461	1-day	0.22	0.52	0.10	NR	NR	NR
T19 138' (Ringold)	7-day	2.07	4.02	0.68	25.70	141.59	61.87
	28-day	18.96	8.64	11.47	NR	NR	NR

NR is not reported because concentrations in the desorption solution were below detection.

A value of "0" was assigned to any computed K_d value of less than zero.

Table 30. Calculated partitioning coefficients for spiked-contaminant experiments using the artificial groundwater recipe (Table 9) for samples B35434 and B35461 with multiple spiked-contaminant concentrations.

		Uranium					
		adsorption (mL/g) 100 µg/L	adsorption (mL/g) 500 µg/L	adsorption (mL/g) 1000 µg/L	desorption (mL/g) 100 µg/L	desorption (mL/g) 500 µg/L	desorption (mL/g) 1000 µg/L
Initial Concentration							
C9507-B35434	1-day	NR	NR	NR	NR	NR	NR
T19 14C (CCUz)	7-day	NR	NR	NR	NR	NR	NR
	28-day	NR	NR	NR	NR	NR	NR
C9507-B35461	1-day	NR	NR	NR	NR	NR	NR
T19 138' (Ringold)	7-day	NR	NR	NR	NR	NR	NR
	28-day	NR	NR	NR	NR	NR	NR
		Tc-99 (pertechnetate)					
		adsorption (mL/g) 5 µg/L	adsorption (mL/g) 10 µg/L	adsorption (mL/g) 50 µg/L	desorption (mL/g) 5 µg/L	desorption (mL/g) 10 µg/L	desorption (mL/g) 50 µg/L
Initial Concentration							
C9507-B35434	1-day	0	0.02	0.04	0.15	0.62	0.26
T19 14C (CCUz)	7-day	0.14	0.10	0.04	1.96	0.46	0
	28-day	0.20	0.08	0.04	0.18	0	0
C9507-B35461	1-day	0	0	0.13	0.01	1.07	2.43
T19 138' (Ringold)	7-day	0.29	0.39	0.27	4.92	6.49	2.35
	28-day	0.20	0.10	0.14	2.41	1.13	0.40
		Iodate					
		adsorption (mL/g) 100 µg/L	adsorption (mL/g) 500 µg/L	adsorption (mL/g) 1000 µg/L	desorption (mL/g) 100 µg/L	desorption (mL/g) 500 µg/L	desorption (mL/g) 1000 µg/L
Initial Concentration							
C9507-B35434	1-day	0.98	0.60	0.18	1.89	1.44	0.22
T19 14C (CCUz)	7-day	1.22	0.82	0.61	1.68	1.18	1.07
	28-day	1.31	1.08	0.62	1.61	1.66	0.98
C9507-B35461	1-day	0.61	0.28	0.12	0.99	0.83	0.05
T19 138' (Ringold)	7-day	0.80	0.38	0.28	0.95	0.67	0.66
	28-day	0.70	0.50	0.33	0.96	1.21	0.83
		Iodide					
		adsorption (mL/g) 100 µg/L	adsorption (mL/g) 500 µg/L	adsorption (mL/g) 1000 µg/L	desorption (mL/g) 100 µg/L	desorption (mL/g) 500 µg/L	desorption (mL/g) 1000 µg/L
Initial Concentration							
C9507-B35434	1-day	0	0.02	0.02	0	0	0
T19 14C (CCUz)	7-day	0	0.02	0.03	0	0.01	0
	28-day	0.02	0.06	0.06	0	0.17	0.09
C9507-B35461	1-day	0	0	0	0	0	0
T19 138' (Ringold)	7-day	0	0.01	0.01	0	0	0
	28-day	0	0.01	0.01	0	0	0
		Chromate					
		adsorption (mL/g) 100 µg/L	adsorption (mL/g) 500 µg/L	adsorption (mL/g) 1000 µg/L	desorption (mL/g) 100 µg/L	desorption (mL/g) 500 µg/L	desorption (mL/g) 1000 µg/L
Initial Concentration							
C9507-B35434	1-day	0.02	0.02	0.03	3.75	0.36	0.22
T19 14C (CCUz)	7-day	0.21	0.05	0.09	6.94	0.33	0.42
	28-day	0.17	0.40	0.21	5.39	2.06	0.97
C9507-B35461	1-day	0.13	0.17	0.05	8.73	18.22	5.39
T19 138' (Ringold)	7-day	2.61	0.73	0.37	NR	18.35	8.06
	28-day	NR	4.08	12.59	NR	36.35	97.93

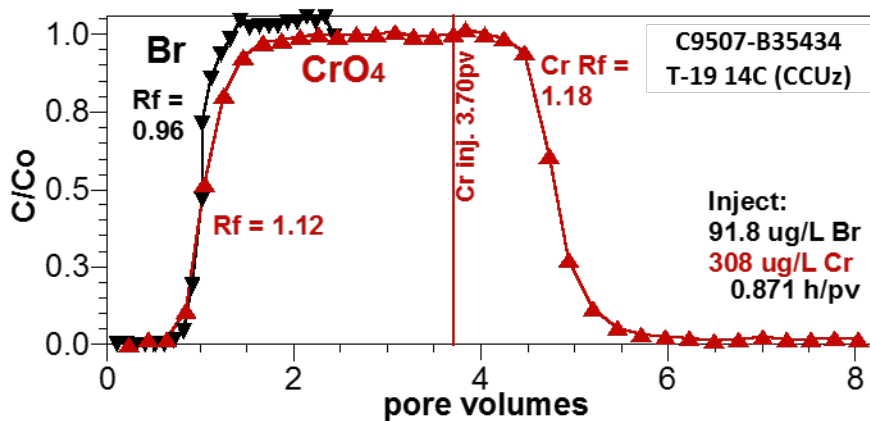
NR is not reported: For uranium, the NR is because the no-sediment control showed large concentration decreases; for chromate, because concentrations in the desorption solution were below detection.

A value of "0" was assigned to any computed K_d value of less than zero.

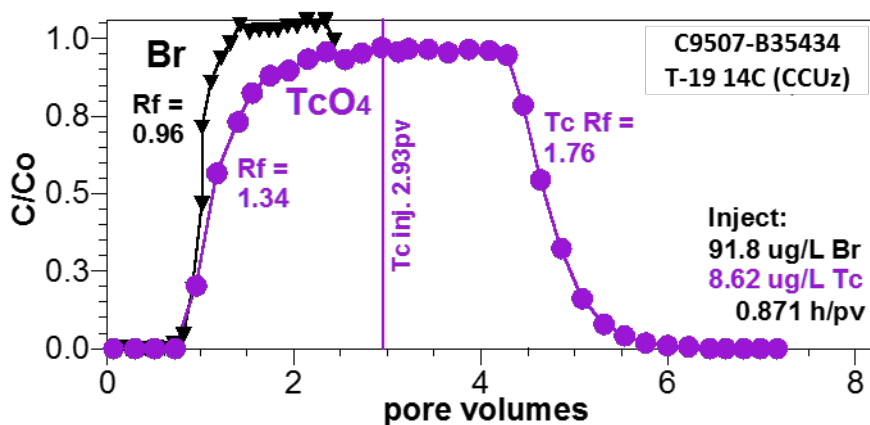
Table 31 shows the adsorption and desorption linear equilibrium partitioning coefficients (K_d) from spiked-contaminant soil-column experiments. Figure 38 through Figure 40 depict the breakthrough and elution curves for the spiked-contaminant soil-column tests. Batch and soil-column experiments provide different types of data that can be used to estimate K_d . There was good agreement between the 1-day batch and the soil-column adsorption K_d estimates in this study for Tc-99, iodine, and chromium. The 1-day batch data were selected for this comparison because of the short residence time used for the soil-column tests. Because batch desorption K_d tests were over a long duration, they are less suitable for comparison to soil-column desorption K_d estimates. Batch experiments with uranium for the simulated groundwater medium were not reportable because the uranium concentration decreased significantly in the no-sediment controls. Soil-column experiments with uranium were also problematic, and effluent concentrations did not show breakthrough or elution responses that could be analyzed for K_d .

Table 31. Calculated partitioning coefficients for spiked-contaminant column experiments.

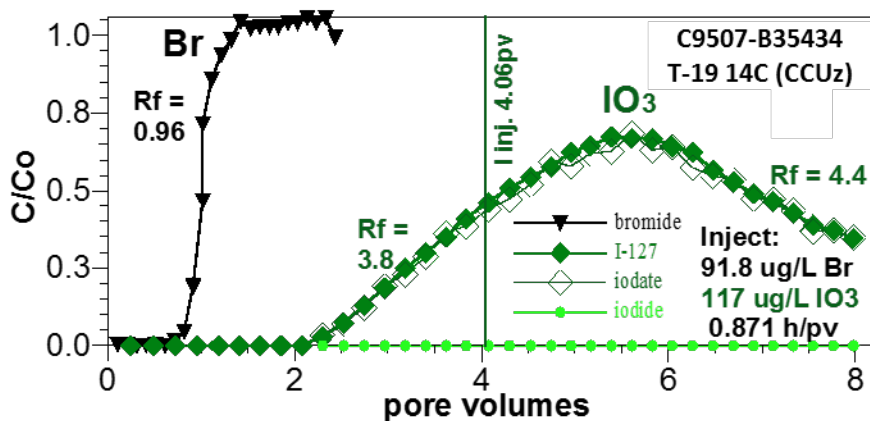
Sample Name	Sample Location	Adsorption			Desorption		
		Tc-99			Tc-99		
		Chromate K_d (mL/g)	(Per technetate) K_d (mL/g)	Iodate K_d (mL/g)	Chromate K_d (mL/g)	(Per technetate) K_d (mL/g)	Iodate K_d (mL/g)
C9507-B35434	T19 14C (CCUz)	0.030	0.086	0.708	0.045	0.192	0.859
C9507-B35461	T19 138' (Ringold)	0.017	0.000	0.677	0.023	0.006	0.529
C9512-B361F3	S-9 20C (H2)	0.025	0.037	0.707	0.028	0.037	0.877



(a)

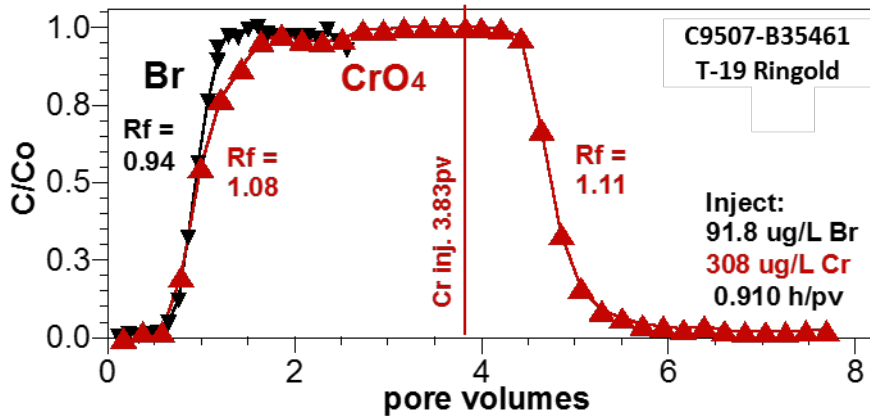


(b)

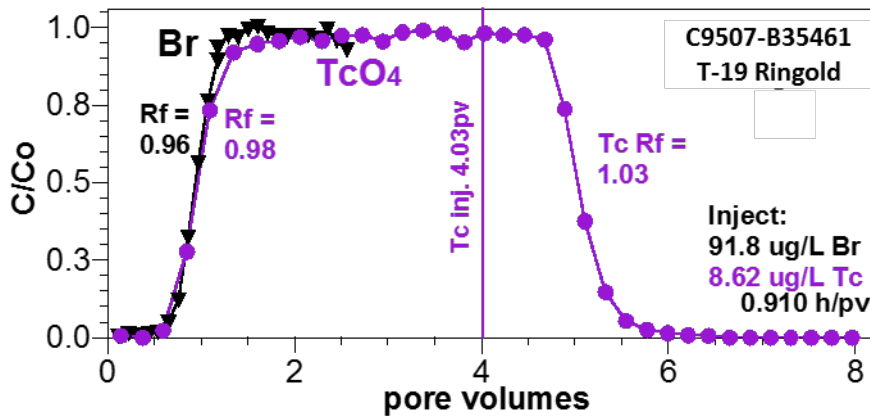


(c)

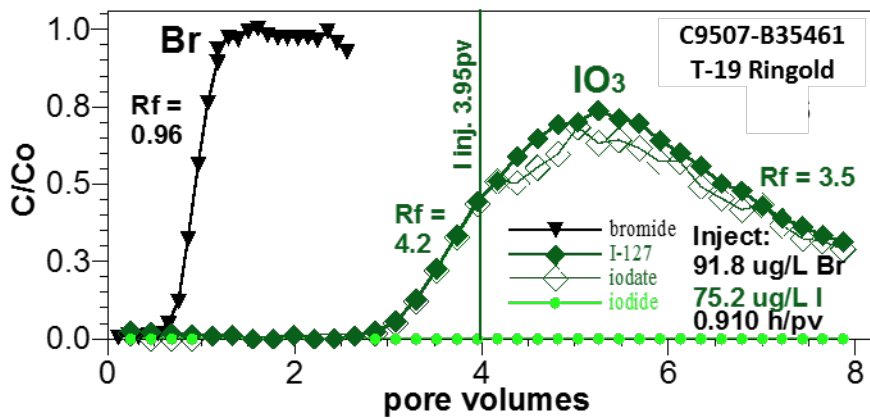
Figure 38. Breakthrough and elution responses for spiked-contaminant soil-column experiments with the C9507-B35434, T19 14C sample for (a) bromide (tracer) and chromate, (b) bromide and pertechnetate, and (c) bromide and iodate.



(a)

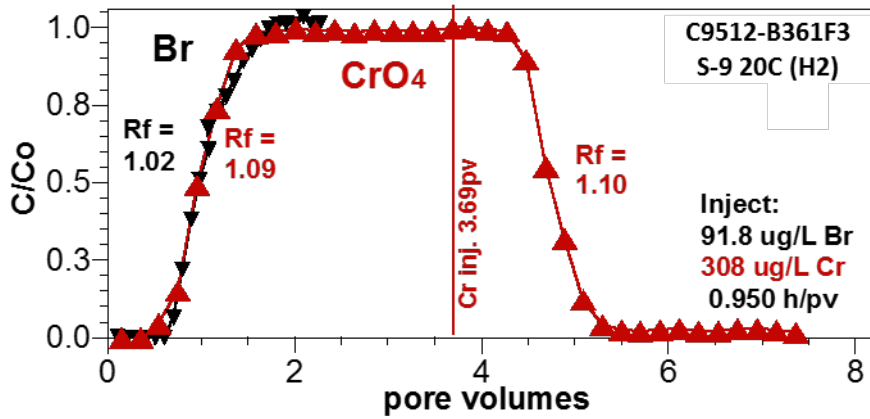


(b)

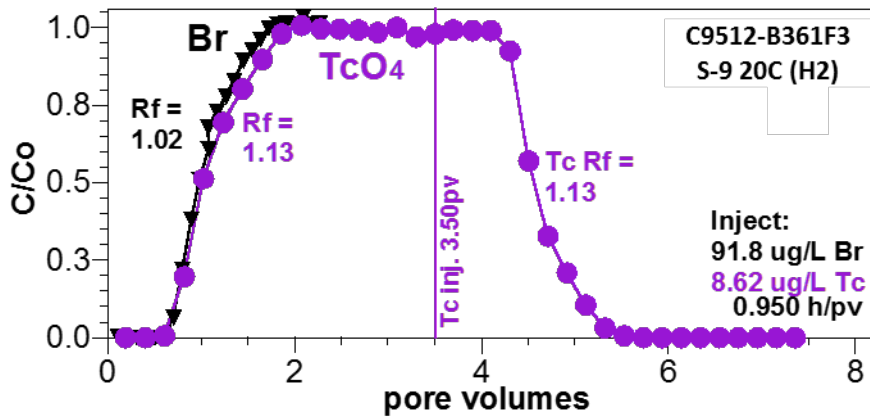


(c)

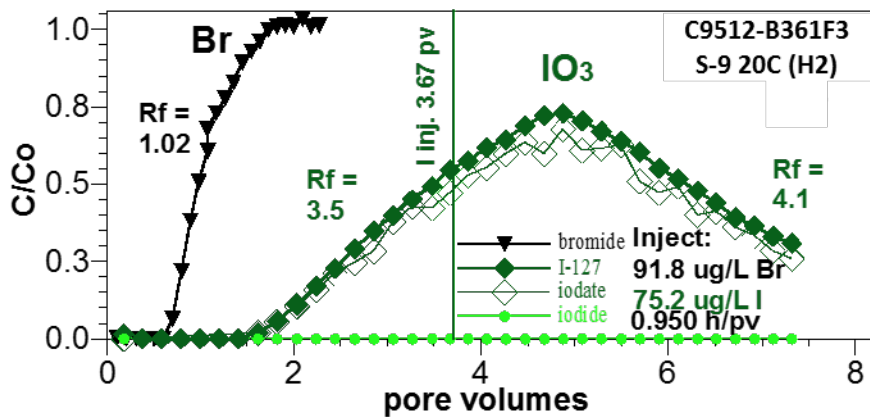
Figure 39. Breakthrough and elution responses for spiked-contaminant soil-column experiments with the C9507-B35461, T19 138' sample for (a) bromide (tracer) and chromate, (b) bromide and pertechnetate, and (c) bromide and iodate.



(a)



(b)



(c)

Figure 40. Breakthrough and elution responses for spiked-contaminant soil-column experiments with the C9510-B361F3, S-9 20C sample for (a) bromide (tracer) and chromate, (b) bromide and pertechnetate, and (c) bromide and iodate.

The batch experiments provide a larger experimental matrix than the soil-column experimental matrix for assessment of variability in K_d across the sample types and for comparison of adsorption and desorption K_d estimates. For both uranium and iodate, adsorption and desorption were highest for samples B35443 and B361N1, where both samples have a high carbonate content. The remaining samples showed moderate K_d values for uranium and iodate. Chromate, iodide, and Tc-99 (pertechnetate) K_d values were all low, except for chromate, where adsorption for days 7 and 28 and desorption (a 28-day test) K_d values were all much higher than the 1-day values. Reduction of chromate in laboratory experiments has been observed over these timeframes for other soil samples (Truex et al. 2015b). Thus, interpretation and use of later-time data for chromate K_d values should consider the possibility that chemical reduction occurred during the test. The effect of potential reduction may have also affected some of the Tc-99 and iodate results, though increases in K_d over time were less dramatic than observed with the chromate data. The desorption K_d values for Tc-99 (pertechnetate), iodate, and chromate are all generally higher than adsorption K_d values. The comparison of adsorption and desorption K_d values for uranium shows a mixed result of higher, lower, and similar values.

Tests for selected samples at multiple spiked-contaminant concentrations provide data to assess the concentration range suitable for use of a K_d -type sorption parameter. Results showing comparable K_d values for each concentration condition indicate use of a K_d -type sorption parameter is reasonable. In some cases, the K_d value decreases as the spiked-contaminant concentration increases, notably for iodate. This result may indicate that sorption sites are limited and a sorption isotherm may be needed to model sorption for higher concentrations. In some treatments, the K_d value increased with increased spiked-contaminant concentration, notably for some uranium treatments. This result may indicate some precipitation is occurring in the treatment.

Soil-column tests show well-behaved breakthrough curves for bromide, chromate, Tc-99 (pertechnetate), and iodate, but not for uranium, as discussed above. Speciation data for iodine shows that injected iodate was not reduced to iodide during the experimental timeframe. The observation that breakthrough of concentrations of chromate and Tc-99 (pertechnetate) are nearly the same as the injected concentrations also suggests no (or very limited) contaminant reduction occurred during the experimental timeframe. For these short-duration soil-column tests, there is minimal difference between measured adsorption and desorption K_d values, in contrast to the batch results. However, batch adsorption (7- and 28-day) and desorption (28-day) tests included much longer contact time of the contaminant and the sediment.

5.0 Recommendations

The laboratory study provided useful data to identify and quantify attenuation and transport processes for the targeted contaminants and the biogeochemical and physical context for these processes. For future laboratory studies of attenuation and transport processes with similar samples, several adjustments can be considered to enhance the laboratory study.

- A number of samples contained low levels of the targeted contaminants. Thus, it is important to quickly analyze sediment intervals for contaminant concentrations and use these data to define the appropriate next analyses. This approach will enable consideration of contaminant concentrations relative to subsequent testing approaches and analysis sensitivity. For the study reported herein, this approach was appropriately applied to limit the number of soil-column leaching experiments and emphasize spiked-contaminant partitioning experiments. Future efforts should implement a first step to evaluate water- and acid-extractable contaminant concentrations and conduct sequential extractions for the sample. These data would be compared to results reported herein to assess leaching potential based on high total contaminant concentrations and high fractions of the contaminants distributed in the first three sequential extraction solutions. These samples would be candidates for batch and soil-column leaching tests. Samples not suitable for leaching would be considered for spiked-contaminant tests as discussed below. Grab samples (e.g., samples other than those originally targeted for attenuation testing) can also be considered to augment the number of samples available for assessing leaching characteristics as described below.
- Some types of attenuation and transport information are best determined from contaminated samples (i.e., as opposed to spiked-contaminant tests). One option for each borehole would be to collect grab samples throughout the borehole at the vertical locations where contaminant of concern analyses are being conducted (i.e., by CHPRC). For those locations with high contaminant levels, a subset of attenuation studies (e.g., repacked column tests, batch leaching tests, sequential extractions, and the basic suite of contaminant and geochemical analyses) could be conducted. These tests do not require an intact sample. While the full suite of analyses for the attenuation laboratory study could not be obtained at these locations, the additional grab-sample data set could provide important information about mobility of contaminants for field-contaminated sediments. Field-contaminated sediments are unique in that they reflect contaminant conditions caused by the history of the waste disposal, contaminant transport, and attenuation processes that have occurred. Thus, these field-contaminated sediments best represent the starting point for future contaminant transport. For this reason, it is important to evaluate additional locations within the borehole that provide this type of representative conditions for evaluating contaminant behavior.
- There were several instances where the sample conditions (e.g., nitrate concentration) limited the applicability of laboratory analyses. Notably, iodine speciation was limited for some of the sample matrices. In addition, iodine speciation was hampered by the ionic strength and acidity of some of the extraction solution properties. Thus, the results reported herein can be used to indicate when matrix interference will occur for iodine speciation.

Based on evaluation of the data collected in this study, several types of additional data collection should be considered for these samples or for future samples.

- Measure the specific surface area of sediments for use in interpreting the partitioning data set. This analysis will be conducted for the existing samples and reported along with the hydraulic and physical

properties in a separate report. It provides another measure of sediment properties beyond just texture and geochemical properties that can be used to assess correlations of partitioning and sediment characteristics.

- The spiked-contaminant studies conducted for the samples in the study reported herein provided a useful set of information for contaminant transport parameters. These data demonstrated that there is variability in these parameters across the different types of samples. Thus, future studies should consider augmenting this set of partitioning information with partitioning studies on samples from other lithologic zones of importance to the 200-DV-1 OU. Candidate samples for additional partitioning tests include those samples that have lithologic and geochemical properties significantly different from the samples included in the large experimental matrix reported herein. These data would augment the current data set to enable evaluate variations in partitioning for a broader set of sediment types.

The data generated in this laboratory study provide a technical basis for updating the site CSMs and transport analyses. The laboratory study was structured to address the information requirements for considering MNA as all or part of a remedy (i.e., EPA 2015) by identifying and quantifying processes that affect contaminant fate and transport. As outlined in the conclusions section, attenuation was demonstrated as contaminant-specific and waste-site specific outcomes of this study. The attenuation processes and transport parameters reported herein and can be used as part of the technical defensibility for identifying attenuated transport through the vadose zone within the remedial investigation and feasibility study for the 200-DV-1 OU.

6.0 Quality Assurance

The PNNL Quality Assurance (QA) Program is based upon the requirements as defined in DOE Order 414.1D, *Quality Assurance*, and 10 CFR 830, “Energy/Nuclear Safety Management, Subpart A, Quality Assurance Requirements. PNNL has chosen to implement the following consensus standards in a graded approach:

- ASME NQA-1-2000, *Quality Assurance Requirements for Nuclear Facility Applications*, Part 1, Requirements for Quality Assurance Programs for Nuclear Facilities.
- ASME NQA-1-2000, Part II, Subpart 2.7, Quality Assurance Requirements for Computer Software for Nuclear Facility Applications, including problem reporting and corrective action.
- ASME NQA-1-2000, Part IV, Subpart 4.2, Guidance on Graded Application of Quality Assurance (QA) for Nuclear-Related Research and Development.

The procedures necessary to implement the requirements are documented through PNNL’s “How Do I...? (HDI), a system for managing the delivery of laboratory-level policies, requirements, and procedures.

The *DVZ-AFRI Quality Assurance Plan* (QA-DVZ-AFRI-001) was applied as the applicable QA document for this work under the NQA-1 QA program. This QA plan conforms to the QA requirements of DOE Order 414.1D and 10 CFR 830, Subpart A. This effort is subject to the *Price Anderson Amendments Act*.

The implementation of the Deep Vadose Zone – Applied Field Research Initiative QA program is graded in accordance with NQA-1-2000, Part IV, Subpart 4.2, Guidance on Graded Application of Quality Assurance (QA) for Nuclear-Related Research and Development. The technology level defined for this effort is Development Research, which consists of developing information that will be used directly by the Hanford Site to support remediation decisions.

This work was conducted under the Development Research level to ensure the reproducibility and defensibility of these experimental results. As such, reviewed calculation packages are available upon request except where experimental information is denoted as a scoping or preliminary study.

This work used PNNL’s Environmental Sciences Laboratory (ESL) for chemical analyses. The ESL operates under a dedicated QA plan that complies with the *Hanford Analytical Services Quality Assurance Requirements Document* (HASQARD; DOE 2007), Rev. 3. ESL implements HASQARD through *Conducting Analytical Work in Support of Regulatory Programs* (CAWSRP). Data quality objectives established in CAWSRP were generated in accordance with HASQARD requirements. Chemical analyses of testing samples and materials were conducted under the ESL QA Plan.

QA reviews of data and analyses were conducted for this work in accordance with the QA plan. There were no reportable QA issues with the data included in this report.

7.0 Conclusions

The data collected in this laboratory study addressed the following three objectives:

- Define the contaminant distribution and the hydrologic and biogeochemical setting.
- Identify attenuation processes and describe the associated attenuation mechanisms.
- Quantify attenuation and transport parameters for use in evaluating remedies.

These objectives are elements of the framework identified in EPA guidance (EPA 2015) for evaluating MNA of inorganic contaminants, and they directly support updating the CSM for these waste sites (and generally for the Hanford Central Plateau). Importantly, the information supports defining suitable contaminant transport parameters that are needed to evaluate transport of contaminants through the vadose zone and to the groundwater. This type of transport assessment supports a coupled analysis of groundwater and vadose zone contamination. The laboratory study information, in conjunction with transport analyses, can be used as input to evaluate the feasibility of remedies for the 200-DV-1 OU. This remedy evaluation will be enhanced by considering these study results that improve the understanding of controlling features and processes for transport of contaminants through the vadose zone to the groundwater.

Interpretation of this laboratory study can be considered from several perspectives relevant to supporting 200-DV-1 OU activities. Results for each contaminant were evaluated across all of the samples to identify contaminant-specific conclusions and to enable consideration of how results from this study may be relevant to other waste sites. Results are also evaluated with respect to conclusions relevant to the specific waste sites included in the study. Lastly, study results were evaluated with respect to updating CSMs and future evaluation of remedies, including the associated fate and transport assessment needed as a basis for remedy evaluation.

The data and information from these attenuation and transport studies were interpreted to support the following conclusions about contaminant behavior observed across the waste sites sampled in this study.

- Uranium
 - Uranium concentrations were low in most samples; therefore, a significant fraction of the uranium may be associated with natural background concentrations.
 - The dominant form of uranium was U(VI), supporting the conclusion that little uranium reduction has occurred in these samples.
 - For samples where uranium concentrations were elevated, only a small fraction of the uranium was present in the aqueous phase or in a form that would be transported in the aqueous phase under equilibrium partitioning conditions. Most of the uranium was associated with precipitates, and transport of uranium would be controlled by dissolution processes. This type of slow-release transport behavior was observed in the batch and soil-column leaching experiments for samples with higher uranium concentrations (B35434, B35443, and B361N1).
 - Uranium K_d values were varied across the different samples tested, with the highest K_d value associated with the sample of the high carbonate CCU material (B35443). Thus, in transport assessments, selection of a K_d value for uranium should consider spatial variation of the K_d value

based on lithologic units and carbonate content. The CCU samples show the highest K_d values for uranium. Thus, carbonate content and smaller particle sizes are important to consider for uranium K_d . Organic carbon content did not appear to be important, but was generally low in all samples. In terms of desorption versus adsorption K_d values, there was no clear trend across all of the samples. However, only the pore-water (Table 10) K_d tests provided useful data, not the tests with artificial groundwater (Table 11).

- Iodine

- I-129 concentrations in the vadose zone were non-detect for all samples. Total iodine concentrations were moderate and suitable for conducting attenuation and transport studies. Because total iodine and I-129 form the same chemical species, attenuation and transport behavior for total iodine and I-129 will be the same.
- Total iodine speciation in the aqueous phase was mostly dominated by iodide. However, sequential extractions showed only a small fraction of the iodine was present in the aqueous phase or in a form that would be transported in the aqueous phase under equilibrium partitioning conditions. Most of the iodine was associated with precipitates (likely carbonates), and transport of iodine in these precipitates would be controlled by dissolution processes. Speciation was not possible in the carbonate precipitate extractions for the sequential extraction procedure, but it is likely that the iodine present in these extractions was iodate. Scientific literature has shown co-precipitation of iodate and carbonates (Zhang et al. 2013; Podder et al. 2016) The leaching experiments showed some slow-release behavior of iodine that may be associated with these carbonate precipitates.
- Total iodine K_d values show minimal sorption of iodide and moderate sorption of iodate. Iodate K_d values varied across the different samples tested, with the highest K_d values associated with the samples with high carbonate concentrations (B35443 and B361N1). Thus, in transport assessments, selection of a K_d value for iodate should consider spatial variation of the K_d value based on carbonate content. Unlike uranium, the higher iodate K_d values are not all associated with CCU material (smaller particle sizes). Organic carbon content did not appear to be important, but was generally low in all samples. Transport of iodide and iodate through the vadose zone will be different, and speciation should be considered when conducting transport assessments. Desorption K_d values were mostly higher than adsorption K_d values in the batch experiments that were conducted.

- Tc-99

- Tc-99 was not detected in any of the samples.
- Tc-99 K_d values determined in spiked-contaminant tests were minimal to low, and values varied slightly across the different samples tested. However, the nominal retardation value for Tc-99 from these data would be close to 1. In batch testing, some of the desorption K_d values for Tc-99 were higher than the corresponding adsorption K_d values. Chemical reduction during the experimental timeframe (up to 56 days total) may have contributed to the higher apparent desorption K_d values, noting that reduction of Tc-99 by Hanford sediments has been observed in the laboratory (Szecsody et al. 2014).

- Chromium
 - Cr(VI) was not detected in most samples and, when detected, was present at a low concentration. Total chromium measured in acid extractions was likely from natural background.
 - Cr(VI) K_d values determined in spiked-contaminant tests were low, and values varied slightly across the different samples tested. The measured K_d values generally increased with experiment time (from 1 to 28 days). It is possible that all or some of this increase was due to Cr(VI) reduction, which has been observed in laboratory experiments with Hanford sediment. Desorption K_d values from batch experiments were all higher than adsorption values. However, some of the concentration changes in the batch desorption experiments (up to 56-day duration) may have been due to some Cr(VI) reduction (Truex et al. 2015b).
- Nitrate
 - Nitrate concentrations were high in all of the samples. Two samples showed very low nitrite concentrations as a potential indicator of denitrification. However, nitrite concentrations were 4 to 5 orders-of-magnitude lower than nitrate concentrations, indicating that minimal reduction had occurred.
 - Nitrate behavior in leaching experiments showed rapid elution, consistent with a minimal K_d value. The nominal retardation value for nitrate from these data would be close to 1.
 - Nitrate is a dominant electron acceptor and has influenced the microbial ecology in the samples.

The following conclusions were developed for the specific boreholes/waste sites analyzed in this study.

- T-19
 - Samples for the laboratory study from the T-19 waste site (borehole C9507) were of CCU silt, CCU caliche, and Ringold (silty, sandy gravel) materials. These samples were from locations well below the historical waste discharge and did not show signs of altered biogeochemistry induced by the waste discharge, other than the presence of contaminants. Nitrate concentrations were similar in all of the samples, indicating that waste fluids had penetrated to at least the depth of the lowest sample. The pore-water pH was consistent with a carbonate-saturated system. The highest uranium and (total) iodine concentrations were in the CCU caliche (high carbonate) material, suggesting that uranium and iodine accumulated in this zone as the waste solution passed through. Accumulation could be expected based on the observed high K_d value in this unit and the potential formation of uranium- and iodine-carbonate precipitates. Thus, the CCU is an important unit at this waste site for controlling contaminant transport. Tc-99 was not detected in any of these samples. Cr(VI) was only detected at a very low concentration near the detection limit in the CCU caliche sample.
 - Based on the data collected in this laboratory study, the following attenuation processes are important at this waste site. Sorption processes are important for uranium and iodate, and to a lesser extent for chromate and Tc-99. Formation of uranium- and iodate-carbonate precipitates also appears to be an attenuation mechanism in T-19 borehole samples. Minor indications of reduction were observed in one T-19 sample, and the potential for reduction through biotic (by the microbes found in the samples) or abiotic (e.g., ferrous iron) mechanisms is present, though it would likely have limited effect on future contaminant migration.

- T-25
 - The sample for the laboratory study from the T-25 waste site (borehole C9510) was of CCU silt materials. The sample was from a location well below the historical waste discharge and did not show signs of altered biogeochemistry induced by the waste discharge, other than the presence of contaminants. The presence of high nitrate concentration indicates that waste fluids had penetrated to at least the depth of the sample. The pore-water pH was consistent with a carbonate-saturated system. The CCU silt had high carbonate content, though not as high as the CCU caliche sample from the T-19 site. Uranium and total iodine were present at low concentrations, though concentrations were sufficient for assessment of leachability. High K_d values were measured for uranium and iodine, similar to the high K_d values measured for the T-19 CCU caliche sample that also had a large fraction of carbonate. Accumulation could be expected based on the high observed K_d value in this unit and the potential formation of uranium- and iodine-carbonate precipitates. Thus, the CCU silt is an important unit at this waste site controlling contaminant transport. Tc-99 and Cr(VI) were not detected in any of the samples.
 - Based on the data collected in this laboratory study, the following attenuation processes are important at this waste site. Sorption processes are important for uranium and iodate, and to a lesser extent for chromate and Tc-99. Formation of uranium- and iodate-carbonate precipitates also appears to be an attenuation mechanism in T-25 borehole samples. The potential for reduction through biotic (by the microbes found in the samples) or abiotic (e.g., ferrous iron) mechanisms is present, though it would likely have limited effect on future contaminant migration.
- S-9
 - Samples for the laboratory study from the S-9 waste site (borehole C9512) were of sandy Hanford Formation and transition from Hanford to CCU silt materials. These samples were deep below the historical waste discharge and did not show significant signs of altered biogeochemistry induced by the waste discharge, other than the presence of contaminants. However, the upper sample showed indication of potential reductive activity that, along with the very high nitrate concentration, may indicate some waste solution effects at this depth. Nitrate concentration was very high in the upper sample (the highest concentration of all samples in the laboratory study), and was at a moderately high concentration in the lower sample, indicating that waste fluids had penetrated to at least the depth of the lowest sample. The pore-water pH was consistent with a carbonate-saturated system. The uranium concentration in the lower sample was low, but was an order of magnitude higher than the uranium concentration in the upper sample. Neither sample appeared to be elevated in carbonate. Tc-99 and Cr(VI) were not detected in any of the samples.
 - Based on the data collected in this laboratory study, the following attenuation processes are important at this waste site. Sorption processes are important for uranium and iodate, and to a lesser extent for chromate and Tc-99. Formation of uranium- and iodate-carbonate precipitates also appears to be an attenuation mechanism in S-9 borehole samples. Minor indications of reduction were observed in one S-9 sample and the potential for reduction through biotic (by the microbes found in the samples) or abiotic (e.g., ferrous iron) is present, though it would likely have limited effect on future contaminant migration.

The study provided a set of data that addressed the study objectives and can support future evaluation of remedies, including MNA and the associated fate and transport assessment that is needed as a basis for remedy evaluations. The first objective was to jointly evaluate contaminant concentrations and the biogeochemical and hydrologic setting for these data. This information provides a baseline for interpreting attenuation and transport studies. As noted, there were significant variations in transport parameter values and some attenuation mechanisms linked to specific sediment characteristics (e.g., carbonate content). For scaling and use of this information in fate and transport assessments, these variations should be considered in light of the sample properties. For this study, the sample properties were strongly linked to the sediment units sampled rather than waste stream properties. Thus, scaling and use in future efforts can translate the attenuation and transport information from this laboratory study to other waste sites based on the distribution of similar sediment units (e.g., the CCU silt and CCU caliche).

Another objective of the study was to identify attenuation processes that appear to be active in these samples and that will affect contaminant transport through the vadose zone. Sorption processes are important for uranium and iodate, and to a lesser extent for chromate and Tc-99. Carbonate content appeared to be important for uranium and iodate K_d . Accumulation in carbonate precipitates was identified as an attenuation mechanism for uranium and iodate. Slow release of uranium and total iodine was evident in leaching experiments. Geochemical signatures of reducing conditions were minimal or non-existent in the samples. However, there was indication of potential catalysts for reductive processes, including the presence of microbes and reduced iron and manganese phases. These reductive catalysts may be responsible for some of the difficult-to-extract contaminant phases (e.g., precipitated phases) observed in sequential extraction analysis. Attenuation mechanisms relevant to chromium and Tc-99 (other than sorption) could not be fully assessed because of the low/non-detect concentrations of these contaminants.

A key objective of the study was to quantify attenuation and transport parameters to support parameterization of fate and transport assessments. This type of assessment will be needed to evaluate transport of contaminants through the vadose zone, to evaluate the coupled vadose zone-groundwater system, and to assess the need for, magnitude of, and/or design of remediation. The contaminant- and sample-specific values from stop-flow portions of soil-column experiments, batch leaching, and K_d experiments provide a set of information that can be directly used to develop transport parameters. Soil-column effluent concentration data can also be compared to one-dimensional simulations to assess fate and transport model configurations for K_d or for surface complexation models.

Collectively, the information from this laboratory study can be considered in terms of updating the CSM for contaminants in the vadose zone. It can also provide input to describing the coupled vadose zone-groundwater system that needs to be considered for remedy determinations. CSM elements from this laboratory study are listed below. These elements will need to be incorporated with other data collected during the 200-DV-1 OU remedial investigation as part of updating the CSMs for the 200-DV-1 OU component waste sites.

- Sequential extraction experiments (and more coarsely indicated by comparison of water- and acid-extraction contaminant data) show that only a small fraction of the uranium and iodine mass in samples is in a mobile form that would transport under equilibrium-partitioning conditions. Leaching experiment results confirmed that slow-release processes affect the transport of these contaminants. The relative amount of uranium and iodine mass in the mobile versus functionally immobile phases affects the potential for future mass discharge from the vadose zone to the groundwater.

- Laboratory data suggest that formation and dissolution of uranium- and iodate-carbonate precipitates is a potential attenuation mechanism affecting the relative mobile and immobile mass fractions and the transport characteristics of uranium and iodine.
- Attenuation and sorption are not uniform in the vadose zone, especially for uranium and the iodate form of iodine. Lithology (e.g., the presence and extent of layers such as the CCU) and carbonate content affected the transport parameter values for these contaminants.
- For the waste sites included in this study, the effects of waste chemistry (e.g., altered sediment pH or biogeochemistry), other than contaminant concentrations, did not penetrate deep into the vadose zone. The biogeochemical signature of samples shows that a transport evaluations at these waste sites will not need to include properties modified by waste chemistry for the deep portion of the vadose zone.
- While the CSM should acknowledge the potential for transformation processes (e.g., biotic or abiotic reduction), minimal evidence was observed that these processes are active. However, biotic and abiotic transformation may have occurred in the past and contributed to the currently observed contaminant distribution within the sediment and pore water.
- Oxygen and hydrogen isotope data were collected and primarily show correlation to regional precipitation with some variations from evaporative and condensation processes.
- It will be important to incorporate variations in physical property data into the CSM to augment existing data and correlate to indirect measures of lithology (e.g., geophysical logging). Some additional hydraulic property data were collected for this laboratory study and will be documented in a separate report.

This laboratory study extended the characterization of the 200-DV-1 OU to include identification and quantification of contaminant attenuation processes and parameters that will be needed to evaluate transport of contaminants through the vadose zone into the groundwater. This type of site-specific information enhances the technical basis to support remedy evaluation. Quantifying transport of contaminants in the vadose zone in terms of a source to groundwater under existing and future conditions without additional intervention is a basic element of remedy evaluation for the vadose zone. This type of evaluation and the supporting laboratory data describing the factors that affect transport (i.e., attenuation processes) are used in the process of considering MNA as all or part of a remedy. For cases where future contaminant discharge from the vadose zone will create or continue plumes of concern in the groundwater, the transport behavior and magnitude of the source discharge are used to define the target for vadose remediation (i.e., the extent of an engineered remedy needed in addition to natural attenuation) and assess potential remedy options. Thus, the information in this laboratory study was included in the 200-DV-1 OU characterization efforts to support the upcoming remedy evaluation in the feasibility study.

8.0 References

10 CFR 830, “Energy/Nuclear Safety Management,” Subpart A, Quality Assurance Requirements. *Code of Federal Regulations*, as amended.

ASME NQA-1-2000, *Quality Assurance Requirements for Nuclear Facility Applications*. American Society of Mechanical Engineers, New York, New York.

Beckett P. 1989. “The use of extractants in studies on trace metals in soils, sewage sludges, and sludge-treated soils.” In *Advances in Soil Science*, Volume 9, Springer-Verlag, New York, New York, pp. 144-176.

Benson DA, K Clark, I Karsch-Mizrachi, DJ Lipman, J Ostell, and EW Sayers. 2015. “GenBank.” *Nucleic Acids Research* 43(Database issue): D30-D35.

Brina R and AG Miller. 1992. “Direct detection of trace levels of uranium by laser induced kinetic phosphorimetry.” *Analytical Chemistry* 64(13):1413-1418.

Callos Y, F Mornet, A Sciandra, N Waser, A Larson, and PJ Harrison. 1999. “An optical method for the rapid measurement of micromolar concentrations of nitrate in marine phytoplankton cultures.” *Journal of Applied Phycology* 11(2):179-184.

Chao T and L Zhou. 1983. “Extraction techniques for selective dissolution of amorphous iron oxides from soils and sediments.” *Soil Science Society of America Journal* 47(2):225-232.

CHPRC. 2015a. *Conceptual Site Models for the 200-DV-1 Operable Unit Waste Sites in the T Complex Area, Central Plateau, Hanford, Washington*. SGW-49924, Rev. 0, CH2M Hill Plateau Remediation Company, Richland, Washington.

CHPRC. 2015b. *Conceptual Site Models for the 200-DV-1 Operable Unit Waste Sites in the S Complex Area, Central Plateau, Hanford, Washington*. SGW-50280, Rev. 1, CH2M Hill Plateau Remediation Company, Richland, Washington.

Cole JR et al. 2013. “Ribosomal Database Project: data and tools for high throughput rRNA analysis.” *Nucleic Acids Research*: gkt1244.

Craig H. “1961 Isotopic variations in meteoric waters.” *Science* 133:1702-1703.

DePaolo DJ, ME Conrad, K Maher, and GW Gee. 2004. “Evaporation effects on oxygen and hydrogen isotopes in deep vadose zone pore fluids at Hanford, Washington.” *Vadose Zone Journal* 3:220-232.

DOE. 1992. *Hanford Site Groundwater Background*. DOE/RL-92-23, U.S. Department of Energy, Richland Operations Office, Richland, Washington.

DOE. 2007. *Hanford Analytical Services Quality Assurance Requirements Document*. DOE/RL-96-68, Rev. 3, U.S. Department of Energy, Richland, Washington.

DOE. 2012. *Characterization Sampling and Analysis Plan for the 200-DV-1 Operable Unit*. DOE/RL-2011-104, U.S. Department of Energy, Richland Operations Office, Richland, Washington.

DOE. 2016. *Remedial Investigation/Feasibility Study and RCRA Facility Investigation/Corrective Measures Study Work Plan for the 200-DV-1 Operable Unit*. DOE/RL-2011-102, U.S. Department of Energy, Richland Operations Office, Richland, Washington.

DOE Order 414.1D, *Quality Assurance*. U.S. Department of Energy, Washington, D.C.

EPA. 2004. *Quality Assurance/Quality Control Guidance for Laboratories Performing PCR Analyses on Environmental Samples*. EPA/815/B-04/001, U.S. Environmental Protection Agency, Washington, D.C.

EPA. 2007a. *Monitored Natural Attenuation of Inorganic Contaminants in Ground Water- Volume 1, Technical Basis for Assessment*. EPA/600/R-07/139, U.S. Environmental Protection Agency, Washington, D.C.

EPA. 2007b. *Monitored Natural Attenuation of Inorganic Contaminants in Ground Water- Volume 2, Assessment for Non-Radionuclides Including Arsenic, Cadmium, Chromium, Copper, Lead, Nickel, Nitrate, Perchlorate, and Selenium*. EPA/600/R-07/140, U.S. Environmental Protection Agency, Washington, D.C.

EPA. 2010. *Monitored Natural Attenuation of Inorganic Contaminants in Ground Water- Volume 3, Assessment for Radionuclides Including Tritium, Radon, Strontium, Technetium, Uranium, Iodine, Radium, Thorium, Cesium, and Plutonium-Americium*. EPA/600/R-101093, U.S. Environmental Protection Agency, Washington, D.C.

EPA. 2015. *Use of Monitored Natural Attenuation for Inorganic Contaminants in Groundwater at Superfund Sites*. OSWER Directive 9283.1-36, U.S. Environmental Protection Agency, Office of Solid Waste and Emergency Response, Washington, D.C.

Gould W, M Stichbury, M Francis, L Lortie, and D Blowes. 2003. "An MPN method for the enumeration of iron-reducing bacteria." In *14th International Symposium on Environmental Biogeochemistry: Mining and the Environment Conference*.

Graham DL. 1983. *Stable isotopic composition of precipitation from the Rattlesnake Hills area of south-central Washington State*. RHO-BW-ST-44 P, Rockwell Hanford Operations, Richland, Washington.

Grebel JE, JA Charbonnet, and DL Sedlak. 2016. "Oxidation of organic contaminants by manganese oxide geomedia for passive urban stormwater treatment systems." *Water Research* 88:481-491.

Gleyzes C, S Tellier, and M Astruc. 2002. "Fractionation studies of trace elements in contaminated soils and sediments: a review of sequential extraction procedures." *Trends in Analytical Chemistry* 21:(6 & 7):451-467.

Goebel TS and RJ Lascano. 2012. System for high throughput water extraction from soil material for stable isotope analysis of water. *Journal of Analytical Sciences, Methods and Instrumentation* 2:203-207.

- Hall G, J Vaive, R Beer, and N Hoashi. 1996. "Selective leaches revisited, with emphasis on the amorphous Fe oxyhydroxides phase extraction." *Journal of Geochemical Exploration* 56:59-78.
- Hearn PP Jr., WC Steinkampf, DG Horton, GC Solomon, LD White, and JR Evans. 1989. "Oxygen-isotope composition of ground water and secondary minerals in Columbia Plateau basalts: Implications for the paleohydrology of the Pasco Basin." *Geology* 17:606-610.
- Heron G, C Crozet, AC Bourg, and TH Christensen. 1994. "Speciation of Fe(II) and Fe(III) in contaminated aquifer sediments using chemical extraction techniques." *Environmental Science and Technology* 28:1698-1705.
- Kohler M, DP Curtis, DE Meece, and JA Davis. 2004. "Methods for estimating adsorbed uranium (VI) and distribution coefficients of contaminated sediments." *Environmental Science and Technology* 38: 240-247.
- Larner B, A Seen, and A Townsend. 2006. "Comparative study of optimized BCR sequential extraction scheme and acid leaching of elements in certified reference material NIST 2711." *Analytica Chimica Acta* 556:444-449.
- Lee BD, JJ Moran, MK Nims, and DL Saunders. 2017. *Stable Hydrogen and Oxygen Isotope Analysis of B-Complex Perched Water Samples*. PNNL-26341, Pacific Northwest National Laboratory, Richland, Washington.
- McKinney CR, JM McCrea, S Epstein, HA Allen, and HA Urey. 1950. "Improvements in mass spectrometers for the measurement of small differences in isotope abundance ratios." *Review of Scientific Instruments* 21:724-730.
- O'Leary NA, MW Wright, JR Brister, S Ciuffo, D Haddad, R McVeigh, B Rajput, B Robbertse, B Smith-White, D Ako-Adjei, A Astashyn, A Badretdin, Y Bao, O Blinkova, V Braver, V Chetvernin, J Choi, E Cox, O Ermolaeva, CM Farrell, T Goldfarb, T Gupta, D Haft, E Hatcher, W Hlavina, VS Joardar, VK Kodali, W Li, D Maglott, P Masterson, KM McGarvey, MR Murphy, K O'Neill, S Pujar, SH Rangwala, D Rausch, LD Riddick, C Schoch, A Shkeda, SS Storz, H Sun, F Thibaud-Nissen, I Tolstoy, RE Tully, AR Vatsan, C Wallin, D Webb, W Wu, MJ Landrum, A Kimchi, T Tatusova, M DiCuccio, P Kitts, TD Murphy, and KD Pruitt. 2015. "Reference sequence (RefSeq) database at NCBI: current status, taxonomic expansion, and functional annotation." *Nucleic Acids Research*: gkv1189.
- Podder J, J Lin, W Sun, SM Botis, J Tse, N Chen, Y Hu, D Li, J Seaman, and Y Pan. 2016. "Iodate in calcite and vaterite: Insights from synchrotron X-ray absorption spectroscopy and first-principles calculations." *Geochimica et Cosmochimica Acta*, doi: <http://dx.doi.org/10.1016/j.gca.2016.11.032>
- Prudic D, D Stonestrom, and R Streigl. 1997. *Tritium, Deuterium, and Oxygen-18 in Water Collected from Unsaturated Sediments near a Low-Level Radioactive-Waste Burial Site South of Beatty, Nevada*. Water Resources Investigations Report 97-4062, U.S. Geological Survey, Reston, Virginia.
- Qafoku NP, CC Ainsworth, JE Szecsody, and OS Qafoku. 2004. "Transport-controlled kinetics of dissolution and precipitation in the sediments under alkaline and saline conditions." *Geochimica et Cosmochimica Acta* 68(14):2981-2995.

- Rehm HL, SJ Bale, P Bayrak-Toydemir, JS Berg, KK Brown, JL Deignan, MJ Friez, BH Funke, MR Hegde, E Lyon, and the Working Group of the American College of Medical Genetics. 2013. "ACMG clinical laboratory standards for next-generation sequencing." *Genetics in Medicine* 15(9):733-747.
- Rice EW, RB Baird, AD Eaton, and LS Clesceri (eds). 2012. *Standard Methods for the Examination of Water and Wastewater*, 22nd Edition. American Public Health Association, Washington, D.C.; American Water Works Association, Denver, Colorado; and Water Environment Federation, Alexandria, Virginia.
- Serne RJ, BN Bjornstad, JM Keller, PD Thorne, DC Lanigan, JN Christensen, and GS Thomas. 2010. *Conceptual Models for Migration of Key Groundwater Contaminants Through the Vadose Zone and Into the Upper Unconfined Aquifer Below the B-Complex*. PNNL-19277, Pacific Northwest National Laboratory, Richland, Washington.
- Serne RJ, JH Westsik, Jr, BD Williams, HB Jung, and G Wang. 2015. *Extended Leach Testing of Simulated LAW Cast Stone Monoliths*. PNNL-24297, Pacific Northwest National Laboratory, Richland, Washington.
- Singleton MJ, EL Sonnenthal, ME Conrad, DJ DePaolo, and GW Gee. 2004. "Multiphase reactive transport modeling of seasonal infiltration events and stable isotope fractionation in unsaturated zone pore water and vapor at the Hanford site." *Vadose Zone Journal* 3:775-785.
- Spane FA Jr. 1999. *Effects of Barometric Fluctuations on Well Water-Level Measurements and Aquifer Test Data*. PNNL-13078, Pacific Northwest National Laboratory, Richland, Washington.
- Spane FA Jr. and WD Webber. 1995. *Hydrochemistry and Hydrogeologic Conditions within the Hanford Site Upper Basalt Confined Aquifer System*. PNL-10817, Pacific Northwest National Laboratory, Richland, Washington.
- Sutherland R and F Tack. 2002. "Determination of Al, Cu, Fe, Mn, Pb, and Zn in certified reference materials using the optimized BCR sequential extraction procedure." *Analytica Chimica Acta* 454:249-257.
- Szecsody JE, BD Lee, MJ Truex, CE Strickland, JJ Moran, MMV Snyder, CT Resch, AR Lawter, L Zhong, BN Gartman, DL Saunders, SR Baum, II Leavy, JA Horner, B Williams, BB Christiansen, EM McElroy, MK Nims, RE Clayton, and D Appriou. 2017. *Geochemical, Microbial, and Physical Characterization of 200-DV-1 Operable Unit Cores from Boreholes C9552, C9487, and C9488, Hanford Site Central Plateau*. PNNL-26266, Pacific Northwest National Laboratory, Richland, Washington.
- Szecsody J, J Zachara, and P Bruckhart. 1994. "Adsorption-Dissolution Reactions Affecting the Distribution and Stability of Co(II)-EDTA in Fe-oxide Sand." *Environmental Science and Technology* 28:1706-1716.
- Szecsody J, M Truex, N Qafoku, D Wellman, T Resch, and L Zhong. 2013. "Influence of acidic and alkaline co-contaminants on uranium migration in vadose zone sediments." *Journal of Contaminant Hydrology* 151:155-175.
- Szecsody JE, D Jansik, JP McKinley, and N Hess. 2014. "Influence of alkaline waste on technetium mobility in Hanford formation sediments." *Journal of Environmental Radioactivity* 135:147-160.

- Truex MJ and KC Carroll. 2013. *Remedy Evaluation Framework for Inorganic, Non-Volatile Contaminants in the Deep Vadose Zone*. PNNL-21815, Pacific Northwest National Laboratory, Richland, Washington.
- Truex MJ, JE Szecsody, N Qafoku, and JR Serne. 2014. *Conceptual Model of Uranium in the Vadose Zone for Acidic and Alkaline Wastes Discharged at the Hanford Site Central Plateau*. PNNL-23666, Pacific Northwest National Laboratory, Richland, Washington.
- Truex MJ, M Oostrom, and GD Tartakovsky. 2015a. *Evaluating Transport and Attenuation of Inorganic Contaminants in the Vadose Zone for Aqueous Waste Disposal Sites*. PNNL-24731, Pacific Northwest National Laboratory, Richland, Washington.
- Truex MJ, JE Szecsody, NP Qafoku, R Sahajpal, L Zhong, AR Lawter, and BD Lee. 2015b. *Assessment of Hexavalent Chromium Natural Attenuation for the Hanford Site 100 Area*. PNNL-24705, Pacific Northwest National Laboratory, Richland, Washington.
- Truex MJ, BD Lee, CD Johnson, NP Qafoku, GV Last, MH Lee, and DI Kaplan. 2016. *Conceptual Model of Iodine Behavior in the Subsurface at the Hanford Site*. PNNL-24709, Rev. 1., Pacific Northwest National Laboratory, Richland, Washington.
- Um W, J Serne, M Truex, A Ward, M Valenta, C Brown, C Iovin, K Geiszler, I Kutnyakov, E Clayton, H Chang, S Baum, R Clayton, and D Smith. 2009. *Characterization of Sediments from the Soil Desiccation Pilot Test (SDPT) Site in the BC Cribs and Trenches Area*. PNNL-18800, Pacific Northwest National Laboratory, Richland, Washington.
- West AG, SJ Patrickson, and JR Ehleringer. 2006. "Water extraction times for plant and soil materials used in stable isotope analysis." *Rapid Communication in Mass Spectrometry* 20:1317-1321.
- Xue Y, C Murray, G Last, and R Mackley. 2003. *Mineralogical and Bulk-Rock Geochemical Signatures of Ringold and Hanford Formation Sediments*. PNNL-14202, Pacific Northwest National Laboratory, Richland, Washington.
- Zachara J, C Liu, C Brown, S Kelly, J Christensen, J McKinley, J Davis, J Serne, E Dresel, and W Um. 2007. *A Site-Wide Perspective on Uranium Geochemistry at the Hanford Site*. PNNL-17031, Pacific Northwest National Laboratory, Richland, Washington.
- Zhang S, C Xu, D Creeley, Y-F Ho, H-P Li, R Grandbois, KA Schwehr, DI Kaplan, CM Yeager, D Wellman, and PH Santschi. 2013. "Iodine-129 and Iodine-127 Speciation in Groundwater at the Hanford Site, US: Iodate Incorporation into Calcite." *Environmental Science & Technology* 47(17):9635-9642.

Appendix A
Geologist Descriptions of Samples

Appendix A

Geologist Descriptions of Samples

The following files show the geologist description of the samples used in this study.

BOREHOLE LOG			Page <u>1</u> of <u> </u>
Well ID: <u>C9507</u>		Well Name: <u> </u>	Date: <u>8-11-16</u>
Project: <u>FY16 200-DV-1 Characterization</u>		Reference Measure Point: <u>Ground Surface</u>	
Depth (ft)	Sample	Graphic Log	Sample Description: Sediment Classification, Grain Size Distribution, Color, Moisture Content, Sorting, Angularity, Mineralogy, Particle Size, Reaction to HCl, Other
			Comments: Depth of Casing, Drilling Method, Sampling Method, Sampler Size, Water Level, Other
92	14A		
93	14B		
94	14C		94.1-94.47: Sand (S) v. well-sorted v.f-f SA-SR, lt. brownish gray (2.5y 6.5/2), >90% S, <10% M, mostly v.f S, v. weakly cons., mod. rxn w/ HCl, sl. moist - 94.35-94.47: v.f (<1/2 mm) lt. color finer MS laminations
95	14D		94.47-94.65: Sand (S) f-m _A (75% m, 25% f), SA-SR, 25% mafic, 75% f/sic, (v. heterolithic), well-sort., mod. rxn w/ HCl, lt. brownish gray (2.5y 6/2).
96	14E		94.65-94.67: Silty Sand (mS) <70% S (v.f) >30% M, sl. moist, st. cohesive when pressed, non-plastic, mod. rxn w/ HCl, lt. brownish gray (2.5y 6/2)
97			94.67-95.1: Sand (S) >90% v.f-f, <10% M, v. well-sort, SA-SR, v. weakly cons., sl. moist, mod. rxn w/ HCl, lt. brownish gray (2.5y 6/2)
98			

Reported By:			
<u>Jake Horner</u> <small>Print Name</small>	<u>Geologist</u> <small>Title</small>	<u>Jake Horner</u> <small>Signature</small>	<u>8-11-16</u> <small>Date</small>
Reviewed By:			
<small>Print Name</small>	<small>Title</small>	<small>Signature</small>	<small>Date</small>

For Office Use Only	
OR Doc Type: <u> </u>	WMU Code(s): <u> </u>

BOREHOLE LOG				Page <u>1</u> of <u>1</u>
Well ID: <u>C9507</u>		Well Name:		Date: <u>7-26-16</u> <u>8-29-16</u>
Project: <u>FY16 200-DV-1 Characterization</u>			Location: <u>8-29-16</u>	
Reference Measure Point: <u>Ground Surface</u>				
Depth (ft)	Sample	Graphic Log	Sample Description:	Comments:
			Sediment Classification, Grain Size Distribution, Color, Moisture Content, Sorting, Angularity, Mineralogy, Particle Size, Reaction to HCl, Other	Depth of Casing, Drilling Method, Sampling Method, Sampler Size, Water Level, Other
103			<u>103.4'-103.9': Gravelly Sand (GS)</u> 5% M, 20% G (w/ pebbles & caliche nodules up to 5mm), 75% S (70% vt-f, 20% m, 10% c-vc), well-cons. wk. cem. v. st. rxn w/ HCl, sl. moist, mod. sort., lt. ol. brn. (2.5y 5.5/2) S is ≥ 80% felsic	Core #16B 103.4'-104.4' HEIS# 1335422
			<u>103.9'-104.0': Sandy Gravel (SG)</u> 60% S (vt-vc; 40% vt-f, 30% m, 30% c-vc), 35% G (vt-f matrix-dom. pebb.) S-80% felsic, mod. cons. non-cem. st. rxn w/ HCl, lt. gray (2.5y 7/2), v. sl. moist.	
104			<u>104.0'-104.3': Sandy Gravel (SG)</u> as above but w/ well-cem. caliche nodules.	
			<u>104.3'-104.4': Gravel fraction ↑ 40%</u> with abundant caliche nodules.	
			<u>104.4'-104.57': Sandy Gravel (SG)</u> 10% vt-f matrix-dom. pebbles, 45% well-cem. caliche nodules (v. st. rxn w/ HCl, contains vt-f G in cemented matrix-supported M), ≈ 40% vt-m felsic -	Core #16C 104.4'-105.4' HEIS# 1335443
105			dom. Sand 5% M, max nodules = 2.5cm, lt. yellowish brn. (2.5y 7.5/3), dry	
			<u>104.57'-105.05': gravelly silty Sand (GS)</u> 10-20% caliche nodules, 30-40% M, 40-60% Sand (vt-vc; 90% vt-f, 10% m-vc)	
			77.5% felsic Mottled zones 10YR 7/2 - 10YR 8/2, M-rich zones of mS (2.5y 6/2)	
			lt. brn. 10YR zones have pinkish rim, sl. moist, mod. cons., mod. rxn w/ HCl.	
106			<u>105.05'-105.4': Sandy Gravel (SG)</u> > 60% caliche nodules, SR-SA, up to 2cm, 35% vt-vc S, 5% M, poorly sorted, wk-mod consolidated, pale yellow (2.5y 6.5/4), st. rxn w/ HCl, Sand is felsic-dom.	

Reported By: Jake Horner Geologist Jake Horner 8-29-16
 Print Name Title Signature Date

Reviewed By: _____
 Print Name Title Signature Date

For Office Use Only

OR Doc Type: _____ WMU Code(s): _____

BOREHOLE LOG				Page <u>1</u> of <u>1</u>
Well ID: <u>C9507</u>		Well Name:		Date: <u>8-2-16</u>
Project: <u>FY16 200-DV-1 Characterization</u>		Location:		Reference Measure Point: <u>Ground Surface</u>
Depth (ft)	Sample	Graphic Log	Sample Description: Sediment Classification, Grain Size Distribution, Color, Moisture Content, Sorting, Angularity, Mineralogy, Particle Size, Reaction to HCl, Other	Comments: Depth of Casing, Drilling Method, Sampling Method, Sampler Size, Water Level, Other
137			<p><u>137.6' - 139.6' examined at end caps</u> <u>138.1' (bottom of "A", top of "B")</u> Silty Sandy Gravel (ms G), 60-70% G, 2-5 cm, max = 7 cm, R-WR w/ broken csts 25-35% S (60% m, 20% c-vc, 20% f-vc R-SR 5-10% M, secondary alteration appears as mottled clay-rich zones Sand matrix is dm. pale yellow (2.5y 7/3) S is felsic dm. mottled colors range from grayish-brn. (2.5y 5/2) to pale yellow (2.5y 7/3) & some white (2.5y 8/1) mostly dark brn. on M-rich cobble rinds Dry to v. sl. moist, no rxn w/ HCl. well-cons. cobbles compacted, but matrix breaks up & crumbles easily.</p>	
138	A			HELS#s <u>#1335461/1336408</u> <u>8-2-16</u>
139	B			
139	C			
139	D		<p><u>139.1' - 139.6' (liner "D"):</u> Silty Sandy Gravel (ms G) 65% G, 25-30% S, 5-10% M. Same as above.</p>	
140				

Reported By: Jake Horner Geologist [Signature] 8-2-16
Print Name Title Signature Date

Reviewed By: _____
Print Name Title Signature Date

For Office Use Only

OR Doc Type: _____ WMU Code(s): _____

BOREHOLE LOG				Page 1 of
Well ID: C9510		Well Name:		Date: 8-29-16
Project: FY16 200-DV-1 Characterization		Location:		Reference Measure Point: Ground Surface
Depth (ft)	Sample	Graphic Log	Sample Description: Sediment Classification, Grain Size Distribution, Color, Moisture Content, Sorting, Angularity, Mineralogy, Particle Size, Reaction to HCl, Other	Comments: Depth of Casing, Drilling Method, Sampling Method, Sampler Size, Water Level, Other
113	Core #14B		113.3' - 114.3': Sand (S) 85% v-f S Core #14B 113.3'-114.3'	
			5-10% M, 5% v-f pebbles, well-cons., HEIS#13361M9 wk-cemented, felsic-dam., ol. brn. (2.5 1/4) strong rxn. w/ HCl, well-sorted sl. moist, sparse pebbles & white caliche nodules up to 5mm, lg. pebbles/ modules v. sparse. -113.8-113.9' 10-15% caliche nodules.	
114	Core #14C		114.3' - 115.3': Sand (S) 95% S Core #14C 114.3'-115.3'	
			(>80% f-v-f, 10% m, 10% c-v-c), 5% HEIS#13361N1 v-f pebbles. Pebbles are 50% mafic dam., S is >75% felsic, SA-SR, st. rxn w/ HCl, mod. consolidated, mod. com., sl. moist, dk grayish brn. (2.5 1/2 moist) & lt gray (2.5 1/2) when dry. Sparse caliche nodules up to 1cm.	
115				
116				

Reported By: Jack Honner Geologist [Signature] 8-29-16

Print Name Title Signature Date

Reviewed By: _____

Print Name Title Signature Date

For Office Use Only

OR Doc Type: _____ WMU Code(s): _____

BOREHOLE LOG				Page <u>1</u> of <u> </u>
Well ID: <u>C9512</u>		Well Name: <u>200-DV-1 Characterization</u>		Date: <u>8-29-12</u>
Project: <u>FY16</u>		Reference Measure Point: <u>Grand Surface</u>		
Depth (ft)	Sample	Graphic Log	Sample Description: Sediment Classification, Grain Size Distribution, Color, Moisture Content, Sorting, Angularity, Mineralogy, Particle Size, Reaction to HCl, Other	Comments: Depth of Casing, Drilling Method, Sampling Method, Sampler Size, Water Level, Other
63	Core #8B		63.2 - 64.2: Sand (S) 99% S (upper fn. - lower crs; 15% f, 70% m, 15% crs), 70% felsic SA-SL, wk. CONS., non-cem, no rxn w/ HCl, 1% M, lt. gray (2.5y 7/2).	Core #8B (8-29-16) Core #8B HEIS#36175
			- 63.83' - 63.85': thin gS layer, 80% S (fn-v.c.) 15% f, 45% m, 40% c-vc, up to 20% G (ve-f, up to 4 mm pebbles, SA-A, matrix-dominated).	
64			- 63.85' - a thin ± 1mm layer of lt. ol. brown (2.5y 5/6), sl. moist M. - 63.85' - 63.97': Sand (S) 90% med. S as above G/M stringers gradlag to coarser S.	
	Core #8C		- 63.97' - 64.2' Sand (S) 95% S (10% f, 50% m, 40% c-vc), 60-70% felsic, A, ± 5% vf pebb, unconsolidated, dry, lt. grayish brn. (2.5y 6/2.5).	
65			64.2' - 65.2': Sand (S) 98% S (5% f, 90% m-c, 5% vc) 2% pebbles up to 2cm, well-sorted, SA sand, 70% felsic, uncons., non-cemented, v. weak to no rxn w/ HCl, lt. yellowish brn. (2.5y, 6/2)	Core #8C HEIS# 1336177
66				

Reported By: Steve Horner Geologist Steve Horner 8-29-16
Print Name Title Signature Date

Reviewed By: _____
Print Name Title Signature Date

For Office Use Only

OR Doc Type: _____ WMU Code(s): _____

BOREHOLE LOG				Page <u> </u> of <u> </u>
Well ID: <u>C9512</u>		Well Name: <u>FY16 200-DV-1 Chev.</u>		Date: <u>8-29-16</u>
Project: <u>FY 200-29-16</u>		Reference Measure Point: <u>GROUND SURFACE</u>		
Depth (ft)	Sample	Graphic Log	Sample Description:	Comments:
			Sediment Classification, Grain Size Distribution, Color, Moisture Content, Sorting, Angularity, Mineralogy, Particle Size, Reaction to HCl, Other	Depth of Casing, Drilling Method, Sampling Method, Sampler Size, Water Level, Other
123	Core # B70		123.0'-123.25': Sand (S) 100% well-sorted Sand (109% f, 60% m, 30% c), SA, uncons. v. wk. rxn w/ HCl, 50% matric, sl. moist, lt. yellowish brn. (2.5y, 6/3).	Core #2015 123'-124' HEIS# B361F1
			123.25'-123.35': Sand (S) cont... grain size decreases to 40% vf-f, 50% m, 10% c, sl. moist, (2.5y, 6/3), v. wk. rxn HCl.	
124			Core # C70	
	123.55'-124.0': Sand (S) ^{125.0' @ 8-29-16} >95% vf-f Sand, <5% M, v. wk. cons., wk. cement, moist, felsic-dom. (90%), lt. ol. brn. (2.5y, 5/4), sl. moldable sand with very little silt, well-sorted.			
125		-124.4' ~ 1cm thick layer of sl. coarser (mostly ^{2.5-5.0mm} fine) sand. -124.5' ~ 1cm thick layer of coarser fn. sand.		
126				

Reported By: Jack Horner Geologist Jack Horner 8-29-16
Print Name Title Signature Date

Reviewed By: _____
Print Name Title Signature Date

For Office Use Only

OR Doc Type: _____ WMU Code(s): _____

Appendix B

Spiked-Contaminant Batch Experiments Individual Treatment Results

Appendix B

Spiked-Contaminant Batch Experiments Individual Treatment Results

The table below shows the individual treatment results for spiked-contaminant batch tests conducted to estimate the linear equilibrium partitioning coefficient (K_d). For this table, some data show negative computed K_d values. Negative K_d values are interpreted as indicating an estimate of zero for the K_d value.

Sample Name/Spike/Duration	Uranium			Tc-99 (pertechnetate)			Iodate			Iodide			Chromate		
	Adsorption	Desorption	K _d	Adsorption	Desorption	K _d	Adsorption	Desorption	K _d	Adsorption	Desorption	K _d	Adsorption	Desorption	K _d
	(mL/g)	(mL/g)	(mL/g)	(mL/g)	(mL/g)	(mL/g)	(mL/g)	(mL/g)	(mL/g)	(mL/g)	(mL/g)	(mL/g)	(mL/g)	(mL/g)	(mL/g)
Base Concentration Results in Pore-Water Matrix (Table 8)															
PW-B35434 Spike-A-1d	1.89	0.61	0.16	0.72	0.78	3.33	0.03	-0.04	0.18	0.03	-0.04	0.18	0.03	-0.04	2.04
PW-B35434 Spike-B-1d	1.75	0.98	0.27	1.56	0.94	1.39	0.02	-0.15	0.11	0.02	-0.15	0.11	0.02	-0.15	2.75
PW-B35443 Spike-A-1d	8.67	6.46	0.19	10.43	3.77	4.51	-0.26	-1.63	0.25	-0.26	-1.63	0.25	-0.26	-1.63	2.21
PW-B35443 Spike-B-1d	9.52	7.53	0.25	17.52	4.05	6.73	-0.27	-1.58	0.25	-0.27	-1.58	0.25	-0.27	-1.58	2.62
PW-B361N1 Spike-A-1d	5.06	5.73	0.21	0.72	6.73	7.59	-0.07	-0.78	0.20	-0.07	-0.78	0.20	-0.07	-0.78	1.74
PW-B361N1 Spike-B-1d	5.35	6.79	0.19	0.58	6.45	4.26	-0.11	-1.10	0.16	-0.11	-1.10	0.16	-0.11	-1.10	1.89
PW-B35461 Spike-A-1d	1.81	0.73	0.13	1.12	0.88	1.39	-0.05	-0.42	0.76	-0.05	-0.42	0.76	-0.05	-0.42	NR
PW-B35461 Spike-B-1d	1.46	1.02	0.08	0.70	0.75	1.26	-0.06	-0.56	0.28	-0.06	-0.56	0.28	-0.06	-0.56	NR
PW-B361F3 Spike-A-1d	2.49	1.53	0.10	0.20	0.78	1.30	0.08	0.06	0.12	0.08	0.06	0.12	0.08	0.06	1.34
PW-B361F3 Spike-B-1d	2.23	1.56	0.13	0.38	0.74	1.30	0.01	-0.13	0.15	0.01	-0.13	0.15	0.01	-0.13	1.23
PW-B36177 Spike-A-1d	0.86	0.39	0.07	0.13	0.89	2.52	0.00	-0.06	0.09	0.00	-0.06	0.09	0.00	-0.06	11.49
PW-B36177 Spike-B-1d	0.88	0.33	0.04	0.00	1.18	2.51	-0.03	-0.17	0.12	-0.03	-0.17	0.12	-0.03	-0.17	11.05
PW-B35434 Spike-A-7d	1.56	1.23	0.14	0.64	2.17	2.65	-0.31	-1.63	0.21	-0.31	-1.63	0.21	-0.31	-1.63	2.63
PW-B35434 Spike-B-7d	1.59	1.06	0.28	0.80	3.22	3.13	0.01	0.00	0.20	0.01	0.00	0.20	0.01	0.00	1.49
PW-B35443 Spike-A-7d	9.83	11.40	0.33	3.15	3.86	5.12	-0.24	-1.63	0.15	-0.24	-1.63	0.15	-0.24	-1.63	1.25
PW-B35443 Spike-B-7d	11.14	9.08	0.29	9.08	4.20	7.61	-0.25	-1.79	0.40	-0.25	-1.79	0.40	-0.25	-1.79	2.18
PW-B361N1 Spike-A-7d	5.73	4.98	0.14	0.40	5.79	6.17	-0.09	-0.93	0.30	-0.09	-0.93	0.30	-0.09	-0.93	1.64
PW-B361N1 Spike-B-7d	5.97	5.55	0.08	0.08	6.27	9.64	-0.09	-0.74	0.10	-0.09	-0.74	0.10	-0.09	-0.74	0.51
PW-B35461 Spike-A-7d	1.26	0.65	0.11	0.60	0.97	1.90	-0.03	-0.31	2.44	-0.03	-0.31	2.44	-0.03	-0.31	141.59
PW-B35461 Spike-B-7d	1.06	0.77	0.02	0.08	1.53	3.16	-0.07	-0.57	5.60	-0.07	-0.57	5.60	-0.07	-0.57	NR
PW-B361F3 Spike-A-7d	2.95	2.13	0.00	-0.12	1.57	2.25	0.05	0.12	0.29	0.05	0.12	0.29	0.05	0.12	1.24
PW-B361F3 Spike-B-7d	2.74	1.87	0.06	-0.03	1.75	2.22	0.02	-0.05	0.29	0.02	-0.05	0.29	0.02	-0.05	1.62
PW-B36177 Spike-A-7d	0.69	0.66	-0.04	-0.48	1.39	3.37	0.06	0.29	0.21	0.06	0.29	0.21	0.06	0.29	17.88
PW-B36177 Spike-B-7d	0.80	0.21	-0.01	-0.06	1.28	2.95	0.03	0.03	0.27	0.03	0.03	0.27	0.03	0.03	13.44
PW-B35434 Spike-A-28d	1.23	0.91	0.16	0.36	1.23	3.70	-0.03	-0.27	0.64	-0.03	-0.27	0.64	-0.03	-0.27	3.54
PW-B35434 Spike-B-28d	1.57	1.03	0.28	0.60	1.03	3.83	0.00	-0.16	0.48	0.00	-0.16	0.48	0.00	-0.16	3.07
PW-B35443 Spike-A-28d	8.00	9.87	1.01	8.35	3.50	3.23	-0.34	-1.18	0.34	-0.34	-1.18	0.34	-0.34	-1.18	1.25
PW-B35443 Spike-B-28d	8.12	10.73	0.51	10.47	2.95	3.79	-0.35	-1.08	0.49	-0.35	-1.08	0.49	-0.35	-1.08	1.73
PW-B361N1 Spike-A-28d	5.99	6.93	0.23	0.55	5.30	7.75	-0.14	-0.99	0.71	-0.14	-0.99	0.71	-0.14	-0.99	2.93
PW-B361N1 Spike-B-28d	4.85	6.34	0.11	-0.01	4.95	10.37	-0.10	-0.86	0.59	-0.10	-0.86	0.59	-0.10	-0.86	2.11
PW-B35461 Spike-A-28d	0.34	0.43	0.19	0.65	0.79	1.74	-0.10	-0.40	NR	-0.10	-0.40	NR	-0.10	-0.40	NR
PW-B35461 Spike-B-28d	0.78	0.98	0.30	0.88	0.75	2.20	-0.11	-0.55	8.64	-0.11	-0.55	8.64	-0.11	-0.55	NR
PW-B361F3 Spike-A-28d	1.56	3.54	0.14	0.04	0.60	0.90	0.00	-0.13	0.72	0.00	-0.13	0.72	0.00	-0.13	3.47
PW-B361F3 Spike-B-28d	2.27	1.59	0.07	-0.03	0.59	2.15	-0.02	-0.20	0.63	-0.02	-0.20	0.63	-0.02	-0.20	2.47
PW-B36177 Spike-A-28d	0.41	0.25	0.06	-0.12	1.16	5.25	-0.02	-0.18	0.96	-0.02	-0.18	0.96	-0.02	-0.18	11.40
PW-B36177 Spike-B-28d	0.46	0.51	0.00	-0.25	0.97	2.40	0.01	0.02	0.99	0.01	0.02	0.99	0.01	0.02	12.08

Sample Name/Spike/Duration	Uranium				Tc-99 (pertechnetate)				Iodate				Iodide				Chromate			
	Adsorption		Desorption		Adsorption		Desorption		Adsorption		Desorption		Adsorption		Desorption		Adsorption		Desorption	
	K _d (mL/g)																			
Base Concentration Results in Artificial Groundwater Matrix (Table 9)																				
AGW-B35434 Spike-A-1d	NR	NR	-0.06	-0.27	0.91	1.86	-0.04	-0.41	0.03	0.44										
AGW-B35434 Spike-B-1d	NR	NR	0.14	0.79	1.06	1.92	-0.07	-0.52	0.01	0.27										
AGW-B35443 Spike-A-1d	NR	NR	0.09	2.81	2.23	5.19	-0.40	-2.01	0.14	1.21										
AGW-B35443 Spike-B-1d	NR	NR	-0.01	0.86	2.18	3.72	-0.40	-2.19	0.03	0.56										
AGW-B361N1 Spike-A-1d	NR	NR	0.04	0.25	5.81	7.31	-0.17	-1.22	0.11	0.65										
AGW-B361N1 Spike-B-1d	NR	NR	0.05	0.35	6.07	7.40	-0.20	-1.47	0.07	0.53										
AGW-B35461 Spike-A-1d	NR	NR	0.03	0.98	0.60	1.06	-0.13	-1.00	0.21	16.93										
AGW-B35461 Spike-B-1d	NR	NR	0.23	3.88	0.62	0.93	-0.11	-0.99	0.13	19.51										
AGW-B361F3 Spike-A-1d	NR	NR	0.05	0.25	0.80	1.25	-0.04	-0.36	0.05	0.22										
AGW-B361F3 Spike-B-1d	NR	NR	0.06	0.27	0.78	1.00	-0.03	-0.29	0.07	0.31										
AGW-B36177 Spike-A-1d	NR	NR	-0.11	-0.58	0.65	1.28	-0.11	-0.82	0.01	0.22										
AGW-B36177 Spike-B-1d	NR	NR	-0.01	-0.14	0.70	1.33	-0.08	-0.57	0.01	0.29										
AGW-B35434 Spike-A-7d	NR	NR	0.01	-0.04	1.25	1.65	-0.03	-0.37	0.06	0.29										
AGW-B35434 Spike-B-7d	NR	NR	0.07	-0.01	1.19	1.71	-0.05	0.28	0.05	0.37										
AGW-B35443 Spike-A-7d	NR	NR	0.34	1.69	2.67	4.59	-0.42	-1.97	0.13	0.99										
AGW-B35443 Spike-B-7d	NR	NR	0.29	1.40	2.55	2.90	-0.40	-2.14	0.12	0.94										
AGW-B361N1 Spike-A-7d	NR	NR	0.07	0.10	5.90	4.67	-0.22	-1.36	0.09	0.50										
AGW-B361N1 Spike-B-7d	NR	NR	0.06	0.05	4.30	3.40	-0.17	-1.29	0.14	0.56										
AGW-B35461 Spike-A-7d	NR	NR	0.33	2.51	0.88	1.01	-0.10	-0.85	0.95	21.84										
AGW-B35461 Spike-B-7d	NR	NR	0.20	2.19	0.72	0.89	-0.12	-0.93	0.51	14.85										
AGW-B361F3 Spike-A-7d	NR	NR	0.10	0.23	0.93	1.04	0.01	-0.23	0.22	0.67										
AGW-B361F3 Spike-B-7d	NR	NR	0.05	0.33	0.96	1.23	-0.03	-0.32	0.16	0.55										
AGW-B36177 Spike-A-7d	NR	NR	-0.04	-0.40	0.72	1.27	-0.06	-0.43	0.25	1.11										
AGW-B36177 Spike-B-7d	NR	NR	-0.01	NR	0.77	1.38	-0.04	-0.40	0.05	0.47										
AGW-B35434 Spike-A-28d	NR	NR	0.04	-0.43	1.33	1.64	0.04	-0.05	0.40	1.64										
AGW-B35434 Spike-B-28d	NR	NR	0.03	0.07	1.29	1.58	-0.01	-0.32	0.41	2.48										
AGW-B35443 Spike-A-28d	NR	NR	0.25	0.54	2.62	3.83	-0.40	-1.90	0.16	0.83										
AGW-B35443 Spike-B-28d	NR	NR	0.21	0.83	2.36	2.40	-0.41	-1.95	0.36	1.30										
AGW-B361N1 Spike-A-28d	NR	NR	-0.06	-0.36	5.09	9.91	-0.21	-1.25	0.44	1.67										
AGW-B361N1 Spike-B-28d	NR	NR	-0.06	-0.21	4.69	8.27	-0.21	-1.38	0.39	1.49										
AGW-B35461 Spike-A-28d	NR	NR	0.23	0.99	0.70	1.06	-0.09	-0.88	3.03	31.81										
AGW-B35461 Spike-B-28d	NR	NR	0.05	-0.19	0.70	0.85	-0.12	-0.93	5.13	40.88										
AGW-B361F3 Spike-A-28d	NR	NR	-0.05	-0.01	0.87	1.25	0.02	-0.16	0.18	0.93										
AGW-B361F3 Spike-B-28d	NR	NR	-0.02	-0.26	0.88	1.20	-0.02	-0.39	0.16	0.46										
AGW-B36177 Spike-A-28d	NR	NR	-0.11	-0.70	0.85	1.53	0.01	-0.04	0.11	1.06										
AGW-B36177 Spike-B-28d	NR	NR	-0.09	-1.14	0.93	1.62	-0.04	-0.44	0.34	2.08										

Sample Name/Spike/Duration	Uranium			Tc-99 (pertechnetate)			Iodide			Chromate		
	Adsorption	Desorption	K _d	Adsorption	Desorption	K _d	Adsorption	Desorption	K _d	Adsorption	Desorption	K _d
	(mL/g)	(mL/g)	(mL/g)	(mL/g)	(mL/g)	(mL/g)	(mL/g)	(mL/g)	(mL/g)	(mL/g)	(mL/g)	(mL/g)
Alternate Concentration Results (Spike 2 and Spike 3) in Pore-Water Matrix (Table 8)												
PW-B35434 Spike 2-A-1d	1.04	-0.95	-0.07	0.17	1.27	0.57	0.00	-0.26	0.10	0.10	-0.26	4.49
PW-B35434 Spike 2-B-1d	1.31	-0.88	0.15	1.43	2.89	1.34	-0.02	-0.46	0.08	0.08	-0.46	NR
PW-B35461 Spike 2-A-1d	1.35	-0.44	0.14	3.63	1.34	0.57	-0.05	-0.68	0.21	0.21	-0.68	NR
PW-B35461 Spike 2-B-1d	1.80	0.41	-0.02	0.01	2.79	1.01	-0.01	-0.38	0.24	0.24	-0.38	NR
PW-B35434 Spike 3-A-1d	2.03	0.51	-0.03	0.51	0.49	0.31	0.08	0.15	0.04	0.04	0.15	0.38
PW-B35434 Spike 3-B-1d	1.46	1.46	-0.03	0.35	1.27	0.74	0.08	0.20	0.02	0.02	0.20	0.44
PW-B35461 Spike 3-A-1d	1.64	0.80	-0.10	-0.89	0.37	0.25	0.00	-0.23	0.09	0.09	-0.23	NR
PW-B35461 Spike 3-B-1d	1.52	0.70	0.04	0.54	0.85	0.37	-0.01	-0.21	0.11	0.11	-0.21	NR
PW-B35434 Spike 2-A-7d	1.87	0.99	0.58	1.29	1.39	0.68	0.16	0.35	0.14	0.14	0.35	3.82
PW-B35434 Spike 2-B-7d	1.25	-0.32	0.53	1.04	0.67	0.25	-0.01	-0.17	0.17	0.17	-0.17	NR
PW-B35461 Spike 2-A-7d	1.79	1.16	0.67	7.68	0.63	0.30	-0.03	-0.38	1.68	1.68	-0.38	NR
PW-B35461 Spike 2-B-7d	1.15	0.81	0.76	8.35	0.20	0.34	-0.07	-0.60	2.45	2.45	-0.60	25.70
PW-B35434 Spike 3-A-7d	2.77	2.30	0.46	1.72	1.11	0.62	0.06	0.01	0.06	0.06	0.01	0.37
PW-B35434 Spike 3-B-7d	2.73	2.03	0.45	1.51	2.51	0.85	0.01	-0.09	0.11	0.11	-0.09	0.68
PW-B35461 Spike 3-A-7d	1.65	1.49	0.32	2.08	1.66	0.71	-0.01	-0.23	0.85	0.85	-0.23	92.31
PW-B35461 Spike 3-B-7d	2.64	2.22	0.51	4.11	1.63	0.59	0.01	-0.07	0.51	0.51	-0.07	31.43
PW-B35434 Spike 2-A-28d	1.15	-0.37	0.67	1.09	0.17	0.52	0.05	-0.06	0.65	0.65	-0.06	6.01
PW-B35434 Spike 2-B-28d	1.53	-0.28	0.56	1.04	0.21	0.59	0.03	0.03	0.92	0.92	0.03	-1.21
PW-B35461 Spike 2-A-28d	1.18	1.32	0.39	2.08	-0.48	0.13	0.01	-0.01	20.59	20.59	-0.01	NR
PW-B35461 Spike 2-B-28d	0.70	-0.21	0.27	1.40	0.23	0.42	0.03	0.03	17.33	17.33	0.03	NR
PW-B35434 Spike 3-A-28d	1.69	1.56	0.39	0.90	0.21	0.43	0.13	0.25	0.32	0.32	0.25	1.74
PW-B35434 Spike 3-B-28d	4.30	3.60	0.43	0.87	0.50	0.59	-0.02	-0.23	0.42	0.42	-0.23	2.25
PW-B35461 Spike 3-A-28d	3.63	2.50	2.04	10.12	-0.59	0.04	-0.01	-0.18	18.80	18.80	-0.18	NR
PW-B35461 Spike 3-B-28d	1.84	2.83	0.20	1.16	0.16	0.29	0.01	-0.04	4.13	4.13	-0.04	NR
Alternate Concentration Results (Spike 2 and Spike 3) in artificial Groundwater Matrix (Table 9)												
AGW-B35434 Spike 2-A-1d	NR	NR	0.04	0.50	1.56	0.67	0.01	-0.12	0.01	0.01	-0.12	3.75
AGW-B35434 Spike 2-B-1d	NR	NR	-0.06	-0.20	1.32	0.54	0.04	0.02	0.03	0.03	0.02	NR
AGW-B35461 Spike 2-A-1d	NR	NR	-0.10	0.12	0.72	0.24	-0.05	-0.58	0.21	0.21	-0.58	8.73
AGW-B35461 Spike 2-B-1d	NR	NR	-0.06	-0.10	0.93	0.33	-0.04	-0.37	0.04	0.04	-0.37	NR
AGW-B35434 Spike 3-A-1d	NR	NR	0.04	0.86	0.41	0.22	0.02	-0.03	0.05	0.05	-0.03	0.48
AGW-B35434 Spike 3-B-1d	NR	NR	0.00	0.37	0.02	0.13	NR	NR	0.01	0.01	NR	-0.05
AGW-B35461 Spike 3-A-1d	NR	NR	-0.08	0.95	-0.05	0.12	-0.03	-0.19	0.04	0.04	-0.19	6.35
AGW-B35461 Spike 3-B-1d	NR	NR	0.02	1.20	0.15	0.13	-0.02	-0.13	0.06	0.06	-0.13	4.42
AGW-B35434 Spike 2-A-7d	NR	NR	0.12	3.46	1.11	0.90	0.04	0.02	0.29	0.29	0.02	7.12
AGW-B35434 Spike 2-B-7d	NR	NR	0.16	0.45	1.25	0.75	0.01	0.00	0.14	0.14	0.00	6.77
AGW-B35461 Spike 2-A-7d	NR	NR	0.30	2.71	0.69	0.39	0.02	0.12	2.84	2.84	0.12	NR
AGW-B35461 Spike 2-B-7d	NR	NR	0.28	7.13	0.65	0.38	-0.01	-0.14	2.39	2.39	-0.14	NR
AGW-B35434 Spike 3-A-7d	NR	NR	0.09	0.35	0.93	0.59	0.04	0.01	0.05	0.05	0.01	0.25
AGW-B35434 Spike 3-B-7d	NR	NR	0.11	0.57	1.20	0.63	0.02	-0.06	0.11	0.11	-0.06	0.59

Sample Name/Spike/Duration	Uranium						Tc-99 (pertechnetate)						Iodate						Chromate																	
	Adsorption		Desorption		K _d		Adsorption		Desorption		K _d		Adsorption		Desorption		K _d		Adsorption		Desorption		K _d		Adsorption		Desorption		K _d							
	(mL/g)	(mL/g)	(mL/g)	(mL/g)	(mL/g)	(mL/g)	(mL/g)	(mL/g)	(mL/g)	(mL/g)	(mL/g)	(mL/g)	(mL/g)	(mL/g)	(mL/g)	(mL/g)	(mL/g)	(mL/g)	(mL/g)	(mL/g)	(mL/g)	(mL/g)	(mL/g)	(mL/g)	(mL/g)	(mL/g)	(mL/g)	(mL/g)	(mL/g)	(mL/g)						
AGW-B35461 Spike 3-A-7d	NR	NR	NR	NR	0.51	8.76	0.27	0.66	0.02	0.00	0.37	7.77	NR	NR	NR	NR	0.51	8.76	0.27	0.66	0.02	0.00	0.37	7.77	NR	NR	NR	NR	0.51	8.76	0.27	0.66	0.02	0.00	0.37	7.77
AGW-B35461 Spike 3-B-7d	NR	NR	NR	NR	0.28	4.22	0.28	0.67	0.00	-0.11	0.37	8.35	NR	NR	NR	NR	0.28	4.22	0.28	0.67	0.00	-0.11	0.37	8.35	NR	NR	NR	NR	0.28	4.22	0.28	0.67	0.00	-0.11	0.37	8.35
AGW-B35434 Spike 2-A-28d	NR	NR	NR	NR	0.23	0.24	1.09	1.61	0.07	0.26	0.42	8.52	NR	NR	NR	NR	0.23	0.24	1.09	1.61	0.07	0.26	0.42	8.52	NR	NR	NR	NR	0.23	0.24	1.09	1.61	0.07	0.26	0.42	8.52
AGW-B35434 Spike 2-B-28d	NR	NR	NR	NR	0.17	0.12	1.06	1.72	0.06	0.08	-0.09	2.27	NR	NR	NR	NR	0.17	0.12	1.06	1.72	0.06	0.08	-0.09	2.27	NR	NR	NR	NR	0.17	0.12	1.06	1.72	0.06	0.08	-0.09	2.27
AGW-B35461 Spike 2-A-28d	NR	NR	NR	NR	-0.06	-0.21	0.54	1.35	0.00	-0.14	NR	NR	NR	NR	NR	NR	-0.06	-0.21	0.54	1.35	0.00	-0.14	NR	NR	NR	NR	NR	NR	NR	NR	NR	NR	NR	NR		
AGW-B35461 Spike 2-B-28d	NR	NR	NR	NR	0.46	5.03	0.47	1.08	0.01	-0.03	NR	NR	NR	NR	NR	NR	0.46	5.03	0.47	1.08	0.01	-0.03	NR	NR	NR	NR	NR	NR	NR	NR	NR	NR	NR	NR		
AGW-B35434 Spike 3-A-28d	NR	NR	NR	NR	0.13	0.15	0.65	1.01	0.08	0.18	0.18	0.81	NR	NR	NR	NR	0.13	0.15	0.65	1.01	0.08	0.18	0.18	0.81	NR	NR	NR	NR	0.13	0.15	0.65	1.01	0.08	0.18	0.18	0.81
AGW-B35434 Spike 3-B-28d	NR	NR	NR	NR	0.03	-0.21	0.59	0.95	0.05	0.00	0.25	1.13	NR	NR	NR	NR	0.03	-0.21	0.59	0.95	0.05	0.00	0.25	1.13	NR	NR	NR	NR	0.03	-0.21	0.59	0.95	0.05	0.00	0.25	1.13
AGW-B35461 Spike 3-A-28d	NR	NR	NR	NR	0.11	1.02	0.33	0.83	0.02	0.05	3.44	97.93	NR	NR	NR	NR	0.11	1.02	0.33	0.83	0.02	0.05	3.44	97.93	NR	NR	NR	NR	0.11	1.02	0.33	0.83	0.02	0.05	3.44	97.93
AGW-B35461 Spike 3-B-28d	NR	NR	NR	NR	0.09	1.24	0.34	0.83	0.00	-0.14	21.75	NR	NR	NR	NR	NR	0.09	1.24	0.34	0.83	0.00	-0.14	21.75	NR	NR	NR	NR	NR	NR	NR	NR	NR	NR	NR	NR	

1 External Distribution		L Zhong	(PDF)
CH2M Hill Plateau Remediation		MK Nims	(PDF)
Company		DL Saunders	(PDF)
Mark Byrns	(PDF)	BD Williams	(PDF)
		JA Horner	(PDF)
24 Local Distribution		II Leavy	(PDF)
Pacific Northwest National Laboratory		SR Baum	(PDF)
MJ Truex	(PDF)	BB Christiansen	(PDF)
JE Szecsody	(PDF)	RE Clayton	(PDF)
NP Qafoku	(PDF)	EM McElroy	(PDF)
CE Strickand	(PDF)	D Appriou	(PDF)
JJ Moran	(PDF)	KJ Tyrrell	(PDF)
BD Lee	(PDF)	ML Striluk	(PDF)
MM Snyder	(PDF)	Information Release	(PDF)
AR Lawter	(PDF)		
CT Resch	(PDF)		
BN Gartman	(PDF)		



Pacific Northwest
NATIONAL LABORATORY

*Proudly Operated by **Battelle** Since 1965*

902 Battelle Boulevard
P.O. Box 999
Richland, WA 99352
1-888-375-PNNL (7665)

U.S. DEPARTMENT OF
ENERGY

www.pnnl.gov